Analytical Modelling of Two-Phase Multi-Component Flow in Porous Media with Dissipative and Non-equilibrium Effects

---

Sara Borazjani, B.Sc.(Hons), M.Sc.

A thesis submitted for the degree of

Doctor of Philosophy (Ph.D.)

Australian School of Petroleum
Faculty of Engineering, Computer & Mathematical Sciences
The University of Adelaide

November 2015

To

my husband, Ali

who has been a constant source of support and encouragement during the challenges of my study and life.

and my mother, Zahra, who has always loved me unconditionally.

I am truly thankful for having you in my life.

Table of Contents

Abstract

Hereby I present a PhD thesis by publications. The thesis includes five journal papers, of which two have already been published and three have been submitted for publication and are presently under review. The journals include high-impact-factor ones (Water Resources Research, Applied Mathematics Letters and Transport in Porous Media), and also Journal of Petroleum Science and Engineering, which is a major academic journal in petroleum industry.

The thesis develops a *new version of so-called splitting theory*. The current 2006-version of the theory encompasses analytical modelling of thermodynamically-equilibrium conservation law systems for two-phase multicomponent flow in porous media. The theory allows the derivation of numerous analytical solutions. The thesis generalizes the splitting method and applies it for flow systems with dissipation, non-equilibrium phase transitions and chemical reactions. It is shown how the general $n\times n$ system is split into an $(n\text{-}1)\times(n\text{-}1)$ auxiliary system and one scalar lifting equation. The auxiliary system contains thermodynamic parameters only, while the lifting equation contains transport properties and solves for phase saturation.

First application of the splitting method is developed for low-salinity water-flooding. Two major effects are accounted for: the wettability alternation and the induction of fines migration, straining and attachment. One-dimensional (1D) problems of sequential injection of high-salinity water slug, low salinity water slug and high-salinity water chase drive corresponds to one of the most promising modern processes of Enhanced Oil Recovery, which currently is under intensive investigation in major world oil companies. Both auxiliary and lifting problems allow for exact solutions. The exact analytical solution consists of implicit formulae for profiles of

phase saturations, salinity and fine particle concentrations. The exact solution allows for deriving explicit formulae in oil recovery. The solution permits the comparative study of the impact of both effects, which are the wettability alternation and the induction of fines migration, on incremental recovery. It was found out that both effects are significant for typical values of the physics constants. The exact solution allows for multi-variant study to optimize the injected water composition in a concrete oilfield.

The *second application* of the splitting method corresponds to 1D displacement of oil by a low-salinity polymer slug followed by a low-salinity water slug and, finally, high salinity water chase drive. This problem corresponds to the Enhanced Oil Recovery Method that merges two traditional methods of polymer- and low-salinity water-floods. The exact analytical solutions are the result of the splitting system. The method was also generalized for the case of several low-salinity slugs and Non-Newtonian properties of the polymer solution. The exact solution yields explicit formulae for propagation of saturation and concentration shocks, dynamics of different flow zones and explicit formulae for incremental oil recovery. The analytical model developed allows optimizing polymer concentration and its slug size, salinity concentration and sizes of slugs for secondary and tertiary oil recovery.

The *third application* of the new splitting method is oil displacement by suspensions and colloids of solid micro particles. The injection of one suspension or colloid with multiple particle capture mechanisms is assumed. The novelty of this work is considering numerous particle capture mechanisms and kinetic equations for the capture rates, which do not have a conservation law type. However, the system is susceptible for splitting by the introduction of Lagrangian co-ordinate and using it

instead of time as an independent variable in the general system of Partial Differential Equations (PDEs). Introduction of the concentration potential linked with retention concentrations yields an exact solution for auxiliary problem. The exact formulae allow predicting the profiles and breakthrough histories for the suspended and retained concentrations and phase saturations. It also allows the calculation of penetration depth.

The analytical models derived in the thesis are applicable also in numerous environmental and chemical engineering processes, including the disposal of industrial wastes in aquifers with propagation of contaminants and pollutants, industrial water treatment, injection of hot- or low-salinity water into aquifers and water injection into geothermal reservoirs.

Declaration

I certify that this work contains no material which has been accepted for the award of any other degree or diploma in my name, in any university or other tertiary institution and, to the best of my knowledge and belief, contains no material previously published or written by another person, except where due reference has been made in the text. In addition, I certify that no part of this work will, in the future, be used in a submission in my name, for any other degree or diploma in any university or other tertiary institution without the prior approval of the University of Adelaide and where applicable, any partner institution responsible for the joint-award of this degree. I give consent to this copy of my thesis when deposited in the University Library, being made available for loan and photocopying, subject to the provisions of the Copyright Act 1968. The author acknowledges that copyright of published works contained within this thesis resides with the copyright holder(s) of those works.

I also give permission for the digital version of my thesis to be made available on the web, via the University's digital research repository, the Library Search and also through web search engines, unless permission has been granted by the University to restrict access for a period of time.

Acknowledgment

I would never have been able to finish my dissertation without the guidance of my supervisors, help from friends, and support from my family and husband.

Firstly, I would like to express my sincere gratitude to my supervisor, Prof. Pavel Bedrikovetsky, for his excellent guidance, caring and patience, without his expertise and supports I would not been able to complete my PhD thesis.

A very special thanks to my co-supervisor Prof. Tony Roberts for persevering with me over the past few years and helping me to develop my background in mathematics.

A big thank you to all of the fantastic people I have been fortunate enough to work and collaborate with, Dr. Rouhi Farajzadeh (Shell Research), Dr. Artem Alexeev (Technical University of Denmark), Dr. Aron Behr, Dr. Luis Genolet and Dr. Antje Van der net (Wintershall), Dr. Zhenjiang You, Dr. Abbas Zeinijahromi, Dr. Themis Carageorgos, Dr. Alireza Keshavarz, Dr. Azim Kalantariasl and Yulong Yang (The University of Adelaide). Thank you all for inspiration, mentoring, motivation, technical assistance and detailed review of my work.

A sincere THANK YOU to my friends Graham and Jo Penson, their friendship and hospitality have supported and enlightened me over the past four years. Thanks also go out to my friend in Australian School of Petroleum, Stephanie, Tessa, Carmine, Mohammad, Jess, Sara, Mojtaba, Jack and Alireza. Thanks for being my friends.

Lastly, I would like to thank my family for all their love and encouragement. To my mother Zahra and my brother Pouya, they were the first community that encouraged me to find my passion and shown belief in me. To my best friend

my loving, supportive, encouraging, and patient husband, Ali, without him I would not have finished this thesis. Thank you.

Thesis by Publication

Published Journal Papers

Borazjani, S., Bedrikovetsky, P., Farajzadeh, R.: Exact Solution for Non-Self-Similar Wave-Interaction Problem during Two-Phase Four-Component Flow in Porous Media, Abstract Applied Analysis, 2014, 13 (2014)

Borazjani, S., Roberts, A.J., Bedrikovetsky, P.: Splitting in Systems of PDEs for Two-Phase Multicomponent Flow in Porous Media, Applied Mathematics Letter, 53: 25-32 (2016)

Borazjani, S., Bedrikovetsky, P., Farajzadeh, R.: Analytical Solutions of Oil Displacement by Polymer Slug with Varying Salinity, Journal of Petroleum Science and Engineering, 140, 28-40 (2016)

Submitted Journal Papers

Borazjani, S., Behr, A., Genolet, L., Van Der Net, A., Bedrikovetsky, P. Effects of fines migration on low-salinity water-flooding: analytical modelling, submitted to Journal of Transport in Porous Media

Borazjani, S., Bedrikovetsky, P. Exact solutions for two-phase colloidal-suspension transport in porous media, submitted to Water Resources Research

Borazjani, S., Bedrikovetsky, P. Exact Solutions for 1-D Polymer Flooding Accounting for Mechanical Entrapment, submitted to Water Resources Research

International conference papers and presentations

Zeinijahromi, A., **Borazjani, S.**, Rodrigues, T., Bedrikovetsky, P. Low salinity fines-assisted water-flood: analytical modelling and reservoir simulation, presented at SPE Asia Pacific Oil & Gas Conference and Exhibition, Society of Petroleum Engineers, Adelaide, Australia (2014). A full volume Conference paper, 19 pages

Borazjani, S., Farajzadeh, R., Roberts, A., Bedrikovetsky, P. Exact non-self-similar solutions for two-phase four-component flows in porous media, presented at 7th International Conference on Porous Media, Padova, Italy (2015)

1 Contextual Statement

Significance of the project Nowadays, under falling oil prices, petroleum industry is looking for new cost-effective Enhanced Oil Recovery (EOR) techniques with negligible environmental effects and simple process operations. Therefore, presently the development of improved versions of water flooding and new EOR technologies is the topic of "hot" research for numerous strong groups worldwide (Lager et al. 2008; Rezaeidoust et al. 2009; Austad et al. 2010; Morrow and Buckley 2011; Mohammadi and Gary 2012; Sheng 2014).

The development of new technologies and its application in a specific field condition is based on the results of laboratory studies and mathematical modelling. The development of a mathematical model is an essential part of the technology development, in particular derivation of equations for two-phase multi-component flow in porous media. Analytical modelling provides fast calculations, clear structure of flow phenomena, straight-forward interpretation of laboratory data and visual representation of oil recovery mechanisms. Therefore, derivation of new mathematical models for improved water flooding and analytical solutions is significant challenges in oil sciences and petroleum industry.

State of the art Consider 1D two-phase flow of water and oil in porous media, which is the simplest case of oil recovery processes. The system consists of mass conservation laws for water and is described in large scale approximation by a quasi linear first order hyperbolic equation

$$\frac{\partial s}{\partial t}+\frac{\partial f\left(s\right)}{\partial x}=0 \tag{1.1}$$

where s is water saturation and f is fractional flow function. t and x are dimensionless coordinates define as

$$x \to \frac{x}{l}, \quad t \to \frac{ut}{\phi l} \tag{1.2}$$

Here l is reservoir size; u is total velocity and ϕ is porosity.

The explicit formulae for exact solution of the problem (1.1) have been obtained by Buckley and Leverett in 1942 (Lake, 1989, Bedrikovetsky, 1993).

In general, injection of water with n low-concentration adsorbing components (such as salt and polymer) is described by the mass conservation laws for water and for each component

$$\frac{\partial s}{\partial t} + \frac{\partial f\left(s, \overline{c}\right)}{\partial x} = 0 \tag{1.3}$$

$$\frac{\partial \left(s\overline{c} + a\left(\overline{c}\right)\right)}{\partial t} + \frac{\partial \overline{c} f\left(s, \overline{c}\right)}{\partial x} = 0 \tag{1.4}$$

where $\overline{c}$ =(c_1, c_2,…, c_n) and $\overline{a}$ =(a_1, a_2, …, a_n) are vectors of concentrations for water composition and adsorbed matters, respectively.

The exact solutions for continuous injection have been obtained by numerous authors during 1954-2015 (the detailed reference lists are presented in Lake, 1989 and Bedrikovetsky, 1993). The analytical solutions for eqs (1.3, 1.4) subject to following boundary and initial conditions

$$t = 0, s = s_I, \overline{c} = \overline{c}_I \tag{1.5}$$

$$x = 0, f = f_J, \overline{c} = \overline{c}_J \tag{1.6}$$

are self-similar and depend on the group $\xi = x/t$ (Pope 1980; Johansen et al. 1988 and 1989; Dahl et al. 1992; Rhee et al. 1998).

However in multi-component EOR flooding, only a fraction of the reservoir pore volume (a slug) of EOR chemical (polymer for example), is injected and then followed by either lower concentrations of the chemical or water (low salinity or high salinity). This injection option is applied in order to reduce the costs of the low-salinity/polymer EOR flooding. The analytical solutions of system (1.3, 1.4) describing the slug injection are not self-similar. The methods of hyperbolic wave interactions are used in order to derive the analytical solutions for slug injection (Fayers 1962; Bedrikovetsky 1993). However, for the general case, where the adsorbed concentrations $\bar{a}$, depend on concentrations of all components $\bar{c}$, the analytical solutions are not available in the literature.

Pires, et al. (2006) introduced a new mathematical technique (so called the splitting method) that allows separating the $(n+1)\times(n+1)$ hyperbolic system for two-phase multicomponent flow in porous media into $n\times n$ thermodynamic auxiliary equations and one scalar equation (lifting) for saturation. In various cases, where the auxiliary system allows for analytical solutions, the general system is reduced to the solution of a single scalar lifting equation.

The above justifies half-century efforts on exact solutions for 1D two-phase multicomponent flows in porous media. It includes the above mentioned splitting technique, which was used for analytical modelling of several natural and industrial processes. However, this technique hasn't been applied for two-phase multi-component flows in porous media with dissipation, non-equilibrium phase transitions and chemical reactions, which encompass the majority of the new water flooding technologies.

Scope of the work The main achievements of the thesis are creation of

- an analytical model for low-salinity water flooding accounting for wettability alternation and induced fines migration (presented in Chapter 3)
- an exact model for 1D oil displacement by low salinity polymer slug followed by low salinity water slug and high salinity water chase drive (presented in Chapter 4)
- the derivation of a new splitting technique and analytical model for oil displacement by suspension and colloidal particles (presented in Chapter 5)
- the development of the splitting technique presented by Pires, et al. (2006) for system of equation describing chemical flooding in porous media accounting for the dissipative capillary effects and non-equilibrium phenomena (presented in Chapter 6)

1.1 Thesis Structure

This is a PhD thesis by publication. Five journal papers are included in the thesis, of which two papers have been published in peer reviewed journals and three papers have been submitted to academic journals and are currently under review.

The thesis body is formed by six Chapters. The *first Chapter* contains an introduction of the importance of the work for the petroleum industry. The *second Chapter* presents a critical analysis of contemporary literature on analytical modelling and two-phase multicomponent flows in natural reservoirs and, derivation of the basic equations for two-phase flow in porous media accounting for low salinity water flooding, low salinity polymer flooding and fines migration assisted water-flooding in porous media. The corresponding mathematical models have the form of the “multi-component polymer flooding”. In addition, this Chapter contains the detailed derivation of the analytical method so-called splitting and its application in solving

the system of equations for multi component two-phase-flows in porous media. *Chapters three, four, five and six* are the novel original parts of the thesis.

Paper	Chapter	Title	Status
1	Chapter 3	Effects of fines migration on Low-Salinity Water-flooding: analytical modelling	Submitted for publication
2	Chapter 4	Exact solution for non-self-similar wave-interaction problem during two-phase four-component flow in porous media	Published
3	Chapter 4	Analytical Solutions of oil displacement by polymer slug with varying salinity	Published
4	Chapter 4	Exact solutions for 1-D polymer flooding accounting for mechanical entrapment	Submitted for publication
5	Chapter 5	Exact solutions for two-phase colloidal-suspension transport in porous media	Submitted for publication
6	Chapter 6	Splitting in systems of PDEs for two-phase multicomponent flow in porous media	Published

Despite a strong demand of petroleum industry for reliable prediction of low salinity water flooding, the mathematical models describing the detailed equations of oil displacement with low salinity water flooding accounting for fines mobilization, migration, straining, non-equilibrium contact angle alternation and dissipative capillary effects are not available in the open literature. Thus, the complete set of equations for displacement of oil by varying water's salinity accounting for above mentioned effects are derived in *Chapter three*. The system contains five dimensionless groups defining dissipative effects of capillary pressure, dispersion, kinetics of the contact angle variation and kinetics of fines straining and detachment. Analyzing the dimensionless groups allows for low-velocity, high-velocity and large-scale approximations. It is shown that for large scale approximation, instant transfer of the excess of attached particle concentration over its maximum value into strained concentration results in instant permeability damage for aqueous phase. The analytical solution is presented for continuous low salinity water-flooding, and the results are

compared with normal water flooding. The impact of separate effects of fines migration and wettability effect alteration is analysed. The splitting technique is used to solve 3×3 hyperbolic system of equations subject to the slug injection of low salinity water flooding. Using the splitting technique separates the initial system to 2×2 auxiliary system for concentrations and one scalar equation for saturation, which allows for full integration of non-self-similar problems. Therefore, *third Chapter* contains the derivation of self-similar solutions for continuous injection of low salinity polymer, derivation of non-self-similar solutions for slug injection of water and polymer with different salinities, derivation of new formula for oil recovery and sensitivity analysis for polymer slug size. The new analytical solutions allow for explicit formula for saturation, concentration and salinity front trajectories.

Using the splitting method allows for a non-self-similar solution of two-phase multi-component problems of polymer slug with alternated water salinity injections in oil reservoirs, which is presented in *Chapter four*. Non-Newtonian properties of the injected polymer are accounted for in the mathematical modelling and results in a velocity-dependent fractional-flow function. The exact solution for 3×3 hyperbolic system of conservation laws that corresponds to two-phase, four-component flow is derived. Using the splitting technique separates the initial system into 2×2 auxiliary system for concentrations and one scalar equation for saturation, which allows for full integration of non-self-similar problems. Therefore, the Chapter contains the derivation of self-similar solutions for continuous injection of low salinity polymer, derivation of non-self-similar solutions for slug injection of water and polymer with different salinities, explicit expressions for water saturation, polymer and salt concentrations, an implicit expression for polymer- and salt-slug trajectories,

derivation of new formula for oil recovery and sensitivity analysis for polymer slug size. The analytical solution also allows calculating the minimum size of the low-salinity slug preventing mixing between polymer and high salinity water chase drive. The analytical solution also allows calculating the minimum size of the low-salinity slug preventing mixing between polymer and high salinity water chase drive. This chapter also obtains non-self-similar solutions for one-dimensional problem of oil displacement by polymer solution accounting for mechanical entrapment of the polymer macro-molecules by the rock.

Suspension flow in porous media with fine particles detachment and capture is important in numerous industrial areas, such as environmental, chemical, and petroleum industries. In petroleum industry, permeability impairment due to fine particle release and capture is a well-known phenomenon (so called deep bed filtration). This phenomenon can be described by system (1.3, 1.4) along with the kinetic equation of particle attachment. Despite of several publications in analytical solutions for single phase suspension flow in porous media (Bedrikovetsky et al. 2008, 2011, 2012) the exact solution for two-phase flow is not found in the literature. Therefore, in *Chapter five*, analytical solutions for two-phase flow of particles with multiple capture mechanisms are derived. Introduction of the splitting technique allows for exact solution of the provided system. Propagation of concentration and saturation waves along with trajectories of shock fronts for water and suspension is discussed in this Chapter.

Splitting technique introduced by Pires, et al. (2006) is only valid for system of equations in large scale approximation where the dissipative effects of capillary pressure and non-equilibrium effects are neglected. In *Chapter six*, a new version of

splitting method for the system of PDE equations accounting for two-phase *n*-component flow in porous media is developed. Here, the system of equations consists of dissipative and non-equilibrium phenomena. It was shown that for several dissipative and non-equilibrium systems, using the new splitting method separates the general $(n+1)\times(n+1)$ system into an $n\times n$ auxiliary system and one scalar lifting equation. In numerous cases, where the auxiliary system allows for exact solution, the general flow problem is reduced to solution of one non-linear lifting equation. The Chapter also discusses the exact solution of the inverse problem for the system of equations under thermodynamic equilibrium and two-phase flows with inter-phase mass transfer.

1.2 How the Publications are related to the Thesis

The paper "Effects of fines migration on low-salinity water-flooding: analytical modelling" derives 1D equations for displacement of oil by varying water's salinity and fines mobilization, migration and straining. The model is simplified for the cases of low-velocity, high-velocity and large-scale approximations. The analytical solutions for self-similar and non-self-similar problems are provided.

In the paper "Exact solution for non-self-similar wave-interaction problem during two-phase four-component flow in porous media" the analytical model for low salinity polymer flooding is derived. As polymer is injected along with the low salinity water into the reservoir, one more equation describing polymer transport is added into the system of equations for low-salinity waterflooding in large scale approximation. Using splitting technique allows for exact solution of non-self-similar

problems for slug injection during the low salinity polymer flooding. The explicit formulae for water saturation and component concentrations are provided.

The derived analytical solution in the previous paper does not account for non-Newtonian rheology of polymer; the salinity effects on relative permeability are neglected and the salinity variation of the injected water has not been considered. Therefore, in the paper, "Analytical solutions of oil displacement by polymer slug with varying salinity", the non-Newtonian properties of polymers are incorporated into the fractional flow yielding the velocity dependency of the fractional flow function. Also, wettability alternation is accounted for in relative phase permeability modifications. Comparing to the previous publication, where the slug injection of polymer is modelled analytically, here the analytical solution is expanded for the sequential injection of low-salinity polymer slug followed by low-salinity and high-salinity water. Using the splitting technique allows for the exact solution and calculating the minimum size of the low-salinity water slug preventing the contact between the polymer and high salinity water drive. The focus of the previous paper was to provide mathematical model while in this paper a numerical example is used to analyze the results, and sensitivity analysis. In the paper "Exact solutions for 1-D polymer flooding accounting for mechanical entrapment" non-self-similar solutions for one-dimensional problem of two-phase flow accounting for mechanical entrapment and adsorption of component by the rock is obtained. To be specific, the component is called "the polymer", since that exhibits both retention and adsorption in porous media.

In the paper "Exact solutions for two-phase colloidal-suspension transport in porous media", the splitting method is generalized for suspended-colloidal flow with

quasi-linear kinetics of the particle capture, and the analytical solutions for two-phase flow with multiple capture mechanisms (m mechanisms) are derived. The splitting procedure separates the $(m+2)\times(m+2)$ system into $(m+1)\times(m+1)$ auxiliary system containing one suspension and m retained concentrations, and a single lifting equation for saturation. The analytical solution of the auxiliary system is found for any form of filtration coefficient. The lifting equation permits for exact solution for the case of zero formation damage coefficients. It was found out that in the case of constant filtration coefficients, the suspended concentration is steady-state behind the concentration front, and all retained concentrations are proportional to the amount of passing suspended particles. The exact solution allows for calculation of propagation depth. It was shown that at infinite time the propagation depths for suspended and retained particles are the same and equal to those for a one-phase flow.

Previous publications in splitting technique (Pires 2004; 2006) derive the analytical solution for the system of equations in large reservoir scales; however, often only short cores are available for laboratory core-flooding, so system (1.3, 1.4) cannot be fulfilled. The paper "Splitting in systems of PDEs for two-phase multicomponent flow in porous media" develops the splitting technique for the system with dissipative and non-equilibrium effects.

Finally, the above mentioned 5 journal papers present the mathematical modeling and the analytical solution of multi-component two phase flow in porous media, accounting for low salinity; low salinity polymer and fines assisted water flooding. Furthermore, the development of the new splitting technique allows for the analytical solution for the system of equation with dissipative and non-equilibrium effects.

1.3 References

Austad, T., RezaeiDoust, A., Puntervold, T.: Chemical mechanism of low salinity water flooding in sandstone reservoirs, presented in SPE improved oil recovery symposium, Oklahoma (2010)

Bedrikovetsky, P.: Mathematical theory of oil and gas recovery: with applications to ex-USSR oil and gas fields. Kluwer Academic, Dordrecht (1993)

Bedrikovetsky, P.: Upscaling of stochastic micro model for suspension transport in porous media, Transp. Porous Media, 75(3), 335-369 (2008)

Bedrikovetsky, P., Siqueira, F. D., Furtado, C. A., Souza, A.L.S.: Modified particle detachment model for colloidal transport in porous media, Transp. Porous Media, 86(2), 353-383 (2011)

Bedrikovetsky, P., Zeinijahromi, A., Siqueira, F. D., Furtado, C. A., De Souza, A. L. S.: Particle detachment under velocity alternation during suspension transport in porous media, Transp. Porous Media, 91(1), 173-197 (2012)

Dahl, O., Johansen, T., Tveito, A., Winther, R.: Multicomponent chromatography in a two phase environment, SIAM J. Appl. Math., 52(1), 65-104 (1992)

Fayers, F.:Some theoretical results concerning the displacement of a viscous oil by a hot fluid in a porous medium, J. Fluid Mech. 13, 65-76 (1962)

Johansen, T., Winther, R.: The solution of the Riemann problem for a hyperbolic system of conservation laws modelling polymer flooding, SIAM J. Math. 19, 3, 541-566 (1988)

Johansen, T., Tveito, A., Winther, R.: A Riemann solver for a two-phase multicomponent process, SIAM J. Sci. Stat. Comput. 10, 5, 846-879 (1989)

Mohammadi, H., Gary, J.: Mechanistic modeling of the benefit of combining polymer with low salinity water for enhanced oil recovery, SPE153161, presented at the SPE improved oil recovery symposium in Tulsa, Oklahoma (2012)

Morrow, N., Buckley, J.: Improved oil recovery by low-salinity waterflooding, J. Pet. Technol., 63(05), 106-112 (2011)

Lager, A., Webb, K., Black, C., Singleton, M., Sorbie, K.: Low salinity oil recovery--An experimental investigation, Petrophysics 49(1), 28 (2008)

Lake, L.W.: Enhanced oil recovery, Prentice Hall, Englewood Cliffs, N.J (1989)

Pires, A., Bedrikovetsky, P., Shapiro, A.: Splitting between Thermodynamics and Hydrodynamics in Compositional Modelling, Presented in 9th European conference on the mathematics of oil recovery (2004)

Pires, A.P., Bedrikovetsky, P.G., Shapiro, A.A.: A splitting technique for analytical modelling of two-phase multicomponent flow in porous media, J. Pet. Sci. Eng., 51(1), 54-67 (2006)

Pope, G.A.: The application of fractional flow theory to enhanced oil recovery, SPE J. (1980)

Sheng, J.: Critical review of low-salinity waterflooding, J. Pet. Sci. Eng. 120, 216-224 (2014)

Sorbie, K.S.: Polymers-improved oil recovery, Blackie and Son Ltd., Glasgow (1991)

Rezaeidoust, A., Puntervold, T., Strand, S., Austad, T.: Smart water as wettability modifier in carbonate and sandstone: A discussion of similarities/differences in the chemical mechanisms. Energy & fuels 23(9), 4479-4485 (2009)

Rhee, H-K., Aris, R., Amundson, N.R.: Theory and application of hyperbolic systems of quasilinear equations, Vol. 2, Prentice-Hall, Englewood Cliffs (1998)

2 Literature Review

2.1 Introduction

The scientific novelty of the present thesis is the generalization of a new version of splitting method for two-phase multi-component flow systems with dissipative capillary effects, non-equilibrium phase transitions and chemical reactions. The version described by Pires et al. (2006) encompasses analytical modelling of thermodynamically-equilibrium conservation law which allows the derivation of various exact solutions. Therefore, the thesis also develops the splitting technique for low-salinity water-flooding; low salinity polymer flooding and two-phase colloidal-suspension transport in porous media. Thus, the literature review first covers the analytical solutions for two-phase multi-component flows in porous media (Section 2.2); self-similar solutions, which are the basics for the solution of non-self-similar problems, are presented in Section 2.2.1. Section 2.2.2 reviews the solution of non-self-similar problems and more recent a powerful splitting method is investigated in Section 2.2.3.

With regards to the derivation of new models accounting for low salinity water flooding, low salinity polymer flooding and suspension-colloidal flow in porous media, Sections (2.3), (2.4) and (2.5) review the previous works in low-salinity water flooding, polymer flooding and suspension-colloidal flow, respectively.

The main conclusion of the literature review is the significance of the research project on analytical modelling of two-phase multi-component flows in porous media, due to wide spreading of these processes in petroleum, environmental and chemical

engineering. The review is finalized by the statement that the solution of this problem is not available in the literature.

2.2 Analytical solutions

Two-phase flow of incompressible fluids with *n* low-concentration adsorbing components is described by the mass conservation laws for water and for each component

$$\frac{\partial s}{\partial t}+\frac{\partial f\left(s,\bar{c},\bar{a}\right)}{\partial x}=-\varepsilon_c k_{ro}\left(s,\bar{c},\bar{a}\right)\frac{\partial J\left(s,\bar{c},\bar{a}\right)}{\partial x} \tag{2.1}$$

$$\frac{\partial\left(\bar{c}s+\bar{a}\right)}{\partial t}+\frac{\partial cf\left(s,\bar{c},\bar{a}\right)}{\partial x}=\text{-}\varepsilon_c\frac{\partial}{\partial x}\left[\bar{c}k_{ro}(s,\bar{c})\,f\left(s,\bar{c},\bar{a}\right)\frac{\partial\left(\mathrm{E}\left(s,\bar{c},\bar{a}\right)J\left(s,\bar{c},\bar{a}\right)\right)}{\partial x}\right]+\varepsilon_D\frac{\partial}{\partial x}\left(s\frac{\partial\bar{c}}{\partial x}\right), \tag{2.2}$$

$$\bar{c}=\left(\bar{c}_1,...,\bar{c}_i,...,\bar{c}_n\right),\ \bar{a}=\left(\bar{a}_1,...\bar{a}_i,...,\bar{a}_n\right),i=1,2...,n$$

$$\varepsilon_t\frac{\partial\bar{a}}{\partial t}=\left[a\left(\bar{c}\right)-\bar{a}\right]f\left(s,\bar{c},\bar{a}\right),\ \ a=\left(a_1,...,a_i,...a_n\right),a_i=a_i\left(\bar{c}\right),\ i=1,2,...,n \tag{2.3}$$

where $\bar{a}$ is non-equilibrium adsorbed concentrations, k_{ro} is relative permeability for oil, J is capillary pressure, ε_D is Schmidt's number, ε_c and ε_t are dimensionless groups for capillary pressure and delay, respectively. Here $f(s,c,\bar{a})$, $k_{ro}(s,c,\bar{a})$, $J(s,c,\bar{a})$ and $a(c)$ are known functions (Ewing 1983; Bedrikovetsky 1983).

In large reservoir scale approximation where dimensionless numbers ε_D, ε_c and ε_t tend to zero the system (2.1-2.3) is equivalent to system (1.3, 1.4) (Bedrikovetsky 1983). Therefore, the system (1.3, 1.4) models the flow in large scale approximation, where the large length scale (reservoir size) yields domination of advective fluxes of water and of components over dissipative fluxes induced by the capillary pressure and component concentration gradients.

For large number of components existing in the aqueous phase, interaction of several discontinuities in the solutions of slug problems (discontinuous boundary

condition) makes major difficulties in numerical modelling. While the analytical solutions provide trajectories of the shock interactions and the parameter jumps across the trajectories, further 1-D exact solutions make the basis for stream-line and front tracking simulators of 3-D flows in porous media (Ewing 1983; Holden 2002). Analytical solutions are also useful in understanding the physics behind the multicomponent flow and can be used to explain the core flood laboratory analysis, such as breakthrough concentrations and fractional flow of the fluid.

Therefore, this Section reviews the analytical solutions for self-similar and no-self-similar problems of two-phase flow in porous media.

2.2.1 Self-similar solutions

The equations (1.3, 1.4), is a first order quasilinear hyperbolic system of conservation laws, for two independent variables x and t, with n+1, s and $\bar{c}$ dependent variables.

Boundary and initial conditions play an important role in the solution of quasi-linear hyperbolic system. Continuous injection of a fluid with constant component concentrations into the reservoir, saturated by another constant composition fluid, corresponds to the Riemann problems. Self-similar solutions of the Riemann problems have been presented in numerous works (Fayers 1962; Johansen 1988; Entov 1989, Bedrikovetsky 1993).

For n=0 in large scale approximation system (1.3-1.6) agrees with the Buckley-Leveret problems (eq (1.1)), continuous injection of water corresponds to self-similar solutions that depends on the group x/t

$$s(x,t) = s(\zeta), \quad \zeta = x/t \tag{2.4}$$

Eq (1.1) in self-similar coordinate ζ takes the form

$$\frac{ds}{d\zeta}\left(\zeta - \frac{\partial f}{\partial s}\right) = 0 \tag{2.5}$$

with following Initial and boundary conditions

$$\begin{aligned} &\zeta \to \infty: \quad s = s_I \\ &\zeta = 0: \quad f(s_J) = 1 \end{aligned} \tag{2.6}$$

Eq (2.5) results in two types of solution

$$\begin{aligned} &s = const \\ &\zeta = \frac{\partial f}{\partial s} \end{aligned} \tag{2.7}$$

Depend on the fractional flow function the solution contains shock, rarefaction or the combination of both. The detailed solution of system (1.1-1.6) is presented by Lake (1989) and Bedrikovetsky (1993).

Fig.1 shows the typical S-shaped of fractional flow as a function of saturation. The self-similar parameter ζ is presented as the tangent line of the fractional flow function eq (2.7).

In order to have the continuous solution, ζ must increase along the path connecting points of boundary (*J*) and initial (*I*) conditions. Therefore in S-shaped fractional flow function (Fig.1), it is impossible to have the continuous solution only.

The Rankine–Hugoniot conditions or the conservation of volume of aqueous phase on the discontinuity define the relationship between the states on both sides of a

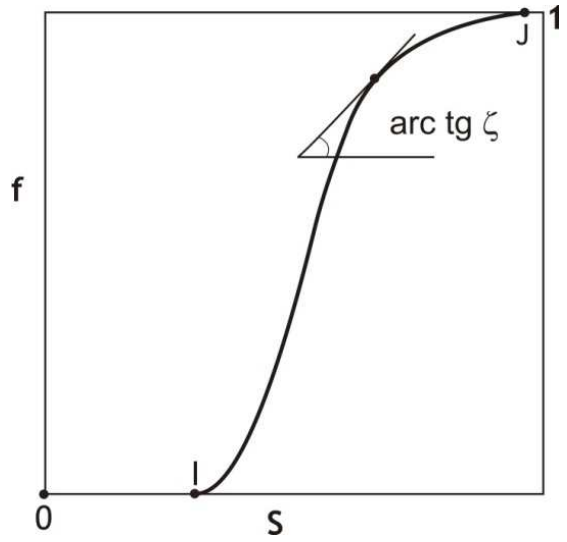

Fig.1 Typical form of fractional flow curve and the graphical presentation of self similat coordinate in (*s*, *f*) plane (Bedrikovetsky 1993)

discontinuous solution (shock wave). Usually the superscripts *l* (or –) and *r* (or +) denote the left and right-hand sides of a discontinuity and [] indicates the quantity of jump across the discontinuity (Gelfand 1959; Logan 2008; Whitham 2011).

The Rankine–Hugoniot condition for eq(1.1) is

$$s^-\left(\frac{f(s^-)}{s^-}-D\right)=s^+\left(\frac{f(s^+)}{s^+}-D\right)$$
$$D=\frac{f^+-f^-}{s^+-s^-} \tag{2.8}$$

where D is the velocity of shock front. To have a unique single-valued solution the Lax entropy condition needs to be satisfied (Whitham 2011)

$$\frac{\partial f\left(s^-\right)}{\partial s}<D<\frac{\partial f\left(s^+\right)}{\partial s} \tag{2.9}$$

Finally the solution of eq (1.1) subject to boundary and initial condition (1.5, 1.6) with c_I=c_J=0 is

$$s(\zeta)=\begin{cases} s_J & 0<\zeta<f'(s_J) \\ \zeta=f'(s) & f'(s_J)<\zeta<\dfrac{f(s_f)-f(s_I)}{s_f-s_I} \\ s_I & \dfrac{f(s_f)-f(s_I)}{s_f-s_I}<\zeta<\infty \end{cases} \tag{2.10}$$

where s_f is found from the contact discontinuity condition (for detailed of derivations see Bedrikovetsky 1993)

$$f_s'(s_f)=\frac{f(s_f)-f(s_I)}{s_f-s_I} \tag{2.11}$$

Solutions of Riemann problem for different mono-component chemical flooding, (n=1) are presented by De Nevers 1964; Claridge and Bondor 1974; Helfferich 1981 and Hirasaki 1981.

For the case of n=2 and a_i=a_i(c_i), the self-similar solutions have been derived in works by Braginskaya and Entov 1980. The solutions show distinct jumps of each component which result in a chromatographic separation of the components. However some Riemann problems allow multiple evolutionary solutions that are stable by Lax condition and the non-uniqueness problem doesn't solve by the introduction of the dissipative effects on the system of conservation laws (1.3, 1.4). The Riemann solutions for n=2 where the sorption isotherms depend on both aqueous concentrations a_i=a_i(c_1, c_2) are derived by Entov and Zazovskii (1982). The simultaneous jumps of the two components are investigated in the solution.

Johansen and Winther (1988, 1989) projected the solution of two-phase flow system into the solution of one phase flow problem, (i.e. s=f=1 in eqs (1.3, 1.4)) to

solve the Riemann problems for $n>2$. The procedure consists of solution of single phase flow and its lifting to the solution of two-phase flow. However, the projection doesn't allow for two-phase flow solution with non-uniform initial or boundary conditions (slug injection of different components).

2.2.2 Non-self-similar solutions

Piecewise injections of fluid into reservoirs (slug injection) correspond to non-self-similar problems.

Qualitative non-self-similar solutions of displacement of oil by hot and cold water sequential slugs are presented by Fayers (1962).

Bedrikovetsky (1982, 1993) showed the exact integration of slug problems with decomposition of the piece-wise constant initial and boundary condition problems into the local Riemann problems and solution of interactions of the elementary wave. The solution allows for explicit formulae for trajectories of curvilinear fronts and for saturation and concentrations distributions.

The exact integration for the case $a_i=a_i(c_i)$ shows the interaction of different concentration slugs after the injection, however the transmitted waves finally separated into the individual component slugs moving in order of reducing the derivative values of $\partial a_i(c_i)/\partial c_i$ (Rhee et al. 1970 for one-phase flows).

Nevertheless, for the general case, where the sorption isotherms strongly depend on concentrations of all aqueous components, the exact solution is not available in the literature.

2.2.3 Splitting method

Pires et al. (2006) introduced the splitting technique based on the existence of a stream function $\varphi(x, t)$ such as

$$s = -\frac{\partial \varphi}{\partial x}, \qquad f = \frac{\partial \varphi}{\partial t} \tag{2.12}$$

where the stream function $\varphi(x, t)$ is the volume of water flowing through the trajectory $x=x(t)$ starts at $x=0$ at the moment t.

$$\varphi(x,t) = \int_{0,0}^{x,t} f dt - s dx \tag{2.13}$$

Using $\varphi(x, t)$ instead of time t yields the following transformation of (1.3, 1.4) in co-ordinates (x, φ). Expressing dt from (2.13) and calculating its differential yields the expressions for eq (1.3) in (x, φ)-plane

$$\begin{aligned} &\frac{\partial U}{\partial x} + \frac{\partial F}{\partial \varphi} = 0 \\ &F = \frac{-s}{f(s,\bar{c})}, \quad U = \frac{1}{f(s,\bar{c})} \end{aligned} \tag{2.14}$$

Applying Green's theorem, over any arbitrary domain ϖ to eq. (1.6) and accounting for (2.13) yields

$$\begin{aligned} &\oint_{\partial\varpi} (\bar{c}f)\,dt - (\bar{c}s + \bar{a})\,dx = \oint_{\partial\varpi} \bar{c}\,(f dt - s dx) - \bar{a} dx = \oint_{\partial\varpi} \bar{c} d\varphi - \bar{a} dx = \\ &\iint_{\varpi} \left(\frac{\partial \bar{a}}{\partial \varphi} + \frac{\partial \bar{c}}{\partial x} \right) dx d\varphi = 0 \end{aligned} \tag{2.15}$$

therefore eq (1.6) in (x, φ)-plane becomes

$$\frac{\partial(\bar{a}(\bar{c}))}{\partial \varphi} + \frac{\partial \bar{c}}{\partial x} = 0 \tag{2.16}$$

The system for (n+1) unknowns (s, $\bar{c}$) is separated into the $n\times n$ auxiliary system (2.16) for unknown $\bar{c}(x, \varphi)$ and a scalar hyperbolic lifting equation (2.14) with unknown $s(x, \varphi)$. The auxiliary system (2.16) contains the thermodynamic terms $\bar{c}$ and$\bar{a}$, while the lifting equation contains hydrodynamic variables $f(s, \bar{c})$ and s, with already known $\bar{c}(x,\varphi)$ from the solution of eq (2.16). On the contrary to the proposed method by Johansen and Winther (1989), that is valid for Riemann problems only, the projection (2.13) allows splitting for any initial and boundary conditions.

For constant initial data s_I and $\bar{c}_I$, the initial conditions now apply along the straight line $\varphi=-s_I x$

$$\varphi = -s_I x: \;\; s = s_I, \; \bar{c} = \bar{c}_I \tag{2.17}$$

For continuous injection of $\bar{c}_J$in aqueous phase, the boundary condition in plane is

$$x = 0: \;\; f = 1, \bar{c} = \bar{c}_J \tag{2.18}$$

Figs 2(a) and (b) show mapping the co-ordinate (x, t) into (x,φ). As it follows from the projection K, the shock trajectory $x_0(t)$ with velocity D maps into the trajectory $x_0(\varphi)$ with velocity V.

Taking the derivative in x from both sides of Eq. (2.14) results in the relationship between the real D and V velocities

$$\frac{1}{V} = \frac{f}{D} - s \tag{2.19}$$

The Hugoniot-Rankine conditions on a discontinuity for system (1.3, 1.4) project onto the jump conditions for the auxiliary system (2.14, 2.16). The Lax's stability

conditions for discontinuity of system (1.3, 1.4) project onto the Lax conditions for auxiliary system (2.14, 2.16) (Lax 1972; Rozdestvenskii and Janenko 1983).

Therefore the solution of the hyperbolic system (1.3, 1.4) is constructed by the splitting method in three steps:

- Solution of the auxiliary system (2.16) subject to boundary conditions eq. (2.18) and initial conditions (2.17),
- Solution of the lifting equation (2.14) subject to boundary condition (2.18) and initial condition (2.17),
- Inversion of the mapping from (x, φ) to (x, t) by calculating dt from eq. (2.13) as

$$dt = \frac{d\varphi}{f} + \frac{S\ dx}{f} \tag{2.20}$$

and integrating it in dφ and dx.

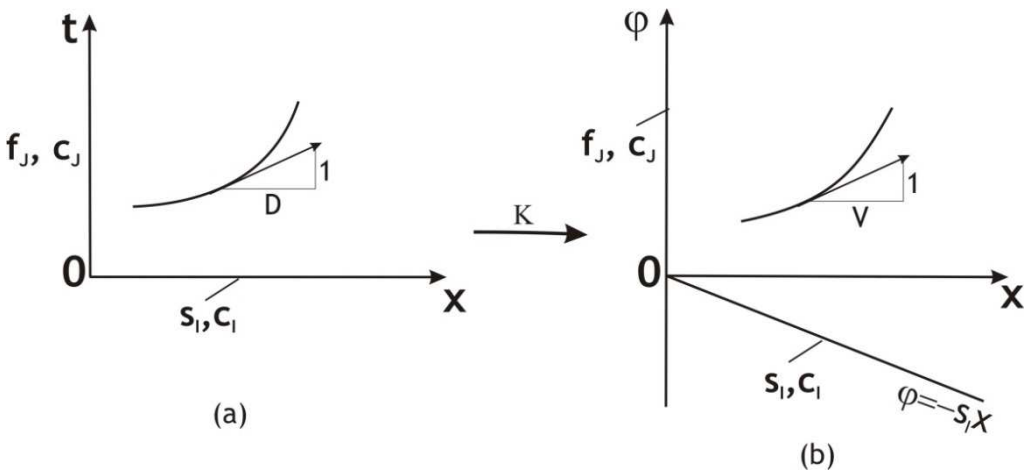

Fig.2 Coordinate transformation using splitting technique and expressing the speed of a water particle in (x, t) and (x,φ) planes

The auxiliary system (2.16) is a hyperbolic system of equation (Courant and Hilbert 1962; Smoller 1994). Initial and boundary conditions with constant values correspond to the Riemann problems that allow for self-similar solutions: $\bar{c}(x,\varphi)=C(\varphi/x)$. Solutions of the initial-boundary problem with piecewise-constant values are found by interactions of Riemann configurations. For many cases the exact solution of auxiliary system (2.16) is available in the literature, for example Rhee et al. (1970 and 1998) derived complete solution of the auxiliary system (2.16) for Langmuir sorption isotherms. The lifting eq (2.14) can be solved either numerically or analytically subject to boundary and initial conditions (2.17, 2.18) with the known solution of auxiliary problem (2.16).

The characteristic form of the lifting equation can be express as

$$\frac{d\varphi}{dx}=\frac{\partial F}{\partial U},\quad \frac{dU}{dx}=0 \tag{2.21}$$

The analytical solution corresponding to the slug injection of polymer (boundary condition (2.22)) for linear sorption ($a=\Gamma c$, where Γ is constant) is presented in Pires et al. (2006)

$$x=0: c=\begin{cases}1 & t>1\\ 0 & 0<t<1\end{cases},\ f(s_J)=1 \tag{2.22}$$

The auxiliary solution of eq (2.16) subject to initial condition (2.17) and boundary condition (2.22) is

$$c(x,\varphi)=\begin{cases}0, -s^I\ x<\varphi<\Gamma x\\ 1, \Gamma x<\varphi<\Gamma x+1\\ 0, \Gamma x+1<\varphi<+\infty\end{cases} \tag{2.23}$$

With known function $c(x,\varphi)$ in eq (2.23), Pires et al. (2006) solved lifting equation (2.14) to determine U and consequently s.

Fig.3 shows the graphical presentation of the lifting solution subject to the boundary condition (2.22) and initial condition (2.17). The solution for $\varphi<1$, consists of s_J-2 rarefaction wave, 2→3 shock, constant state 3 and 3→*I* shock. At $\varphi=1$ s_J-2 rarefaction wave transmit through the *c* shock.

The lifting solution in (x,φ) plane is

$$s(x,\varphi)=\begin{cases} s_3 & -s^I\ x<\varphi<\Gamma x \\ s^0\left(\dfrac{\varphi}{x_D}\right) & \Gamma x<\varphi<\Gamma x+1 \\ s^-\left(x_D,\varphi\right) & \Gamma x+1<\varphi<+\infty \end{cases} \tag{2.24}$$

where s_0, s_3 , s_2 and s^- are calculated from the following equations

$$F_U^{/}\left(U^0,c=1\right)=\frac{\varphi}{x} \tag{2.25}$$

$$\frac{U_2-U_3}{F_2-F_3}=\frac{1}{F_U^{/}\left(U_2,1\right)}=\Gamma \tag{2.26}$$

$$\Gamma=\frac{F\left(U^+,1\right)-F\left(U^-,0\right)}{U^+-U^-} \tag{2.27}$$

$$\begin{aligned} &U\left(x,\varphi\right)=U^-\left(x',\varphi'\right) \\ &\frac{\varphi-\varphi'}{x-x'}=F_U^{/}\left(U^-,0\right) \end{aligned} \tag{2.28}$$

The inverse mapping from (x,φ) to $(x,\ t)$ was performed using (2.20), and finally the solution was provided in $(x,\ t)$ plane

$$\begin{pmatrix} s(x,t) \\ c(x,t) \end{pmatrix} = \begin{cases} s_3, \ c=0, & \dfrac{\left(s_3 - s^I\right)}{f_3} x < t < \dfrac{\left(s_3 + \Gamma\right)}{f_3} x \\ s^0\left(\dfrac{x}{t}\right), \ c=1, & \dfrac{\left(s^0\left(\dfrac{x}{t}\right) + \Gamma\right)}{f\left(s^0\left(\dfrac{x}{t}\right)\right)} x < t < \dfrac{\left(s^0\left(\dfrac{x}{t}\right) + \Gamma\right) x + f\left(s^0\left(\dfrac{x}{t}\right)\right)}{f\left(s^0\left(\dfrac{x}{t}\right)\right)} \\ s^-(x,t), \ c=0, & \dfrac{\left(s^-(x,t) + \Gamma\right) x + f\left(s^-(x,t)\right)}{f\left(s^-(x,t)\right)} < t < +\infty \end{cases} \quad (2.29)$$

Pires et al (2006) and Dutra et al. (2009) also applied the splitting to various EOR methods such as gas-flooding, Water Alternating Gas (WAG) injection, carbonized water-flooding and non-isothermal water-flooding.

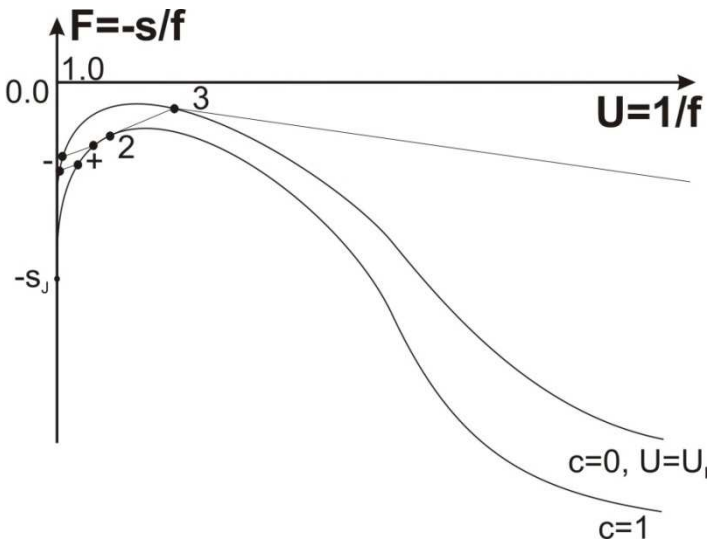

Fig 3. Graphical presentation of the lifting problem in plane (*U*, *F*) (Pires et al. 2006)

The system of equations describing gas-flooding in porous media where *n* components are distributed between the aqueous and gas phases is

$$\frac{\partial C_i}{\partial t} + \frac{\partial F_i}{\partial x} = 0, \ \ C_i = c_i\, s + y_i\,(1-s), F_i = c_i\, f + y_i\,(1-f), \ i = 1,2,...,n-1 \quad (2.30)$$

where c_i, y_i and C_i are the concentrations in water, gas and two-phase fluid, respectively. The concentrations c_1, $c_2 \ldots c_{n-1}$ and y_1 are functions of concentrations y_2, $y_3 \ldots y_{n-1}$ and f is the fractional flow of liquid. The (n-1)×(n-1) system (2.30) has (n-1) unknowns y_2, $y_3 \ldots y_{n-1}$ and s.

Pires et al. (2006) transformed the system (2.30) into (2.33) by introduction of thermodynamic variables α_i and β_i

$$\alpha_i(c_2 \ldots c_{n-1}) = \frac{c_i - y_i}{c_1 - y_1}, \beta_i(c_2 \ldots c_{n-1}) = y_i - \alpha_i y_1, \; i = 2, 3, \ldots, n-1 \tag{2.31}$$

$$\frac{\partial C_1}{\partial t} + \frac{\partial F_1(C, \beta)}{\partial x} = 0, \; \frac{\partial(\alpha_i(\beta) C_1 + \beta_i)}{\partial t} + \frac{\partial(\alpha_i(\beta) F_1 + \beta_i)}{\partial x} = 0, \; \beta = (\beta_2, \beta_3 \ldots \beta_{n-1}) \tag{2.32}$$

By using the potential ϕ and variable ψ instead of independent variables x and t

$$C = -\frac{\partial \phi}{\partial x}, F = \frac{\partial \phi}{\partial t}, \quad \psi = x - t \tag{2.33}$$

the (n-2)×(n-2) auxiliary equation (2.35) is separated from the equation (2.34)

$$\frac{\partial}{\partial \phi}\left(\frac{C_1}{F_1 - C_1}\right) - \frac{\partial}{\partial \psi}\left(\frac{1}{F_1 - C_1}\right) = 0 \tag{2.34}$$

$$\frac{\partial \beta_i}{\partial \phi} + \frac{\partial \alpha_i(\beta)}{\partial \psi} = 0 \tag{2.35}$$

Equation (2.35) contains only thermodynamic terms and can be solved independently from eq (2.34).

Oil displacement by carbonized water in large scale approximation is defined as

$$\frac{\partial s}{\partial t} + \frac{\partial f(s, \bar{c})}{\partial x} = 0 \tag{2.36}$$

$$\frac{\partial\left(\bar{c}s+b(\bar{c})(1-s)\right)}{\partial t}+\frac{\partial\left(\bar{c}f\left(s,\bar{c}\right)+b\left(\bar{c}\right)\left(1-f\left(s,\bar{c}\right)\right)\right)}{\partial x}=0 \tag{2.37}$$

Here $\bar{c}$ is the concentration of gas in injected water and $b(\bar{c})$ is the equilibrium concentration of gas in oil phase. Using coordinates φ and ψ instead of variables x and t results in the following separated auxiliary and lifting equations

$$\frac{\partial}{\partial\phi}\left(\frac{C}{q-C}\right)-\frac{\partial}{\partial\psi}\left(\frac{1}{q-C}\right)=0 \tag{2.38}$$

$$\frac{\partial\left(\bar{c}-b(\bar{c})\right)}{\partial x}+\frac{\partial\left(b(\bar{c})\right)}{\partial\psi}=0 \tag{2.39}$$

The solution of system (2.34, 2.35) and (2.38, 2.39) is presented in Pires et al. (2006) and Dutra et al. (2009).

The aim of the thesis is creation of the analytical solution based on the splitting method for non-self-similar problems of low salinity water flooding, low-salinity polymer flooding and colloidal suspension flow in porous media. Regarding the derivation of new equations for the mentioned EOR processes, next Section contains the review of the previous works in low-salinity water flooding, polymer flooding and colloidal transport.

2.3 Low salinity water flooding

In recent years, injection of low-salinity water into oil reservoirs for recovery enhancement has become an attractive method as it shows more benefits than chemical EOR processes, such as low cost, negligible environmental effect and simple process operations. Widespread experimental studies in the past decades offered different mechanisms of oil displacement during low salinity water flooding. It is reported that in sandstone reservoirs, presence of clay, polar components in oil,

formation water and multicomponent ions in the formation water are necessary requirements for the successful Low Salinity Water (LSW) flooding (Lager 2008; 2011).

Recently, Sheng (2014) provides a critical review of seventeen proposed LSW mechanisms. Most of these mechanisms are related to each other, and among them, wettability alternation of formation rock from oil wet to water wet, fines migration, mineral dissolution, increased pH and multicomponent ion exchange (MIE) are widely agreed mechanisms.

The modification of rock wettability during the injection of LSW has been reported by many authors (Salatheil 1973; Kovscek et al. 1993; Agbalaka et al. 2008; Rezaeidoust et al. 2099; Takahashi et al. 2010; Kim 2013; Mahani et al 2015 a,b). It has been shown that low salinity water has an important impact on the shape of relative permeability curves. LSW flooding results in a decline in water relative permeability and an increase in oil relative permeability. This behavior can be described by the ionic exchange between the injection and initial water.

Jerauld et al. (2008) provided a mathematical model for low salinity water flooding based on the salinity dependent oil and water relative permeabilities. In this work all salt groups in one pseudo-component (so called lumped model). Although the results of the proposed mathematical model in tertiary recovery agree with some experimental observation, however other mechanisms such as fines migration and multicomponent ion exchange were not accounted in this study.

An increase in pH during LSW flooding is observed in several studies (Austad et al. 2010, Pu et al., 2010), which is explained due to the exchange of hydrogen ions in water with adsorbed sodium ions. The negative clay surface acts as a cation

exchanger. Primarily cations (mostly Ca^{2+}) from formation water and polar components in the oleic phase are attached on to the clay surface. Injection of LSW disturbs the equilibrium between the positive components and negative charge of the clay. This effects result in the desorption of cations (Ca^{2+}), to neutralize the negative charge of the clay proton H^{+} from the water adsorbed onto the clay, therefore pH close to the clay surface increases. A reaction between adsorbed oil components and available OH^{-} occurs due to an increase in the local pH an oil component detaches from the rock surface resulting in lower residual oil saturation and higher oil relative permeability.

Multicomponent ion exchange during LSW flooding is another mechanism that was proposed by Lager et al. (2008). The mechanism explains the mobilization of polar oil components previously attached to the clay by divalent ion bonding. In LSW flooding monovalent ions mainly sodium (Na^{+}) replace the divalent ion such as calcium and magnesium (Ca^{2+} and Mg^{2+}) with a consequent oil detachment (Lager et al. 2008, 2011).

Numerical models accounting for multi-component ion exchange that include monovalent and divalent anions with active-mass-law kinetics of their adsorption on clay sites, and cations in brine are presented in works by Omekeh et al. (2013); Dang et al. (2013); Nghiem et al. (2015).

Tang and Morrow (1999) observed the detachment of in-situ fines from rock surface by injecting low salinity water. Fines detachment occurs if the ionic strength of injected water is less than a critical salinity from where particles start to mobilize. The critical salinity is a function of the concentration of ions in the aqueous phase. The mobilized particles mainly clay and silt, flow with water. Water flow is more

intense in high permeable zones. The particles dispersed in water become trapped in pore throats with smaller size than the moving particles. This blockage results in decrease of water relative permeability, therefore the water is forced to take other flow paths, to the zones with lower permeability, this consequently increases the sweep efficiency of the oil displacement (Morrow et al. 2011).

Effective fines migration management with varying injected water composition is based on the mathematical modelling. The equations for two-phase flow with fines migration have been presented for homogeneous reservoirs in large scale approximation (Yuan and Shapiro 2011; Zeinijahromi et al. 2013). Zeinijahromi et al (2013) derived the basic equations for two-phase flow with fines migration in aqueous phase. The introduction of the maximum retention function allows the modelling of the fine-particle detachment. It was shown that the large-scale system can be represented in the form equivalent to that of the polymer-flooding model, which allows using the available polymer-flooding simulator for modelling of the low-salinity water-flood with induced migration of fines. The sweep efficiency enhancement due to the water relative permeability reduction was shown in this work.

Despite the aforementioned works in modelling LSW flooding into reservoirs, to the best of our knowledge, the basic equations for low-salinity water-flooding (LSW) accounting for fines mobilisation, migration and straining and the local non-equilibrium and dissipative effects are not available in the literature.

In the current thesis (Chapter 3), the equations describe two-phase flow with single salt concentration in water accounting for fines mobilization, migration and aqueous phase permeability impairment are derived. The dissipative effects include non-equilibrium wettability alteration, capillary pressure, dispersion and deep bed

filtration. The provided system of equations in large scale approximation allows for exact solution. The analytical solution permits for sensitivity analysis of the impact of contact angle alteration and fines migration on incremental recovery as a separate physics factors.

2.4 Low salinity polymer flooding

Sweep efficiency is an important factor in oil displacement by water, which is linked to the mobility ratio of the displacing (water) and displaced (oil) phases. As the viscosity of water is often lower than that of oil, its mobility is higher, therefore, water usually by-passes the oil toward the production wells. Finally, the large area of the porous media remains un-swept.

Adding polymer to the injected water increases the viscosity of the displacing agent and improves the mobility ratio between water and oil, which results in the sweep efficiency enhancement (Sorbie 1991).

Section 2.3 shows that injection of water with lower salinity can improve oil recovery comparing to normal or high salinity water flooding. In some cases of tertiary LSW flooding, an unstable shock front due to high mobility of water is reported; adding polymer to the water phase can improve the stability of the shock front. A laboratory core-flood test on low- and high-salinity polymer flooding showed that adding polymer to the LSW improves the oil recovery to an extra 10% above the LSW-flood (Mohammadi, Gary 2012).

Also, for a certain polymer concentration the viscosity of polymer solutions increases by decreasing salt concentration. This leads to injection of lower amount of polymer for a certain oil viscosity target. It is also reported that low salinity water reduces polymer adsorption (Sorbie 1991).

Therefore, the combined effect of LSW flooding and polymer flooding can be utilized simultaneously to improve the oil recovery in economically and operationally favorable conditions.

Generally speaking, the high-concentration polymer solution is a non-Newtonian fluid. The rheology of non-Newtonian polymer solution depends on several parameters such as polymer concentration, velocity, and salt concentration. Bird et al. (1960) summarized many theoretical and experimental models for different one phase non-Newtonian fluids. Sorbie (1991) presents the rheological models of polymer solution in porous media. The power-law non-Newtonian fluid has been used extensively in the study of non-Newtonian fluid flow through porous media. Hirasaki and Pope (1974) described the apparent viscosity of the polymer as a power law function of the Darcy velocity. Wu et al. (1991) extended the power law model for two-phase flow.

Effects of low salinity polymer flooding can be modelled through modifications of the fractional-flow functions (Mohammadi, Gary 2012). Analytical methods can be used to describe the underlying physics of LSW polymer injection.

In polymer flooding, often a slug of polymer is injected and then is followed by either lower concentrations of polymer or water (low salinity or high salinity). Injection of multi-component slugs, corresponds to non-self-similar problems, interaction of several discontinuities in the solutions of slug problems makes major difficulties in analytical solutions. Despite several attempts to derive the analytical solution for system (1.3, 1.4) subject to the slug injection (Fayers 1962; Dahl et al. 1992; Bedrikovetsky 1993), for the general case, where the adsorbed concentrations depend on concentrations of all components, to the best of our knowledge the

analytical solution is not available in the literature. The current thesis (Chapter 4) presents analytical solution of a non-self-similar two-phase multi-component problem of polymer slug injection with varying water salinity in oil reservoirs.

2.5 Two-phase colloidal flow in porous media

Suspension-colloidal flow in porous media occurs in numerous areas of environmental, chemical and geo-engineering, like disposal of industrial wastes in aquifers with propagation of contaminants and pollutants, industrial water treatment and filtering (Bradford et al., 2011, 2012). A large body of literature has reported fines mobilization with permeability decline as a result of reduction of the salinity of aqueous phase, increased flow velocity and changed of pH (Lever and Dawe 1984; Khilar and Fogler 1998; Civan 2007, 2015).

Particles may detach from the rock surface, as the electrostatic attraction between the particle-rock surface decreases due to the double layer expansion. This detachment increases the relative permeability slightly, hence plugging of small pore throats leads to substantial permeability decline. Muecke (1979), Tang and Morrow (1999) showed that in two- phase flow, the fine particles are mobilized and strained inside the water phase. Therefore, the mobilized fines affect the relative permeability of the water phase. The laboratory studies in two-phase flow of oil with low-salinity water, carried out by Liu and Civan (1996), Bennion and Thomas (2005), and Civan (2007) showed similar results.

Therefore, as it was discussed in Section 2.3, the traditional vision is avoiding fines migration due to well productivity and injectivity decline. However, the

reduction in relative permeability in water-swept zone during water-flooding may be used to provide mobility control for improved performance of the water-flood.

Design of the above mentioned technologies is based on the results of mathematical modelling. The exact models are used for interpretation of the laboratory core-flooding data and determination of the model coefficients. In particular, comparison of the concentration and phase saturations calculated by the analytical models with the breakthrough of particles and water along with the pressure drop yields more understanding of the processes. For example, Alvares et al., (2007) determine the filtration function from the effluent concentration and permeability damage function from the pressure drop growth along the core.

The model for a one-phase suspension-colloidal flow in porous media consists of mass balance for suspended and retained particles and Darcy's law accounting for permeability damage by the retained particles. Herzig et al. (1970) presented the analytical solutions for 1-D flows for constant, linear and power-law filtration functions. The exact solution for a particular case, where the filtration function remains zero above some critical retention concentration is presented by Santos and Barros, 2010.

A mathematical model for the detachment of particles was derived by Bedrikovetsky et al. (2011). It is based on mechanical equilibrium of the torque balance of drag, lifting, electrostatic, and gravity forces, acting on the particle from the moving fluid and rock surface. The torque balance defines maximum retention concentration during the particle straining. A dimensionless ratio between the drag and normal forces exerting the particle determines the particle torque equilibrium and closes system of equations. Bedrikovetsky et al. (2011) derived the exact solution for

1-D colloid transport with particle release, under the assumptions of constant filtration coefficient and porosity. The explicit formulae allow the calculation of maximum retention concentration, filtration and formation damage coefficients from the pressure drop across the core during the injection. The exact solution for continuous suspension flooding was successfully matched with the core-flood laboratory data.

Flow of suspensions in porous media with particle capture and detachment under alternate flow rates is discussed in Bedrikovetsky (2012). The mathematical model contains the maximum retention concentration function of flow velocity that is used instead of equation for particle detachment kinetics from the classical filtration model.

Payatakes (1974) presents a population balance model accounting for average particle and pore sizes. The analytical solution is obtained for mono-sized particles in the rock with the pores distributed by sizes; see Bedrikovetsky (2008). The exact solution provides the averaged flow, yielding the generalization of the model that accounts for the pore volume, inaccessible for finite-size particles, and the fractional flows via the accessible and inaccessible parts of the porous space.

The stochastic models, for single-phase colloidal-suspension flows including the particle- trajectory calculations are presented in Payatakes (1974) and for the random-walk equations are provided in Shapiro (2007) and Yuan and Shapiro (2010).

The numerical models for two-phase colloidal-suspension flows have been developed for propagation of viruses and nano-particles in porous media (Zhang et al., 2013).

Despite of several studies in analytical modelling of colloidal flow in one phase flow in porous media, to the best of our knowledge, the analytical models describing

two-phase suspensions and colloids flow in porous media are not available in the literature.

In the present thesis (Chapter 5), the analytical solutions for two-phase flow of particles with multiple capture mechanisms are presented. Introduction of the splitting technique allows for separating auxiliary equations containing only suspension and retained concentrations from one lifting equation for unknown phase saturation. The auxiliary system allows for exact solution for any form of filtration functions. The lifting equation allows for exact solution for the case of constant filtration coefficients and zero formation damage coefficients. Semi analytical solution was provided for the general case of lifting equation, where fractional flow is a function of suspended and retained concentrations. The propagation of concentration and saturation waves along with trajectories of shock fronts for water and suspension is discussed.

2.6 Conclusions

The mathematical models for two-phase multicomponent flow in porous media with non-equilibrium phase transitions and chemical reactions describe numerous industrial and natural processes in chemical, environmental, geo- and petroleum engineering. Planning and design of the above mentioned technologies is based on the results of mathematical modelling. The exact analytical solutions are used for interpretation of the results of laboratory coreflooding and calculation of the model coefficients. The comparison of the concentration and saturation waves provided by the analytical models with the breakthrough of colloids and water during the corefloods or field tests yields more profound understanding of the processes. The analytical models are also widely used in three-dimensional reservoir simulation using the stream-line and front-tracking techniques.

The above applications motivated almost 70-year history of glorious studies on exact solutions for 1D two-phase multicomponent flows in porous media. It includes the recent splitting technique, which was used for analytical modelling of numerous natural and industrial processes. However, this technique hasn't been applied for two-phase multi-component flows in rocks with dissipation, non-equilibrium phase transitions and chemical reactions, which encompass the majority of the above mentioned processes and technologies. The critical literature analysis presented in this Chapter shows that the solution of this problem is not available in the literature.

2.7 References

Agbalaka, C.C., Dandekar, A.Y., Patil, S.L., Khataniar, S., Hemsath, J.R.: Coreflooding studies to evaluate the impact of salinity and wettability on oil recovery efficiency. Transp. Porous Media, 76(1), 77-94 (2009)

Alvarez, A. C., Hime, G., Marchesin, D., Bedrikovetsky, P.: The inverse problem of determining the filtration function and permeability reduction in flow of water with particles in porous media, Transp. Porous Media, 70(1), 43-62 (2007)

Austad, T., Rezaeidoust, A., Puntervold, T.: Chemical mechanism of low salinity water flooding in sandstone reservoirs, Presented in SPE improved oil recovery symposium, Oklahoma (2010)

Bedrikovetsky, P.: Displacement of oil by a chemical slug with water drive, J. Fluid Dyn. USSR Academy of Sciences, 3, 102-111 (1982)

Bedrikovetsky, P.: Mathematical theory of oil and gas recovery: with applications to ex-USSR oil and gas fields. Kluwer Academic, Dordrecht (1993)

Bedrikovetsky, P.: Upscaling of stochastic micro model for suspension transport in porous media, Transp. Porous Media, 75(3), 335-369 (2008)

Bedrikovetsky, P., Siqueira, F. D., Furtado, C. A., Souza, A.L.S.: Modified particle detachment model for colloidal transport in porous media, Transp. Porous Media, 86(2), 353-383 (2011)

Bedrikovetsky, P., Zeinijahromi, A., Siqueira, F. D., Furtado, C. A., De Souza, A. L. S.: Particle detachment under velocity alternation during suspension transport in porous media, Transp. Porous Media, 91(1), 173-197 (2012)

Bennion, D. and Thomas F.: Formation damage issues impacting the productivity of low permeability, low initial water saturation gas producing formations, J. Energy Resour. Technol.-Trans., 127 (3) 240-247 (2005)

Bird, R. B, Stewart W.E, Lightfoot, E.N.:Transport phenomena, John Wiley and Sons, New York (1960)

Bradford, S. A., S. Torkzaban, and J. Simunek.: Modeling colloid transport and retention in saturated porous media under unfavorable attachment conditions, Water Resour. Res., 47(10) (2011)

Bradford, S. A., S. Torkzaban, H. Kim, J. Simunek.: Modeling colloid and microorganism transport and release with transients in solution ionic strength, Water Resour. Res., 48(9) (2012)

Braginskaya, G., Entov, V.: Nonisothermal displacement of oil by a solution of an active additive, J. Fluid Dyn. 15, 6, 873-880 (1980)

Civan, F.: reservoir formation damage: Fundamentals, modeling, assessment, and mitigation, Gulf professional publishing, Elsevier, Burlington (2007)

Civan, F.: Non-isothermal permeability impairment by fines migration and deposition in porous media including dispersive transport, Transp. Porous Media., 85(1), 233-258 (2010)

Claridge, E., Bondor, P.: A graphical method for calculating linear displacement with mass transfer and continuously changing motilities, SPE J. 14, 6, 609-618 (1974)

Courant, R., Hilbert, D.: Methods of mathematical physics: partial differential equations, Interscience, New York (1962)

Dahl, O., Johansen, T., Tveito, A., Winther, R.: Multicomponent chromatography in a two phase environment, SIAM J. Appl. Math., 52(1), 65-104 (1992)

Dang, C.T., Nghiem, L.X., Chen, Z., Nguyen, Q.P., Nguyen, N.T.: State-of-the art low salinity waterflooding for enhanced oil recovery, Presented in SPE Asia pacific oil and gas conference and exhibition, Jakarta (2013)

De Nevers, N.: A calculation method for carbonated water flooding, SPE J. 4, 01, 9-20 (1964)

Dutra, T.A., Pires, A.P., Bedrikovetsky, P.:A new spliting scheme and existance of elliptic region for gas flood modeling, SPE J., (2009)
Entov, V. M., Zazovskii, A.F.: Displacement of oil by a solution of two additives (active and passive). Izv. Akad. Nauk SSSR, Mekh. Zhidk. Gaza 6 (1982)
Entov, V., Zazovskii, A.: Hydrodynamics of Enhanced Oil Recovery Processes, Nauka, Moscow (1989) (in Russian)
Ewing, R.E.: The Mathematics of Reservoir Simulation, SIAM, Philadelphia (1983)
Fayers, F.: Some theoretical results concerning the displacement of a viscous oil by a hot fluid in a porous medium, J. Fluid Mech., 13, 65-76 (1962)
Gel'fand, I.M.: Some problems in the theory of quasi-linear equations, Usp. Mat. Nauk, 14, 2, 87-158 (1959)
Holden, H., Risebro N.H.: Front Tracking for Hyperbolic Conservation Laws, Springer-Verlag, New York (2002)
Helfferich, F.G.: Theory of multicomponent multiphase displacement in porous media, SPE J. 21, 01, 51-62 (1981)
Herzig, J., Leclerk, D., Legoff, P.: Flow of suspensions through porous media, J. Ind. Eng. Chem., 62(5), 8-35 (1970)
Hirasaki, G.: Application of the theory of multicomponent, multiphase displacement to three-component, two-phase surfactant flooding, SPE J. 21, 2, 191-204 (1981)
Jerauld, G.R., Lin, C., Webb, K.J., Seccombe, J.C.: Modelling low-salinity waterflooding, SPE Reserv. Eval. Eng., 11(6), 1000 (2008)
Johansen, T., Winther, R.: The solution of the Riemann problem for a hyperbolic system of conservation laws modelling polymer flooding, SIAM J. Math., 19, 3, 541-566 (1988)
Johansen, T., Tveito, A., Winther, R.: A Riemann solver for a two-phase multicomponent process. SIAM J. Sci. Stat. Comput., 10, 5, 846-879 (1989)
Khilar, K. and Fogler, H.: Migrations of fines in porous media, Kluwer Academic Publishers, Dordrecht (1998)
Kim, T.W., Kovscek, A.R.: Wettability alteration of a heavy oil/brine/carbonate system with temperature, Energy Fuels, 27(6), 2984-2998 (2013)
Kovscek, A., Wong, H., Radke, C.: A pore level scenario for the development of mixed wettability in oil reservoirs, AICHE J., 39(6), 1072-1085 (1993)
Lager, A., Webb, K., Black, C., Singleton, M., Sorbie, K.: Low salinity oil recovery-An experimental investigation, Petrophysics, 49(1), 28 (2008)
Lager, A., Webb, K., Seccombe, J.: Low salinity waterflood, Endicott, Alaska: Geochemical study & field evidence of multicomponent ion exchange. In: IOR-16th European Symposium on Improved Oil Recovery (2011)
Lake, L.W.: Enhanced oil recovery, Prentice Hall, Englewood Cliffs, N.J (1989)
Lax, P.D.: Hyperbolic systems of conservation laws and the mathematical theory of shock waves, SIAM, Philadelphia, (1972)
Lever, A., Dawe, R.: Water-sensitivity and migration of fines in the hopeman sandstone. J. Pet. Geol., 7 (1) 97-107 (1984)
Liu, X., Civan, F.: Formation damage and filter cake buildup in laboratory core tests: modeling and model-assisted analysis, SPE Form. Eval., 11.01 26-30 (1996)
Logan, J.: An introduction to nonlinear partial differential equations, John Wiley & Sons, New Jersey (2008)
Mahani, H., Berg, S., Ilic, D., Bartels, W.-B., Joekar-Niasar, V.: Kinetics of Low-Salinity-Flooding Effect, SPE J., 20 (1), 8−20 (2015a)
Mahani, H., Keya, A.L., Berg, S., Bartels, W.-B., Nasralla, R., Rossen, W.R.: Insights into the mechanism of wettability alteration by low-salinity flooding (lsf) in carbonates, Energy Fuels 29(3), 1352-1367 (2015b)
Muecke, T.W.: Formation fines and factors controlling their movement in porous media. J. Pet. Technol., 31 (2) 144-150 (1979)

Mohammadi, H., Gary, J.: Mechanistic modeling of the benefit of combining polymer with low salinity water for enhanced oil recovery. SPE153161, presented at the SPE improved oil recovery symposium in Tulsa, Oklahoma (2012)
Morrow, N., Buckley, J.: Improved oil recovery by low-salinity waterflooding, J. Pet. Technol., 63(05), 106-112 (2011)
Nghiem, L., Dang, C., Nguyen, N., Nguyen, Q., Chen, Z.: Modelling and optimization of low salinity waterflood. In SPE reservoir simulation symposium, Texas (2015)
Omekeh, A.V., Evje, S., Friis, H.A.: Modeling of low salinity effects on sandstone rocks, Int. J. Numer. Anal. Model., 1(1), 1-18 (2013)
Payatakes, A., Rajagopalan, R., Tien, C.: Application of porous media models to the study of deep bed filtration, Can. J. Chem. Eng., 52(6), 722-731 (1974)
Pires, A., Bedrikovetsky, P., Shapiro, A.: Splitting between Thermodynamics and Hydrodynamics in Compositional Modelling. In 9th European Conference on the Mathematics of Oil Recovery (2004)
Pires, A.P., Bedrikovetsky, P.G., Shapiro, A.A.: A splitting technique for analytical modelling of two-phase multicomponent flow in porous media, J. Pet. Sci. Eng., 51(1), 54-67 (2006)
Pope, G.A.: The application of fractional flow theory to enhanced oil recovery, SPE J., (1980)
Pu, H., Xie, X., Yin, P., Morrow, N.: Low-salinity waterflooding and mineral dissolution, Paper SPE 134042 presented at the SPE annual technical confrence and exhibition, Florence, Italy, (2010)
Salathiel, R.: Oil recovery by surface film drainage in mixed-wettability rocks, J. Pet. Technol., 25, 1216-1224 (1973)
Santos, A., Barros, H.: Multiple particle retention mechanisms during filtration in porous media, Environ. Sci. Technol., 44 7 (2010)
Sarkar, A.K., Sharma, M.M.: Fines migration in two-phase flow. J. Pet. Technol., 42 (5): 646-652 (1990)
Shapiro, A. A.: Elliptic equation for random walks: Application to transport in microporous media, Physica A, 375(1), 81-96 (2007)
Sheng, J.: Critical review of low-salinity waterflooding, J. Pet. Sci. Eng., 120, 216-224 (2014)
Smoller, J.: Shock waves and reaction diffusion equations. Springer Science & Business Media, (1994)
Sorbie, K.S.: Polymers-Improved Oil Recovery, Blackie and Son Ltd., Glasgow (1991)
Rezaeidoust, A., Puntervold, T., Strand, S., Austad, T.: Smart water as wettability modifier in carbonate and sandstone: A discussion of similarities/differences in the chemical mechanisms. Energy Fuels 23(9), 4479-4485 (2009)
Rhee, H.-K., Rutherford A., Amundson, N.: On the theory of multicomponent chromatography. Philos. Trans. R. Soc. Lond. Ser. A-Math. Phys. Eng. Sci.: 419-455 (1970)
Rhee, H-K., Aris, R., Amundson, N.R.: Theory and application of hyperbolic systems of quasilinear equations, Vol. 2, Prentice-Hall, Englewood Cliffs (1998)
Rozdestvenskii, B.L., Janenko, N.N.: Systems of quasilinear equations and their applications to gas dynamics, American Mathematical Society, Providence (1983)
Takahashi, S., Kovscek, A.R.: Wettability estimation of low-permeability, siliceous shale using surface forces. J. Pet. Sci. Eng. 75(1), 33-43 (2010)
Tang, G.Q., Morrow, N.R.: Influence of brine composition and fines migration on crude oil/brine/rock interactions and oil recovery. J. Pet. Sci. Eng 24(2), 99-111 (1999)
Yuan, H., and Shapiro, A. A.: Modeling non-Fickian transport and hyperexponential deposition for deep bed filtration, Chem. Eng. J., 162(3), 974-988 (2010)
Whitham, G. B.: Linear and nonlinear waves, John Wiley & Sons, California (2011)
Wu, Y-S., Pruess, K., Witherspoon, P. A:. Displacement of a Newtonian fluid by a non-Newtonian fluid in a porous medium, Transp. Porous Media. 6, 115-142 (1991)

Zhang, Q., Hassanizadeh, M., Karadimitriou, N., Raoof, A., Liu, B., Kleingeld, P., Imhof :Retention and remobilization of colloids during steady-state and transient two-phase flow, Water Resour. Res., 49(12), 8005-8016 (2013)

Zeinijahromi, A., Nguyen, T.K.P., Bedrikovetsky, P.: Mathematical model for fines-migration-assisted waterflooding with induced formation damage. SPE. J. 18(03), 518-533 (2013)

3 Effects of Fines Migration on Low-Salinity Water-Flooding: Analytical Modelling

S. Borazjani, A. Behr, L. Genolet, A. Van Der Net, P. Bedrikovetsky

Journal of Transport in Porous Media, submitted 08/ 2015

Statement of Authorship

Title of Paper	Effects of fines migration on Low-Salinity Water-flooding: analytical modelling
Publication Status	☐ Published ☐ Accepted for Publication ☑ Submitted for Publication ☐ Unpublished and Unsubmitted w ork w ritten in manuscript style
Publication Details	S. Borazjani, A. Behr, L. Genolet, A. Van Der Net, P. Bedrikovetsky. (2015). Effects of fines migration on Low-Salinity Water-flooding: analytical modelling. Submitted to Transport in Porous Media

Principal Author

Name of Principal Author (Candidate)	Sara Borazjani
Contribution to the Paper	Derivation of the mathematical model, Derivation of exact solution, Analysis of results, Writing the manuscript
Overall percentage (%)	80%
Certification:	This paper reports on original research I conducted during the period of my Higher Degree by Research candidature and is not subject to any obligations or contractual agreements with a third party that would constrain its inclusion in this thesis. I am the primary author of this paper.
Signature	Date: 22.11.2015

Co-Author Contributions

By signing the Statement of Authorship, each author certifies that:

i. the candidate's stated contribution to the publication is accurate (as detailed above);

ii. permission is granted for the candidate in include the publication in the thesis; and

iii. the sum of all co-author contributions is equal to 100% less the candidate's stated contribution.

Name of Co-Author	Aron Behr
Contribution to the Paper	Problem formulation, Analysis of results
Signature	on behalf of Aron Behr Date: 19.11.2015

Name of Co-Author	Luis Genolet
Contribution to the Paper	Problem formulation, Analysis of results
Signature	Date: 18.11.2015.

Please cut and paste additional co-

Name of Co-Author	Antje Van Der Net
Contribution to the Paper	Problem formulation, Analysis of results
Signature	Date 18-11-2015

Name of Co-Author	Pavel Bedrikovetsky
Contribution to the Paper	Derivation of exact solution
Signature	Date 18-11-2015

Effects of fines migration on Low-Salinity Water-flooding: analytical modelling

S. Borazjani, A. Behr, L. Genolet, A. Van Der Net, P. Bedrikovetsky

Abstract

We derive the governing system for oil-water flow with varying water composition. The model accounts for wettability alteration, affecting the relative permeability and capillary pressure, and for the fines migration, induced by the salinity variation and causing the permeability damage for water. The aqueous phase composition is lumped into a single salt. The model is simplified for asymptotic cases of low- and high-velocities as well as in large scale approximation. One-dimensional displacement of oil by low-salinity water at large scales allows for self-similar solution. Non-self-similar solution for high-salinity water-flood followed by the low-salinity-slug injection is derived using the splitting method. The effects of wettability alteration and fines migration on oil recovery as two separate physics mechanisms are analysed using the analytical models. For the typical reservoir conditions, the significant effects of both mechanisms are observed.

Keywords: low-salinity water-flooding; fines migration; wettability; non-self-similar solution; analytical model; oil recovery

Nomenclature

A	Specific rock-liquid surface, L^{-1}
A_{132}	Hamekar constant, J
c	Volumetric concentration of particles in water
C	Normalised particle concentration in water
D	Front velocity in (x, t) coordinates
D_μ	Molecular diffusion, L^2T^{-1}
E	Dimensionless product of interfacial tension and contact angle cosine
f	Fractional flow for water
J	Leverett function
k	Absolute permeability, L^2
k_r	Relative permeability
k^*	End point relative permeability
L	Reservoir size, L
n	Corey exponent
U	Overall flow velocity, LT^{-1}
u	Velocity, LT^{-1}
p	Pressure, $ML^{-1}T^{-2}$
p_c	Capillary pressure, $ML^{-1}T^{-2}$
s	Saturation
S_a	Dimensionless concentration of attached particles
S_s	Dimensionless concentration of strained particles
s_{or}	Residual oil saturation

t	Time
V	Front velocity in (x, φ) coordinates
x	Coordinate

Greek letters

α_L	Dispersivity, L
β	Formation damage coefficient
γ	Brine concentration, molL^{-3}
θ	Contact angle
θ_e	Equilibrium contact angle
λ	Filtration coefficient, L^{-1}
Λ	Dimensionless filtration coefficient
μ	Viscosity, ML^{-1}T^{-1}
σ_a	Volumetric concentration of attached particles
σ_{cr}	Maximum volumetric concentration of attached particles
σ_s	Volumetric concentration of strained particles
σ_{wo}	Water-oil interfacial tension, MT^{-2}
τ	Delay time, T
ε_c	Capillary-viscous ratio
ε_θ	Delay dimensionless number for contact angle
ε_σ	Delay dimensionless number for maximum retention
ϕ	Porosity
φ	Potential function
Ω_H	Volume of injected formation water, L^3

Subscripts

H	High salinity water
I	Initial value
J	Injected value
L	Low salinity water
o	Oil
w	Water

1. Introduction

Injection of low-salinity (LS) or “smart” water into oilfields for recovery enhancement has several advantages, such as low cost relative to other Enhanced Oil Recovery techniques, often readily available injectant, negligible environmental impact and easy field process implementation. Planning and designing of the water-flood with alternative composition includes study of numerous physics mechanisms of incremental recovery; the degree of freedom for possible injection compositions highly exceeds those for “normal” flooding (Agbalaka et al. 2009; Austad et al. 2010; Sheng 2014; Brady et al. 2015). The injected water composition strongly affects the success of “smart” water-flooding; it’s optimal choice is extremely sensitive to numerous factors, like formation water and crude composition, mineral contents of the rock, etc. (Tang and Morrow 1999; RezaeiDoust et al. 2009; Morrow and Buckley 2011; Fogden et al. 2011). Therefore, the decision-making on low-salinity or “smart” waterflood must include multi-variant sensitivity study with reliable laboratory-based mathematical modelling.

The corresponding mathematical models have the form of “multi-component polymer flooding” (Braginskaya and Entov 1980; Pope 1980; Lake 1989; Barenblatt et al., 1989; Dahl et al. 1992). One-component “lumped” model, presented by Jerauld et al. 2008, groups all salts in one pseudo-component, referring to salinity as the “ionic strength”. The multi-component models include monovalent and divalent anions with active-mass-law kinetics of their adsorption on clay sites, and cations in brine (Omekeh et al. 2013; Dang et al. 2013; Nghiem et al. 2015). The models also account for dissolution of calcite cement in the brine, and sorption of some oleic components on the rock surface (Al Shalabi et al. 2014a, b; Alexeev et al. 2015).

Planning and design of low-salinity or “smart” waterflood includes fines management (Civan 2007, 2010, 2011). Often the injected water salinity is chosen to avoid fines mobilisation and migration in order to restrict the consequent formation damage (Scheuerman and Bergersen 1990; Pingo-Almada et al. 2013). However, the fines-induced permeability damage decelerates the injected water resulting in sweep efficiency enhancement (Zeinijahromi et al. 2013). Effective fines migration management with varying injected water composition is based on mathematical modelling. The equations for two-phase flow with fines migration have been presented for homogeneous reservoirs in large scale approximation (Yuan and Shapiro 2011; Zeinijahromi et al. 2013). Their averaging in layer-cake formations yields pseudo-relative permeability equations (Lemon et al. 2011). However, to the best of our knowledge, the basic equations for low-salinity (LS) water-flooding accounting for fines mobilisation, migration and straining and the local non-equilibrium and dissipative effects are not available in the literature.

In the present work, we derive equations merging two-phase immiscible flow model with the “lumped” salt concentration in water, with the model of fines mobilization, migration and aqueous phase permeability impairment. The dissipative effects include non-equilibrium ion exchange with wettability alteration and fines release, capillary pressure, dispersion and deep bed filtration. For the case where the initial concentration of attached fines is below its maximum value, we proposed the extrapolation of the maximum retained function into the area where particle mobilisation does not occur, in order to avoid working with two different

systems of equations in different (x,t)-domains. In reservoir scale approximation, the dissipative and non-equilibrium effects are neglected, and the governing system is simplified up to the fractional flow model. The 1-D LS water-flooding problems allow for exact solutions. The solution for secondary recovery with continuous injection of low-salinity water is self-similar. The exact solution for tertiary recovery with "normal" waterflood followed by the injection of low-salinity water slug with high-salinity (HS) chase drive is non-self-similar; the solution is obtained by the splitting method. The exact solution provides explicit formulae for concentration and saturation profiles, front velocities, breakthrough concentration and the recovery factor. The analytical model allows for sensitivity analysis of the impact of two separate physics factors, i.e. contact angle alteration and fines migration, on incremental oil recovery.

The structure of the paper is as follows. The governing equations including large scale approximation are derived in Section 2, Appendixes A, B and C. Derivations of exact solutions corresponding to secondary and tertiary LS water-flooding are presented in Section 3 and Appendix D. Section 4 contains the results of analytical modelling and analysis of incremental oil recovery with LS water-flooding applications.

2. Governing equations

The basic equations for two-phase flow with varying salinity and induced fines mobilisation and straining are presented in its dimensionless form in Section 2.1 along with the estimates of the dimensionless groups. The detailed derivations with formulation of initial and boundary conditions are shown in Appendixes A and B. The large-scale approximation of the governing system is presented in Section 2.2 and Appendix C.

2.1. Dimensionless governing system

Let us discuss the governing equations for oil displacement by low-salinity water. The overall molar concentration of cations is represented by the equivalent sodium ion concentration γ (so-called ionic strength). Two phases are assumed to be immiscible and incompressible (see Fig.1). Variation of small sodium concentration does not change the aqueous phase density. Other assumptions of the model include constant oil viscosity; relative phase permeabilities depend on the contact angle; the equilibrium contact angle depends on salinity; porosity is constant. It is also assumed that the dispersivity coefficients for salt and fines particles are equal (Geiger et al. 2012). Small fines concentrations c yield significant permeability decline but does not affect water viscosity and density (Muecke, 1979, Khilar and Fogler, 1998), which is assumed too.

Fig. 1 shows attached and strained fine particles, retained in the rock, and the mobilised fines suspended in aqueous phase (with concentrations σ_a, σ_s and c, respectively). The attached particles are mobilised into the suspension with the following straining in thin pore throats. The attached fines coat the grain surfaces and pore walls. So, the particle detachment by drag force yields non-significant increase in porosity and permeability. The significant permeability reduction by small amount of suspended mobilised particles is explained by the form of clay fines (thin large plates of kaolinite and shells of chlorite, long illite fines), where

a small-volume fine can strain even a large pore throat (Muecke, 1979, Lever and Dawe, 1984, Sarkar and Sharma, 1990). So, the pore structure can be alternated by straining of the low-concentration fines suspension. Therefore, it is assumed that fines mobilisation does not change water viscosity, but the water relative permeability and capillary pressure are strained-concentration dependent. Fines are strained by the rock fraction where the aqueous suspension flows, so relative permeability of water depends on the strained fine concentration and oil relative permeability is independent of the concentration of strained fines. The mobilised fine particles are assumed to be water-wet and transported by the aqueous phase (Muecke, 1979, Yuan and Shapiro, 2011).

The mechanical equilibrium of particles on the rock surface is determined by the torques balance for drag, lifting, electrostatic and gravitational forces, i.e. the total of torques is equal to zero (Khilar and Fogler, 1998; Bradford et al., 2006 and 2011). For each particle, the torque balance determines, whether this particle is mobilised or remains attached for a given force values. So, the torque balance determines the amount of attached fines, which is called the critical retention function (Bedrikovetsky et al. 2011, 2012). Since the above mentioned forces depend on velocity and salinity, the critical retention concentration is a function of velocity and salinity. Under constant flow velocity, the attached concentration is a salinity function only. However, it takes some time for salt to diffuse from the particle-rock contact space to the bulk solution in the pore centre, so the attached concentration takes values of the maximum retention function with some delay (Mahani et al. 2015a, b).

Sarkar and Sharma 1990 investigated the permeability damage with injection of low salinity water. The lower formation damage under the presence of polar residual oil or at the presence of non-polar oil, if compared with a single-phase flow is observed. The phenomenon is attributed to incomplete accessibility of water to rock surface in the case of partial wettability by oil. Fig. 2 shows the fractions of the overall solid-liquid interface A accessible to water A_w and oil A_o, which is one of the schemas for oil and water distribution in mixed-wet rocks (Salathiel 1973; Kovscek et al. 1993; Kim and Kovscek 2013). The amount of fines attached to area A_o is not affected by salinity, while that on the A_w-surface depends on salinity (Schembre and Kovscek 2005; Schembre et al. 2006, Zeinijahromi et al. 2013). Both fractions are the saturation functions. So, the fines detachment occurs due to changing both salinity and water saturation.

The model also assumes that the drag force acting on a particle from the flowing oil is not enough for its mobilization.

The overall specific rock-liquid surface is a total of those accessible to water and oil:

$$A = A_w(s,\theta) + A_o(s,\theta) \tag{1}$$

The higher is water saturation and the lower is the contact angle, the higher is the accessible to water surface A_w. Consequently, the surface A_o is monotonically decreasing function of s and monotonically increasing function of θ.

Therefore, the overall attached fine particle concentration in the rock is a total of those attached to water-accessible and oil-accessible surfaces; the corresponding fractions depend on phase saturations and wettability. The attached fines can be mobilized by drag forces exerting from water with decreasing salinity, resulting in weakening of the attractive

electrostatic particle-grain forces (Khilar and Fogler 1998; Israelachvili 2011). Xxx For the case of instant fine particles release, the attached concentration is determined by the torque balance of forces exerting the particle attached to the water-accessible surface A_w and is called the maximum retention function of water composition (Bradford et al. 2006, 2011). The plot of the function is given in Fig. 3. For the points below the maximum retention curve, the attaching torques of electrostatic and gravitational forces exceed those for detaching drag and lifting forces. The initial point corresponds to "under-saturated" state, i.e. it takes the salinity decrease from γ_I to γ_{cr} in order to start the fine particle mobilisation. Therefore, the path corresponds to horizontal line without fines release followed by the curve with the release of some amount of fines, denoted as σ_s. The critical salinity is determined as a minimum salinity where fines are released by the flow:

$$\sigma_{cr}(\gamma_{cr}) = \sigma_{a0} \tag{2}$$

For the case of instant fines release, the attached concentration is equal to the maximum retention function of the rock, where the attached particles on the rock surface accessible to water can be removed, plus the attached particles on the accessible to oil surface that cannot be removed (Yuan and Shapiro 2011; Zeinijahromi et al. 2013):

$$\sigma_a(s,\gamma,\theta) = \sigma_{cr}(\gamma)\frac{A_w(s,\theta)}{A} + \sigma_{a0}\frac{A - A_w(s,\theta)}{A} \tag{3}$$

Let us introduce the following dimensionless co-ordinates and parameters into the system of dimensional equations derived in Appendix A:

$$x \to \frac{x}{L}, \quad t \to \frac{1}{\phi L}\int_0^t U(t)dt, \; \mathrm{E}(\gamma,\theta) = \frac{\sigma_{wo}(\gamma)\cos\theta}{\sigma_{wo}(\gamma_I)\cos\theta(\gamma_I)}, \; \varepsilon_c = \frac{\sigma_{wo}(\gamma_I)\cos\theta(\gamma_I)\sqrt{k\phi}}{\mu_o UL}; \tag{4}$$
$$\varepsilon_D = \frac{\alpha_L}{L}, \varepsilon_\sigma = \frac{U\tau_\sigma}{\phi L}, \; \varepsilon_\theta = \frac{U\tau_\theta}{\phi L}, \Lambda = \lambda L, \; S_a = \frac{\sigma_a}{\sigma_{a0}}, \quad S_s = \frac{\sigma_s}{\sigma_{a0}}, \quad C = \frac{\phi c}{\sigma_{a0}}$$

Substitution of the dimensionless parameters (4) along with expression (A-12) into the governing system (A-1,A-5, A-6-A-9) yields

$$\frac{\partial s}{\partial t} + \frac{\partial f(s,\theta,S_s)}{\partial x} = -\varepsilon_c \frac{\partial}{\partial x}\left[k_{ro}(s,\theta) f(s,\theta,S_s) \frac{\partial\left(\mathrm{E}(\gamma,\theta) J(s,\gamma,S_s)\right)}{\partial x} \right] \tag{5}$$

$$\frac{\partial \gamma s}{\partial t} + \frac{\partial \gamma f(s,\theta,S_s)}{\partial x} = -\varepsilon_c \frac{\partial}{\partial x}\left[\gamma k_{ro}(s,\theta) f(s,\theta,S_s) \frac{\partial\left(\mathrm{E}(\gamma,\theta) J(s,\gamma,S_s)\right)}{\partial x} \right] + \varepsilon_D \frac{\partial}{\partial x}\left(s\frac{\partial \gamma}{\partial x} \right) \tag{6}$$

$$\varepsilon_\sigma \frac{\partial S_a}{\partial t} = S_{cr}(\gamma)\frac{A_w(s,\theta)}{A} + S_{a0}\frac{A - A_w(s,\theta)}{A} - S_a \tag{7}$$

$$\varepsilon_\theta \frac{\partial \theta}{\partial t} = \theta_e(\gamma) - \theta \tag{8}$$

$$\frac{\partial S_s}{\partial t} = \Lambda(\gamma, S_s) C\left[f(s,\theta,S_s) + \varepsilon_c \, k_{ro}(s,\theta) f(s,\theta,S_s) \frac{\partial\left(\mathrm{E}(\gamma,\theta) J(s,\gamma,S_s)\right)}{\partial x} \right] \tag{9}$$

$$\frac{\partial}{\partial t}\left(sC+S_a+S_s\right)+\frac{\partial Cf}{\partial x}=-\varepsilon_c\frac{\partial}{\partial x}\left(Ck_{ro}(s,\theta)f(s,\theta,S_s)\frac{\partial\left(\mathrm{E}(\gamma,\theta)J(s,\gamma,S_s)\right)}{\partial x}\right)+\varepsilon_D\frac{\partial}{\partial x}\left(s\frac{\partial C}{\partial x}\right) \tag{10}$$

System of 6 equations (5-10) determines 6 unknowns: saturation s, salinity γ, attached fines concentration S_a, concentration of strained fines S_s, suspended fines concentration C and contact angle θ.

The system contains the following dimensionless groups: capillary-viscous ratio ε_c, Schmidt's number $\varepsilon_D=\alpha_L/L$ (inverse to Peclet's number), filtration coefficient $\Lambda=\lambda L$ and two delay numbers ε_θ and ε_σ. The dimensionless groups correspond to different dissipative processes. Capillary-viscous ratio and Schmidt's number correspond to "diffusion" of variables s, γ and C. The delay numbers corresponds to delay in establishing the equilibrium contact angle and the maximum retention values for attached fines concentration.

Let us calculate the dimensionless groups (4) for the laboratory coreflood, described further in Section 4. The properties of rock and fluids are: L=0.08 m, k=0.135×10^{-12} m^2, ϕ=0.13, U=1.4×10^{-5} m/s, μ_o=0.11 Pas, μ_w=10^{-3} Pas, α_L=4.1×10^{-6}m, λ=100 1/m, σ_{wo}=0.04 N/m, D_μ=10^{-12} m^2/s, $\theta=\pi/6$, τ_θ=100 s. The dimensionless groups (4) are: ε_c=0.04; ε_D=0.00005; ε_θ=0.13; ε_σ=0.002; Λ=8. Dissipative numbers ε_n, $n=c$, D, θ and σ, are significantly smaller than one, while the dimensionless filtration coefficient highly exceeds unit, i.e. large scale approximation conditions are fulfilled, (see Appendix C). It means that the laboratory coreflood data must be matched by the simple model (11-13) rather than by the detailed model (5-10).

2.2. Large scale approximation

Approximations of the system (5-10) for the cases of high and low velocities of laboratory corefloods and large reservoir scale are presented in Appendix C. In this Section, we present equations for large scale approximation (Bedrikovetsky 1993; Hussain et al. 2013):

$$\frac{\partial s}{\partial t}+\frac{\partial f(s,\gamma)}{\partial x}=0 \tag{11}$$

$$S_s=\left(S_{a0}-S_{cr}(\gamma)\right)\frac{A_w(s,\gamma)}{A},\ f(s,\gamma)=f(s,\gamma,S_s) \tag{12}$$

$$\frac{\partial \gamma s}{\partial t}+\frac{\partial \gamma f(s,\gamma)}{\partial x}=0 \tag{13}$$

It corresponds to water transport by pressure gradient only, advective salt transfer, equilibrium attached concentration that is equal to maximum retention function and instant straining of the released fines.

The governing system (11-13) is 2×2 hyperbolic system of quasi linear equations for two variables s and γ (Courant and Friedrichs 1976).

The initial conditions correspond to reservoir saturation and salinity of formation water before the injection:

$$t=0:\ s=s_J,\ \gamma=\gamma_J \tag{14}$$

Entrance boundary conditions for continuous low-salinity water injection are fixed fraction of injected water and injected salt concentration:

$$x=0:\ f(s,\gamma_J)=1,\ \gamma=\gamma_J \tag{15}$$

For formation water injection followed by the injection of low-salinity-water slug with high-salinity drive, the volume of injected formation water Ω_H is used to dimensionalise co-ordinates x and t in (4); the dimensionless co-ordinate of the core outlet (production well row) becomes $\phi L/\Omega_H$. The inlet boundary conditions are:

$$x=0:\ f(s,\gamma_J)=1,\ \gamma=\begin{cases}\gamma_I & 0<t<1\\ \gamma_J & 1<t<t_s\\ \gamma_I & t_s<t<\infty\end{cases} \tag{16}$$

3. Analytical models for Low-Sal Waterflood with fines migration

In this Section we present exact solutions for fines-assisted low-salinity waterflooding in large scale approximation (11-13). The splitting procedure is used for the exact integration (Appendix D). Secondary recovery corresponds to continuous injection of low-salinity water and self-similar solution (Section 3.1). Tertiary recovery follows "normal" waterflooding and the solution is non-self-similar (Section 3.2).

3.1. Self-similar solutions for continuous injection of low-salinity water

The solutions of continuous injection problem (14, 15) for system (11-13) are well known (Pope 1980; Lake 1989). The solutions are self-similar and depend on the group x/t. Fig.4a presents the graphical solution. Points 6, 2 and 4 are tangent points of straight lines I-6, 0-2 and 0-4 to the fractional flow curves $\gamma=\gamma_I$, $\gamma=\gamma_J$. The corresponding slopes are the speeds of the jumps, where the points ahead and behind the jumps are located on those straight lines I-6, 0-2 and 0-4.

The solution corresponds to the path in (s, f)-plane consisting of rarefaction wave from the saturation s_L^0 to point 2, γ-jump from 2 to 3 and s-jump from 3 to s_I:

$$s_3<s_6:\ s_L^0-2\to 3\to I \tag{17}$$

Fig. 4b shows the saturation profiles for injection of formation water (solid curve), low salinity water (dotted curve) and medium salinity water (dashed curve). The salinity profile is a step-function, given by a γ-jump with velocity D_2. Water-cut history is shown in Fig. 4c. The graphic-analytical technique for solution is available from Lake, 1989 and Bedrikovetsky, 1993.

If the intersection point 5 is located above the point 6, the corresponding path is

$$s_5>s_6:\quad s_L^0-4\to 5-6\to I \tag{18}$$

Figs. 4b and c show profiles of saturation and water-cut history for normal water-flooding (solid curves), intermediate-salinity flood (dashed curves) and low-salinity water-flooding (dotted curves). As it follows from the curve shapes, for 1-D continuous water injection, low

salinity water-flooding results in later breakthrough if compared with formation water injection; it also causes decreased water-cut during production of oil-water bank and during a short period after the breakthrough of the injected water. It also results in lower oil residual at the late stage of the water-flooding. Oil production with intermediate-salinity water injection coincides with normal flooding from the beginning of injection until some moment after water breakthrough. Afterwards, normal waterf-lood exhibits higher water-cut and higher residual oil.

3.2. Non-self-similar solutions for displacement of oil by formation water followed by low-salinity water slug

Let us discuss displacement of oil by HS water followed by injection of LS water slug with HS-water chase drive. The solution of the large-scale system (11-13) subject to boundary conditions (16) is non-self-similar. The corresponding interactions of saturation- and concentration-waves have been investigated in Barenblatt et al. 1989, Entov and Zazovskii 1989, Bedrikovetsky 1993. The exact solution of the problem (11-13, 14, 16) is derived in Appendix D using the splitting method. The method uses the stream-function (Lagrangian co-ordinate) $\varphi(x,t)$ as an independent variable in the governing system (11-13) instead of time t (eq D-2). The corresponding mapping K is presented in Fig. 5. It transforms mass balance for water(11) into conservation law (D-4). The graphical solution of the slug problem (D-9) is presented in the plane of fractional flow curves (s,f) and in the plane of density and flux (U,F) of conservation law (D-4) in Figs. 6 a and b, respectively. The corresponding characteristics and front trajectories are presented in planes (x,φ) and (x,t) (Figs. 7 and 8).

The solution of eq (D-6) subject to initial and boundary conditions (D-8) and (D-9) is:

$$\gamma(\frac{\varphi}{x}) = \begin{cases} \gamma_I, & -s_I < \frac{\varphi}{x} < 0 \\ \gamma_I, & 0 < x < \infty, 0 < \varphi < 1 \\ \gamma_J, & 0 < x < \infty, 1 < \varphi < t_s \\ \gamma_I, & 0 < x < \infty, t_s < \varphi < \infty \end{cases} \tag{19}$$

The solution $s(x,\varphi)$ of eq (D-4) subject to initial and boundary conditions (D-8), (D-9) is discontinuous. The front trajectories $\varphi_L(x)$ and $\varphi_H(x)$, where the jumps $\gamma_J \to \gamma_I$ and $\gamma_I \to \gamma_J$ occur, respectively, are presented in plane (x, φ) (Fig. 7 a and b). Continuous solutions $s(x, \varphi)$ in zones between the shocks are obtained by method of characteristics and are given by rarefaction and simple waves (Table 1). The geometric procedure to find points 2, 3, …6 is shown in Fig. 6a and b.

The rarefaction wave s^0_H-6$\to I$ propagates from point x=0, t=0 (zones I and II in Table 1). The characteristic lines transport the values from s^0_H to s_4 until the shock trajectory φ=0, where the jump $\gamma_J \to \gamma_I$ occurs. The corresponding points above the front vary from 5 to 2. The boundary value of saturation s^0_L appear for φ>1 due to change of salinity. The corresponding rarefaction s^0_L-5 connects the points along the curve $\gamma=\gamma_J$ in Fig. 7 b (zones III and IV). The simple wave propagates the characteristic lines with points varying from 5 to 2 in zone V. Point 2 is held above the line φ=1+0, $x>x_B$. As it follows from Fig. 7 b, point 3 is held below

this line at φ=1-0, $x>x_B$. Trajectory $\varphi=\varphi_{L2}(x)$ separates zone II of rarefaction wave 4-6 from zone VI with constant state 3. The trajectory is defined by condition on characteristic line

$$\frac{\varphi}{x} = F_U'\left(U, \gamma_I\right) \tag{20}$$

and the Hugoniot-Rankine condition that corresponds to conservation law (D-4):

$$\frac{d\varphi_{L2}}{dx} = \frac{F^- - F_3}{U^- - U_3} \tag{21}$$

Integration of eq (D-4) along the contour (0, 0)→(x_B, t_B)→(x_{L2}, t_{L2})→(0, 0) results in first integral for ordinary differential equation (21), defining the trajectory $x=x_{L2}(\varphi)$:

$$x_{L2}\left(\varphi\right) = \frac{\left(F_4 - F_3\right)\left(\frac{1}{V_4}\right) - U_4 + U_3}{\left(\left(F\left(\varphi/x\right) - F_3\right) + F_U'\left(U\left(\varphi/x\right), \gamma_I\right)\left(U_3 - U\left(\varphi/x\right)\right)\right)} \tag{22}$$

The intersection between front trajectory $\varphi=\varphi_{L2}(x)$ and line $\varphi=-s_I x$ corresponds to point 6 behind the shock. It gives the intersection moment: $\varphi=\varphi_F$. The jump 3→*I* appears after the intersection.

Salinity jump $\gamma_I \rightarrow \gamma_J$ occurs along the front $\varphi=t_s$. Saturation jumps occur along this shock with conservation of the flux $F(U,\gamma)$. The saturation values $s(t_s+0, x)$ propagate in zones VII, X and VIII along the characteristic lines in simple waves. The corresponding formulae are presented in Table 1. Finally, solution for γ and s is obtained for the overall domain $x>0$, $-s_I<\varphi/x<\infty$.

Calculating $t(x,\varphi)$ for each point of the domain by formula (D-3) maps the solution into variables (x, t). Formulae in Table 2 are obtained from those in Table 1 by transfer (D-3). Here points (x, t) and (x', t') in zone V are located on the same characteristic line. Points (x, t) and (x'', t'') in zone X are also located on the same characteristic line. The front $x_{L1}(\varphi)$ is mapped into the following trajectory $x_{L1}(t)$, determined parametrically:

$$x_{L1}\left(t\right) = \frac{\partial f\left(s^+, \gamma_I\right)}{\partial s} t, \;\; t = \frac{1}{\Delta\left(s^+, \gamma_I\right)}, \; s^+ = s^+\left(x_{L1}\left(t\right)\right) \tag{23}$$

here

$$\Delta\left(s, \gamma\right) = f\left(s, \gamma\right) - s f_s'\left(s, \gamma\right) \tag{24}$$

In Fig. 6 a, $AO=\Delta(s^+,\gamma_I)$ and $BO=\Delta(s^+,\gamma_I)/f_s'(s^+,\gamma_I)$. It allows for graphical expression of the dependency $x_{L1}=x_{L1}(t)$: point *A* is determined by $AO=1/t$ for any arbitrary t; point *B* is determined by tangent line A-s^+ to fractional flow curve $\gamma=\gamma_I$; the front co-ordinate x_{L1} is determined by $BO=1/x_{L1}(t)$. Trajectories $x_{L2}(t)$, $x_{H1}(t)$ and $x_{H2}(t)$ are determined in the same way.

Fig. 8 presents trajectories of saturation and concentration shocks in (x, t)-plane. The displacement zone consists of the following reference patterns:

0– Unperturbed zone of initial water saturation;

I– Zone with residual immobile oil and injected formation water;

II– Zone of oil flow together with injected formation water, saturation changes from s_H^0 to s_6 at the displacement front;

III– Zone with residual immobile oil and injected low-salinity water;

IV– Zone with low-mobility oil and injected low-salinity water, which substitutes zone I during the displacement;

V– Zone with mobile oil and injected low-salinity water;

VI – Oil-water bank with saturation s_3;

VII– Zone of immobile oil with saturation s^0_L;

VIII– Zone of immobile oil with saturation varying from s^0_L to s^0_H;

IX– Zone of immobile oil with saturation s^0_H;

X– Zone with injected high-salinity water, which substitutes zone V during the displacement;

XI– Oil-water bank with saturation s_4.

Implicit formulae for front trajectories (23) and straight lines for characteristics allow explicit calculation of the recovery factor

$$RF(t) = \frac{\langle s \rangle (x,t) - s_I}{1 - s_I} \tag{25}$$

Let us derive formula for average water saturation $<s>(x, t)$ at the moment t_2. Integrate eq (11) by rectangular, bounded by the contour $(0,0)\to(0,t_2)\to(\phi L/\Omega_H, t_2)\to(\phi L/\Omega_H,0)\to(0,0)$, i.e. during LS water injection. Following Green's formula, the mass integral is equal to the integral of mass flux fdt-sdx along this contour. The integral over the side $(0, t_2)\to(\phi L/\Omega_H, t_2)$ is equal to $<s>(t_2)\times \phi L/\Omega_H$. The integral over the interval $(0,0)\to(0,t_2)$ is equal to t_2 and the integral over $(\phi L/\Omega_H,0) \to(0,0)$ is equal to $s_I\times\phi L/\Omega_H$. Finally, the average water saturation at the moment t_2 is (see Fig. 8 (a)):

$$\langle s \rangle (t_2) = \frac{t_2 + s_I \left(\dfrac{\phi L}{\Omega_H} \right)}{\dfrac{\phi L}{\Omega_H}} \tag{26}$$

Average saturation (26) is substituted into formula (25) for recovery factor calculation. Similarly, the recovery factor is calculated for any arbitrary moment *t*.

4. Results

In this Section, the water-flood cases of injection of formation and low salinity waters are compared. The effects of low-salinity water on relative permeability and on fines mobilisation and straining are treated together in the mathematical model (11-13). However, those are separate physics mechanisms that act independently. The effect of low-salinity on contact angle reduction is expressed in eq (A-2) by reduction of relative permeability for water, decrease of residual oil saturation and some increase in relative permeability for oil. It is expressed by the contact angle-dependency of both relative permeabilities on contact angle (eq (A-2)), which in turn depends on salinity ($\theta=\theta_e(\gamma)$). The above mechanisms yield the reduction in fractional flow for water and increase of the fractional flow for oil, leading to enhanced oil recovery.

As it is explained at the beginning of Section 2.1, fine particle mobilisation is triggered by weakening of electrostatic particle-grain attraction, which decreases as salinity decreases. Fines mobilisation and migration follow by particle straining in thin pore throats. Since the particles are transported by water, it results in declining of relative permeability for water, see eq (A-3). The main effect of induced fines migration is the reduction of relative permeability for water and deceleration of the aqueous phase. However, sweep on the micro scale can increase, resulting in the reduction of the residual oil saturation. Those effects also cause reduction of fractional flow function for water and consequent oil recovery enhancement.

A separate effect of salinity on relative permeability, where the fines are not mobilised corresponds to $\beta=0$ in (A-3). A separate effect of fines-induced formation damage, where the contact angle remains constant with salinity decrease, corresponds to salinity-independent relative permeability for water $k^{/}_{rw}$ in eq (A-3). The effects of fractional flow reduction on 1D displacement of oil are described at the end of Section 3.1.

The maximum retention function is calculated for poly-layers of mono-sized particles in cylindrical capillary (see Bedrikovetsky et al. 2011, 2012). The sandstone rock with kaolinite fines attached to the grain surfaces is assumed. The typical values of physics properties are: for salinity equal to 0.5 *M NaCl* are Hamaker constant A_{132}= 9.5561E-21 J, electrostatic potentials for quartz-brine and kaolinite brine are -19.1 and -10.7 mV, respectively, and for 0.1 M *NaCl*, Hamaker constant A_{132}=9.5938E-21 J, electrostatic potentials for quartz-brine and kaolinite brine are -34.9 and -23.0 mV, respectively, mean particle size r_s=3 μm, drag factor ω=60 ; formation damage coefficient β=1000 (Khilar and Fogler 1998; Israelachvili 2010). The plot is given by a bold curve in Fig. 3; the dashed curve $\sigma_s(\gamma)$ corresponds to the amount of strained fines that have been captured by size exclusion mechanism. The curve $\sigma_s(\gamma)$ is approximated by a positive function for $\gamma_{cr}<\gamma<\gamma_i$, where a positive but negligibly small amounts of fines are released for salinities above the critical value, i.e. the fines release occurs at any salinity below the initial salinity. So, the governing system (5-10) can be used in the overall interval for salinity variation.

Relative permeability $k^{/}_r(s,\gamma)$ is expressed by Corey's formulae. The typical values for the relative permeability at HS and LS waters are taken from Lager et al. 2007, 2008, 2011 and

are presented in Table 3. The fractions of rock surface accessible to water and oil have been calculated from the porous space model of a bundle of parallel capillaries. The values of formation damage parameters follow the works by Bradford et al., 2006, 2011; Civan, 2011; Hussain et al., 2013. The same Corey coefficients are used for LS water for the cases of wettability effect only and for both effects. For the case of LS water with fines migration effect only, Corey's coefficients for HS are utilized. At the cases of HS and LS water accounting for wettability effect only, the formation damage coefficient is equal zero, β=0.

Fractional flow curves for HS and three above mentioned LS cases are shown in Fig. 9. Water-cut and recovery factors as calculated from the analytical model (11-13) subject to initial and boundary condition (14-15) are presented in Figs. 10 a, b. Blue fractional flow curve is located below the black curve, i.e. the impact of fines-induced formation damage is higher than that of wettability alteration. Fines straining does not alternate the residual oil saturation, so blue curve in Fig. 10 b tends to green curve at large times. Wettability variation does alternate the residual oil, so the black and red curves converge at large times. If compared with HS flood, LS flood yields 0.35 incremental oil after 1 PVI due to both effects. Separately, the wettability alteration and fines migration effects after 1 PVI bring 0.14 and 0.21 of incremental oil, respectively.

The results of recovery factor calculations for different volumes of HS injected before the LS water is given in Fig. 11. The trajectories of concentration and saturation fronts in plane (x, t) are shown in Fig. 8a. Here time and linear coordinate are dimensionalised using the volume Ω_H of HS water injected, i.e. $x \to \phi x/\Omega_H$, $t \to ut/\Omega_H$. The dimensionless moment of switching from HS to LS is constant and equal to unity, while the dimensionless coordinate of the production line $x=\phi L/\Omega_H$ depends on the volume Ω_H. With increasing of the volume Ω_H of injected HS water, the solution in (x, t)-plane is intact, while the line of production wells $x=\phi L/\Omega_H$ moves to the left.

Fig. 8a shows that for a small volume Ω_H of injected HS water, that $x_F<\phi L/\Omega_H$, the bank of formation water and oil with composition 3 arrives at the production row after water breakthrough; the injected LS water arrives after the bank production with water-cut 2 (Fig. 6a), which will monotonically rise, i.e. the solution asymptotically tends to that for continuous injection of LS water. For larger HS volumes, the arrival time, water-cut at the arrival and its further growth coincide with that of continuous HS waterflood; the water-cut decrease occurs after the arrival of LS water front. For so large HS volume that $\phi L/\Omega_H$ is equal to maximum coordinate of zone I, the production fully coincide with HS flood exactly until the 100%-water-cut. LS water arrives at that moment, and water-cut falls up to the point 5 with further increase during oil production with LS water.

Fig. 11 presents the recovery curves for different volumes of HS injected before the LS waterflood. The higher is the injected HS volume, the lower is the recovery. At high HS volumes, it tends to recovery at HS water injection. As low volumes of injected HS water, the recovery tends to that of continuous LS flood from the very beginning.

Let us compare a specific contribution of wettability alteration and fines-migration to oil recovery. The data for calculations are presented in Table 3. For both effects, if compared with "normal" 1-D waterflooding, injection of water with salinity with typical conditions results in increase of the water-less production period from 0.34 to 0.48, decrease of water-

cut from 0.83 to 0.41 before the salinity front breakthrough and increase of recovery factor after 1 PVI from 0.47 to 0.82.

For wettability alteration effect only (the case of zero formation damage coefficient), if compared with “normal” 1-D waterflooding, injection of low salinity water results in increase of the water-less production period from 0.24 to 0.39, decrease of water-cut from 0.83 to 0.58 before the salinity front breakthrough and increase of recovery factor after 1 PVI from 0.47 to 0.62.

For the effect of fines-migration only (water relative permeability in the nominator in eq (A-3)) is independent of salinity, if compared with “normal” 1-D water-flooding, injection of low salinity water results in increase of the water-less production period from 0.34 to 0.43, decrease of water-cut from 0.83 to 0.42 before the salinity front breakthrough, increase of recovery factor after 1 PVI from 0.47 to 0.68.

5. Discussions

Impact of wettability alternation and fines migration on LS water-flood The distinguished physics effects of low-salinity water-flood are wettability alteration and fines-migration-induced formation damage, both triggered by the difference between salinities of formation and injected waters. In order to compare low-salinity and “normal” water-flooding, we discuss water-flood by formation water, where no salinity alteration occurs. So, the term “high salinity” in this paper assumes equality of connate and injected HS waters.

The explicit analytical formulae for sequential injection of HS slug, LS slug and HS drive presented in Tables 2 and 3 can be implemented in Excel or MatLab and used for sensitivity study and low-salinity EOR screening (Excel 2010; MATLAB 2015).

The 1D analytical modelling, presented in Section 4 shows that for typical values of wettability alteration and induced formation damage by application of LS water, either effect can make a major contribution to incremental oil recovery if compared with HS water. For example, for typical conditions of secondary low-salinity waterflood (Table 3), the incremental recovery after 1 PVI due to collective effects of wettability alteration and fines migration is 0.35, while for each effect separately the incremental recovery is 0.14 and 0.25, respectively. For tertiary low-salinity-slug injection with wettability alteration effect only, the incremental recovery after 1.5 PVI is 0.22, 0.20 and 0.09, with secondary injection of 0.1, 0.3 and 1.0 PVI of HS water.

The effects of wettability alternation and fines migration affect also 2D LS water-flooding. The wettability alternation causes the reduction in residual oil and more complete oil displacement from the swept areas. The induced fines migration and consequent permeability damage in swept area decrease water flux and diverts it into unswept zones, yielding sweep efficiency enhancement. The 2D effects of sweep increase with LS water injection have been discussed in details by Lemon et al., 2011 and Zeinijahromi et al., 2013. The derived analytical model can be used for 3D reservoir simulation in stream-line or front-tracking modes (Oladyshkin, Panfilov, 2007; Holden, Risebro, 2013).

Roles of dissipative and non-equilibrium effects The model for low-salinity water-flooding accounting for wettability alterations and fines migration (5-10) accounts for "vanishing viscosity" effects of capillary pressure and dispersivity and non-equilibrium fines

mobilisation, migration and straining along with the contact-angle-alteration kinetics. The capillary pressure effect smooths the saturation shocks, while other effects of dispersivity and non-equilibrium smooth the concentration shocks.

Thickness Δ of smoothed zones for the saturation-concentration shocks is determined from the travelling wave solutions (Dujin and Knabner 1992; Dujin et al. 1997). A travelling wave converges to each shock with the dissipative dimensionless groups tending to zero. The condition $\Delta << L$ is more precise estimate of large scale approximation than inequalities for small dimensionless groups ε_c, ε_D, ε_θ, ε_σ, $\Lambda^{-1} << 1$ (Bedrikovetsky 1993).

Let us consider determination of relative permeabilities from low salinity core flood data measuring rates of two phases and pressure drop across the core. In large scale approximation, where six dimensionless parameters for the long cores are significantly smaller than one, the exact recalculation is based on self-similarity of solution (see eq (17) or (18)) using the generalised Weldge-JBN method for system (11-13) (Bedrikovetsky, 1993; Jerald et al., 2008). If the dimensionless numbers ε_c, ε_D, ε_σ, ε_θ and $1/\Lambda$ are not small, the dissipative and non-equilibrium terms cannot be neglected. In this case, the overall system (5-10) must be solved numerically, and the relative permeabilities are determined by tuning of the laboratory data into the mathematical model, using the iterative optimization algorithms. However the dissipative and non-equilibrium parameters in this case are not known (capillary pressure, delay times, dispersivity and contact angle). If compared with the generalised Weldge-JBN method, using the general model (5-10) increases the uncertainty in determining of the unique tuning data, i.e. in order to determine the same level of uncertainty as with Weldge-JBN method, the Leverett function and delay times must be known.

Recently obtained semi-analytical and exact solutions for two-phase multi-component systems with dissipation and non-equilibrium simplify the solution of inverse problem for the general system (Schmid et al., 2010, 2013; Geiger et al., 2012; Borazjani et al., 2015).

Example in Section 2.1 shows that the reservoir-scale conditions can be reached during laboratory coreflooding. So, the experimental data can be matched using simpler model (11-13) rather than the detailed system of equations (5-10). In this case, the modelling results are independent of the capillary pressure, dispersion, delay times for contact angle and fines detachment and the filtration coefficient. It significantly reduces the number of tuning parameters. The above advantages encourage reaching the conditions of large scale approximation by selecting proper velocity, oil viscosity, core length, etc in the laboratory tests.

More complex mathematical models More sophisticated model rather than that of single-salinity is the multi-component ionic exchange model, which reflects the effect of different cations on rock surface and wettability alteration during their adsorption on clay sites (Omekeh et al. 2013; Nesterov et al. 2015).

The wettability alteration results in s_{or}- and k_{rw}-decrease (Omekeh et al. 2013; Dang et al. 2013; Nghiem et al. 2015), leading to displacement coefficient enhancement, like it is the case for chemical EOR (Lake 1989). Fines-migration-induced formation damage for water yields the injected water re-direction into un-swept zones, leading to sweep enhancement, like it is with the mobility-control EOR.

Different behaviour of oil-wet, mixed-wet and water-wet fines during low-salinity water-flooding has been reported in the literature (Sarkar and Sharma 1990; Tang and Morrow 1999). Here we discuss initially oil-wet fine particles, like those of kaolinite or illite. The oil-wet particles are coated by oil, so there is no direct contact between the particles and water. However, arrival of low-salinity water causes alternation of wettability, resulting in oil displacement from the rock surface and exposing it to the injected water. From this moment on, particle equilibrium on the rock surface is determined by torque balance of drag and electrostatic forces. The electrostatic particle-rock attraction decreases with salinity decrease, resulting in particle mobilisation.

In the current paper we discussed two EOR mechanisms of low-salinity water flooding: the wettability and interfacial tension alternations resulting in changing the relative permeability, and the induced formation damage to aqueous phase by mobilising and straining of the natural reservoir fines. However, numerous other EOR mechanisms are presently under intensive investigation. Sheng 2014 reviewed the mechanisms of fine migration, mineral dissolution, increased pH effect and reduced interfacial tension, saponification, multicomponent ion exchange, wettability alteration, etc. Morrow and Buckley (2011) briefly mentioned osmotic pressure as an important factor leading to incremental oil recovery. Sandengen and Arntzen (2013), provided a detailed description of how osmosis could operate. The mentioned works claim that the mechanisms for LS water flooding are presently not well understood and their modelling is a subject of forthcoming research.

6. Conclusions

Development of the mathematical model for LS-water flood accounting for wettability alternation and fines migration, derivation of the exact solution for 1D slug problem and recovery prediction by the analytical modelling allow drawing the following conclusions:

1. One-dimensional equations for displacement of oil by varying salinity water with wettability alternation, lumped salt and fines mobilisation, migration and straining contain five dimensionless groups describing dissipative effects of capillary pressure, dispersion of components, kinetics of the contact angle alteration and kinetics of fines detachment and straining.
2. The model allows for simplified versions in low-velocity, high-velocity and large-scale approximations.
3. In large scale approximation, the excess of the attached particle concentration over the maximum retention value is instantly transferred to strained concentration, yielding instant permeability damage for aqueous phase. The governing equations are equivalent to the fractional flow model of oil displacement by chemical solution.
4. Well-known analytical EOR model describes a lumped-salt LS water-flooding accounting for both wettability alteration and induced fines migration.
5. Continuous low salinity water-flooding results in later breakthrough if compared with formation water injection; it causes decreased water-cut during production of oil-water bank and during a short period after the breakthrough of the injected water. It also results in lower oil residual at the late stage of the water-flooding.

6. With injection of intermediate salinity water, the breakthrough moment and water cut during some times after the breakthrough coincide with the formation-water-flooding. Afterwards, water-cut at the intermediate salinity water is lower. The residual oil is lower also.
7. One-dimensional problem for oil displacement by formation water with further injection of LS slug and HS chase drive allows for exact solution. The saturation and salinity front trajectories are described by explicit formulae.
8. For short time formation water injection before low-salinity-water flooding, the solution asymptotically tends to that for oil displacement by low-salinity water. For long time formation water injection, the solution tends to that for oil displacement with high initial water saturation by low-salinity water.

References

Agbalaka, C.C., Dandekar, A.Y., Patil, S.L., Khataniar, S., Hemsath, J.R.: Coreflooding studies to evaluate the impact of salinity and wettability on oil recovery efficiency. Transport in Porous Media 76(1), 77-94 (2009)

Al Shalabi, E.W., Sepehrnoori, K., Delshad, M.: Mechanisms behind low salinity water injection in carbonate reservoirs. Fuel 121, 11-19 (2014a)

Al Shalabi, E.W., Sepehrnoori, K., Delshad, M., Pope, G.: A Novel Method to Model Low-Salinity-Water Injection in Carbonate Oil Reservoirs. In: SPE EOR conference at OGWA, Muscat (2014b)

Alexeev, A., Shapiro, A., Thomsen, K.: Modelling of Dissolution Effects on Waterflooding. Transport in Porous Media 106(3), 545-562 (2015)

Austad, T., RezaeiDoust, A., Puntervold, T.: Chemical mechanism of low salinity water flooding in sandstone reservoirs. In SPE improved oil recovery symposium, Oklahoma (2010)

Barenblatt, G.I., Entov, V.M., Ryzhik, V.M.: Theory of fluid flows through natural rocks, Kluwer, Dordrecht (1989)

Bedrikovetsky, P.: Mathematical theory of oil and gas recovery: with applications to ex-USSR oil and gas fields. Kluwer Academic, Dordrecht (1993)

Bedrikovetsky, P., Siqueira, F.D., Furtado, C.A., Souza, A.L.S.: Modified particle detachment model for colloidal transport in porous media. Transport in porous media 86(2), 353-383 (2011)

Bedrikovetsky, P., Zeinijahromi, A., Siqueira, F.D., Furtado, C.A., de Souza, A.L.S.: Particle detachment under velocity alternation during suspension transport in porous media. Transport in porous media 91(1), 173-197 (2012)

Borazjani, S., Roberts, A.J., Bedrikovetsky, P.: Splitting in systems of PDEs for two-phase multicomponent flow in porous media. Applied mathematics letter, 53, 25-32 (2015)

Bradford, S.A., Tadassa, Y.F., Jin, Y.: Transport of coliphage in the presence and absence of manure suspension. Journal of environmental quality 35(5), 1692-1701 (2006)

Bradford, S.A., Torkzaban, S., Wiegmann, A.: Pore-scale simulations to determine the applied hydrodynamic torque and colloid immobilization. Vadose Zone Journal 10(1), 252-261 (2011)

Brady, P.V., Morrow, N.R., Fogden, A., Deniz, V., Loahardjo, N.: Electrostatics and the Low Salinity Effect in Sandstone Reservoirs. Energy & Fuels 29(2), 666-677 (2015)

Braginskaya, G., Entov, V.: Nonisothermal displacement of oil by a solution of an active additive. Fluid Dynamics 15(6), 873-880 (1980)

Civan, F.: Temperature effect on power for particle detachment from pore wall described by an Arrhenius-type equation. Transport in porous media 67(2), 329-334 (2007)

Civan, F.: Non-isothermal permeability impairment by fines migration and deposition in porous media including dispersive transport. Transport in porous media 85(1), 233-258 (2010)
Civan, F.: Reservoir formation damage. Gulf Professional Publishing, Burlington (2011)
Courant, R., Friedrichs, K.O.: Supersonic flow and shock waves. Interscience publisher LTD., London (1976)
Dahl, O., Johansen, T., Tveito, A., Winther, R.: Multicomponent chromatography in a two phase environment. SIAM Journal on Applied Mathematics 52(1), 65-104 (1992)
Dang, C.T., Nghiem, L.X., Chen, Z., Nguyen, Q.P., Nguyen, N.T.: State-of-the Art Low Salinity Waterflooding for Enhanced Oil Recovery. In: SPE Asia Pacific Oil and Gas Conference and Exhibition, Jakarta (2013)
Duijn, C.J.V., Knabner, P.: Travelling Waves in the Transport of Reactive Solutes Through Porous Media: Adsorption and Binary Ion Exchange – Part 2. Transport in Porous Media 8, 199-225 (1992)
Duijn, C.J.V., Grundy, R.E., Dawson, C.N.: Large Time Profiles in Reactive Solute Transport. J. Transp. Porous Media 27, 57-84 (1997)
Entov, V., Zazovskii, A.: Hydrodynamics of Enhanced Oil Recovery Processes. Nedra, Moscow (in Russian) (1989)
Excel 2010, Microsoft Corporation, United States (2010)
Fogden, A., Kumar, M., Morrow, N.R., Buckley, J.S.: Mobilization of fine particles during flooding of sandstones and possible relations to enhanced oil recovery. Energy & Fuels 25(4), 1605-1616 (2011)
Geiger, S., Schmid, K.S., Zaretskiy, Y.: Mathematical analysis and numerical simulation of multi-phase multi-component flow in heterogeneous porous media. Current Opinion in Colloid & Interface Science 17(3), 147-155 (2012)
Herzig, J., Leclerc, D., Goff, P.L.: Flow of suspensions through porous media-application to deep filtration. Industrial & Engineering Chemistry 62(5), 8-35 (1970)
Holden, H., Risebro, N. H.: Front tracking for hyperbolic conservation laws, Springer (2013)
Hussain, F., Zeinijahromi, A., Bedrikovetsky, P., Badalyan, A., Carageorgos, T., Cinar, Y.: An experimental study of improved oil recovery through fines-assisted waterflooding. Journal of Petroleum Science and Engineering 109, 187-197 (2013)
Israelachvili, J.N.: Intermolecular and surface forces: revised third edition. Academic press, Waltham (2011)
Jerauld, G.R., Lin, C., Webb, K.J., Seccombe, J.C.: Modelling low-salinity waterflooding. SPE Reservoir Evaluation & Engineering 11(6), 1000 (2008)
Khilar, K.C., Fogler, H.S.: Migrations of fines in porous media, vol. 12. Kluwer, Dordrecht (1998)
Kim, T.W., Kovscek, A.R.: Wettability alteration of a heavy oil/brine/carbonate system with temperature. Energy & Fuels 27(6), 2984-2998 (2013)
Kovscek, A., Wong, H., Radke, C.: A pore-level scenario for the development of mixed wettability in oil reservoirs. AIChE Journal 39(6), 1072-1085 (1993)
Lagasca, J., Kovscek, A.: Fines migration and compaction in diatomaceous rocks. Journal of Petroleum Science and Engineering 122, 108-118 (2014)
Lager, A., Webb, K., Black, C.: Impact of brine chemistry on oil recovery. In: 14th European Symposium on Improved Oil Recovery, (2007)
Lager, A., Webb, K., Black, C., Singleton, M., Sorbie, K.: Low salinity oil recovery--An experimental investigation. Petrophysics 49(1), 28 (2008)

Lager, A., Webb, K., Seccombe, J.: Low salinity waterflood, Endicott, Alaska: Geochemical study & field evidence of multicomponent ion exchange. In: IOR-16th European Symposium on Improved Oil Recovery, (2011)
Lake, L.W.: Enhanced oil recovery. Prentice Hall, Englewood Cliffs, N.J (1989)
Lemon, P., Zeinijahromi, A., Bedrikovetsky, P., Shahin, I.: Effects of injected-water salinity on waterflood sweep efficiency through induced fines migration. Journal of Canadian Petroleum Technology 50(9), 82 (2011)
Lever, A., Dawe, R.A.: Water-Sensitivity and Migration of Fines in the Hopeman Sandstone. Journal of Petroleum Geology 7 (1) 97-108 (1984)
Mahani, H., Berg, S., Ilic, D., Bartels, W.-B., Joekar-Niasar, V.: Kinetics of Low-Salinity-Flooding Effect. SPE Journal. 20 (1), 8−20 (2015a)
Mahani, H., Keya, A.L., Berg, S., Bartels, W.-B., Nasralla, R., Rossen, W.R.: Insights into the Mechanism of Wettability Alteration by Low-Salinity Flooding (LSF) in Carbonates. Energy & Fuels 29(3), 1352-1367 (2015b)
MATLAB R2015a, The MathWorks, Inc., Natick, Massachusetts, United States (2015)
Morrow, N., Buckley, J.: Improved oil recovery by low-salinity waterflooding. Journal of Petroleum Technology 63(05), 106-112 (2011)
Muecke, T. W.: Formation Fines and Factors Controlling their Movement in Porous Media, Journal of Petroleum Technology, 31(2) 144-150 (1979)
Nesterov, I., Shapiro, A., Kontogeorgis, G., Multicomponent Adsorption Model for Polar and Associating Mixtures. Ind. Eng. Chem. Res. 54, 3039−3050 (2015)
Nghiem, L., Dang, C., Nguyen, N., Nguyen, Q., Chen, Z.: Modelling and Optimization of Low Salinity Waterflood. In: SPE Reservoir Simulation Symposium, Texas (2015)
Oladyshkin, S., Panfilov, M.: Streamline splitting between thermodynamics and hydrodynamics in a compositional gas–liquid flow through porous media, Comptes Rendus Mécanique, 335(1), 7-12 (2007).
Omekeh, A.V., Evje, S., Friis, H.A.: Modeling of low salinity effects on sandstone rocks. International Journal of Numerical Analysis and Modelling 1(1), 1-18 (2013)
Pingo-Almada, M., Pieterse, S., Marcelis, A., van Haasterecht, M., Brussee, N., van der Linde, H.: Experimental investigation on the effects of very low salinity on Middle Eastern sandstone corefloods. In: SPE International Conference and Exhibition on European Formation Damage, Noordwijk (2013)
Pires, A., Bedrikovetsky, P., Shapiro, A.: Splitting between Thermodynamics and Hydrodynamics in Compositional Modelling. In: 9th European Conference on the Mathematics of Oil Recovery (2004)
Pires, A.P., Bedrikovetsky, P.G., Shapiro, A.A.: A splitting technique for analytical modelling of two-phase multicomponent flow in porous media. Journal of Petroleum Science and Engineering 51(1), 54-67 (2006)
Pope, G.A.: The application of fractional flow theory to enhanced oil recovery. Society of Petroleum. Engineers (1980). doi: 0197·7520/80/0006·7660$00.25
RezaeiDoust, A., Puntervold, T., Strand, S., Austad, T.: Smart water as wettability modifier in carbonate and sandstone: A discussion of similarities/differences in the chemical mechanisms. Energy & fuels 23(9), 4479-4485 (2009)
Salathiel, R.: Oil recovery by surface film drainage in mixed-wettability rocks. Journal of petroleum technology, 25, 1216-1224 (1973)
Sandengen, K., Arntzen O. J.: Osmosis during low salinity water flooding, paper presented at 17th European Symposium on Improved Oil Recovery, European Association of Geoscientists and Engineers, EAGE, Saint Petersburg (2013)

Sarkar, A.K., Sharma, M.M.: Fines migration in two-phase flow. Journal of petroleum technology 42(05), 646-652 (1990)
Schembre, J., Kovscek, A.: Mechanism of formation damage at elevated temperature. Journal of energy resources technology 127(3), 171-180 (2005)
Schembre, J., Tang, G.-Q., Kovscek, A.: Wettability alteration and oil recovery by water imbibition at elevated temperatures. Journal of Petroleum Science and Engineering 52(1), 131-148 (2006)
Scheuerman, R.F., Bergersen, B.M.: Injection-Water Salinity Formation Pre-treatment and Well-Operations Fluid-Selection Guidelines. Journal of Petroleum Technology 42(07), 836-845 (1990)
Schmid, K.S., Geiger, S., Sorbie, K.S.: Analytical solutions for co-and counter current imbibition of sorbing–dispersive solutes in immiscible two-phase flow. In: 12th European Conference on the Mathematics of Oil Recovery (2010)
Schmid, K.S., Geiger, S.: Universal scaling of spontaneous imbibition for arbitrary petro-physical properties: Water-wet and mixed-wet states and Handy's conjecture. Journal of Petroleum Science and Engineering 101 44–61 (2013)
Shapiro, A.A.: Two-Phase Immiscible Flows in Porous Media: The Mesocopic Maxwell–Stefan Approach. Transport in Porous Media, 1-29 (2014)
Sheng, J.: Critical review of low-salinity waterflooding. Journal of Petroleum Science and Engineering 120, 216-224 (2014)
Takahashi, S., Kovscek, A.R.: Wettability estimation of low-permeability, siliceous shale using surface forces. Journal of Petroleum Science and Engineering 75(1), 33-43 (2010)
Tang, G.-Q., Morrow, N.R.: Influence of brine composition and fines migration on crude oil/brine/rock interactions and oil recovery. Journal of Petroleum Science and Engineering 24(2), 99-111 (1999)
Tikhonov, A.N., Samarskii, A.A.: Equations of mathematical physics, vol. 39. Courier Corporation, (1990)
Yuan, H., Shapiro, A.A.: Induced migration of fines during waterflooding in communicating layer-cake reservoirs. Journal of Petroleum Science and Engineering 78(3), 618-626 (2011)
Zeinijahromi, A., Nguyen, T.K.P., Bedrikovetsky, P.: Mathematical model for fines-migration-assisted waterflooding with induced formation damage. SPE Journal 18(03), 518-533 (2013)

Appendix A. Derivation of governing equations

Mass balance equations for incompressible immiscible water and oil phases are (Lake 1989):

$$\phi \frac{\partial s}{\partial t} + \frac{\partial u_w}{\partial x} = 0, \ \phi \frac{\partial (1-s)}{\partial t} + \frac{\partial u_o}{\partial x} = 0 \tag{A-1}$$

Momentum balances for aqueous and oil phases are expressed by modified Darcy's law

$$u_w = -\frac{k\, k_{rw}(s,\theta,\sigma_s)}{\mu_w} \frac{\partial p_w}{\partial x}, \ u_o = -\frac{k\, k_{ro}(s,\theta)}{\mu_o} \frac{\partial p_o}{\partial x} \tag{A-2}$$

The effect of wettability variation with salinity is expressed in the contact-angle-dependency of relative permeabilities, see eq (A-2). The formation damage to aqueous phase due to straining of the released fines is expressed as

$$k_{rw}(s,\theta,\sigma_s) = \frac{k'_{rw}(s,\theta)}{1+\beta\sigma_s} \tag{A-3}$$

i.e. the effect of attached particles on relative permeability for water is assumed to be negligible (Civan 2007, 2010). Here $k'_{rw}(s, \theta)$ is relative permeability for water for fines-free flow.

The capillary pressure is the difference between pressures in oil and water

$$p_o - p_w = p_c, \ \ p_c = \frac{\sigma_{wo}(\gamma)\cos\theta}{\sqrt{k/\phi}} J(s,\gamma,\sigma_s) \tag{A-4}$$

Mass conservation law for salt includes the advective salt transfer by the carrier aqueous phase and its advective dispersion

$$\phi \frac{\partial \gamma s}{\partial t} + \frac{\partial \gamma u_w}{\partial x} = \alpha_L U \frac{\partial}{\partial x}\left(s \frac{\partial \gamma}{\partial x}\right) \tag{A-5}$$

Establishing the salinity-dependent contact angle $\theta_e(\gamma)$ occurs with some delay due to diffusion of salt from connate water layer into the injected water, $\tau = \alpha_L^2/D_\mu$ (Mahani et al. 2015a, b):

$$\tau_\theta \frac{\partial \theta}{\partial t} = \theta_e(\gamma) - \theta \tag{A-6}$$

Concentration of the attached particles reaches the critical retention function (3) with delay τ_σ.

$$\tau_\sigma \frac{\partial \sigma_a}{\partial t} = \sigma_{cr}(\gamma) \frac{A_w(s,\theta)}{A} + \sigma_{a0} \frac{A - A_w(s,\theta)}{A} - \sigma_a \tag{A-7}$$

The delay is due to the ion diffusion time into the contact area between fine particles and rock surface, resulting in the particle mobilisation. For the case of instant fine particles release, the attached concentration is equal to the maximum retention function (3).

The kinetics of fines straining is proportional to the advective flux of suspended fines

$$\frac{\partial \sigma_s}{\partial t} = \lambda(\gamma, \sigma_s) c u_w \tag{A-8}$$

where the proportionality coefficient λ is called the filtration coefficient. Since the attaching electrostatic force is a salinity function, and the particle capture probability depends on the pore space geometry, the filtration coefficient is a function of salinity and strained concentration (Herzig et al. 1970). Here we assume that attached particles coat the grains and do not change the pore space geometry.

The conservation law for suspended, attached and strained fines is

$$\frac{\partial}{\partial t}\left(\phi s c + \sigma_a + \sigma_s\right) + \frac{\partial c u_w}{\partial x} = \alpha_L U \frac{\partial}{\partial x}\left(s \frac{\partial c}{\partial x}\right) \tag{A-9}$$

For the reservoir part where the salinity is higher than the critical salinity, the reservoir fines remain attached $\left(\gamma > \gamma_{cr}, \sigma_s = 0\right)$, and the model comprises Buckley-Leverett equations with changing salinity and contact angle (A-1,A-2,A-4-A-6) without fines migration, i.e. c=σ_s=0 and σ_a=σ_{a0}.

Adding two eq (A-1) results in conservation of the total flux of two incompressible phases:

$$u = u_w + u_o = U(t) \tag{A-10}$$

Calculation of the total flux U by adding two eq (A-2) and substituting the expression for pressure in oil phase from (A-4) into the resulting formula, yields

$$U = -k\left(\frac{k_{rw}(s,\theta,\sigma_s)}{\mu_w} + \frac{k_{ro}(s,\theta)}{\mu_o}\right)\frac{\partial p_w}{\partial x} - \frac{k\, k_{ro}(s,\theta)}{\sqrt{k/\phi}\mu_o}\frac{\partial\left(\sigma_{wo}(\gamma)\cos\theta J\right)}{\partial x} \tag{A-11}$$

Expressing pressure gradient from (A-11) and its substitution into first eq (A-2) results in the following expression for water flux

$$u_w = f\left[U + \frac{k\, k_{ro}}{\sqrt{k/\phi}\mu_o}\frac{\partial\left(\sigma_{wo}(\gamma)\cos\theta J\right)}{\partial x}\right],\quad f(s,\theta,\sigma_s) = \frac{\frac{k_{rw}(s,\theta,\sigma_s)}{\mu_w}}{\frac{k_{rw}(s,\theta,\sigma_s)}{\mu_w} + \frac{k_{ro}(s,\theta)}{\mu_o}}, \tag{A-12}$$

In (A-12), the total flux of water consists of the advective flux moved by pressure gradient, and the capillary flux due to saturation gradient.

Appendix B. Initial and boundary conditions for 1-D displacement

System (5-10) has time derivatives for six unknowns: saturation s, salinity γ, attached fines concentration S_a, concentration of strained fines S_s , contact angle θ and suspended fines concentration C, which corresponds to transient behaviour of those parameters during the

displacement. Therefore, initial conditions must be posed for six unknowns: s, γ, S_a, S_s ,θ and C:

$$t=0: s=s_I, C=0, S_s=0, S_a=S_{a0}, \gamma=\gamma_I, \theta=\theta_0 \tag{B-1}$$

corresponding to their values in the reservoir before the injection.

System contains first order x-derivatives for three unknowns s, γ and C. The x-derivatives for three unknowns s, γ and C corresponds to the carrier fluxes, transporting the corresponding species (water, salt and suspended fines).. Therefore, three entrance boundary conditions must be set for those variables. It includes unity overall water flux carried by pressure and capillary pressure gradients, zero fine particle flux transported by the overall water and particle diffusive fluxes, given flux of salt transported by the overall water and salt diffusive fluxes and given injection pressure:

$$\begin{gathered} x=0: f\left[1+\varepsilon_c k_{ro}(s,\theta)\frac{\partial\left(\mathrm{E}(\gamma,\theta)J\right)}{\partial x}\right]=1, Cf\left[1+\varepsilon_c k_{ro}(s,\theta)\frac{\partial\left(\mathrm{E}(\gamma,\theta)J\right)}{\partial x}\right]-\varepsilon_D s\frac{\partial C}{\partial x}=0, \\ \gamma f\left[1+\varepsilon_c k_{ro}(s,\theta)\frac{\partial\left(\mathrm{E}(\gamma,\theta)J\right)}{\partial x}\right]-\varepsilon_D s\frac{\partial \gamma}{\partial x}=\gamma_J \end{gathered} \tag{B-2}$$

which corresponds to injected concentrations of fines and salt and the water fraction in the injected fluid. Here we discuss the particular case where no fine particles are injected.

The attached and strained fine particles are immobile, their fluxes are equal zero. The equation (A-6) for kinetics of the contact angle also does not contain the advective term. Therefore, their concentrations at the entrance x=0 are determined from kinetics of their variations (see Tikhonov and Samarskii 1990 on so-called Goursat problem). The ordinary differential equations for attached fines concentration at the entrance $S_a(0, t)$ and contact angle, follow from kinetics eqs (A-7), (A-6)

$$\varepsilon_\sigma\frac{dS_a(0,t)}{dt}=S_{cr}(\gamma_J)\frac{A_w(1-s_{or},\theta)}{A}+S_{a0}\frac{A-A_w(1-s_{or},\theta)}{A}-S_a(0,t) \tag{B-3}$$

$$\varepsilon_\theta\frac{\partial\theta(0,t)}{\partial t}=\theta_e(\gamma_J)-\theta(0,t) \tag{B-4}$$

The initial condition for ordinary differential equations (B-3) and (B-4) corresponds to initial concentrations of attached fines on rock surface accessible to water and oil and the initial contact angle:

$$S_a(0,0)=S_{a0},\quad \theta(0,0)=\theta_0 \tag{B-5}$$

The solution of the problem (B-4) is obtained by separation of variables

$$\theta(0,t)=-e^{-\frac{t}{\varepsilon_\theta}}\left(\theta_e(\gamma_J)-\theta_0\right)+\theta_e(\gamma_J) \tag{B-6}$$

The solution of eq (B-3) is obtained by solving the ordinary differential equation

$$\varepsilon_\sigma \frac{dS_a(0,t)}{dt} = S_{cr}(\gamma_J)\frac{A_w\left(1-s_{or},-e^{-\frac{t}{\varepsilon_\theta}}\left(\theta_e(\gamma_J)-\theta_0\right)+\theta_e(\gamma_J)\right)}{A}+S_{a0}\frac{A-A_w\left(1-s_{or},-e^{-\frac{t}{\varepsilon_\theta}}\left(\theta_e(\gamma_J)-\theta_0\right)+\theta_e(\gamma_J)\right)}{A}-S_a(0,t)$$

(B-7)

As it follows from kinetics of straining (9) and boundary condition (B-2) for injected fines, the ordinary differential equation for strained fines at the entrance x=0 and corresponding boundary conditions are:

$$\frac{dS_s(0,t)}{dt}=0,\quad S_s(0,t=0)=0 \tag{B-8}$$

resulting in zero-solution:

$$S_s(0,t)=0 \tag{B-9}$$

System of governing equations contains second order x-derivatives for saturation, salinity and suspended fines concentration. It corresponds to capillary flux for water and dispersive fluxes for salt and suspended fines. Therefore, boundary conditions at the outlet x=1 must be set for s, γ and C.

The boundary condition for saturation is so-called end-effect (Barenblatt et al. 1989)

$$x=1:\ (s-1-s_{or})\left(f+\varepsilon_c k_{ro} f\frac{\partial J}{\partial x}\right)=0 \tag{B-10}$$

As it follows from (B-10), s=s_I before the water breakthrough; afterwards capillary pressure is equal zero, and oil saturation takes the oil residual value.

Dispersive fluxes are zero at the outlet

$$x=1:\ \frac{\partial\gamma}{\partial x}=\frac{\partial C}{\partial x}=0 \tag{B-11}$$

corresponding to the assumption that a salt or fine particle that exited the core by advective flux, never diffuses back.

System of governing equations (5-10) subject to initial (B-1) and boundary conditions (B-2, B-7-B-11) provides a unique solution, stable with respect to small perturbations (Bedrikovetsky 1993).

Appendix C. Large scale approximation

Let us discuss the case of large L, such that three dimensionless groups are negligibly small and dimensionless filtration coefficient is infinitely large, i.e. L is significantly larger than four values (see eq (4)):

$$L>>\frac{\sigma_{wo}\cos\theta\sqrt{k\phi}}{\mu_o U};\ L>>\alpha_L,\ L>>\frac{U\tau}{\phi},L>>\frac{1}{\lambda} \tag{C-1}$$

Left hand side of eq (9) is limited and independent of L. Tending Λ to infinity corresponds to tending C to zero. Tending C to zero in eq (10) results in

$$\frac{\partial}{\partial t}(S_a + S_s) = 0 \tag{C-2}$$

Therefore, the total retained concentration is found from initial conditions (B-1)

$$S_a(x_D, t_D) + S_s(x_D, t_D) = S_{a0} \tag{C-3}$$

Eq (C-3) means that all released particles are strained instantly, and there are no suspended particles.

Tending ε_θ and ε_σ to zero in left hand side of eqs (7) and (8) and accounting for (C-3), we obtain the equilibrium values for strained concentration (first eq (12)) and contact angle $\theta_e(\gamma)$. Straining concentration in (12) becomes the difference between the initial and current values of the maximum retention function. Tending ε_c to zero in left hand side of eqs (5-10) eliminates the capillary-pressure-driven flux if compared with advection flux $f=f(s,\theta,S_s)$.

Finally, large scale approximation of the system (5-10) is given by eqs (11-13).

However, often only short cores are available for laboratory coreflooding, so the conditions (C-1) cannot be fulfilled. Some simplification of the basic system (5-10) can be achieved by going to extremes of high and low velocities.

Slow displacement approximation corresponds to negligible delay numbers. Tending ε_θ and ε_σ to zero in left hand side of eqs (7) and (8) results in “instant” maximum retention function, given by eq (3), and equilibrium contact angle $\theta_e(\gamma)$. So, the slow-displacement system consists of 5 equations (5, 6, 9-10) with equilibrium maximum retention functions and contact angle.

Fast displacement approximation corresponds to negligible capillary-viscous ratio (see eq (4)). The governing system at fast displacement approximation consists of eqs (5-10) with ε_c =0.

Appendix D. Splitting method for equations of two-phase multicomponent mass transfer in porous media

Following papers by Pires et al. 2004, 2006, here we briefly present the splitting procedure for hyperbolic system (11-13). Let us introduce the hydrodynamic potential φ from the conservation law (11):

$$s = -\frac{\partial \varphi}{\partial x}, \qquad f = \frac{\partial \varphi}{\partial t} \tag{D-1}$$

As it follows from (D-1), the potential has the following form

$$d\varphi = f dt - s dx$$

$$\varphi(x,t) = \int_{(0,0)}^{(x,t)} f dt - s dx \tag{D-2}$$

Differential dt can be expressed from eq (D-2)

$$dt = \frac{d\varphi}{f} + \frac{s dx}{f} \tag{D-3}$$

The equality of second mixed derivatives of function $t=t(x, \varphi)$ in (C-3) yields

$$\frac{\partial F(U,\gamma)}{\partial \varphi} + \frac{\partial U}{\partial x} = 0,$$

$$U = \frac{1}{f(s,\gamma)}, \; F(U,\gamma) = -\frac{s}{f(s,\gamma)} \tag{D-4}$$

Eq (D-4) is the result of the eq (11) transform to co-ordinates (x,φ).

Applying Green's theorem over any arbitrary domain ϖ with continuous boundary $\partial\varpi$, to Eq (12) and accounting for eq (D-3),

$$0 = \oint_{\partial\varpi} (\gamma f) dt - (\gamma s) dx = \oint_{\partial\varpi} \gamma (f dt - s dx) = \oint_{\partial\varpi} \gamma d\varphi = \iint_{\varpi} \frac{\partial \gamma}{\partial x} dx d\varphi \tag{D-5}$$

yields the transformation of this equation to (x,φ)-coordinates

$$\frac{\partial \gamma}{\partial x} = 0 \tag{D-6}$$

So, the original system (11-13) in (x, φ)-coordinates has the form (D-4, D-6).

Fig. 5a, b shows the mapping K: $(x,t)\rightarrow(x,\varphi)$ along with the images of the initial-condition axis $t=0$ and the boundary-condition axis $x=0$. The images depend on initial and boundary data.

Inlet boundary conditions for continuous injection (15) become

$$x = 0 : U = 1, \; \gamma = \gamma_J \tag{D-7}$$

Initial conditions (14) take the form

$$\varphi = -s_I x : \gamma = \gamma_I, \; U \rightarrow \infty \tag{D-8}$$

Inlet boundary condition for formation water injection followed by the injection of low-salinity water (16) becomes

$$x=0:\gamma=\begin{cases}\gamma_I,\ 0<\varphi<1\\ \gamma_J,\ 1<\varphi<t_s\\ \gamma_I,\ t_s<\varphi<\infty\end{cases} \tag{D-9}$$

Speeds of rarefaction and shock waves in planes (x,φ) and (x, t) (V and D, respectively) are related as

$$\frac{1}{V}=\frac{f}{D}-s \tag{D-10}$$

The geometric interpretation of Eulerian and Lagrangian speeds D and V are shown in Fig. 5c.

The Hugoniot-Rankine conditions of flux continuity on the discontinuities for two conservation laws (D-4) and (D-6) are (Courant and Friedrichs 1976)

$$[U]=V[F],\ [\gamma]=0 \tag{D-11}$$

As it follows from (D-11), for shocks with salinity and saturation jumps,

$$[F]=0,\ [\gamma]=\forall,\ V=\infty \tag{D-12}$$

For saturation shocks with continuous salinity,

$$\frac{1}{V}=\frac{[F]}{[U]},[\gamma]=0 \tag{D-13}$$

Eq (D-6) for unknown γ separates from eq (D-4) and is solved independently (Fig. 7a). Then, eq (D-4) is solved with respect to unknown $s(x,\varphi)$ for known $\gamma(x,\varphi)$ using method of characteristics (Fig. 6b). This is so-called lifting problem. As it follows from the shock conditions (D-12, D-13), the solutions for initial-boundary problems with piecewise constant γ-values contain those values only. Fig. 6a shows the form of flux curves $F=F(U, \gamma)$ for γ-values γ_I and γ_J appearing in initial and boundary conditions (D-8) and (D-9). Finally, the transformation of solution $s(x,\varphi)$, $\gamma(x,\varphi)$ to co-ordinates (x,t) is performed by calculation of $t(x,\varphi)$ from eq (D-3):

$$t(x,\varphi)=\int^{(x,\varphi)}\frac{d\varphi}{f}+\frac{sdx}{f} \tag{D-14}$$

where any arbitrary point (x, φ) is connected to the point with φ=0 or x=0, where the connections are the characteristic lines.

Solutions for continuous injections in co-ordinates (x, t) are self-similar and depend on the group x/t. The corresponding solutions in (x,φ)-plane are also self-similar and depend on the group φ/x. The solution $\gamma(x,\varphi)$ for continuous injection (D-7) is achieved by a single infinite-

speed jump along the axes φ=0. The solution $s(\varphi/x)$ corresponds to rarefaction wave J-2, jump 2→3 and jump 3→I in Fig. 6a. The solution $s(x/t)$, $\gamma(x/t)$ corresponds to rarefaction wave J-2, jump 2→3 and jump 3→I in Figs. 6b.

Figures

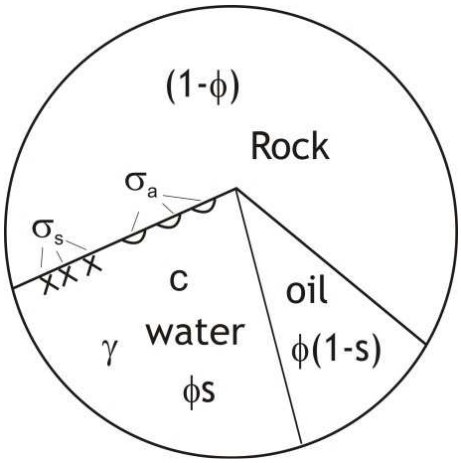

Figure 1. Schematic for porosity, phase saturations and component concentrations in porous space; the fine particles are in suspension (c), can be attached (σ_a) or retained by the rock (σ_s)

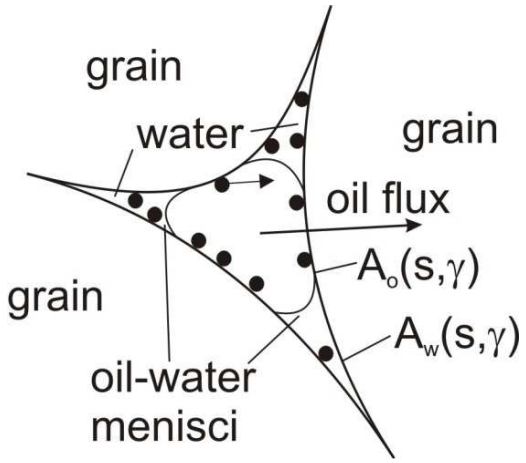

Figure 2. The attached particles can be mobilised by the injected water from the rock surface accessible to water A_w, fines attached to the surface A_o remain immobile

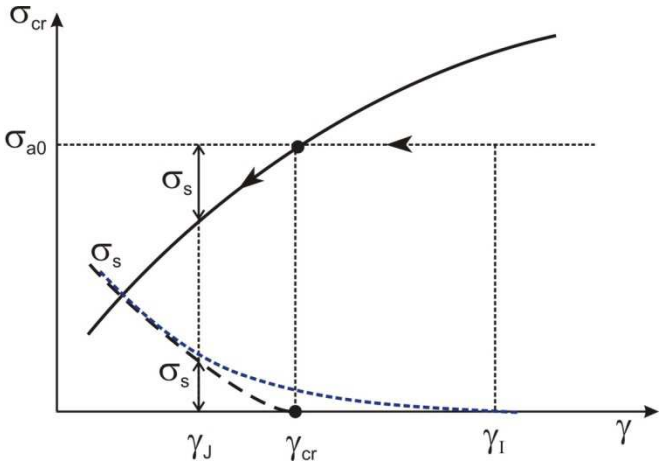

Figure 3. Strained concentration σ_s in large scale approximation is determined by the maximum retention function $\sigma_{cr}(\gamma)$; here concentrations σ_s and $\sigma_{cr}(\gamma)$ are approximated by the vanishing function into the domain $\sigma<\sigma_{cr}(\gamma)$ where no particles are mobilised

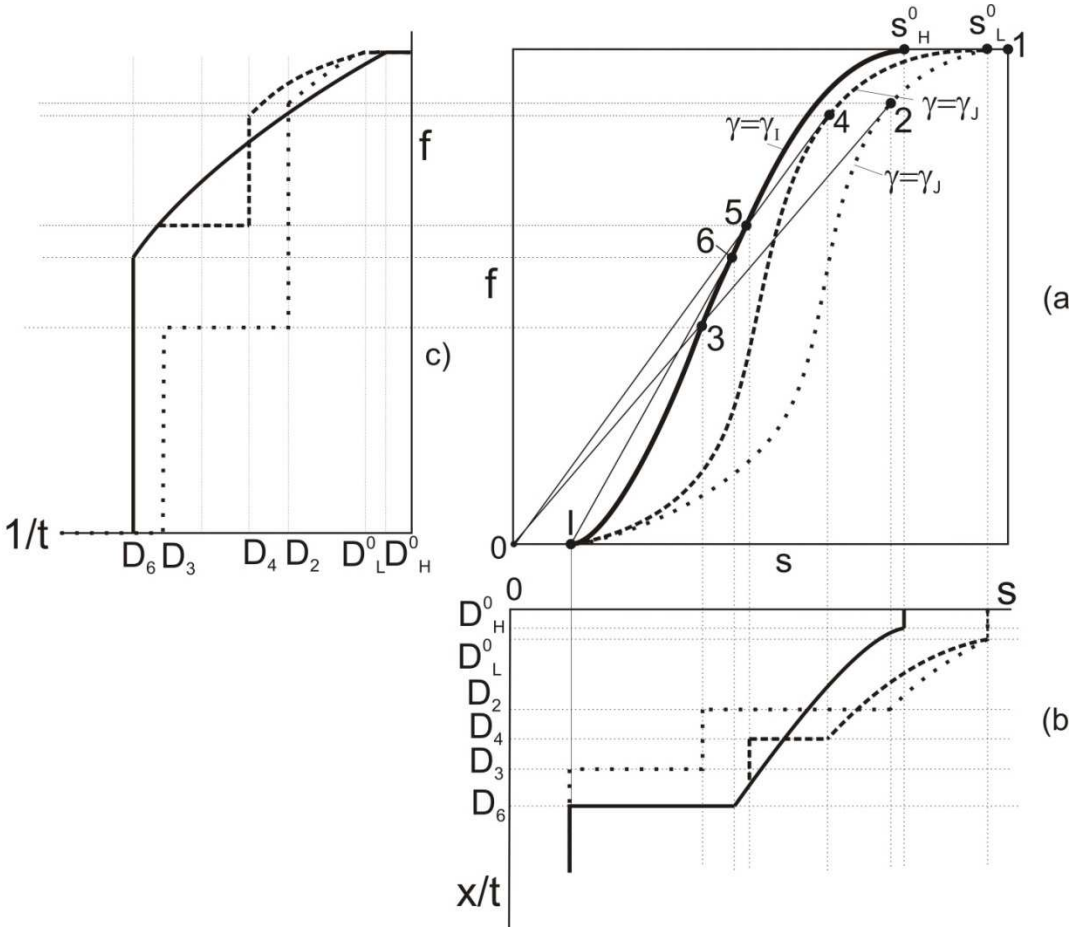

Figure 4. Analytical model and graphical solution for continuous low-salinity water injection: (a) solutions for formation water injection (S^0_H-6->*I*), medium salinity (S^0_L-4->5-6->*I*) and low-salinity flooding (S^0_L-2->3->*I*) on the fractional flow curves; (b) profiles for saturation for three displacement cases; (c) water-cur history for three cases of displacement

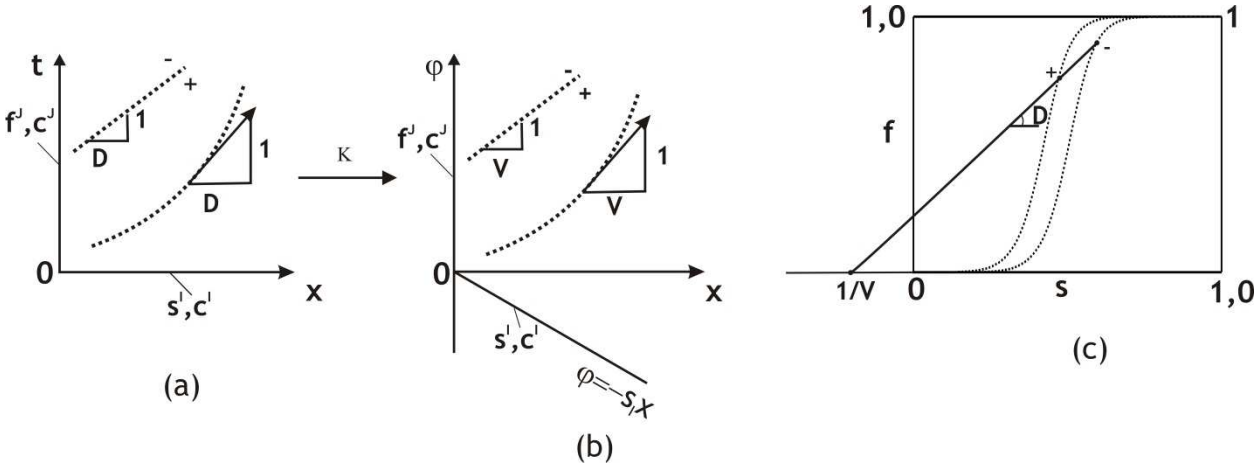

Figure 5. Mapping using the stream function $\varphi(x,t)$: (a) initial and boundary conditions and front velocity at the plane (x,t); (b) mapped initial and boundary conditions and front velocity at the plane (x, φ); (c) graphical presentation of Lagrangian speed V and Eulerian speed D in (s,f) plane

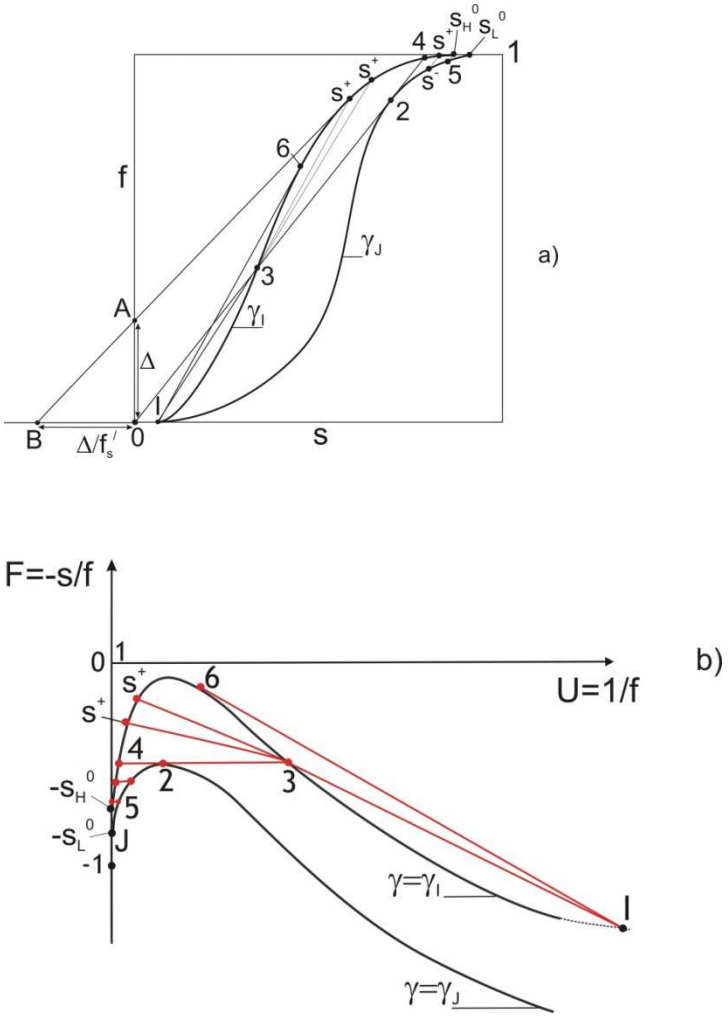

Figure 6. Graphical solution for 1D displacement of oil by formation water followed by the LS slug and HS water chase drive: (a) fractional flow curves and typical saturations corresponding to points 2,3…6; (b) lifting of the solution for auxiliary problem in (*F*, *U*)-plane

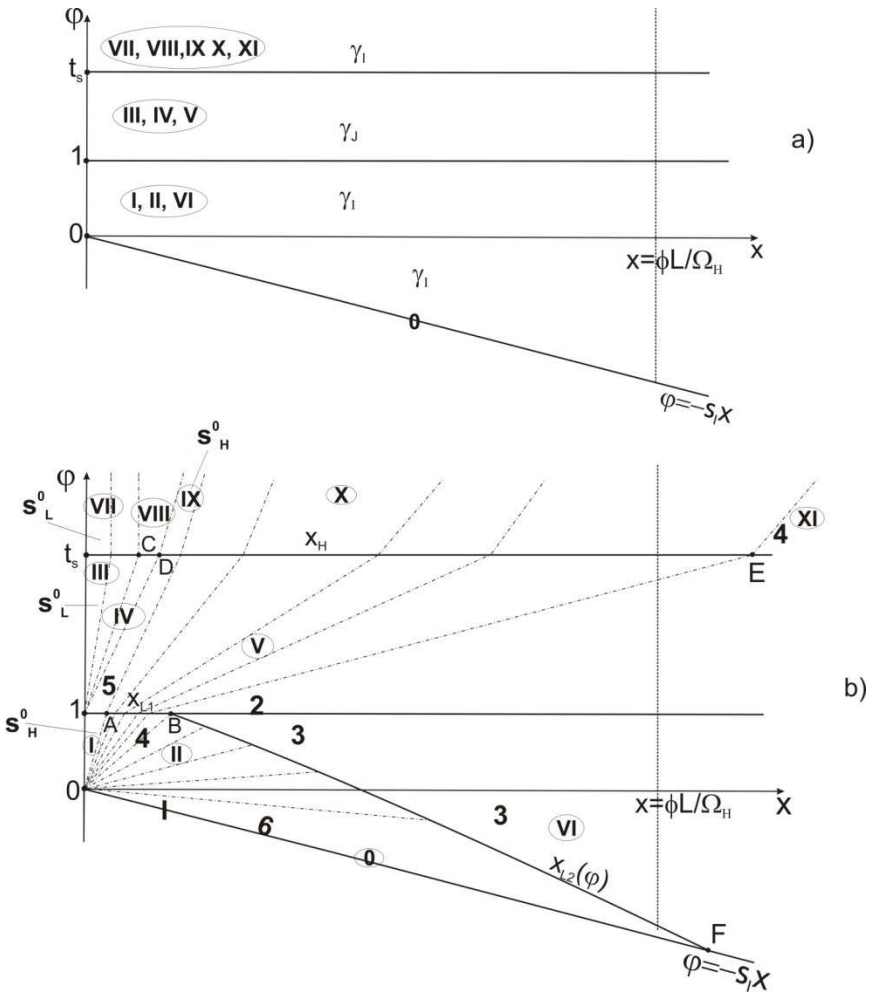

Figure 7. Solution of the problem for HS and LS slugs followed by HS water chase drive in (x, φ) co-ordinates: (a) solution of the auxiliary system; (b) solution of the lifting equation

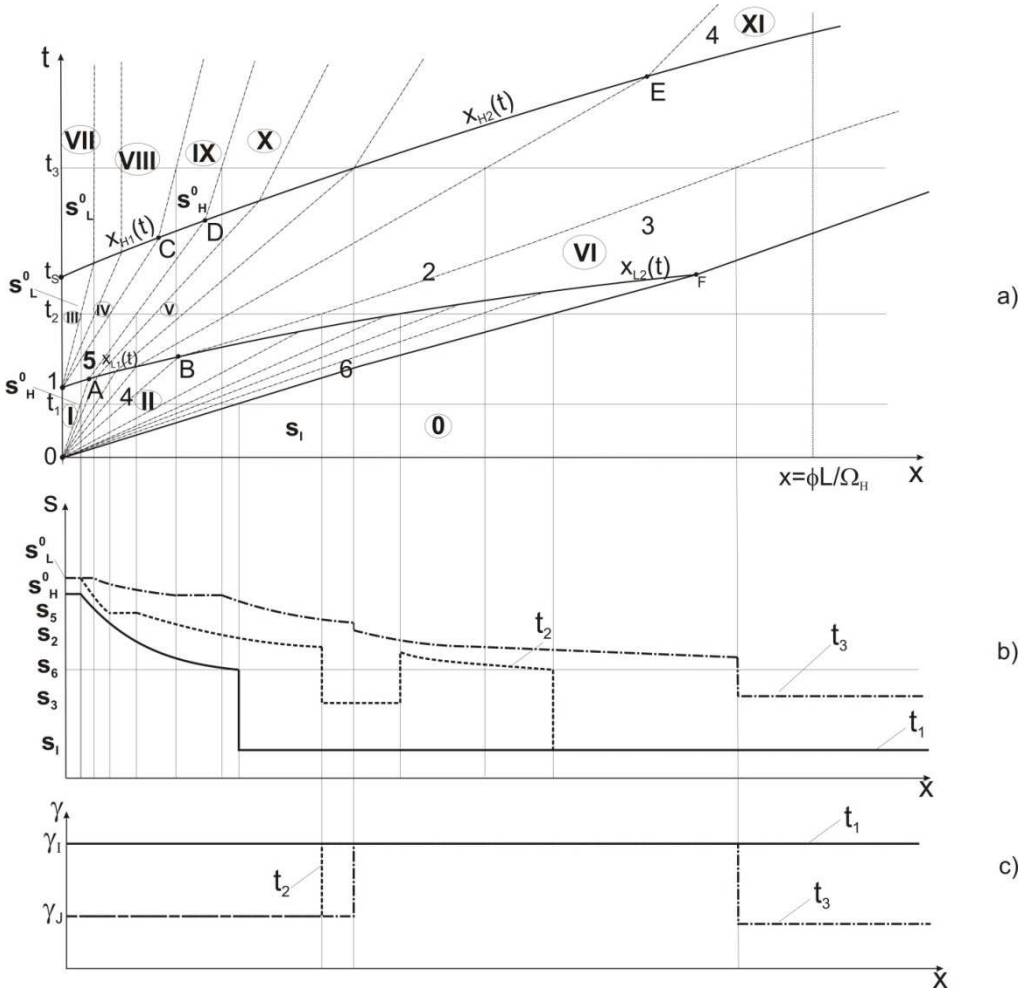

Figure 8. Analytical model for 1D injection problem of HS and LS slugs followed by HS water drive in (*x*, *t*) co-ordinates: (a) Trajectories of saturation and concentration waves in (*x*, *t*)-plane along with typical zones I,II…XI; (b) saturation profiles in three different moments; (c) salinity profiles in three different moments

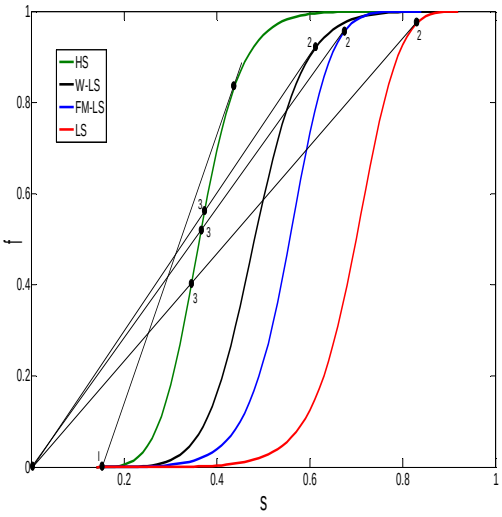

Figure 9. Fractional flow curves for injection of formation water and low salinity water: green curve correspond to injection of formation water; red curve encompasses both effects of wettability alternation and induced fines migration; the case of fines-free and wettability-affected low-salinity flood is presented by black curve; blue curve corresponds to no wettability alternation and fines mobilisation with straining during low-salinity waterflood.

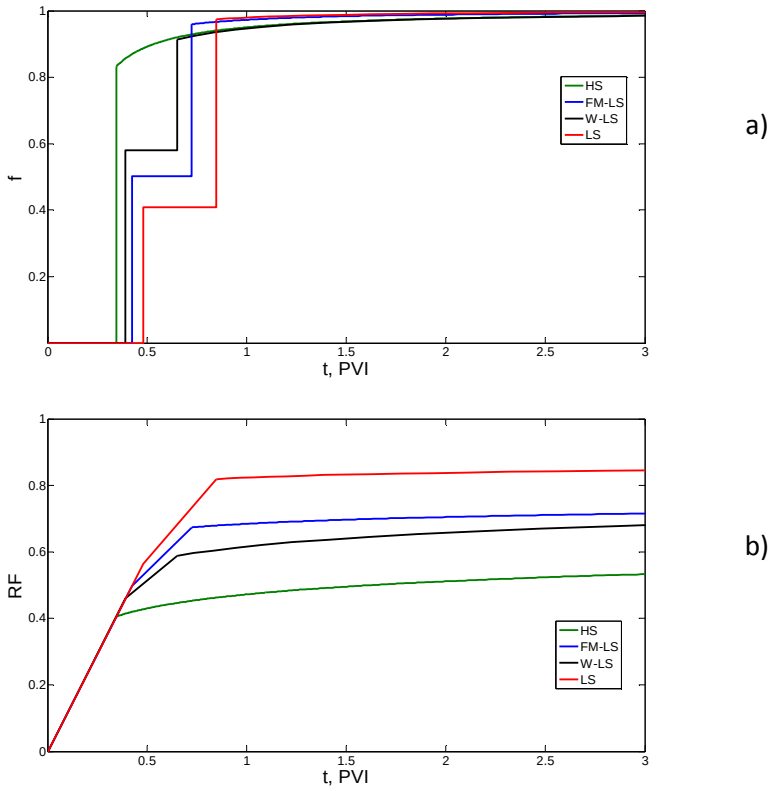

Figure 10. Comparison between cases of oil displacement by formation HS water (green), by LS water accounting for wettability alteration effect only (black), by LS water accounting for fines migration effect only (blue), by LS water accounting for both effects (red): a) water cut history; b) recovery factor versus PVI

Tables

Table 1. Exact solution for 1D oil displacement by formation water and low-salinity slug in (x, φ) domain

zones	***U(x,φ)***	***γ(x,φ)***	**domain**
0	s_I	γ_I	$\varphi = -s_I x$
I	$s^0{}_H$	γ_I	$0 < \varphi < 1, \quad \varphi > F_U^{/}\left(U_H^0, \gamma_I\right) x$
II	$\dfrac{\varphi}{x} = F_U^{/}\left(U, \gamma_I\right)$	γ_I	$\varphi < 1, \quad -s_I x < \varphi < F_U^{/}\left(U_H^0, \gamma_I\right) x, \quad x < x_{L2}\left(\varphi\right)$
III	$s^0{}_L$	γ_J	$1 < \varphi < t_s, \ \varphi > F_U^{/}\left(U_L^0, \gamma_J\right) x + 1$
IV	$\dfrac{\varphi - 1}{x} = F_U^{/}\left(U, \gamma_J\right)$	γ_J	$1 < \varphi < t_s, \quad F_U^{/}\left(U_5, \gamma_J\right) x + 1 < \varphi < F_U^{/}\left(U_L^0, \gamma_J\right) x + 1$
V	$\dfrac{\varphi - 1}{x - x'} = F_U^{/}\left(U, \gamma_J\right)$	γ_J	$1 < \varphi < t_s, \quad \varphi < F_U^{/}\left(U_5, \gamma_J\right)\left(x - x_A\right) + 1$
VI	s_3	γ_I	$\varphi\left(x_{L2}\right) < \varphi < 1$
VII	$s^0{}_L$	γ_I	$\varphi > t_s, \ \varphi > F_U^{/}\left(U_L^0, \gamma_J\right) x + t_s$
VIII	$F\left(U, \gamma_I\right) - F\left(U, \gamma_J\right) = 0$ $F_L^0 < F < F_H^0$	γ_I	$\varphi > F_U^{/}\left(U_0^H, \gamma^I\right)\left(x - x_D\right) + t_s$
IX	$s^0{}_H$	γ_I	$t_s < \varphi, \ F_U^{/}\left(U_H^0, \gamma_I\right)\left(x - x_D\right) + t_s < \varphi < F_U^{/}\left(U_H^0, \gamma_I\right)\left(x - x_C\right) + t_s$
X	$\dfrac{\varphi - t_s}{x - x''} = F_U^{/}\left(U, \gamma_I\right)$	γ_I	$t_s < \varphi, \ F_U^{/}\left(U_4, \gamma_I\right)\left(x - x_E\right) + t_s < \varphi < F_U^{/}\left(U_H^0, \gamma_I\right)\left(x - x_D\right) + t_s$
XI	s_4	γ_I	$t_s < \varphi < F_U^{/}\left(U_4, \gamma_J\right)\left(x - x_E\right) + t_s$

Table 2. Exact solution for 1D oil displacement by formation water and low-salinity slug in (x, t) domain

zones	***s***	γ	**domain**
0	s_I	γ_I	$0<t<f_s^{/}\left(s_6,\gamma_I\right)^{-1}x,\ x<x_F,\quad t<\frac{s_3-s_I}{f_3}\left(x-x_F\right),x>x_F$
I	$s^0{}_H$	γ_I	$t<1+s_H^0x,\quad t>f_s^{/}\left(s_H^0,\gamma_I\right)^{-1}x$,
II	$\frac{x}{t}=f_s^{/}\left(s,\gamma_I\right)$	γ_I	$t<t\left(x_{L1}\right),\ f_s^{/}\left(s_4,\gamma_I\right)^{-1}x<t<f_s^{/}\left(s_H^0,\gamma_I\right)^{-1}x,x<x_B$ $t<t\left(x_{L2}\right),\ f_s^{/}\left(s_6,\gamma_I\right)^{-1}x<t<f_s^{/}\left(s_4,\gamma_I\right)^{-1}x,\ x_B<x<x_F$
III	$s^0{}_L$	γ_J	$t\left(x_{L1}\right)<t<t\left(x_H\right),\quad t>f_s^{/}\left(s_L^0,\gamma_J\right)^{-1}x+1$
IV	$\frac{x}{t-1}=f_s^{/}\left(s,\gamma_J\right)$	γ_J	$t\left(x_{L1}\right)<t<t\left(x_H\right),\quad f_s^{/}\left(s_5,\gamma_J\right)^{-1}x+1<t<f_s^{/}\left(s_L^0,\gamma_J\right)^{-1}x+1$
V	$\frac{x-x'}{t-t'}=f_s^{/}\left(s,\gamma_J\right)$	γ_J	$f_s^{/}\left(s_2,\gamma_J\right)^{-1}\left(x-x_B\right)+t_B<t<f_s^{/}\left(s_5,\gamma_J\right)^{-1}\left(x-x_A\right)+t_A,$ $t\left(x_{L1}\right)<t<t\left(x_H\right)$
VI	s_3	γ_I	$t\left(x_{L2}\right)<t<f_s^{/}\left(s_2,\gamma_J\right)^{-1}\left(x-x_B\right)+t_B,\ x_B<x<x_F$ $t>\frac{s_3-s_I}{f_3}\left(x-x_F\right),x>x_F$
VII	$s^0{}_L$	γ_I	$t>s_L^0x+t_s,\quad 0<x<x_G$
VIII	$F\left(U,\gamma^I\right)-F\left(U,\gamma_J\right)=0$ $F_L^0<F<F_H^0$	γ_I	$t(x_H)<t,\ \ x_G<x<x_C$
IX	$s^0{}_H$	γ_I	$t(x_H)<t,\ f_s^{/}\left(s_H^0,\gamma_I\right)^{-1}\left(x-x_D\right)+t_D<t<f_s^{/}\left(s_H^0,\gamma_I\right)^{-1}\left(x-x_C\right)+t_C$
X	$\frac{x-x''}{t-t''}=f_s^{/}\left(s,\gamma_I\right)$	γ_I	$t(x_H)<t,\ f_s^{/}\left(s_4,\gamma_I\right)^{-1}\left(x-x_E\right)+t_E<t<f_s^{/}\left(s_H^0,\gamma_I\right)^{-1}\left(x-x_D\right)+t_D$
XI	s_4	γ_I	$t(x_H)<t,\ \ t<f_s^{/}\left(s_4,\gamma_I\right)^{-1}\left(x-x_E\right)+t_E$

Table 3. Recovery factor calculations during sequential injection of formation- and low-salinity water

	s_I	$k^*{}_w$	s_{or}	$k^*{}_o$	n_w	n_o	β
HS water	0.15	0.5	0.2	1	2.77	4.5	0
LS water, wet	0.14	0.5	0.1	1	4.1	3.15	0
LS water, fines	0.15	0.5	0.2	1	2.77	4.5	1000
LS water, both	0.14	0.5	0.1	1	4.1	3.15	1000

4 Analytical Solutions of Oil Displacement by Low Salinity Polymer Flooding

4.1 Exact Solution for Non-Self-Similar Wave-Interaction Problem during Two-Phase Four-Component Flow in Porous Media

S. Borazjani, P. Bedrikovetsky, R. Farajzadeh

Abstract and Applied Analysis, Volume 2014, Article ID 731567, 13 pages.

Statement of Authorship

Title of Paper	Exact solution for non-self-similar wave-interaction problem during two-phase four-component flow in porous media
Publication Status	☑ Published ☐ Accepted for Publication ☐ Submitted for Publication ☐ Unpublished and Unsubmitted work written in manuscript style
Publication Details	S. Borazjani, P. Bedrikovetsky, R. Farajzadeh. (2014). Exact solution for non-self-similar wave-interaction problem during two-phase four-component flow in porous media. Abstract and Applied Analysis, Hindawi Publishing Corporation.

Principal Author

Name of Principal Author (Candidate)	Sara Borazjani
Contribution to the Paper	Derivation of the mathematical model, Derivation of exact solution, Analysis of the results, Writing the manuscript
Overall percentage (%)	85%
Certification:	This paper reports on original research I conducted during the period of my Higher Degree by Research candidature and is not subject to any obligations or contractual agreements with a third party that would constrain its inclusion in this thesis. I am the primary author of this paper.
Signature	Date 22.11.2015

Co-Author Contributions

By signing the Statement of Authorship, each author certifies that:

i. the candidate's stated contribution to the publication is accurate (as detailed above);

ii. permission is granted for the candidate in include the publication in the thesis; and

iii. the sum of all co-author contributions is equal to 100% less the candidate's stated contribution.

Name of Co-Author	Pavel Bedrikovetsky
Contribution to the Paper	Supervised development of the work, Manuscript review and assessment
Signature	Date 22.11.2015

Name of Co-Author	Rouhi Farajzadeh
Contribution to the Paper	Literature review; Problem formulation
Signature	Date 23-11-2015

Please cut and paste additional co-autho

Hindawi Publishing Corporation
Abstract and Applied Analysis
Volume 2014, Article ID 731567, 13 pages
http://dx.doi.org/10.1155/2014/731567

Research Article

Exact Solution for Non-Self-Similar Wave-Interaction Problem during Two-Phase Four-Component Flow in Porous Media

S. Borazjani,[1] P. Bedrikovetsky,[1] and R. Farajzadeh[2,3]

[1] *Australian School of Petroleum, The University of Adelaide, SA 5005, Australia*
[2] *Shell Global Solutions International, Rijswijk, The Netherlands*
[3] *Delft University of Technology, The Netherlands*

Correspondence should be addressed to S. Borazjani; sara.borazjani@adelaide.edu.au

Received 6 September 2013; Revised 27 December 2013; Accepted 29 December 2013; Published 12 March 2014

Academic Editor: Shuyu Sun

Analytical solutions for one-dimensional two-phase multicomponent flows in porous media describe processes of enhanced oil recovery, environmental flows of waste disposal, and contaminant propagation in subterranean reservoirs and water management in aquifers. We derive the exact solution for 3×3 hyperbolic system of conservation laws that corresponds to two-phase four-component flow in porous media where sorption of the third component depends on its own concentration in water and also on the fourth component concentration. Using the potential function as an independent variable instead of time allows splitting the initial system to 2×2 system for concentrations and one scalar hyperbolic equation for phase saturation, which allows for full integration of non-self-similar problem with wave interactions.

1. Introduction

Exact self-similar solutions of Riemann problems for hyperbolic systems of conservation laws and non-self-similar solutions of hyperbolic wave interactions have been derived for various flows in gas dynamics, shallow waters, and chromatography (see monographs [1–8]). For flow in porous media, hyperbolic systems of conservation laws describe two-phase multicomponent displacement [9, 10]. Consider

$$\frac{\partial s}{\partial t} + \frac{\partial f(s,c)}{\partial x} = 0 \tag{1}$$

$$\frac{\partial (cs + a(c))}{\partial t} + \frac{\partial (cf(s,c))}{\partial x} = 0, \tag{2}$$

where s is the saturation (volumetric fraction) of aqueous phase and f is the water flux. Equation (1) is the mass balance for water and (2) is the mass balance for each component in the aqueous solution. Under the conditions of thermodynamic equilibrium, the concentrations of the components adsorbed on the solid phase (a_i) and dissolved in the aqueous phase (c_i) are governed by adsorption isotherms:

$$a = a(c), \qquad a = (a_1, a_2, \ldots, a_n), \qquad c = (c_1, c_2, \ldots, c_n). \tag{3}$$

Exact and semianalytical solutions of one-dimensional flow problems are widely used in stream-line simulation for flow prediction in three-dimensional natural reservoirs [10]. The sequence of concentration shocks in the one-dimensional analytical solution is important for interpretation of laboratory tests in two-phase multicomponent flow in natural reservoir cores.

The scalar hyperbolic equations (1) and (2), $n = 0$, correspond to displacement of oil by water [9, 10]. The $(n+1) \times (n+1)$ system (1) and (2) describes two-phase flow of oleic and aqueous phases with n components (such as polymer and different salts) that may adsorb and be dissolved in both phases. These flows are typical for so-called chemical enhanced oil recovery displacements, like injections of polymers or surfactants, and for numerous environmental flows [9, 10]. For polymer injection in oil reservoirs, $i = 1$ corresponds to polymer and $i = 2, 3, \ldots, n$ to different ions.

Therefore the system (1) and (2) is called the multicomponent polymer-flooding model [11, 12]. Besides, $(n-1)\times(n-1)$ hyperbolic system (1) and (2) describes two-phase n-component displacement, which is typical for so-called gas methods of enhanced oil recovery [9, 10, 13, 14]. The processes of hot water injection with phase transitions, secondary migration of hydrocarbons with consequent formation of petroleum accumulations, enhanced geothermal energy projects, and injections into aquifers are described by the above systems. The Riemann problems correspond to continuous injection of chemical solutions or gases into oil reservoirs; the solutions are self-similar [3, 9, 14]. The wave-interaction problems correspond to piece-wise-constant initial-boundary conditions, for which the solutions are non-self-similar [1, 10, 15–17]. The wave-interaction solutions describe injection of limited slugs (banks) of chemical solutions or gaseous solvents driven in the reservoirs by water or gas [9, 10].

Riemann problem (1) and (2) with $n = 1$ has been solved with applications to various injections of polymers [17, 18], carbonized water and surfactants [19, 20], and so forth. More complex self-similar solutions of (1) and (2) for $n = 2, 3$ were obtained by Barenblatt et al. [21] and Braginskaya and Entov [22] and later by Johansen et al. and Winther et al. [11, 12, 23–25]. Analogous solutions for gas injection and $n = 3, 4, \ldots$ have been obtained by Orr and others [9, 13, 26–31].

The system (1) and (2) describes two-phase multicomponent displacements in large scale approximation, where the dissipative effects of capillary pressure, diffusion, and thermodynamic nonequilibrium are negligible if they are compared with advective fluxes under the large length scale of the natural subterranean reservoirs. Travelling waves near to shock discontinuities in dissipative systems have been presented in [10, 32]. A semianalytical global solutions have been obtained by Geiger et al. [33] and Schmid et al. [34]; see also [16].

The particular case of so-called multicomponent polymer flooding is the dependency of the component sorption concentration of its own concentration only $a_i(c_1, c_2, \ldots, c_n) = a_i(c_i)$. Exact solutions of the Riemann problem for this case show that the concentration of each component performs the jump without shocks of other components (see the corresponding solution in the books [10, 21]). Therefore, in concentration profiles, the shocks are located in order of decrease of derivatives of the sorption functions. In the case of Henry isotherms $a_i(c_i) = \Gamma_i c_i$, the shocks are located in order of increase of Henry's sorption coefficients Γ_i.

The distinguished invariant feature of $(n + 1) \times (n + 1)$ conservation law systems for two-phase multicomponent flows in porous media with sorption and phase transitions equations (1) and (2) is its splitting into an $n \times n$ auxiliary system for concentrations $c_i(x, t)$ and a scalar hyperbolic equation for saturation $s(x, t)$ [35, 36]. This splitting explains the simple form of Riemann problem solutions for system (1) and (2) as compared with gas dynamics or chromatography [1, 2, 37].

The non-self-similar solution of system (1) and (2), $n = 2$, for slug injections has been considered by Fayers [17], where the qualitative behaviour of characteristic lines and shocks has been described. The exact solutions of system (1) and (2) for $n = 2$ and 3 have been obtained in [15] (see book [10] for detailed derivations, in which the sorption of component depends on its own concentration only $a_i = a_i(c_i)$, $i = 1, 2, \ldots$). Numerous interactions of different saturation-concentration shocks occur after the injection, resulting in appearance of moving zones with different combinations of components. However, after all interactions, different component slugs are separated from each other. As in the case of continuous injection, the slugs are finally positioned in the order of decreasing sorption isotherm derivatives (da_i/dc_i). It seems that this simplified case draws the line where the analytical solutions can be found from the analysis of system (1) and (2) directly. Consideration of cross-effects $a_i = a_i(c_1, c_2, \ldots, c_n)$ in sorption functions equation (3) introduces significant difficulties into wave analysis, and even the Riemann problem cannot be solved for any arbitrary case $n = 2$ (see [38], where the Riemann solutions have been obtained for several particular cases).

The splitting technique reduces number of equations in (1) and (2) by one, allowing for exact solutions in more complex multicomponent cases [35–40]. The Riemann problem with cross-effects for adsorption $a_i = a_i(c_1, c_2)$ has been solved in [39, 41, 42] for continuous polymer injection with varying salinity using the splitting method. In the current paper, the exact solution for non-self-similar problem of injection of polymer slug with varying salinity followed by water drive is obtained.

The structure of the text is as follows. The particular case of the general system (1) and (2) that is discussed in the current work is introduced in Section 2 along with physics assumptions and initial-boundary conditions for slug injection problem. The detailed description of the splitting procedure for the system is discussed along with formulation of initial and boundary conditions for the auxiliary system which is presented in Section 3. Section 4 contains derivation of the Riemann solution that corresponds to the first stage of the slug injection. The wave-interaction slug injection problem is solved in Section 5. Section 6 contains a simplified solution for the particular case where the initial chemical concentration is zero, which corresponds to the case of polymer slug injection. The paper is concluded by physical interpretation of the solution obtained for chemical slug injection with different water salinity into oilfield (Sections 7 and 8).

2. Formulation of the Problem

Let us discuss the displacement of oil by aqueous chemical solution with water drive accounting for different salinities of formation and injected waters. In the following text, the component $n = 1$ is called the polymer, and that $n = 2$ is called the salt. The assumptions of the mathematical model are as follows: both phases are incompressible, dispersion and capillary forces are neglected, there are two phases (oleic and aqueous phases) and two components dissolved in water (polymer and salt), water and oil phases are immiscible, chemical and salt concentrations in water are negligibly small and do not affect the volume of the aqueous phase,

the fractional flow of the aqueous phase is affected by concentration of the dissolved chemical, the fractional flow is independent of salt concentration, chemical and salt do not dissolve in oil, linear sorption for the polymer $a = \Gamma c$, Henry's sorption coefficient Γ is salinity-dependent, salt does not adsorb on the rock, and temperature is constant.

The system of governing equations consists of mass balance equations for aqueous phase, for dissolved and adsorbed chemical, and for dissolved salt [8, 9]:

$$\frac{\partial s}{\partial t} + \frac{\partial f(s,c)}{\partial x} = 0 \tag{4}$$

$$\frac{\partial (cs + a(c,\beta))}{\partial t} + \frac{\partial (cf(s,c))}{\partial x} = 0 \tag{5}$$

$$\frac{\partial (\beta s)}{\partial t} + \frac{\partial (\beta f(s,c))}{\partial x} = 0, \tag{6}$$

where s is the water saturation, f is the fractional flow function, a is the polymer sorption isotherm, and c and β are chemical and salt concentrations, respectively.

The fractional flow function (water flux) depends on the water saturation s and on the chemical concentration c. The typical S-shapes of fractional flow functions f under $c = \text{const}$ are shown in Figure 1. The fractional flow is a monotonically decreasing function of c. Sorption isotherms are linear for fixed salinity $a(c,\beta) = \Gamma(\beta)c$. The functions f and a are assumed to be bounded and smooth.

The system (4)–(6) is a hyperbolic 3×3 system of conservation laws with unknowns s, c, and β.

The displacement of oil by chemical slug corresponds to the following initial-boundary problem:

$$x = 0 \begin{cases} \beta = 0, & c = c_1, \quad s = s^L, \quad t < 1 \\ \beta = 0, & c = c_2, \quad s = s^L, \quad t > 1 \end{cases} \tag{7}$$

$$t = 0, \quad \beta = 1, \quad c = c_2, \quad s = s^R. \tag{8}$$

For $t < 1$, during continuous injection of chemical solution with different salinity, the solution of system (4)–(6) subject to initial-boundary conditions equations (7) and (8) coincides with the solution of the Riemann problem:

$$x = 0, \quad \beta = 0, \quad c = c_1, \quad s = s^L \tag{9}$$

$$t = 0, \quad \beta = 1, \quad c = c_2, \quad s = s^R. \tag{10}$$

The initial condition is denoted by R in Figure 1 and the boundary condition corresponding to injection of the slug is denoted as L.

Generally $c(x,0) = c_2 > 0$ is positive. Further in the text, the component with concentration c is called "chemical," while for the case of the absence of this component initially in the reservoir $c(x,0) = c_2 = 0$ we use the term "polymer."

The solution of the Riemann problem is self-similar: $s(x,t) = s(\xi)$, $c(x,t) = c(\xi)$, $\beta(x,t) = \beta(\xi)$, $\xi = x/t$ and it can be found in [37, 39, 40]. The solution of the problem (7) and (8) in the neighbourhood of the point $(0,1)$ in (x,t)-plane is also self-similar. The global solution of the system (4)–(6) subject to the initial-boundary conditions equations (7) and (8) is non-self-similar; it expresses the interactions between hyperbolic waves occurring from decays of Riemann discontinuities in points $(0,0)$ and $(0,1)$ in (x,t)-plane.

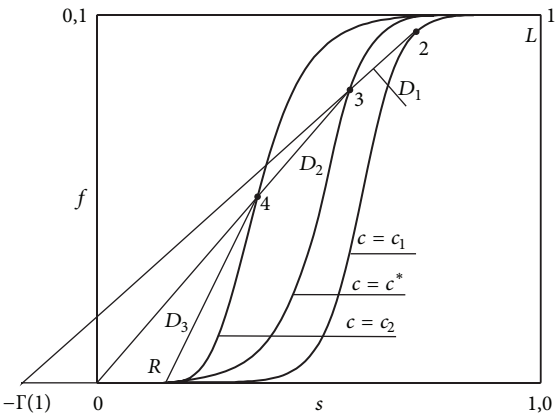

Figure 1: Fractional flow curves and Riemann problem solution, where c_1 is the slug concentration, c_2 is the initial concentration, and c^* is the intermediate concentration.

System of (4)–(6) subject to the initial and boundary conditions equations (9) and (10) is solved in Section 4 using the method so-called splitting procedure [35]. This procedure is explained in the next section.

3. Splitting Procedure

In the present section we briefly explain the splitting method for the solution of hyperbolic system of conservation laws equations (4)–(6).

3.1. Streamline/Potential Function and Auxiliary System. As it follows from divergent (conservation law) form of equation for mass balance for water (1) or (4), there does exist such a potential function $\varphi(x,t)$ that

$$\begin{aligned} s &= -\frac{\partial \varphi}{\partial x} \\ f &= \frac{\partial \varphi}{\partial t}; \end{aligned} \tag{11}$$

that is,

$$d\varphi = f dt - s dx, \tag{12}$$

$$\varphi(x,t) = \int_{0,0}^{x,t} f dt - s dx. \tag{13}$$

Equation (4) is merely the condition of equality of second derivatives of the potential φ as taken in different orders. It also expresses that the differential of the first order form equation (12) equals zero. The splitting procedure consists of changing the independent variables from (x,t) to (x,φ) in system (4)–(6). Figures 2 and 3 show the corresponding mapping [43, 44].

From fluid mechanics point of view, $\varphi(x,t)$ is a potential function, which equals the volume of fluid flowing through

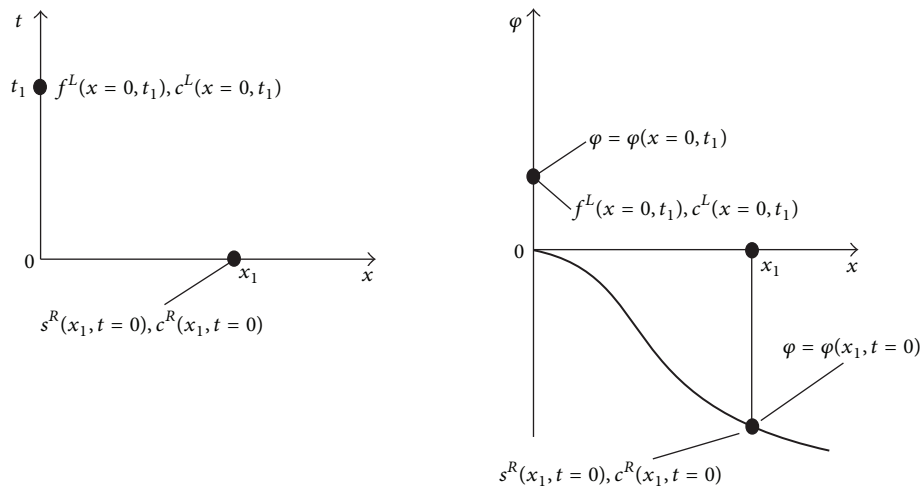

Figure 2: Introduction of potential function (Lagrangian coordinate) and mapping between independent variables.

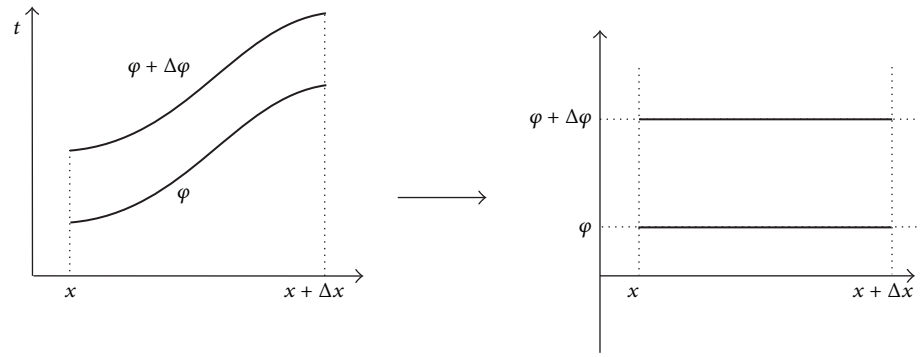

Figure 3: Derivation of mass balance equation in Eulerian and Lagrangian coordinate systems.

a trajectory connecting points $(0, 0)$ and (x, t). As it follows from (12), two streamlines in Figure 3 correspond to constant values of potential, that is, there is no flux through streamlines:

$$\varphi(x, t_2) - \varphi(x, t_1) = \int_{t_1}^{t_2} f(x, t)\, dt. \tag{14}$$

Equation (4) shows that the integral of (13) along the closed contour is equal to zero; that is, the volume of fluid flowing through a trajectory connecting points $(0, 0)$ and (x, t) is independent of trajectory and depends on end points only. The potential function equation (13) is determined in the way that one end of trajectory is fixed at point $(0, 0)$.

Let us derive the relationship between the elementary wave speeds of the system in (φ, x) coordinates and those of the large system in (t, x). Consider the trajectory $x = x_0(t)$ and its image $\varphi = \varphi_0(t)$ by the mapping equation (13):

$$\varphi_0(t) = \varphi(x_0(t), t). \tag{15}$$

Define the trajectory speeds as

$$D = \frac{dx}{dt}, \qquad V = \frac{dx}{d\varphi}. \tag{16}$$

Let us use x as a parameter for both curves $x = x_0(t)$ and $\varphi = \varphi_0(t)$. Taking derivation of both parts of (13) in x along trajectories and using speed definitions in (16), we obtain

$$\frac{1}{V} = \frac{f}{D} - s \tag{17}$$

from which follows the relationship between elementary wave speed in planes (x, t) and (x, φ):

$$D = \frac{f}{s + 1/V}. \tag{18}$$

For example, the eigenvalues of the system of equation in (t, x) plane λ_i and in (φ, x), Λ_i, are related by (Figure 4 [43, 44])

$$\Lambda_i(s, c) = \frac{f}{s + 1/\lambda_i}. \tag{19}$$

From now on, the independent variables (x, φ) are used in (4)–(6) instead of (x, t). Expressing the differential form dt from (12) as

$$dt = \frac{d\varphi}{f} + \frac{s\,dx}{f} \tag{20}$$

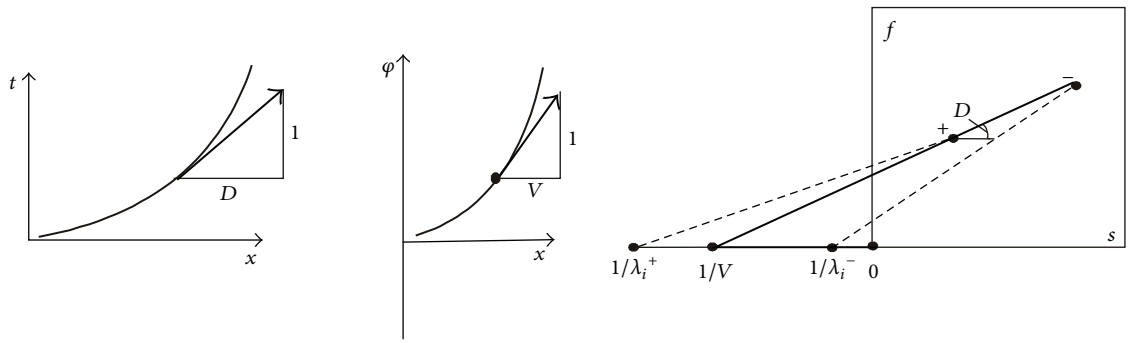

Figure 4: Speeds of a particle in Eulerian and Lagrangian coordinates.

and accounting for zero differential of the form dt

$$d^2t = 0 = \left[\frac{\partial}{\partial x}\left(\frac{1}{f}\right) - \frac{\partial}{\partial \varphi}\left(\frac{s}{f}\right)\right] dx d\varphi \tag{21}$$

we obtain the expression for (4) in coordinates (x, φ)

$$\frac{\partial (s/f)}{\partial \varphi} - \frac{\partial (1/f)}{\partial x} = 0. \tag{22}$$

So, (22) is the mass balance for water; that is, it is (4) rewritten in coordinates (x, φ).

Let us derive (5) in (x, φ) coordinates. The conservation laws for (5) in the integral form are

$$\oint_{\partial\Omega} (cf)\, dt - (cs + a)\, dx = 0, \tag{23}$$

where Ω is a closed domain $\Omega \subset R^2$, so the integral of (23) is taken over the closed contour.

Applying the definition of the potential function equation (13) into (23) yields

$$\oint_{\partial\Omega} c\,(f dt - s dx) - a dx = \oint_{\partial\Omega} c d\varphi - a dx = 0. \tag{24}$$

Tending the domain radius to zero and applying Green's theorem,

$$\frac{\partial a\,(c, \beta)}{\partial \varphi} + \frac{\partial c}{\partial x} = 0. \tag{25}$$

Now let us perform change of independent variables in (6) in (x, φ) coordinates as follows:

$$\iint \left(\frac{\partial (\beta s)}{\partial t} + \frac{\partial (\beta f\,(s, c))}{\partial x}\right) dx\, dt = \oint_{\partial\Omega} \beta s dx - \beta f\,(s, c)\, dt$$
$$= \oint \beta d\varphi = \iint \frac{\partial \beta}{\partial x} = 0. \tag{26}$$

Finally, the $(n + 1) \times (n + 1)$ system of conservation laws for two-phase n component chemical flooding in porous media with adsorption can be split into an $n \times n$ auxiliary system equations (25) and (26) and one independent lifting equation (22). The splitting is obtained from the change of independent variables (x, t) to (x, φ). This change of coordinates also transforms the water conservation law into the lifting equation. The solution of hyperbolic system (22), (25), and (26) consists of three steps: (1) solution of the auxiliary problem, (25), and (26) subject to initial and boundary conditions, (2) solution of the lifting equation, (22), and (3) determining time t for each point of the plane (x, φ) from (13).

The auxiliary system contains only equilibrium thermodynamic variables, while the initial system contains both hydrodynamic functions (phase's relative permeabilities and viscosities) and equilibrium thermodynamic variables.

The above splitting procedure is applied to the solution of displacement of oil by polymer slug with alternated salinity in the next section.

3.2. Formulation of the Splitting Problem for Two-Phase Flow with Polymers and Salt. Introducing new variables "density" F and "flux" U and applying the splitting technique, the 3×3 system (4)–(6) is transformed to the following form:

$$F = -\frac{s}{f}, \qquad U = \frac{1}{f} \tag{27}$$

$$\frac{\partial (F\,(U, c))}{\partial \varphi} + \frac{\partial (U)}{\partial x} = 0 \tag{28}$$

$$\frac{\partial a\,(c, \beta)}{\partial \varphi} + \frac{\partial c}{\partial x} = 0 \tag{29}$$

$$\frac{\partial \beta}{\partial x} = 0. \tag{30}$$

The auxiliary system equations (29) and (30) are independent of (28). The auxiliary system has thermodynamic nature since it contains only sorption function $a(c, \beta)$ and the unknowns are the component concentrations c and β. Equation (28) is the volume conservation for two immiscible phases. For the known auxiliary solution of (29) and (30), equation (28) is a scalar hyperbolic equation. Figure 5 shows the projection of the space of the large system into that of auxiliary system and the lifting procedure [43, 44].

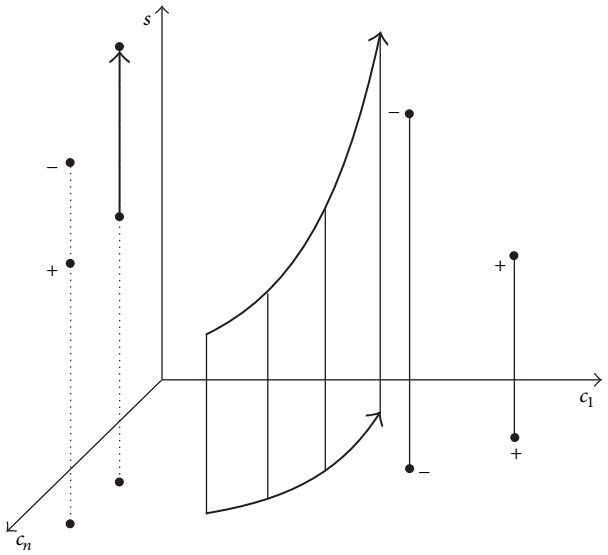

Figure 5: Projection of the space of the large system into that of auxiliary system and the lifting procedure using the solution of auxiliary system.

The boundary conditions for slug problem equation (7) are reformulated for coordinates (x, φ) as

$$x = 0 \begin{cases} \beta = 0, & c = c_1, \quad U = 1, \quad \varphi < 1 \\ \beta = 0, & c = c_2, \quad U = 1, \quad \varphi > 1. \end{cases} \tag{31}$$

Figure 2 shows how the initial and boundary conditions for the large system (4) and (6) are mapped into those for auxiliary system and the lifting equations (28)–(30).

The initial conditions for slug problem equation (8) are reformulated for coordinates (x, φ) as

$$\varphi = -\, s^R x, \quad \beta = 1, \quad c = c_2, \quad U = +\infty. \tag{32}$$

The solution of the Riemann problem for $\varphi < 1$ corresponds to the following initial and boundary conditions:

$$\begin{aligned} x = 0, \quad \beta = 0, \quad c = c_1, \quad U = 1 \\ \varphi = -s^R x, \quad \beta = 1, \quad c = c_2, \quad U = +\infty. \end{aligned} \tag{33}$$

4. Solution for the Riemann Problem

Let us discuss the solution of the problem equations (7) and (8) for $t < 1$, which is self-similar; that is, the boundary and initial conditions become (9) and (10).

The mass balance conditions on shocks which follow from the conservation law (Hugoniot-Rankine condition) form of the system (28)–(30) are

$$\sigma [U] = [F] \tag{34}$$

$$\sigma [c] = [a] \tag{35}$$

$$\sigma [\beta] = 0, \tag{36}$$

where σ is reciprocal to the shock velocity of (28)–(30). As salt and polymer concentration are connected by the thermodynamic equilibrium relationship $a(c, \beta)$, function a is discontinuous if c is discontinuous, so is β. Since F is a function of c and U, discontinuity of c and U yields discontinuity of F.

As it follows from equality (36), either $\sigma = 0$ or $[\beta] = 0$. From (34) and (35) it follows that if $\sigma = 0$, $[a] = 0$ and $[F] = 0$. If $[\beta] = 0$, from (35) and (36) it follows that $\sigma = [a]/[c]$ and $\sigma = [F]/[U]$; therefore it yields to $\sigma = [a]/[c] = [F]/[U]$. Finally from (34), if $[\beta] = 0$ and $[c] = 0$ this leads to $\sigma = [F]/[U]$.

The shock waves must obey the Lax evolutionary conditions [1–4, 9].

4.1. Solution for the Auxiliary System. The solution of auxiliary system is presented in Figure 6 by sequence of c-shock from point L into intermediate point and (c, β)-shock into point R. The corresponding formulae are as follows:

$$\begin{matrix} c(x, \varphi) \\ \beta(x, \varphi) \end{matrix} = \begin{cases} c_1, & \beta = 0, \quad \varphi > \Gamma(0)\, x \\ c^*, & \beta = 0, \quad 0 < \varphi < \Gamma(0)\, x \\ c_2, & \beta = 1, \quad -s^R x < \varphi < 0, \end{cases} \tag{37}$$

where the condition of continuity of function $a(c, \beta)$ on the shock with $\sigma = 0$, and (35) allows finding the intermediate concentration

$$c^* = \frac{\Gamma(1)}{\Gamma(0)} c_2. \tag{38}$$

4.2. Solution for the Lifting Equation. Figure 7 exhibits initial and boundary conditions for hydrodynamics lifting equation (28). Curves $F = F(U, c)$ are shown for constants $c = c_1$, $c = c_2$, and $c = c^*$; they are obtained from fractional flow curves $f = f(s, c)$ for the same constant values of concentration c. Point R corresponds to U tending to infinity and F tending to minus infinity, where the fractional flow f tends to zero. The tangent of the segment $(0, 0)$–(U, F) tends to $-s^R$.

The solution of lifting equation with known concentrations (37) is given by centred wave L–2, (c-U)-shock 2–>3, (β-c-U)-shock 3–>4, and U-shock 4–>R (Figure 7). The centred wave (L–2) is given by (39)

$$\frac{\varphi}{x} = \frac{\partial F\left(U^1, c_1\right)}{\partial U}. \tag{39}$$

Points 2 and 3 are determined by the condition of equality of U and c shock speeds:

$$\frac{\partial F\left(U_2, c_1\right)}{\partial U} = \frac{F_2\left(U_2, c_1\right) - F_3\left(U_3, c^*\right)}{U_2 - U_3} = \Gamma(0). \tag{40}$$

Point 4 is determined by condition of equality of the shock velocities c, β, and U:

$$F_3\left(U_3, c^*\right) = F_4\left(U_4, c_2\right) = 0. \tag{41}$$

Point 4 is connected to point R by U-shock:

$$\frac{F_4\left(U_4, c_2\right) - F_i\left(U_R, c_2\right)}{U_4 - U_i} = \frac{-s_4 f^R + s^R f_4}{f^R - f_4} = -s^R. \tag{42}$$

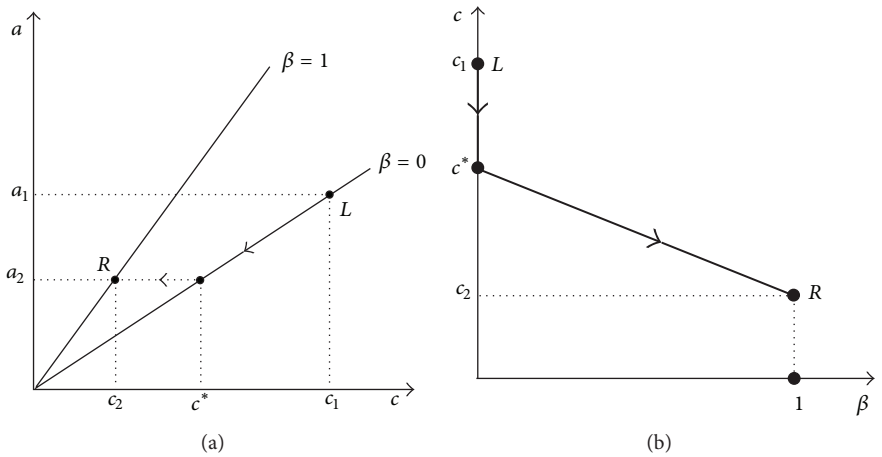

Figure 6: Solution of the auxiliary problem. (a) Adsorption isotherm for chemical for different water salinities and the Riemann problem solution; (b) Riemann problem solution on the plane of chemical concentration c and salinity β.

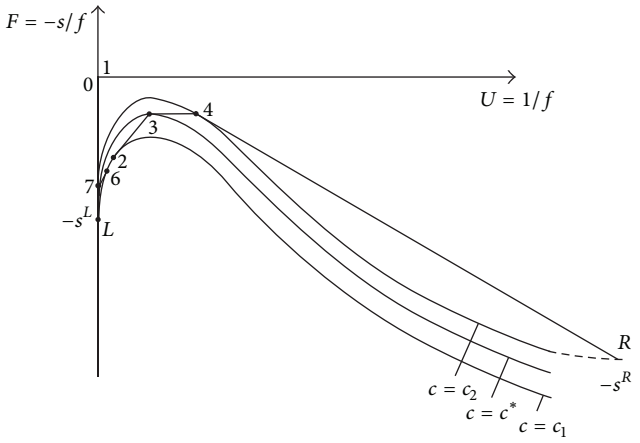

Figure 7: The image of the solution in (F-U) plane.

The solution of the Riemann problem equations (28)–(30) with free variables (x, φ) is given by the following formulae:

$$\begin{matrix} U(x,\varphi) \\ c(x,\varphi) \\ \beta(x,\varphi) \end{matrix} = \begin{cases} U^1\left(\dfrac{\varphi}{x}\right), & c_1, \quad \beta = 0, \quad \varphi > \Gamma(0)\, x \\ U_3, & c^*, \quad \beta = 0, \quad 0 < \varphi < \Gamma(0)\, x \\ U_4, & c_2, \quad \beta = 1, \quad -s^R x < \varphi < 0 \\ \infty, & c_2, \quad \beta = 1, \quad \varphi > -s^R x. \end{cases} \tag{43}$$

The expression $s = -UF(U, c)$ allows calculating saturation $s(x, \varphi)$:

$$\begin{matrix} s(x,\varphi) \\ c(x,\varphi) \\ \beta(x,\varphi) \end{matrix} = \begin{cases} s^1\left(\dfrac{\varphi}{x}\right), & c_1, \quad \beta = 0, \quad \varphi > \Gamma(0)\, x \\ s_3, & c^*, \quad \beta = 0, \quad 0 < \varphi < \Gamma(0)\, x \\ s_4, & c_2, \quad \beta = 1, \quad -s^R x < \varphi < 0 \\ s^R, & c_2, \quad \beta = 1, \quad \varphi < -s^R x. \end{cases} \tag{44}$$

Figure 8 shows the solution of the system (28)–(30) in (φ, x)-plane. For $\varphi < 1$, the solution is self-similar; the wave interaction occurs at $\varphi > 1$.

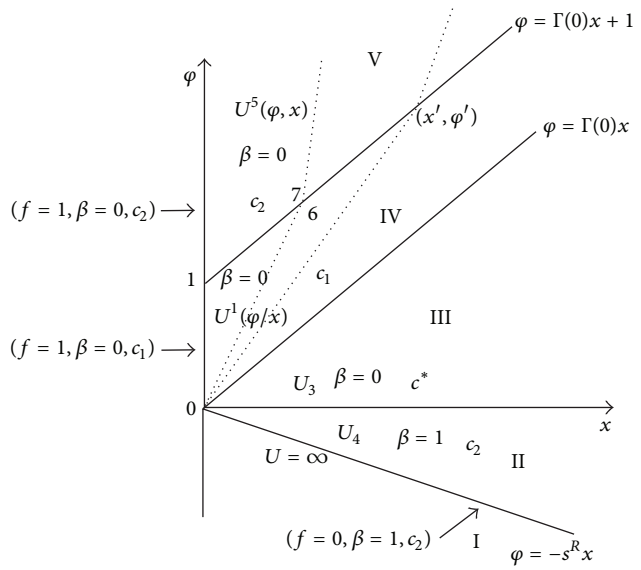

Figure 8: Solution of the auxiliary and lifting system for slug problem in (φ, x)-plane.

4.3. Inverse Mapping: Change of Variables from (φ, x) to (t, x). Time $t = t(x, \varphi)$ for solution is calculated from (12) along any path from point (x, φ) to point $(0, 0)$. The expression for time t in zone II is

$$t = \frac{1}{f_4}\int_0^{\varphi} d\varphi + \frac{s_4}{f_4}\int_0^{x} dx = \left(\frac{-s^R + s_4}{f_4}\right) x. \tag{45}$$

The expression for time t in zone III is

$$t = \frac{1}{f_3}\int_0^{\varphi} d\varphi + \frac{s_3}{f_3}\int_0^{x} dx = \frac{s_3}{f_3} x. \tag{46}$$

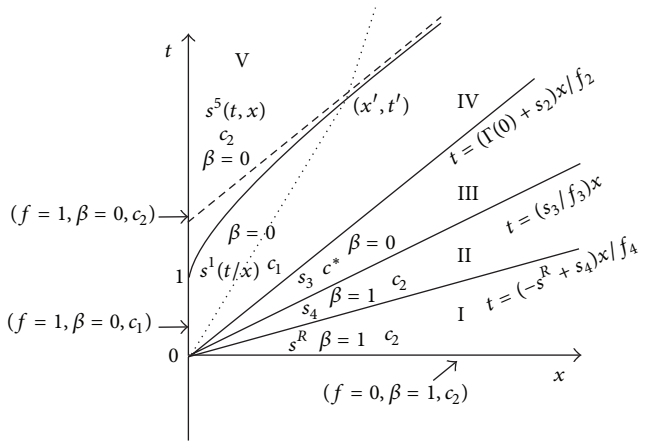

Figure 9: Non-self-similar solution of the problem for wave interactions in (x,t)-plane.

In zone IV, integral for calculation time, $t = \int_{0,0}^{x,\varphi}(d\varphi/f + sdx/f)$ is calculated along the characteristic in centred U-wave:

$$t = \frac{\varphi}{f\left(s^1(\varphi/x), c_1\right)} + \frac{s^1(\varphi/x)}{f\left(s^1(\varphi/x), c_1\right)}x. \tag{47}$$

Figure 9 shows the solution for the Riemann problem at $t < 1$; see Figure 10 for detailed description of the Riemann solution and profiles of unknown functions. Finally, the solution of the Riemann problem for the system (4)–(6) is

$$\begin{matrix} s(x,t) \\ c(x,t) \\ \beta(x,t) \end{matrix} = \begin{cases} s^1\left(\dfrac{t}{x}\right), & c_1, \quad \beta = 0, \quad t > \dfrac{\Gamma(0) + s_2}{f_2}x, \\ s_3, & c^*, \quad \beta = 0, \quad \dfrac{s_3}{f_3}x < t < \dfrac{\Gamma(0) + s_2}{f_2}x, \\ s_4, & c_2, \quad \beta = 1, \quad \dfrac{-s^R + s_4}{f_4}x < t < \dfrac{s_3}{f_3}x, \\ s^R, & c_2, \quad \beta = 1, \quad t < \dfrac{-s^R + s_4}{f_4}x. \end{cases} \tag{48}$$

5. Solution of the Slug Problem

Now let us solve the slug problem equations (31) and (32) for auxiliary system (29) and (30). The solution of Riemann problem at the point $(0,1)$ is given by c-shock with $c^- = c_2$ and $c^+ = c_1$ under constant β:

$$\begin{matrix} c(x,\varphi) \\ \beta(x,\varphi) \end{matrix} = \begin{cases} c_2, & \beta = 0, \quad \varphi > \Gamma(0)x + 1 \\ c_1, & \beta = 0, \quad \Gamma(0)x < \varphi < \Gamma(0)x + 1 \\ c^*, & \beta = 0, \quad 0 < \varphi < \Gamma(0)x \\ c_2, & \beta = 1, \quad -s^R x < \varphi < 0. \end{cases} \tag{49}$$

The solution of the auxiliary system is given by (49).

So, zone I in Figure 8 corresponds to initial conditions, the solution is given by point 4 in zone II, and point 3 holds in zone III. Centred waves equation (39) fills in zone IV. In zone V, $c = c_2$ and $\beta = 0$.

Now let us solve the lifting equation (28) with given $c(x,\varphi)$ and $\beta(x,\varphi)$.

The Hugoniot-Rankine condition for the rear slug front is

$$\frac{F\left(U^+, c_1\right) - F\left(U^-, c_2\right)}{U^+ - U^-} = \Gamma(0). \tag{50}$$

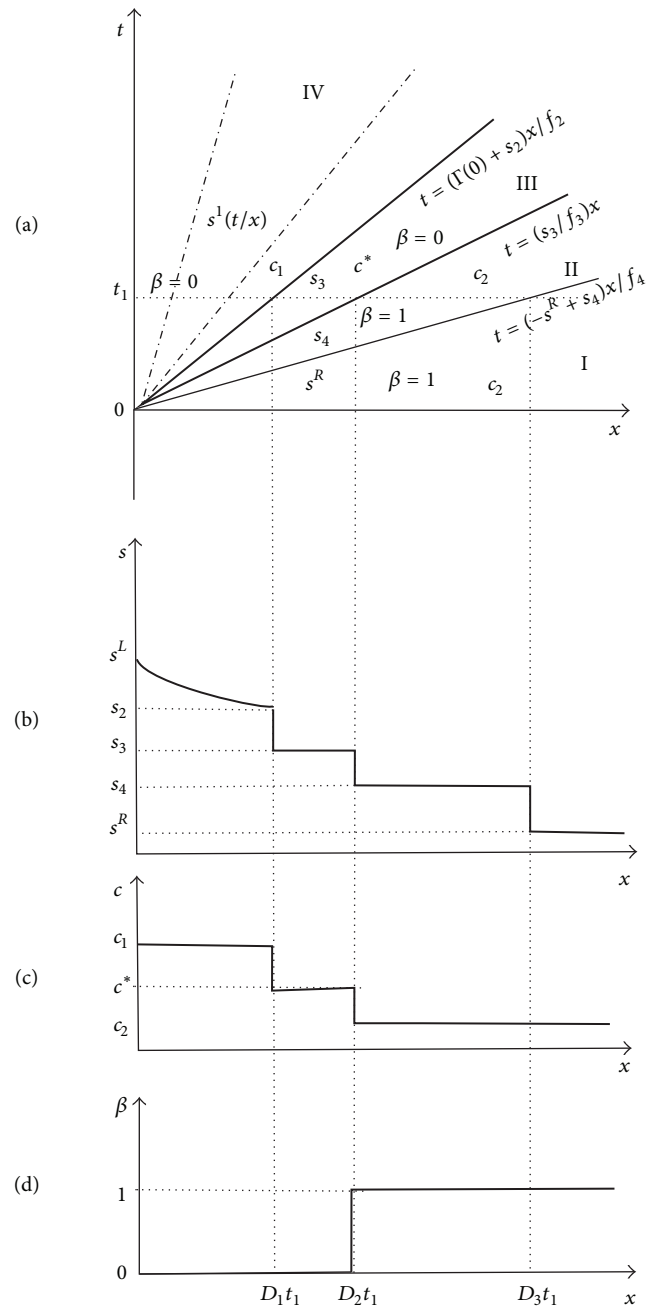

Figure 10: Solution of the Riemann problem: (a) trajectories of shock fronts and characteristic lines in (x,t)-plane; (b) saturation profile; (c) chemical concentration profile; (d) salinity profile.

U is constant along the characteristic lines behind the rear front

$$U_5(x,\varphi) = U^-\left(x',\varphi'\right), \tag{51}$$

where point (x',φ') is located on the rear front and is located on the same characteristic line with point (x,φ):

$$\frac{\varphi-\varphi'}{x-x'} = \frac{\partial F(U_5,c_1)}{\partial U}. \tag{52}$$

The solution of lifting equation $U(x,\varphi)$ is given by different formulae in zones I–V:

$$\begin{matrix} U(x,\varphi) \\ c(x,\varphi) \\ \beta(x,\varphi) \end{matrix} = \begin{cases} U_5(x,\varphi), & c_2, & \beta=0, & \varphi > \Gamma(0)\,x+1 \\ U^1\left(\dfrac{\varphi}{x}\right), & c_1, & \beta=0, & \Gamma(0)\,x<\varphi<\Gamma(0)\,x+1 \\ U_3, & c^*, & \beta=0, & 0<\varphi<\Gamma(0)\,x \\ U_4, & c_2, & \beta=1, & -s^R x<\varphi<0 \\ \infty, & c_2, & \beta=1, & \varphi>-s^R x, \end{cases} \tag{53}$$

where the equation for rear front of the chemical slug in the auxiliary plane is

$$\varphi = \Gamma(0)\,x+1. \tag{54}$$

Finally, the solution of auxiliary problem equation (53) allows calculating $t(x,\varphi)$ for zones I, II, ..., V. Let us start with determining time t along the rear front of the slug. The centred s-wave propagates ahead of the rear front

$$\frac{\varphi}{x} = \frac{f\left(s^+,c_1\right)-s^+f'\left(s^+,c_1\right)}{f'\left(s^+,c_1\right)}. \tag{55}$$

From (54), (55) follow the expression for $x_D(\varphi_D)$ in a parametric form:

$$x_D\left(s^+\right) = \frac{f'\left(s^+,c_1\right)}{f\left(s^+,c_1\right)-f'\left(s^+,c_1\right)\left(s^++\Gamma\right)} = \frac{f'\left(s^+,c_1\right)}{\Delta} \tag{56}$$

$$\begin{aligned} \varphi_D\left(s^+\right) &= \frac{f\left(s^+,c_1\right)-s^{1^+}f'\left(s^+,c_1\right)}{f\left(s^+,c_1\right)-f'\left(s^+,c_1\right)\left(s^++\Gamma\right)} \\ &= \frac{f\left(s^+,c_1\right)-s^{1^+}f'\left(s^+,c_1\right)}{\Delta}. \end{aligned} \tag{57}$$

Integration of the form (41) along the rear front gives

$$\begin{aligned} t_D &= \frac{\varphi}{f\left(s^+(\varphi,x),c_2\right)} + \frac{s^+(\varphi,x)}{f\left(s^+(\varphi,x),c_2\right)}x \\ t_D &= \frac{1}{f\left(s^+,c_1\right)-f'\left(s^+,c_1\right)\left(s^{1^+}+\Gamma\right)} = \frac{1}{\Delta}. \end{aligned} \tag{58}$$

Finally, the solution of the slug problem for the system (4)–(6) subject to initial and boundary conditions equations (7) and (8) is (Figure 9)

$$\begin{matrix} s(x,t) \\ c(x,t) \\ \beta(x,t) \end{matrix} = \begin{cases} s_5(t,x), & c_2, & \beta=0, & t>\dfrac{\Gamma(0)+s_5(t,x)}{f_5\left(s_5(t,x),c_2\right)}x+1 \\ s^1\left(\dfrac{t}{x}\right), & c_1, & \beta=0, & \dfrac{\Gamma(0)+s_2}{f_2}x<t<\dfrac{\Gamma(0)+s_5(t,x)}{f_5\left(s_5(t,x),c_2\right)}x+1 \\ s_3, & c^*, & \beta=0, & \dfrac{s_3}{f_3}x<t<\dfrac{\Gamma(0)+s_2}{f_2}x \\ s_4, & c_2, & \beta=1, & \dfrac{-s^R+s_4}{f_4}x<t<\dfrac{s_3}{f_3}x \\ s^R, & c_2, & \beta=1, & t<\dfrac{-s^R+s_4}{f_4}x. \end{cases} \tag{59}$$

Figure 11 presents trajectories of shock fronts in (x,t)-plane along with profiles of unknowns s, c, and β at typical moments.

Here the trajectory of the rear slug front $x_D = x_D(t)$ is given in a parametric form (Figure 12)

$$\begin{aligned} \frac{1}{x_D} &= s_B+\Gamma(0) \\ \frac{1}{t_D} &= f_A, \end{aligned} \tag{60}$$

where s_B is the abscissa of point B and f_A is the ordinate of point A (Figure 12). Equations (60) can be solved graphically. Straight line AB is a tangent to the fractional flow curve $c = c_1$, the tangent point in $s+$. The rear front position x_D is determined by the interval BC at the moment determined by AC.

6. Particular Case for the Polymer Absence in the Reservoir before the Injection

In reality, there is no chemical initially in the reservoir during the majority of chemical enhanced oil recovery applications; that is, $c(x,0) = 0$. For zero initial polymer concentration, the intermediate polymer concentration is equal to zero, so the points ahead and behind the β-shock coincide in planes (c,a) and (s,f). The particular simplified solution is (Figures 13 and 14)

$$\begin{matrix} s(x,t) \\ c(x,t) \\ \beta(x,t) \end{matrix} = \begin{cases} s_5(t,x), & c=0, & \beta=0, & t>\dfrac{\Gamma(0)+s_5(t,x)}{f_5\left(s_5(t,x),c_2\right)}x+1 \\ s^1\left(\dfrac{t}{x}\right), & c=c_1, & \beta=0, & \dfrac{\Gamma(0)+s_2}{f_2}x<t<\dfrac{\Gamma(0)+s_5(t,x)}{f_5\left(s_5(t,x),c_2\right)}x+1 \\ s_3, & c=0, & \beta=0, & \dfrac{s_3}{f_3}x<t<\dfrac{\Gamma(0)+s_2}{f_2}x \\ s_3, & c=0, & \beta=1, & \dfrac{-s^R+s_3}{f_3}x<t<\dfrac{s_3}{f_3}x \\ s^R, & c=0, & \beta=1, & t<\dfrac{-s^R+s_3}{f_3}x. \end{cases} \tag{61}$$

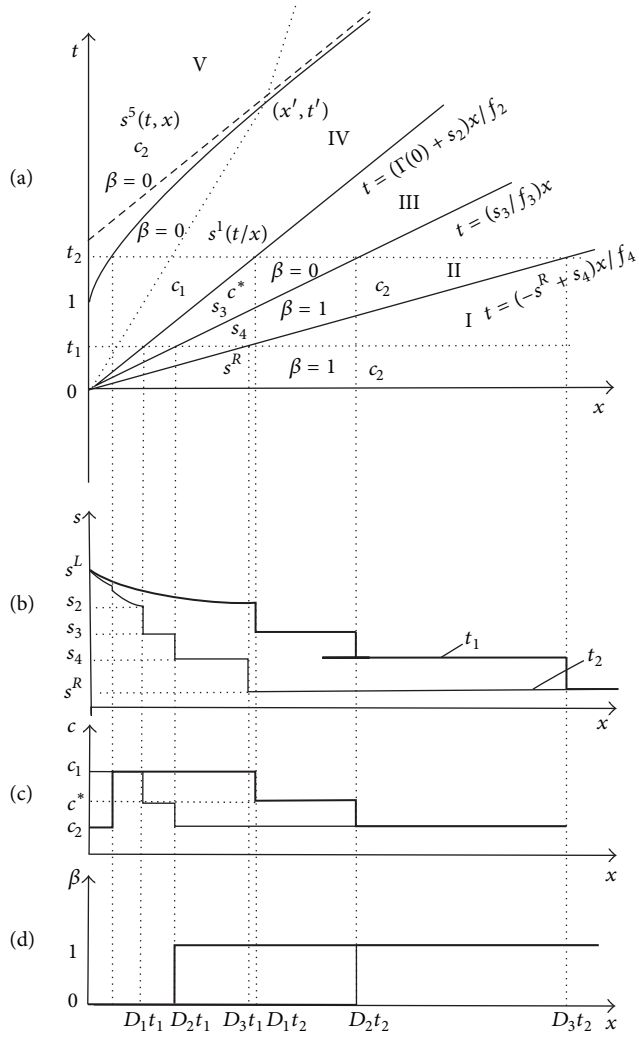

FIGURE 11: The solution of the slug injection problem: (a) trajectories of shock fronts and characteristic lines in (x, t)-plane; (b) saturation profile; (c) chemical concentration profile; (d) salinity profile.

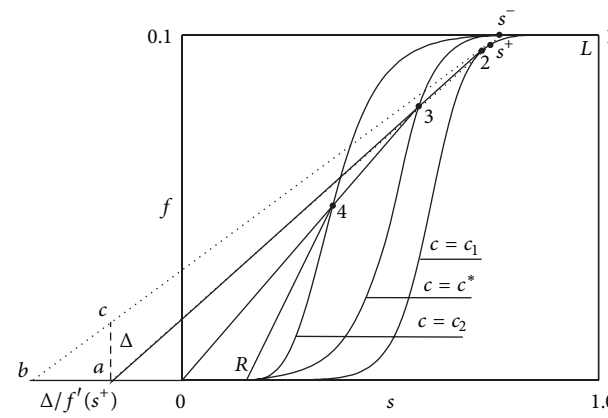

FIGURE 12: Solution of the lifting equation in (s, f)-plane.

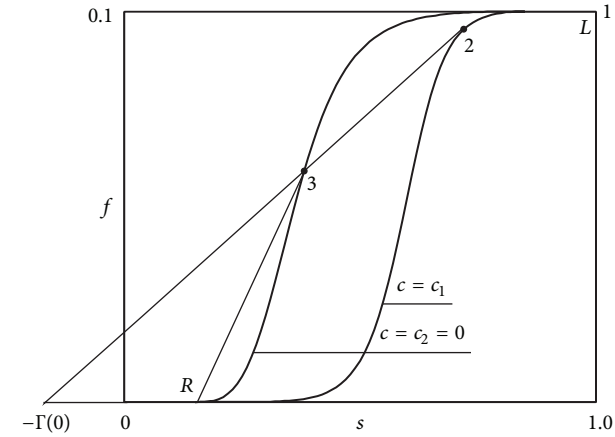

FIGURE 13: Solution of the lifting system in $(f\text{-}s)$ plane when $c_2 = 0$.

7. Fluid Mechanics Interpretation of the Solution

Following exact solution equations (4)–(9), let us describe structure of two-phase flow with chemical and salt additives during chemical slug injection.

During continuous injection $t < 1$, the solution of chemical slug injection coincides with that of continuous chemical injection. Initial conditions equation (10) is shown by point R that corresponds to low initial saturation and initial concentrations of chemical c_2 and of salt $\beta = 1$. The boundary condition at $x = 0$ corresponds to point L of injection of chemical solution with concentration c_1 and salinity $\beta = 0$. The path of Riemann problem solution in plane (s, f) consists of centred s-wave with injected chemical concentration and unity salinity, c-s-shock 2–>3, c, s, β-shock 3–>4, and s-shock 4–>R into initial point (Figure 1). Following nomenclature by Courant and Friedrichs [1] and Lake [9], the Riemann solution is L–2–>3–>4–>R. Shock 2–>3 in plane (c, β) is horizontal; shock 3–>4 is vertical (Figure 6(b)). Shock 2–>3 in plane (c, a) occurs along the sorption isotherm; shock 3–>4 is a horizontal jump from isotherm $c = c^*$ to that $c = c_2$ (Figure 7).

The trajectories of shocks 2–>3, 3–>4, and 4–> R are shown in Figure 7. Shock velocities are constant, so the trajectories are straight lines. Let us fix the position $x = 1$ of the raw of production wells. Before arrival of the front 4–> R at the moment $t = 1/D_3$, oil with fraction of water f^R and initial concentrations of chemical and salt is produced. After arrival of the front, water-oil mixture with water fraction f_4 and initial concentrations of chemical and salt is produced until the arrival of the 3–>4 front at the moment $t = 1/D_2$.

The corresponding profiles of saturation and concentrations are shown in Figure 10. The moment t_1 for profiles is fixed in Figure 10(a), allowing defining positions of all fronts in this moment. Corresponding profiles at that moment for saturation, chemical concentration, and salinity are shown in Figures 10(b), 10(c), and 10(d), respectively. The saturation profile consists of declining interval s^L–s_2 in s-wave, two oil-water banks s_3 and s_4, and the initial undisturbed zone s^R. The chemical concentration profile consists of injected value $c = c_1$ in s-wave, intermediate value c^* in s_3-bank, and initial

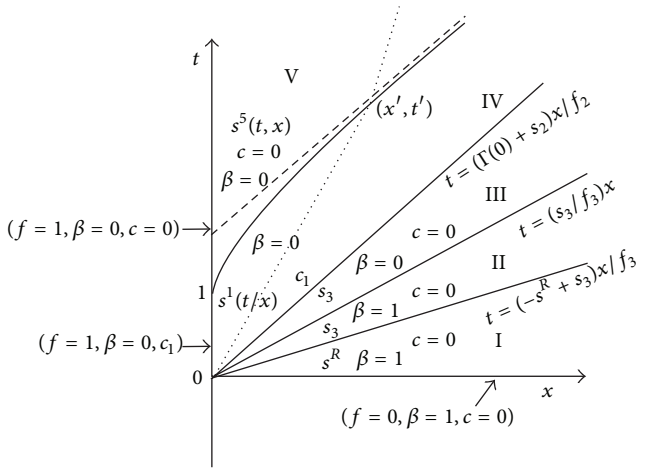

FIGURE 14: Non-self-similar solution of the problem for wave interactions in (x, t)-plane when $c_2 = 0$.

concentration c_2 in s_4-bank and in the initial zone. Salinity β-profile consists of injected value in zones IV and III and initial value in other zones.

Injection of water without chemical and with salinity $\beta = 0$ starts at the moment $t = 1$. The flow is not self-similar anymore. The front trajectories and profiles are shown in Figure 11. The solution for slug problem coincides with the solution for continuous injection ahead of the rear front $x_D(t)$. The profiles taken at the moment $t_1 < 1$ during continuous injection (Figure 11) coincide with those from Figure 10.

The propagation of the rear slug front from the beginning of water drive injection in the reservoir is shown in Figure 11(a). The rear front velocity decreases reaching the value of the forward front D_3 when time tends to infinity. The slug thickness increases and stabilises.

The profiles are shown in Figures 11(b), 11(c), and 11(d) for the moment after the beginning of slug injection $t_2 > 1$. Saturation decreases in a simple wave behind the rear slug front, jumps down on the front, decreases in centred s-wave in the slug, and is constant in zones II, II, and I. Chemical slug dissolution during the water drive injection is shown in Figure 11(c). There does occur the full concentration shock from zero behind the read slug front to the injected value in the slug. Further in the reservoir, there does appear a zone of intermediate chemical concentration c^* in the bank s_3. The concentration is equal to its initial value in banks s_4 and in the initial zone. So, dissolution of slug occurs in the initial water by formation of oil-water bank s_3 with lower chemical concentration. Salinity changes by full shock on the front between zones III and II.

8. Conclusions

Application of the splitting method to 3×3 conservation law system describing two-phase four-component flow in porous media allows drawing the following conclusions.

(1) The method of splitting between hydrodynamics and thermodynamics in system of two-phase multicomponent flow in porous media allows obtaining an exact solution for non-self-similar problem of displacement of oil by chemical slug with different water salinity for the case of linear polymer adsorption affected by water salinity.

(2) The solution consists of explicit formulae for water saturation and polymer and salt concentrations in the continuity domains and of implicit formulae for front trajectories.

(3) First integrals for front trajectories allow for graphical interpretation at the hodograph plane, yielding a graphical method for finding the front trajectories.

(4) For linear sorption isotherms, the solution depends on three fractional flow curves that correspond to initial reservoir state R, injected fluid L, and an intermediate curve for intermediate polymer concentration and injected salinity; the value for intermediate polymer concentration is the part of exact solution.

(5) For linear sorption isotherms, the only continuous wave is s-wave with constants c and β; concentrations c and β change only across the fronts by jumps; thus the solution of any problem with piece-wise constant initial and boundary conditions is reduced to interactions between s-waves and shocks.

(6) Introduction of salinity dependency for sorption of the chemical introduces the intermediate (c, β)-shock into the solution of the Riemann problem; this shock interacts with s-wave and concentration shocks in the solution of any problem with piece-wise constant initial and boundary conditions.

(7) The exact solution shows that the injected chemical slug dissolves in the connate reservoir water rather than in the chemical-free water injected after the slug.

Conflict of Interests

The authors declare that there is no conflict of interests regarding the publication of this paper.

Acknowledgments

Long-term cooperation in hyperbolic systems and fruitful discussions with Professors A. Shapiro (Technical University of Denmark), Y. Yortsos (University of Southern California), A. Roberts (University of Adelaide), A. Polyanin (Russian Academy of Sciences), M. Lurie, and V. Maron (Moscow Oil and Gas Gubkin University) are gratefully acknowledged. The reviewers are gratefully acknowledged for their critical comments yielding to significant improvement of the text.

References

[1] R. Courant and K. O. Friedrichs, *Supersonic Flow and Shock Waves*, Springer, New York, NY, USA, 1976.

[2] I. M. Gel'fand, "Some problems in the theory of quasi-linear equations," *Uspekhi Matematicheskikh Nauk*, vol. 14, no. 2, pp. 87–158, 1959.

[3] A. G. Kulikovskii, N. V. Pogorelov, and A. Yu. Semenov, *Mathematical Aspects of Numerical Solution of Hyperbolic Systems*, vol. 118, Chapman & Hall/CRC Press, Boca Raton, Fla, USA, 2001.

[4] B. L. Rozhdestvenski and N. N. Ianenko, *Systems of Quasilinear Equations and Their Application to the Dynamics of Gases*, vol. 55, American Mathematical Society, 1983.

[5] G. B. Whitham, *Linear and Nonlinear Waves*, vol. 42, John Wiley & Sons, Hoboken, NJ, USA, 2011.

[6] A. Kulikovskii and E. Sveshnikova, *Nonlinear Waves in Elastic Media*, CRC Press, Boca Raton, Fla, USA, 1995.

[7] J. D. Logan, *An Introduction to Nonlinear Partial Differential Equations*, vol. 93, John Wiley & Sons, Hobokon, NJ, USA, 2010.

[8] H. K. Rhee, R. Aris, and N. R. Amundson, *First-Order Partial Differential Equations: Theory and Application of Hyperbolic Systems of Quasilinear Equations*, Dover, New York, NY, USA, 2001.

[9] L. W. Lake, *Enhanced Oil Recovery*, Prentice Hall, Englewood Cliffs, NJ, USA, 1989.

[10] P. Bedrikovetsky, *Mathematical Theory of Oil and Gas Recovery: With Applications to Ex-USSR Oil and Gas Fields*, Kluwer Academic Publishers, Boston, Mass, USA, 1993.

[11] T. Johansen, A. Tveito, and R. Winther, "A Riemann solver for a two-phase multicomponent process," *SIAM Journal on Scientific and Statistical Computing*, vol. 10, no. 5, pp. 846–879, 1989.

[12] T. Johansen and R. Winther, "The Riemann problem for multicomponent polymer flooding," *SIAM Journal on Mathematical Analysis*, vol. 20, no. 4, pp. 908–929, 1989.

[13] R. Johns and F. M. Orr Jr., "Miscible gas displacement of multicomponent oils," *SPE Journal*, vol. 1, pp. 39–50, 1996.

[14] F. M. Orr Jr., *Theory of Gas Injection Processes*, Tie-Line Publications, Copenhagen, Denmark, 2007.

[15] P. Bedrikovetsky, "Displacement of oil by a chemical slug with water drive," *Journal of Fluid Dynamics*, vol. 3, pp. 102–111, 1982.

[16] V. G. Danilov and D. Mitrovic, "Smooth approximations of global in time solutions to scalar conservation laws," *Abstract and Applied Analysis*, vol. 2009, Article ID 350762, 26 pages, 2009.

[17] F. Fayers, "Some theoretical results concerning the displacement of a viscous oil by a hot fluid in a porous medium," *Journal of Fluid Mechanics*, vol. 13, pp. 65–76, 1962.

[18] E. L. Claridge and P. L. Bondor, "A graphical method for calculating linear displacement with mass transfer and continuously changing mobilities," *SPE Journal*, vol. 14, no. 6, pp. 609–618, 1974.

[19] G. J. Hirasaki, "Application of the theory of multicomponent, multiphase displacement to three-component, two-phase surfactant flooding," *SPE Journal*, vol. 21, no. 2, pp. 191–204, 1981.

[20] G. A. Pope, L. W. Lake, and F. G. Helfferich, "Cation exchange in chemical flooding—part 1: basic theory without dispersion," *SPE Journal*, vol. 18, no. 6, pp. 418–434, 1978.

[21] G. I. Barenblatt, V. M. Entov, and V. M. Ryzhik, *Theory of Fluid Flows through Natural Rocks*, Kluwer Academic Publishers, London, UK, 1989.

[22] G. S. Braginskaya and V. M. Entov, "Nonisothermal displacement of oil by a solution of an active additive," *Fluid Dynamics*, vol. 15, no. 6, pp. 873–880, 1980.

[23] O. Dahl, T. Johansen, A. Tveito, and R. Winther, "Mulicomponent chromatography in a two phase environment," *SIAM Journal on Applied Mathematics*, vol. 52, no. 1, pp. 65–104, 1992.

[24] T. Johansen, Y. Wang, F. M. Orr Jr., and B. Dindoruk, "Four-component gas/oil displacements in one dimension—part I: global triangular structure," *Transport in Porous Media*, vol. 61, no. 1, pp. 59–76, 2005.

[25] T. Johansen and R. Winther, "The solution of the Riemann problem for a hyperbolic system of conservation laws modeling polymer flooding," *SIAM Journal on Mathematical Analysis*, vol. 19, no. 3, pp. 541–566, 1988.

[26] P. Bedrikovetsky and M. Chumak, "Riemann problem for two-phase four-and morecomponent displacement (Ideal Mixtures)," in *Proceedings of the 3rd European Conference on the Mathematics of Oil Recovery*, 1992.

[27] V. Entov, F. Turetskaya, and D. Voskov, "On approximation of phase equilibria of multicomponent hydrocarbon mixtures and prediction of oil displacement by gas injection," in *Proceedings of the 8th European Conference on the Mathematics of Oil Recovery*, 2002.

[28] V. Entov and D. Voskov, "On oil displacement by gas injection," in *Proceedings of the 7th European Conference on the Mathematics of Oil Recovery*, 2000.

[29] R. T. Johns, B. Dindoruk, and F. M. Orr Jr., "Analytical theory of combined condensing/vaporizing gas drives," *SPE Advanced Technology Series*, vol. 1, no. 2, pp. 7–16, 1993.

[30] C. Wachmann, "A mathematical theory for the displacement of oil and water by alcohol," *Old SPE Journal*, vol. 4, pp. 250–266, 1964.

[31] A. Zick, "A combined condensing/vaporizing mechanism in the displacement of oil by enriched gases," in *Proceedings of the SPE Annual Technical Conference and Exhibition*, 1986.

[32] O. M. Alishaeva, V. M. Entov, and A. F. Zazovskii, "Structures of the conjugate saturation and concentration discontinuities in the displacement of oil by a solution of an active material," *Journal of Applied Mechanics and Technical Physics*, vol. 23, no. 5, pp. 675–682, 1982.

[33] S. Geiger, K. S. Schmid, and Y. Zaretskiy, "Mathematical analysis and numerical simulation of multi-phase multi-component flow in heterogeneous porous media," *Current Opinion in Colloid and Interface Science*, vol. 17, no. 3, pp. 147–155, 2012.

[34] K. S. Schmid, S. Geiger, and K. S. Sorbie, "Analytical solutions for co- and counter-current imbibition of sorbing, dispersive solutes in immiscible two-phase flow," in *Proceedings of the 12th European Conference on the Mathematics of Oil Recovery*, 2012.

[35] A. P. Pires, P. G. Bedrikovetsky, and A. A. Shapiro, "A splitting technique for analytical modelling of two-phase multicomponent flow in porous media," *Journal of Petroleum Science and Engineering*, vol. 51, no. 1-2, pp. 54–67, 2006.

[36] A. P. Pires, *Splitting between thermodynamics and hydrodynamics in the processes of enhanced oil recovery [Ph.D. thesis]*, Laboratory of Petroleum Exploration and Production, North Fluminense State University UENF, 2003.

[37] H.-K. Rhee, R. Aris, and N. R. Amundson, "On the theory of multicomponent chromatography," *Philosophical Transactions of the Royal Society A*, vol. 267, no. 1182, pp. 419–455, 1970.

[38] V. M. Entov and A. F. Zazovskii, "Displacement of oil by a solution of an active and a passive additive," *Fluid Dynamics*, vol. 17, no. 6, pp. 876–884, 1982.

[39] C. B. Cardoso, R. C. A. Silva, and A. P. Pires, "The role of adsorption isotherms on chemical-flooding oil recovery,"

in *Proceedings of the SPE Annual Technical Conference and Exhibition (ATCE '07)*, pp. 773–780, November 2007.

[40] B. Vicente, V. Priimenko, and A. Pires, "Streamlines simulation of polymer slugs injection in petroleum reservoirs," in *Proceedings of the SPE Latin America and Caribbean Petroleum Engineering Conference*, 2012.

[41] S. Oladyshkin and M. Panfilov, "Splitting the thermodynamlics and hydrodynamics in compositional gas-liquid flow through porous reservoirs," in *Proceedings of the 10th European Conference on the Mathematics of Oil Recovery*, 2006.

[42] P. M. Ribeiro and A. P. Pires, "The displacement of oil by polymer slugs considering adsorption effects," in *Proceedings of the SPE Annual Technical Conference and Exhibition (ATCE '08)*, pp. 851–865, September 2008.

[43] P. Bedrikovetski, A. Pires, and A. Shapiro, "Conservation law system for two-phase n-component flow in porous media: splitting between thermodynamics and hydrodynamics," in *Proceedings of the 10th International Congress on Hyperbolic Problems Theory*, 2004.

[44] A. Pires, P. Bedrikovetsky, and A. Shapiro, "Splitting between thermodynamics and hydrodynamics in compositional modelling," in *Proceedings of the 9th European Conference on the Mathematics of Oil Recovery*, 2004.

4.2 Analytical Solutions of Oil Displacement by a Polymer Slug with Varying Salinity

S. Borazjani, P. Bedrikovetsky, R. Farajzadeh

Journal of Petroleum Science and Engineering, 140 (2016) 28-40

Statement of Authorship

Title of Paper	Oil displacement by polymer slug with varying salinity
Publication Status	☐ Published ☐ Accepted for Publication ☑ Submitted for Publication ☐ Unpublished and Unsubmitted work written in manuscript style
Publication Details	S. Borazjani, P. Bedrikovetsky, R. Farajzadeh, Oil displacement by polymer slug with varying salinity. Submitted to Journal of petroleum science and engineering (2015)

Principal Author

Name of Principal Author (Candidate)	Sara Borazjani
Contribution to the Paper	Derivation of the mathematical model, Derivation of the exact solution, Analysis of the results, Writing the manuscript
Overall percentage (%)	80%
Certification:	This paper reports on original research I conducted during the period of my Higher Degree by Research candidature and is not subject to any obligations or contractual agreements with a third party that would constrain its inclusion in this thesis. I am the primary author of this paper.
Signature	Date 22.11.2015

Co-Author Contributions

By signing the Statement of Authorship, each author certifies that:

i. the candidate's stated contribution to the publication is accurate (as detailed above);

ii. permission is granted for the candidate in include the publication in the thesis; and

iii. the sum of all co-author contributions is equal to 100% less the candidate's stated contribution.

Name of Co-Author	Pavel Bedrikovetsky
Contribution to the Paper	Supervised development of the work, Manuscript review and assessment
Signature	Date 22.11.2015

Name of Co-Author	Rouhi Farajzadeh
Contribution to the Paper	Literature review, Problem formulation, Article review and assessment
Signature	Date 23-11-2015

Please cut and paste additional co-autho

Journal of Petroleum Science and Engineering 140 (2016) 28–40

Contents lists available at ScienceDirect

Journal of Petroleum Science and Engineering

journal homepage: www.elsevier.com/locate/petrol

Analytical solutions of oil displacement by a polymer slug with varying salinity

S. Borazjani [a,*], P. Bedrikovetsky [a], R. Farajzadeh [b,c]

[a] The University of Adelaide, Australia
[b] Shell Global Solutions International, Rijswijk, The Netherlands
[c] Delft University of Technology, The Netherlands

ARTICLE INFO

Article history:
Received 22 September 2015
Received in revised form
7 December 2015
Accepted 3 January 2016
Available online 4 January 2016

Keywords:
Low salinity
Polymer flooding
Exact solution
Splitting method
Slugs with drive chase
Non-Newtonian

ABSTRACT

This paper presents an analytical solution of a non-self-similar, two-phase, multi-component problem of polymer slug injection with varying water salinity (ionic strength) in oil reservoirs. The non-Newtonian properties of polymers are incorporated into the fractional flow, yielding the velocity dependency of the fractional-flow function. Using the Lagrangian coordinate instead of time allows splitting the initial system ($n+1 \times n+1$) into a $n \times n$ system for concentrations and one scalar hyperbolic equation for phase saturation, which allows for full integration of the non-self-similar problem of wave interactions. The solution includes implicit formulae for saturation, polymer, and salt concentrations and front trajectories of the components. The solution allows determining the slug size of the low-salinity water that prevents the contact between the polymer and the high-salinity water.

1. Introduction

Polymer flooding aims at improving sweep efficiency of the water displacement process by increasing the mobility ratio between the displacing agent and the in-situ oil. This is achieved by adding a polymer to the aqueous phase. The rheology of the polymer solution depends on parameters such as polymer concentration, velocity, and salt concentration. For example, if polymer concentration is held constant, the viscosity of a polymer solution increases as salt concentration decreases. This means that for given oil viscosity target, potentially less polymer would be required to maintain mobility control as salinity decreases (Sorbie, 1991). Furthermore, it has been observed that more oil is released from rocks when the salinity of the aqueous phase is reduced. This is mainly attributed to modifications in the wetting state of the rock surface among other mechanisms (Lager et al., 2008; Mahani et al., 2015). This implies that the combined effect of low-salinity water and polymer can in principle be utilized to improve oil recovery in economically and operationally favourable conditions. To minimize the cost of low-salinity polymer (LSP) injection, usually a slug (fraction of the reservoir pore volume) of polymer is injected and then followed by one or more slugs with reduced polymer concentration and, finally, by a water drive.

Effects of the polymer and of lowering the salinity can be modelled through modifying the fractional-flow functions: addition of polymer increases viscosity of the displacing agent, and lowering the salinity affects the relative permeability parameters (Mohammadi and Gary, 2012). Analytical methods are useful in understanding the underlying physics of many enhanced oil recovery processes (Pope, 1980; Bedrikovetsky, 1993; Lake, 1989). These methods can also be used to check the accuracy of the numerical schemes that are employed for large-scale simulations. Multiple discontinuities in the solutions of multi-component slug injections typically create major difficulties in numerical modelling, whereas the analytical solutions provide trajectories for the multiple shocks and the parameter jumps across the trajectories. Moreover, one-dimensional analytical models form the basis for streamline and front-track simulators of three-dimensional flows in heterogeneous formations (Ewing, 1983; Holden and Risebro, 2002).

Continuous injection of a fluid having a constant composition into a reservoir initially saturated by another fluid with a constant composition corresponds to corresponds to so-called Riemann problems, with initial conditions corresponding to the reservoir fluid saturation and composition, and boundary conditions of the injected fluid fractional flow and composition. The Riemann solutions are self-similar (Gel'fand, 1959; Courant and Friedrichs, 1976), and depend on the group $\xi = x/t$. The solutions contain individual discontinuities of each component, and can exhibit chromatographic separation of the components. Numerous

* Corresponding author.
E-mail address: Sara.Borazjani@adelaide.edu.au (S. Borazjani).

http://dx.doi.org/10.1016/j.petrol.2016.01.001
0920-4105/

Nomenclature

a	concentration of adsorbed polymer
c	polymer concentration in water (g/m^3)
c_s	salt concentration in water (g/m^3)
c_s^D	salt concentration in the drive (g/m^3)
D	shock speed for (x, t) co-ordinates
f	water fractional flow
H	power law coefficient (Pa s^n)
K	absolute permeability (m^2)
k_r	relative permeability of liquid phase
L	reservoir size (m)
n	power-law exponential index
p	pressure (Pa)
S	water saturation
t	time
RF	recovery factor
u	total velocity (m/s)
u_w	aqueous phase velocity (m/s)
V	shock speed in (x, φ) co-ordinate
V_p	polymer slug volume per unit area (m^3/m^2)
x	coordinate

Greek letters

Γ	Henry's polymer sorption coefficient
η	self-similar coordinate φ/x
κ	Bulk power law coefficient (Pa s^n)
μ	apparent viscosity (Pa s)
ϕ	porosity of porous media
ξ	self-similar coordinate x/t
φ	potential function

Subscripts

H	high salinity water
L	low salinity water
o	oil
s	salt
w	water

Superscripts

D	drive condition
I	initial condition
J	injection condition
$+$	value ahead of the shock
$-$	value behind the shock
$*$	intermediate point

authors have provided solutions for one- and multi-component, two-phase flow systems that allow for different kinds of dependencies of parameters (De Nevers, 1964; Claridge and Bondor, 1974; Helfferich, 1981; Hirasaki, 1981; Braginskaya and Entov, 1980).

Johansen and Winther (1988) and Johansen et al. (1989) solved the Riemann problem for a multi-component, two-phase system by projecting it onto the solution of a single-phase problem. The authors prove that the direct projection transforms all elementary waves of two-phase system into those for a single-phase system. So, the solution process consists of finding a solution for one-phase flow and extending it to two-phase flow. The projection principle allows for algorithmic integration of an arbitrary Riemann problem for two-phase multi-component with adsorption, based on the corresponding solute transport problem for a single-phase flow. However, the projection is valid for Riemann problems only: the two-phase flow solution with non-constant initial or boundary conditions cannot be mapped onto the corresponding one-phase-flow solution.

Injection of multi-component slugs corresponds to non-self-similar solutions. The qualitative phase plane with characteristics is presented in (Fayers, 1962) for sequential displacement of oil by intercalated slugs of cold and hot water. The exact integration is achieved by decomposition of the problem with piece-wise-constant initial and boundary conditions into local Riemann problems and solution of interactions of the elementary waves (Bedrikovetsky, 1982, 1993). Integration of the conservation law over the invariant contours yields the exact solutions with explicit formulae for trajectories of curvilinear fronts and for saturation and concentration distributions. In the simplified case, where adsorption of a component is a function of its own concentration only, the exact integration shows that the multi-component slugs interact after the injection and finally separate into single-component slugs moving in order of decreasing the sorption derivative values, similar to Rhee et al. (1998) for one-phase flows. Nevertheless, for the general case, where the adsorbed concentrations depend on the concentrations of all components, the analytical solution is not available in the literature.

Pires et al. (2006) and Borazjani et al. (2016) show that the introduction of Lagrangian coordinate φ (stream function) associated with mass conservation for water in n-component two-phase flow problems and using it as an independent variable instead of time t allows separating the $(n+1)\times(n+1)$ hyperbolic system into an $n\times n$ auxiliary one-phase system and one scalar equation (so called lifting) for two-phase flow. The auxiliary system and the lifting equation are the results of transformation of conservation laws for water and for all components, respectively, in co-ordinates (x, φ). In various cases, where the auxiliary system allows for an analytical solution, the general system is reduced to the solution of a single scalar equation (Pires et al., 2006). In contrast to direct projection onto the one-phase solution that is valid for Riemann problems only (Johansen and Winther, 1988; Johansen et al., 1989), this mapping results in splitting for any initial and boundary-value problems.

Generally, the solution of the lifting equation is obtained numerically (Vicente et al., 2014). However, for the case of linear adsorption isotherms, even with the Henry's constants depending on other concentrations, the lifting problem allows for exact solution (Borazjani et al., 2014).

In this paper the splitting method presented by Pires et al. (2006) is applied for hyperbolic systems corresponding to two-phase multi-component flows in the reservoir scale approximation. Yet, recently the splitting method has been extended for two-phase multicomponent systems of parabolic PDEs accounting for capillary pressure and non-equilibrium phase transitions and chemical reactions (Borazjani et al., 2016).

The objective of this work is to provide exact solutions based on the mapping presented in Pires et al. (2006) for the cases when the displacing aqueous phase contains varying viscosity and salinity. Our special focus is to describe the physics of the process when a slug of low-salinity polymer is followed by injection of polymer-free aqueous solutions. The adsorption of the chemical

(and other fractional-flow parameters) is assumed to be salinity dependent.

The structure of the paper is as follows. Section 2 derives the governing equations. Section 3 presents derivations of the exact solutions, corresponding to continuous and slug injections of polymer solution with varying salinity. Section 4 contains the results of this work, provides the mechanisms of physics of low-salinity polymer injection under some simplifying assumptions, and compares it to conventional polymer injection. Section 5 concludes the paper, with an interpretation of the solution.

2. Mathematical model

2.1. Formulation

We consider injection of an aqueous solution with varying viscosity and salinity at a constant temperature into a one-dimensional homogeneous porous medium with length L, permeability K, and porosity ϕ. The system is considered uniform and isotropic. The aqueous phase containing polymer and salt is injected to displace oil. The two phases are assumed to be immiscible and incompressible. The displacing phase can exhibit a shear-thinning behaviour, i.e., its viscosity reduces with increasing velocity; whereas the oil is considered Newtonian. The only rock–fluid interaction considered is the adsorption of polymer on the rock, which depends on the polymer and salt concentrations in the aqueous phase. The polymer and salt concentrations (on the solid and in the aqueous phases) are small enough not to affect the phase density and porosity of the rock. We assume Henry's sorption equation for low-concentration polymer solutions. The modified Darcy's law describes the fluid flow in the porous medium. The relative-phase permeabilities are functions of saturation and of polymer and salt concentrations. We assume no adsorption involving the salt. The gravitational effects are considered to be negligible. Viscous fingering is not accounted for. Furthermore, dissipative effects of dispersion and capillary pressure are ignored. The schematic of the pore space saturated by oil and water with polymer and salt dissolved in water and polymer adsorbing on the rock is shown in Fig. 1.

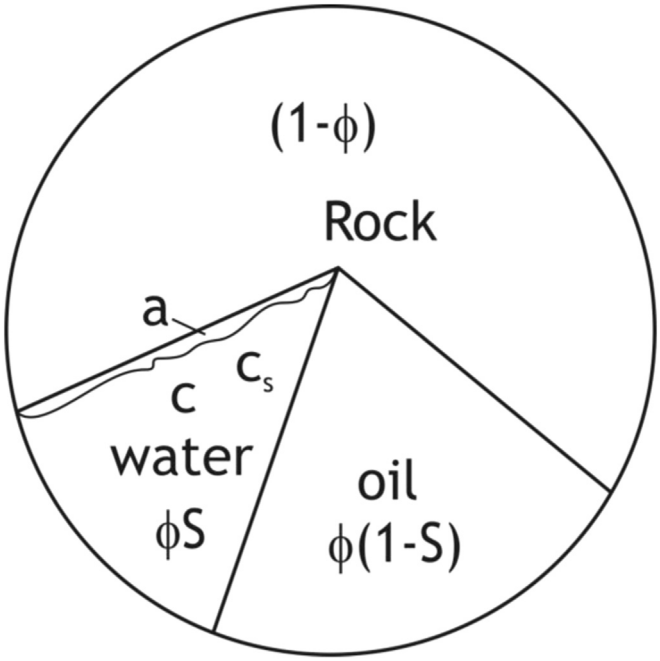

Fig.1. Schematic representation for porosity, phase saturations and component concentrations: oil, aqueous phase, polymer and salt components in aqueous solution and an adsorbed polymer within a pore space.

2.2. Governing equations

Mass-balance equations for two-phase flow with polymer and salt components are

$$\frac{\partial S}{\partial t} + \frac{\partial f(S, u, a, c, c_s)}{\partial x} = 0. \tag{1}$$

$$\frac{\partial (cS + a)}{\partial t} + \frac{\partial \left(cf(S, u, a, c, c_s)\right)}{\partial x} = 0. \tag{2}$$

$$\frac{\partial \left(c_s S\right)}{\partial t} + \frac{\partial \left(c_s f(S, u, a, c, c_s)\right)}{\partial x} = 0. \tag{3}$$

where S is water saturation, f is fractional flow of water ($f=u_w/u$), and $1-f$ is the fractional-flow of oil ($f=u_o/u$), u is overall velocity of oil and water, c, c_s and a are mass concentrations for polymer, salt and adsorbed polymer, respectively. The dimensionless coordinates x and t are defined as

$$x \to \frac{\phi x}{V_p}, \quad t \to \frac{1}{V_p}\int_0^t u(t)dt. \tag{4}$$

V_p is the polymer slug volume per unit area, and the dimensionless position of the outlet is at $l=\phi L/V_p$. Usually the dimensionless time is introduced in terms of the reservoir pore volume ϕL. Definition (4) is more convenient for the solution of polymer slug problem and study of the effect of polymer slug on the performance.

Following Wu et al. (1991) and Sorbie (1991) we assume the power-law model to describe the non-Newtonian behaviour of the polymer solution in porous media:

$$\mu_w = H u_w^{n-1} \tag{5}$$

where μ_w is the apparent aqueous phase viscosity in the porous medium, n is the bulk power-law index, and H for two phase flow is

$$H = \frac{\kappa}{12}\left(9 + \frac{3}{n}\right)^n \left(150 K k_{rw}\phi\left(S - S^l\right)\right)^{(1-n)/2}. \tag{6}$$

Here, κ is the bulk power-law coefficient and S^l is initial water saturation. κ and n are function of polymer and salt concentrations. Formulae (5) and (6) are the results of upscaling of the power-law flow of non-Newtonian fluid in the pore capillary to the Darcy's scale.

Combining modified Darcy's equation for water and (5) yields the expression for aqueous phase flux

$$u_w = \left(\frac{K k_{rw}}{H}\left(-\frac{\partial p}{\partial x}\right)\right)^{1/n}. \tag{7}$$

Using the definition of overall velocity ($u=u_w+u_o$), Darcy's law for oil, and Eq. (7), the following transcendental equation can be derived for the fractional-flow function:

$$u = fu + \frac{k_{ro}H}{\mu_o k_{rw}}(fu)^n. \tag{8}$$

As it follows from Eqs. (5–8), non-Newtonian properties can be incorporated into the fractional flow theory, where the fractional-flow function becomes velocity-dependent (Wu et al., 1991; Bedrikovetsky, 1993).

For small concentrations c and c_s, the equilibrium polymer-adsorption isotherm is described by the linear Henry's sorption

$$a(c, c_s) = \Gamma(c_s)c. \tag{9}$$

Polymer adsorption increases as salinity increases, i.e., $\partial\Gamma(c_s)/\partial c_s > 0$ (Sorbie, 1991).

The boundary condition for polymer-slug injection with varying salinity in the slug is

$$x = 0: \quad f(S, u, a, c, c_s) = 1, \quad c = \begin{cases} c^J, & t < 1 \\ 0, & t > 1 \end{cases}, \quad c_s = c_s{}^J. \tag{10}$$

We assume that initially no polymer is present in the reservoir, i.e.,

$$t = 0: \quad c_s = c_s{}^I, \quad c = 0, S = S^I \tag{11}$$

where $c_s{}^I > c_s{}^J$.

From this point forward, the injection rate is assumed to be constant; therefore, the velocity-dependency of the fractional-flow function need no longer be mentioned.

3. Analytical model for polymer injection with varying salinity

The solutions of the continuous injection ($t < 1$, in Eqs. (10, 11)) for system (1–3) are self-similar and depend on the group x/t (Pope, 1980; Bedrikovetsky, 1993; Lake, 1989), i.e.,

$$S = S(\xi), \quad c = c(\xi), \quad c_s = c_s(\xi), \quad \xi = x/t \tag{12}$$

The self-similarity is obtained from the analysis of dimensions, where only one dimensinless group x/t can be obtained from two independent variables (Landau and Lifshitz, 1987). The solutions for slug injection of low-salinity polymer (LSP) followed by water drive with different salinities are non-self-similar, since the boundary condition (10) contains one extra parameter, which is the slug size. The splitting technique (Pires et al., 2006) is used to derive the exact solutions for non-self-similar problems.

3.1. Splitting procedure

Introduction of a stream function φ associated with mass conservation for water (1),

$$\varphi(x, t) = \int_{0,0}^{x,t} (fdt - Sdx) \tag{13}$$

yields the following form for system (1–3) in coordinates (x, φ)

$$\frac{\partial F(U, a, c, c_s)}{\partial \varphi} + \frac{\partial U}{\partial x} = 0 \tag{14}$$

$$\frac{\partial a}{\partial \varphi} + \frac{\partial c}{\partial x} = 0 \tag{15}$$

$$\frac{\partial c_s}{\partial x} = 0 \tag{16}$$

where

$$U = \frac{1}{f}, \quad F(U, a, c, c_s) = -\frac{S}{f}. \tag{17}$$

The detailed derivations of Eqs. (14–16) are presented in Appendix A.

Eq. (14) is separate from the 2×2 system (15, 16), thus the unknowns c and c_s are found from Eqs. (15, 16) followed by the determination of $U(x, \varphi)$ from Eq. (14). This means that the transformation $(x, t) \to (x, \varphi)$ splits the 3×3 system (1–3) into the 2×2 auxiliary system (15, 16) and the lifting Eq. (14). We present the properties of projection for the elementary waves, along with the continuous and discontinuous solutions in Appendix A.

With this transformation, the abscissa axis $t=0$ transfers to straight line $\varphi = -S^I x$; however, the ordinate axis does not change (i.e., along the straight line $x=0$, $\varphi = t$).

Accordingly, the inlet boundary condition of Eq. (10) in coordinates (x, φ) becomes

$$x = 0: \ c_s = c_s{}^J, \ c = \begin{cases} c^J, & \varphi < 1 \\ 0, & \varphi > 1 \end{cases} \tag{18}$$

$$x = 0: \quad U = 1 \tag{19}$$

and the initial conditions of Eq. (11) take the form

$$\varphi = -S^I x: \ c_s = c_s^I, \ c = 0 \tag{20}$$

$$\varphi = -S^I x \ : \ F = -\infty. \tag{21}$$

3.2. Solution of the auxiliary system

The solution of the auxiliary system (15, 16) subject to boundary condition Eq. (18) and initial condition Eq. (20) is self-similar for $\varphi < 1$, the self-similar group is x/φ. The solution is shown in Fig. 2a (Path 1) by a sequence of c-shock from the injection point ($c_s = C_S^J$, $c = c^J$) to an intermediate point ($c_s = C_S^J$, $c = 0$), represented by Eq. (A-10)

$$\frac{[a]}{[c]} = \frac{\Gamma(c_s{}^J)c^J}{c^J} = \Gamma(c_s^J), \tag{22}$$

followed by a c_s-shock across the line $\varphi = 0$ from the intermediate point into the initial condition ($c_s = C_S^I$, $c = 0$). The shock in c appears before the shock in c_s (Lax condition).

The solution of the Riemann problem for $\varphi < 1$ corresponds to waves $(C_S^J, c^J) \to (C_S^J, 0) \to (C_S^I, 0)$. The terms A–B and $A \to B$ denote a centred wave and a shock connecting states A and B, respectively.

At $\varphi = 1$, a c-shock connects ($c_s = C_S^J$, $c = 0$) to the injection point at $\varphi < 1$ ($c_s = C_S^J$, $c = c^J$) (Path 2 in Fig. 2b). Using Eq. (A-10) to find the velocity of this c-shock yields

$$\frac{1}{V} = \Gamma(c_s{}^J) \to \varphi(x) = \Gamma(c_s{}^J)x + 1. \tag{23}$$

Finally, the solution of the auxiliary system is

$$\begin{pmatrix} c(x, \varphi) \\ c_s(x, \varphi) \end{pmatrix} = \begin{cases} c = 0, & c_s = c_s^J, & \varphi \geq \Gamma(c_s^J)x + 1 \\ c = c^J, & c_s = c_s^J, & \Gamma(c_s^J)x \leq \varphi \leq \Gamma(c_s^J)x + 1 \\ c = 0, & c_s = c_s^J, & 0 \leq \varphi \leq \Gamma(c_s^J)x \\ c = 0, & c_s = c_s^I, & -S^I x \leq \varphi \leq 0 \end{cases}. \tag{24}$$

Zones I, II, III, IV and V in Fig. 3a represent the auxiliary solution of Eq. (24).

3.3. Solution of the lifting equation

For system (14–16), the solution is reduced to one hyperbolic lifting Eq. (14) subject to boundary and initial conditions (19, 21) with the known solution of auxiliary problem (24). The solution for $\varphi < 1$ corresponds to the path in (U, F) and (S, f)-plane consisting of a rarefaction wave from the saturation $-S_0{}^L$ to point 2, c-

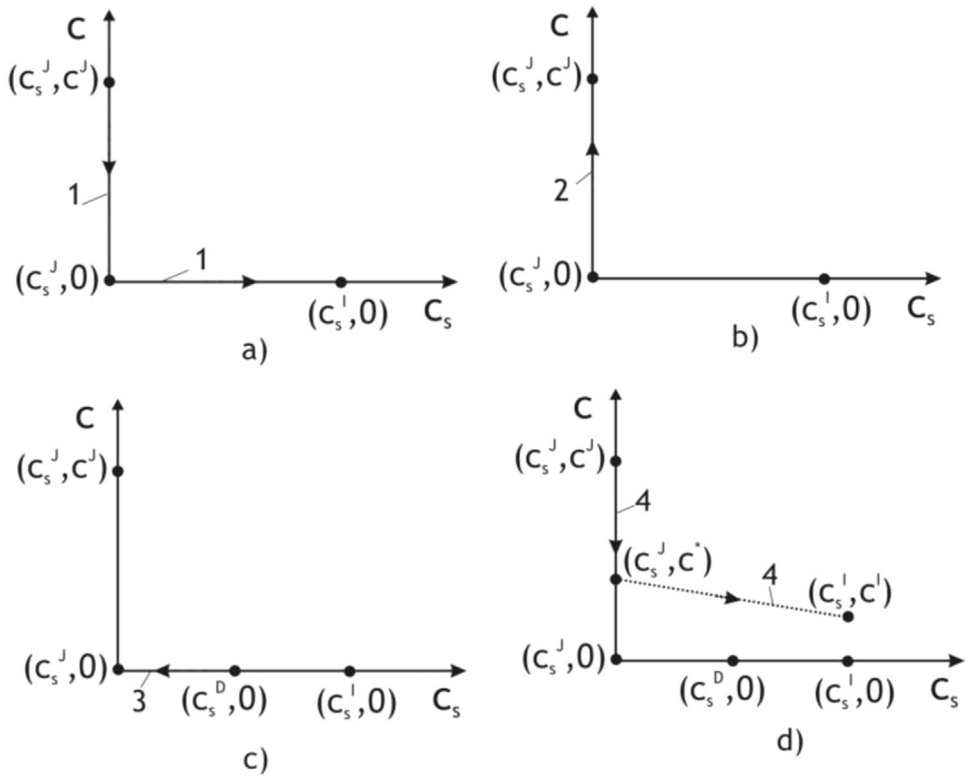

Fig.2. Initial and boundary Riemann values with the solution path; (a) path 1- Riemann problem solution with discontinuity at the point $x=0$, $\varphi=0$ for the case $c^I=0$, consisting of c-jump and c_s-jump;(b) path 2- Riemann solution for discontinuity at the point $x=0$, $\varphi=1$ is a c-jump; (c) path 3- Riemann solution with discontinuity at the point $x=0$, $\varphi=t_s$ is c_s-jump; (d) path 4- Riemann solution for discontinuity at the point $x=0$, $\varphi=0$ for $c^I\neq 0$; consists of c- and c-c_s-jumps.

jump from 2 to 3, c_s-jump from 3 to 4 and a S-jump from 4 to I, $-S_0{}^L$–2→3→4→I; see solid red paths in Figs. 4 and 5.

Eq. (A-12) allows implicit calculation of $U=U_1(x,\ \varphi)$ in the rarefaction wave $-S_0{}^L$–2:

$$\frac{\varphi}{x}=\frac{\partial F\left(U_1(\varphi,\ x),\ c=c^J,\ c_s=c_s{}^J\right)}{\partial U}. \tag{25}$$

Point 2 is calculated from the equality of the S-waves and the characteristic speed of the c-shock given by Eq. (A-9) and Eq. (A-12).

$$\frac{\varphi}{x}=\frac{\partial F\left(U_2,\ c=c^J,\ c_s=c_s^J\right)}{\partial U}=\Gamma\left(c_s^J\right). \tag{26}$$

Point 3 is calculated from the Hugoniot–Rankine condition at the c-shock given by Eq. (A-10).

$$\frac{F\left(U_2,\ c=c^J,\ c_s=c_s^J\right)-F\left(U_3,\ c=0,\ c_s=c_s^J\right)}{U_2-U_3}=\Gamma\left(c_s^J\right). \tag{27}$$

Constant state 3 is shown in zone III in Fig. 3 (for the case $\partial F_3/\partial U<0$).

Point 4 is determined from condition of continuity of F along c_s-jump (see Eq. (A-9)).

$$F\left(U_3,\ c=0,\ c_s=c_s^J\right)=F\left(U_4,\ c=0,\ c_s=c_s^I\right). \tag{28}$$

Jump velocity from point 4 to point I is calculated from the Hugoniot–Rankine condition on S-shock, given in Eq. (A-11).

$$\frac{\varphi}{x}=\frac{F\left(U_4,\ c=0,\ c_s=c_s^I\right)-F\left(U^I,\ c=0,\ c_s=c_s^I\right)}{U_4-U^I}=\ -\ S^I. \tag{29}$$

Next we solve the slug problem, $\varphi>1$. The rarefaction wave ($-S_0{}^L$–2) originating from (0, 0) in the (x, φ) plane interacts with the c-shock originating from point (0, 1). The two waves are transmitted through each other and build the transmitted rarefaction wave and the transmitted shock wave. Values $U_1(x,\varphi)$ and $U_5(x,\varphi)$ ahead of and behind the c-shock are related by the mass-balance condition on the c-shock given by Eq. (A-10).

$$\frac{F\left(U_1,\ c=c^J,\ c_s=c_s^J\right)-F\left(U_5,\ c=0,\ c_s=c_s^J\right)}{U_1-U_5}=\Gamma\left(c_s^J\right). \tag{30}$$

The c-shock velocity remains constant and equal to $1/\Gamma(C_S^J)$ during this transition. U_5 also remains constant along the characteristic lines behind the slug rear, which results in the straight characteristic lines starting from any point (x', φ') on the c-shock.

$$\frac{\varphi-\varphi'}{x-x'}=\frac{\partial F\left(U_5,\ c=0,\ c_s=c_s^J\right)}{\partial U}. \tag{31}$$

The expression $U(x,\varphi)$ in zone V along with the corresponding point (x', φ') on the c-shock front is determined from three transcendental Eqs. (25, 30, 31). The slug path (6→7) for $U_1(x,\varphi)=U_6$ is shown by the dashed lines in Figs. 4 and 5. The initial conditions I in Fig. 5 correspond to initial connate water saturation, i.e. only secondary oil recovery by the polymer flooding is considered.

Finally, the solution of the auxiliary and lifting system is

$$\begin{pmatrix} U(x,\varphi)\\ c(x,\varphi)\\ c_s(x,\varphi)\end{pmatrix}=\begin{cases} U_5(x,\varphi),\ c=0,\ c_s=c_s^J, & \varphi\geq\Gamma\left(c_s^J\right)x+1\\ U_1(\varphi/x),\ c=c^J,\ c_s=c_s^J, & \Gamma\left(c_s^J\right)x\leq\varphi\leq\Gamma\left(c_s^J\right)x+1\\ U_3,\ c=0,\ c_s=c_s^J, & 0\leq\varphi\leq\Gamma\left(c_s^J\right)x\\ U_4,\ c=0,\ c_s=c_s^I, & -S^Ix\leq\varphi\leq 0\\ \infty,\ c=0,\ c_s=c_s^I, & \varphi=\ -\ S^Ix\end{cases} \tag{32}$$

The zones I, II, III, IV and V in Fig. 3 contain the auxiliary and lifting solution (32). The water saturation $S(x,\varphi)$ is obtained from

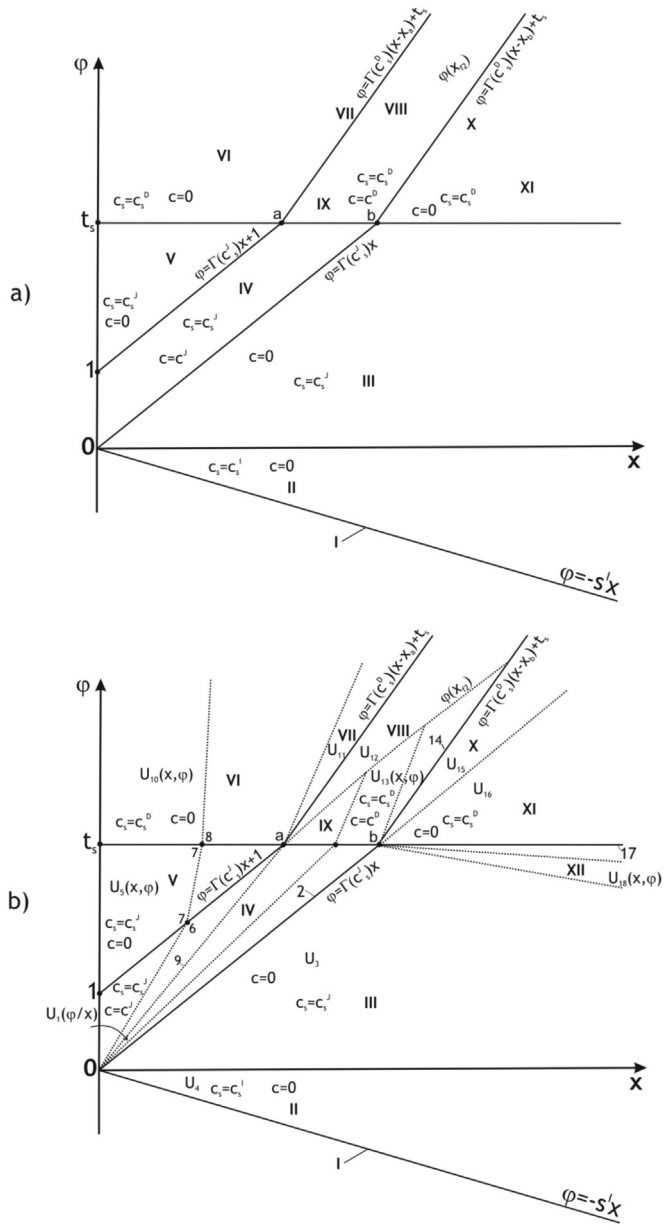

Fig.3. Solution of the auxiliary and lifting equations for oil displacement by low salinity polymer slug with alternated water salinity in the slug and in the water drive in (x, φ) plane (a) solution of the auxiliary equations, (b) solution of the lifting problem.

Eq. (32) using Eq. (17).

3.4. Inverse mapping–change of variables from (x, φ) to (x, t)

Next we reverse the mapping (x, φ) to (x, t) by calculating time $t = t(x, \varphi)$ along any path from point (0, 0) to point (x, φ) (see Eq. (A-3)).

$$t(x, \varphi) = \int_{0,0}^{x,\varphi} (1/f d\varphi + S/f dx). \tag{33}$$

Because S_4 and S_3 are constant in zones II and III, the expressions for time t in these zones are

$$t = \frac{1}{f_4}\int_0^{-S^I x} d\varphi + \frac{S_4}{f_4}\int_0^x dx = \left(\frac{-S^I + S_4}{f_4}\right)x \tag{34}$$

$$t = \frac{1}{f_3}\int_0^0 d\varphi + \frac{S_3}{f_3}\int_0^x dx = \frac{S_3}{f_3}x. \tag{35}$$

Although S is not constant in zone IV, it remains constant through each of the centred waves; therefore, the integral of Eq. (33) along each characteristic line is

$$t = \frac{\varphi}{f\left(S_1(\varphi/x),\, c = c^J,\, c_s = c_s^J\right)} + \frac{S_1(\varphi/x)}{f\left(S_1(\varphi/x),\, c = c^J,\, c_s = c_s^J\right)}x. \tag{36}$$

In zone V, time is calculated along the U_5-rarefaction waves:

$$t = \frac{\varphi}{f\left(S_5(x, \varphi),\, c = 0,\, c_s = c_s^J\right)} + \frac{S_5(x, \varphi)}{f\left(S_5(x, \varphi),\, c = 0,\, c_s = c_s^J\right)}x. \tag{37}$$

Along the polymer-slug rear; i.e., $\varphi = \Gamma(C_s^J)x + 1$,

$$x = \frac{\partial f(S_1, c = c^J, c_s = c_s^J)}{\partial S}\Delta^{-1},\ \Delta = f_1 - \left(S_1 + \Gamma\left(c_s^J\right)\right)\partial f_1/\partial S \tag{38}$$

$$\varphi = \frac{f(S_1, c = c^J, c_s = c_s^J) - S_1\partial f_1/\partial S}{\Delta}, \tag{39}$$

and time t is determined from Eq. (A-3).

$$t = \frac{1}{\Delta}. \tag{40}$$

Fig. 5 shows the graphical expression for the polymer-slug rear, where AD is equal to Δ and AC is equal to $\Delta \times (\partial f_1/\partial s)^{-1}$.

Finally, the solution of the slug problem for system (1–3) subject to the boundary and initial conditions Eqs. (10) and (11) is

$$\begin{pmatrix} S(x, t) \\ c(x, t) \\ c_s(x, t) \end{pmatrix} = \begin{cases} S_5(x, t), & c = 0, \quad c_s = c_s^J, & t \geq \dfrac{\Gamma\left(c_s^J\right) + S_1(x, t)}{f(S_1(x, t))}x + 1 \\ S_1(x/t), & c = c^J, \quad c_s = c_s^J, & \dfrac{\Gamma\left(c_s^J\right) + S_2}{f_2}x \leq t \leq \dfrac{\Gamma\left(c_s^J\right) + S_1(x, t)}{f(S_1(x, t))}x + 1 \\ S_3, & c = 0, \quad c_s = c_s^J, & \dfrac{S_3}{f_3}x \leq t \leq \dfrac{\Gamma\left(c_s^J\right) + S_2}{f_2}x \\ S_4, & c = 0, \quad c_s = c_s^I, & \dfrac{-S^I + S_4}{f_4}x \leq t \leq \dfrac{S_3}{f_3}x \\ S^I, & c = 0, \quad c_s = c_s^I, & 0 \leq t \leq \dfrac{-S^I + S_4}{f_4}x \end{cases} \tag{41}$$

The solution to Eq. (41) in the (x, t) domain is shown in Fig. 6(a) (zones I, II, III, IV and V). The profiles of water saturation and of polymer and salt concentrations at t_1, t_2, and t_3 are presented in Fig. 6(b)–(d), respectively. The water-displacement front moves at velocity $D_s = f_4/(-S^I + S_4)$, the salt front at velocity $D_{cs} = f_3/S_3$, and the polymer front at velocity $D_c = f_2/(\Gamma(C_s^J) + S_2)$. Because salt does not adsorb on the rock, $D_{cs} > D_c$.

The displacement zones during injection of a low-salinity-polymer slug, followed by low-salinity water consist of the following reference patterns:

I. Initial reservoir mixture, S^I, $c = 0$, $c_s = C_S^I$.
II. High-salinity water oil bank formed ahead of the low-salinity water front, S_4, $c = 0$, $c_s = C_S^I$.
III. Low-salinity water oil bank formed ahead of the polymer slug, with a constant saturation. The bank contains no polymer, S_3, $c = 0$, $c_s = C_S^I$.
IV. Polymer slug, S, declines from S_0^L to S_2 on the leading front of slug, $S_1(x/t)$, $c = c^J$, $c_s = C_S^J$.
V. Low-salinity water drive zone with oil, $S_5(x, t)$, $c = 0$, $c_s = C_S^I$.

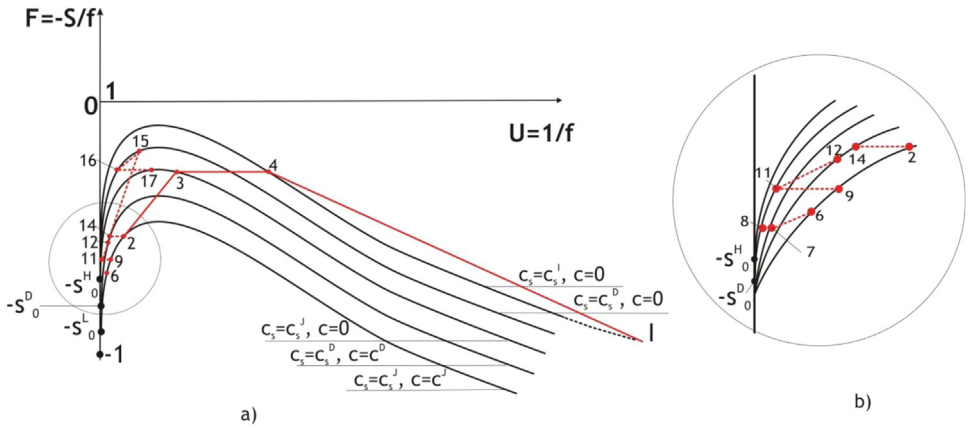

Fig.4. The image of auxiliary and lifting solutions in (U–F) plane (a) graphical determination of the basic points 2, 3…17; (b) zoom near to the point $(0,-S_0^H)$ (For interpretation of the references to color in this figure, the reader is referred to the web version of this article.).

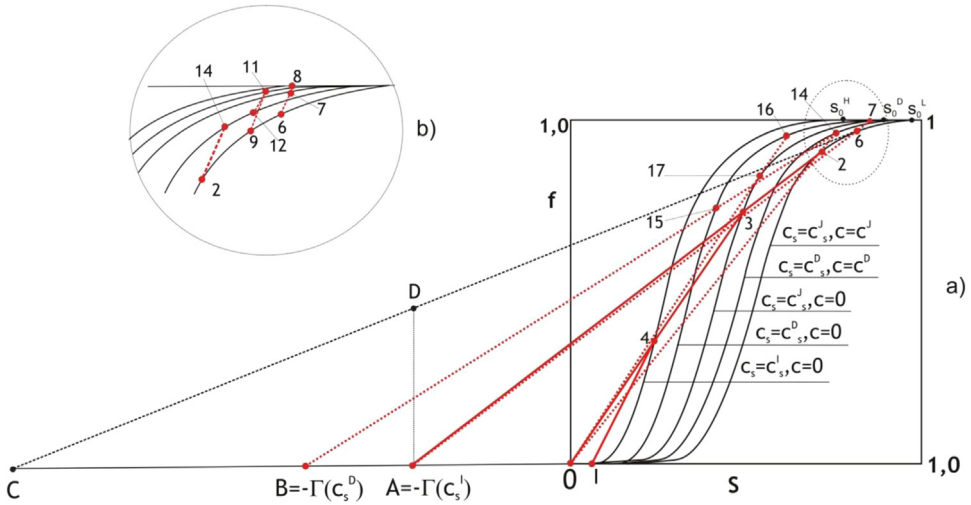

Fig.5. Fractional flow curves and graphical solution of oil displacement by polymer and salt slugs (a) the auxiliary and lifting solutions in (s, f)-plane; (b) zoom near to the point 7 exhibiting the graphical determination of the basic points.

3.5. *Solution of the sequential injection of a low-salinity polymer slug followed by low-salinity and high-salinity water drives*

This section derives the solution of system (1–3), subject to the following boundary condition

$$x=0:\quad f=1,\quad c=\begin{cases} c^J, & t<1,\\ 0, & t>1\end{cases},\quad c_s=\begin{cases} c_s^J, & t<t_s,\\ c_s^D, & t>t_s\end{cases},\quad t_s>1, \tag{42}$$

where t_s is the injection time of high-salinity water C_S^D in the drive, i.e., the low-salinity slug is driven by the high-salinity water, assuming $C_S^J<C_S^D<C_S^I$. The previous section showed that the low-salinity water front moves faster than the polymer-slug front. Therefore, to avoid the negative effect of high salinity on polymer viscosity, the high-salinity water should be injected in an optimum time, t_s. This time can be obtained from the ordinate of the low-salinity slug trajectory at $x=0$, when the low-salinity-slug rear intersects with the polymer-slug rear at the outlet, $x=\phi L/V_p$.

$$t_s=\Gamma\left(c_s^J\right)\frac{\phi L}{V_p}+1. \tag{43}$$

Fig. 3 shows the solution for the auxiliary and lifting problems of system (1–3) subject to the boundary condition of Eq. (42) and the initial condition of Eqs. (20, 21) in the (x,φ) plane. The solution coincides with the solution in Eq. (41) in zones I, II, III, IV and V.

At $\varphi=t_s$, a c_s-shock connects ($c_s=C_S^D$, $c=0$) to the injection point at $\varphi<t_s$ ($c_s=C_S^J$, $c=0$) (Path 3 in Fig. 2). The horizontal line $\varphi=t_s$ corresponds to the infinite c_s-shock velocity V, as shown in Fig. 3.

The rarefaction wave $U_5(x,\varphi)$, interacts with the c_s-shock at $\varphi=t_s$. The values U_5 and U_{10} ahead of and behind the c_s-shock are related by the mass-balance on the c_s-shock:

$$F\left(U_5(x,\varphi),c=0,c_s=c_s^J\right)=F\left(U_{10}(x,\varphi),c=0,c_s=c_s^D\right). \tag{44}$$

For any point on the low-salinity-water-slug trajectory (x'',φ''),

$$\frac{\varphi-\varphi''}{x-x''}=\frac{\partial F\left(U_{10}(x,\varphi),c=0,c_s=c_s^D\right)}{\partial U}. \tag{45}$$

Zone VI in Fig. 3 and lines 7⟶8 in Figs. 4b and 5b show this transition path.

The polymer-slug rear and front intersect with the low-salinity-slug rear at points $a((t_s-1)/\Gamma(C_S^J),\ t_s)$ and $b(t_s/\Gamma(C_S^J),\ t_s)$, respectively (Fig. 3). These intersections result in a constant polymer concentration, c^D, in zones VIII and IX.

$$c^D=\frac{\Gamma\left(c_s^J\right)c^J}{\Gamma\left(c_s^D\right)}. \tag{46}$$

U_{11}, U_{12} and $U_{13}(x,\varphi)$ are obtained from the Hugoniot condition on c and c_s shocks:

$$F_9 = F_{11};\ \frac{F_{11} - F_{12}}{U_{11} - U_{12}} = \Gamma\left(c_s^D\right);\ F_1(x, \varphi) = F_{13}(x, \varphi),\ U_1(x, \varphi) > U_9, \tag{47}$$

where U_9 is found from $U_1(x, \varphi)$ at $x=x_a$ and $\varphi < t_s$.

For any point on the low-salinity-water-slug trajectory (x''', φ''') between a and b,

$$\frac{\varphi - \varphi'''}{x - x'''} = \frac{\partial F_{13}(x, \varphi)}{\partial U}. \tag{48}$$

U_{12} is transferred to $U_{13}(x, \varphi)$ by an S-shock. The shock trajectory $\varphi(x_{f2})$ is found from Eq. (48) and Eq. (49).

$$\frac{d\varphi}{dx} = \frac{F_{12} - F_{13}(x, \varphi)}{U_{12} - U_{13}(x, \varphi)}. \tag{49}$$

U_{14}, U_{15}, U_{16} and U_{17} are found form the Hugoniot condition on c and c_s shocks.

$$F_2 = F_{14};\ \frac{F_{15} - F_{14}}{U_{15} - U_{14}} = \Gamma\left(c_s^D\right);\ \frac{\partial F_{17}}{\partial U} = 0;\ F_{17} = F_{16}. \tag{50}$$

U_{17} transfers to U_3 in zone XII through rarefactions $U_{18}(x, \varphi)$.

$$\frac{\varphi - t_s}{x - x_b} = \frac{\partial F\left(U_{18}(x, \varphi),\ c = 0,\ c_s = c_s^J\right)}{\partial U},\ U_{17} < U_{18}(x, \varphi) < U_3. \tag{51}$$

Table 1 contains solutions in (x, φ) for zones VI, VII, VIII, IX, X and XI.

With a similar inverse mapping $(x, \varphi) \rightarrow (x, t)$ as in Section 3.5, the solution of the problem in Eq. (42) in zones VI, VII, VIII, IX, X and XI in the (x, t) domain is presented in Table 2.

Low-salinity front, $\varphi = t_s$, in zone VI is mapped into the trajectory $t(x_{f1})$:

$$x_{f1} = (t - t'')\frac{\partial f_5}{\partial S},\ t(x_{f1}) = \frac{(t_s - \varphi'')}{\Delta'} + t''$$

$$\Delta' = f_5(x, \varphi) - S_5(x, \varphi)\frac{\partial f_5(x, \varphi)}{\partial S} \tag{52}$$

The front $\varphi = t_s$ in zone IX is mapped into the trajectory $t(x_{f3})$.

$$x_{f3} = t\frac{\partial f_1}{\partial S},\ t = \frac{1}{\Delta}$$

$$\Delta = f_1(x, \varphi) - S_1(x, \varphi)\frac{\partial f_1(x, \varphi)}{\partial S},\ S_2 < S_1(x, \varphi) < S_9 \tag{53}$$

Fig. 6(a) illustrates the solution in the (x, t) plane.

3.6. Injection of polymer slug with salinity higher than the initial salinity of the reservoir

This section presents the Riemann solution of injection of a polymer slug into a reservoir with salinity c_s^H, higher than the initial salinity of the reservoir, c_s^I. The solution for this case depends on the fractional-flow curves corresponding to (c^J, c_s^H), $(0, c_s^H)$, and $(0, c_s^I)$. At a fixed water saturation, the fractional-flow curve corresponding to $(0, c_s^H)$ is located above the fractional-flow curve corresponding to the initial condition of the reservoir, i.e., $f(c^J, c_s^H) < f(0, c_s^I) < f(0, c_s^H)$.

The solution is on the path in the (s, f)-plane and consists of the rarefaction wave from the saturation S_0^H to point 2, c-S jump from 2 to 4, S-jump from 4 to 5, c_s-S-jump from 5 to 3, rarefaction wave from 3 to 6 and an S-shock from 6 to I. This path is shown in Fig. 7.

$$s_0^H - 2 \rightarrow 4 \rightarrow 5 \rightarrow 3 - 6 \rightarrow I. \tag{54}$$

Compared to LSP flooding, injection of the high-salinity polymer results in the appearance of an S-shock, $4 \rightarrow 5$, and an extra oil bank between the polymer and salt shocks. Also, injection of the high-salinity polymer increases the velocity of the water front, causing a decline in the water-free oil production period and faster water breakthrough. The water cut increases sharply from f_3 to f_5 during the production of the second oil bank. Afterwards, the water cut decreases from f_5 to f_4. At the final stage of the production, the high-salinity-polymer flood exhibits higher residual oil than does the LSP injection.

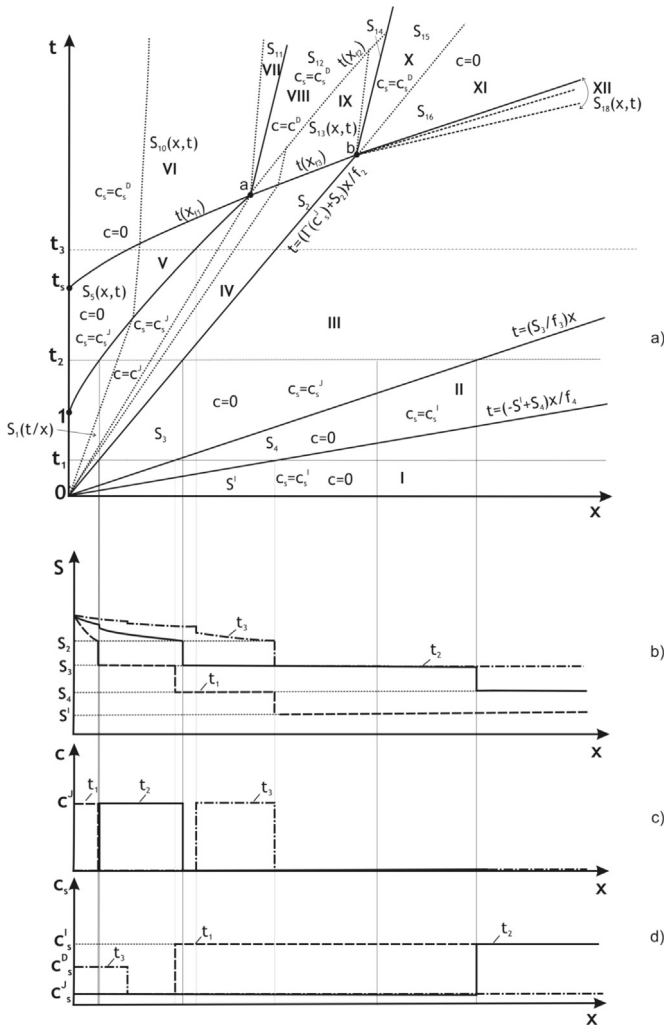

Fig.6. Solution for oil displacement by low-salinity polymer slug with alternated water salinity in the slug and in the water drive and different flow zones (a) trajectories of concentration and saturation fronts in (x, t)-plane separating different zones I, II…XII with different forms of the analytical solution; (b) saturation profiles in three moments; (c) polymer concentration profiles; (d) salt concentration profiles in three moments.

3.7. Analytical model for nonzero initial polymer concentration

For a general case of LSP flooding into the reservoir, where initial polymer (or ion) concentration is not zero, i.e., $c^I \neq 0$, an intermediate concentration of chemical $c^* \neq 0$ will appear in the solution; see Fig. 2 (Path 4). The concentration of c^* is defined by the equality of the sorption functions across the c_s-jump; see (A-9):

$$[a] = \Gamma(c_s^J)c^* - \Gamma(c_s^I)c^I = 0 \ \rightarrow\ c^* = \frac{\Gamma(c_s^I)c^I}{\Gamma(c_s^J)} \tag{55}$$

The Riemann problems with a nonzero initial concentration arise in low-salinity water flooding accounting for multi-component ions in the aqueous phase (Pope et al., 1978). The relative permeability of saline water is a function of ion compositions

(mainly calcium), and eventually, the concentration of c^* affects drastically the relative permeability of aqueous and oil phases.

Consider the following Riemann problems:

(1) Injection of low-salinity, high-concentration polymer solution (J_1) into the rock with high-salinity, low-concentration polymer (I_1);

(2) Injection of high-salinity, high-concentration polymer solution (J_2) into the rock with low-salinity, low-concentration polymer (I_2);

(3) Injection of low-salinity, low-concentration polymer solution (J_3) into the rock with high-salinity, high-concentration polymer (I_3);

(4) Injection of high-salinity, low-concentration polymer solution (J_4) into the rock with low-salinity, high-concentration polymer (I_4).

For conditions 1 to 4, Fig. 8 shows the solution of the auxiliary system (15, 16) in the (a, c) plane. The initial and injected component concentrations have strong effect on c^* concentration. In cases (1) and (4), c^* is between the initial and injected concentrations; whereas in case (2), it is less; and in case (3), it is more than the initial and injected conditions. Thus, adjusting the injected ion concentrations can provide a favourable operating condition for LSP flooding. For the detailed solution of case (1), see Borazjani et al. (2014).

4. Examples

This Section uses the obtained exact solution from Section 3.4 to calculate the fractional-flow functions, saturation and concentration profiles, and recovery factors using some typical parameters.

Phase-relative permeabilities are calculated using Corey's function. The viscosity of the aqueous phase containing polymer is expressed by Eq. (5). The parameters are listed in Table 3, the additional physical properties used are $\phi=0.2$, $K=1$ Darcy, $\mu_o=20$ cp, $L=5$ m, $V_p=0.1$ PVI, and residual resistance factor $R=3$.

The structure of the Riemann solutions (10, 11) depends on the form of fractional flow curves $f(S,u,a,c,c_s)$. Let us show that for conditions under consideration in this Section, the fractional flow curves have S-shape typical for Newtonian fluids. Fig. 9 shows the fractional-flow curves calculated for three flow velocities 10^{-4}, 10^{-5}, and 10^{-6} m/s and for the power-law exponents $n=0.4$, 0.5 and 0.7, under the conditions listed in Table 3. The higher injection rates yield lower fractional flow values at fixed water saturation, which is the result of the shear-thinning behaviour of the polymer solution. In the following, we will use the fractional-flow curve corresponding to $u=10^{-6}$ m/s.

Fig. 10 compares water saturation and polymer and salt concentration profiles of HSP flood (0.2 PVI polymer slug with continuous injection of high-salinity water) and LSP flood (0.2 PVI polymer slug with continuous injection of low-salinity water) into a reservoir initially containing high-salinity water.

Fig. 10(a) shows five zones in LSP flooding profile: 1) LS water, 2) polymer slug, 3) low-salinity water oil bank, 4) high-salinity water oil bank, 5) initial oil–water fluid. The HSP profile exhbits four zones. Compared to HSP injection, an additional oil bank occurs in LSP injection; that is, because of the low-salinity-water front, injection of LSP results in delay of the water breakthrough, increase of oil cut before salinity breakthrough time, and decline of residual oil saturation at the final stage of production from 0.24 to 0.2. In addition, a larger value of the polymer sorption isotherm, a, in HSP results in a larger lag of polymer appearance at the production well ($t=7.8$ PVI in LSP, and $t=8.1$ PVI in HSP). Fig. 10 (b) shows polymer slug position at the given time 2 PVI.

Implicit formulae for front trajectories in Eqs. (38–40) and straight lines for characteristics allow explicit calculation of the recovery factor. We use the contour integration method to determine the oil recovery at any instant of time t; see Appendix B for details. Fig. 11(a) and (b) show the recovery factors and water cut subject to following cases:

1. 0.1 PVI of low-salinity polymer slug followed by low-salinity water.
2. 0.1 PVI of high-salinity polymer slug followed by high-salinity brine.
3. Continuous injection of high-salinity water.

The ultimate oil recovery after 10 PVI of fluid injection for low-salinity polymer flooding is about 32% higher than that for the continuous water flood and 14% higher than that of the polymer flood. The water breakthrough time is 2.11 PVI for Case 3, 2.13 PVI for Case 2, and 2.56 PVI for Case 1. The recovery factors at the breakthrough time for these cases are 0.32, 0.33, and 0.4, respectively.

Fig. 11(b) shows the comparison of water cut for all the cases. The water breakthrough occurs latest for low-salinity polymer flood. Moreover, the water cut is the lowest for low-salinity polymer.

The independent dimensionless variable defined in Eq. (4) relates x and t to the polymer slug volume, V_p. Thus, a change in V_p has no effect on the solution of system (1–3) in the (x, t) domain, only changing the coordinate of the outlet $l=\phi L/V_p$. Therefore, the relation between the recovery factor and slug size can be studied by changing the position of the outlet $l=\phi L/V_p$, from right to left. An example of the sensitivity of the results to the slug volume is presented in Fig. 12. The assumed values are identical to Case 1, and only the slug volume changes from 0.1 to 0.3 PVI. The results show a slight increase in the recovery factor at $t=8$ PVI as the slug size increases, although at $t=1$ PVI, the recovery factor increases from 0.15 to 0.51, and the recovery stabilization time decreases from 9 to 3 PVI.

Table 1
Exact solution for sequential injection of low-salinity polymer slug followed by low-salinity and high-salinity water drives in (x, φ) domain.

Zones	$c(x,\varphi)$	$c_s(x,\varphi)$	$U(x,\varphi)$	Domains
VI	0	C_S^D	$U_{10}(x,\varphi)$	$\varphi>t_s$, $\varphi>F'_{11}(x-x_a)+t_s$
VII	0	C_S^D	U_{11}	$\varphi>t_s$, $\Gamma(C_S^D)(x-x_a)+t_s<\varphi<F'_{11}x-x_a)t_s$
VIII	c^D	C_S^D	U_{12}	$\varphi>t_s$, $\varphi(x_{f2})<\varphi<\Gamma(C_S^{DD})(x-x_a)+t_s$
IX	c^D	C_S^D	$U_{13}(x,\varphi)$	$t_s<\varphi<\varphi(x_{f2})$, $\varphi>\Gamma(C_S^D)(x-x_b)+t_s$
X	0	C_S^D	U_{15}	$\varphi>t_s$, $((F_{16}-F_{15})/(U_{16}-U_{15}))(x-x_b)+t_s<\varphi<\Gamma(C_S^D)(x-x_b)+t_s$
XI	0	C_S^D	U_{16}	$t_s<\varphi<((F_{16}-F_{15})/(U_{16}-U_{15}))(x-x_b)+t_s$
XII	0	C_S^I	$U_{18}(x,\varphi)$	$F'_3(x-x_b)+t_s<\varphi<t_s$

5. Summary and conclusions

The system of governing equations describing two-phase displacement of oil by the aqueous solution of non-Newtonian polymer with varying salinity allows for a fractional flow form and consists of conservation mass laws for aqueous phase, for polymer, for salt and of the modified Darcy's law. The exact solutions of the system allow analysing the non-Newtonian behaviour effects on efficiency of injection of polymer slug with alternating salinity in the slug and the drive chase. For a fixed polymer concentration,

Table 2
Exact solution for sequential injection of low-salinity polymer slug followed by low-salinity and high-salinity water drives in (x, t) domain.

Zones	$c(x, t)$	$c_s(x, t)$	$S(x, t)$	Domains
VI	0	C_S^D	$S_{10}(x, t)$	$t > t(x_{f1})$, $t > (I(C_S^D)+S_{11})/f_{11}(x-x_a)+t_a$
VII	0	C_S^D	S_{11}	$(I(C_S^D)+S_{11})/f_{11}(x-x_a)+t_a < t < ((F'_{11}+S_{11})/f_{11})(x-x_a)+t_a$
VIII	c^D	C_S^D	S_{12}	$t(x_{f2}) < t < (I(C_S^D)+S_{11})/f_{11}(x-x_a)+t_a$
IX	c^D	C_S^D	$S_{13}(x, \varphi)$	$t(x_{f3}) < t < t(x_{f2})$, $t > (I(C_S^D)+S_{14})/f_{14}(x-x_b)+t_b$
X	0	C_S^D	S_{15}	$((F_{16}-F_{15})/(U_{16}-U_{15})+S_{15})/f_{15}(x-x_b)+t_b < t < (I(C_S^D)+S_{14})/f_{14}(x-x_b)+t_b$
XI	0	C_S^D	S_{16}	$S_{17}/f_{17}(x-x_b)+t_b < t < ((F_{16}-F_{15})/(U_{16}-U_{15})+S_{15})/f_{15}(x-x_b)+t_b$
XII	0	C_S^I	$S_{18}(x, \varphi)$	$(F'_3+S_3)/f_3(x-x_b)+t_b < t < t_b+S_{17}/f_{17}(x-x_b)$

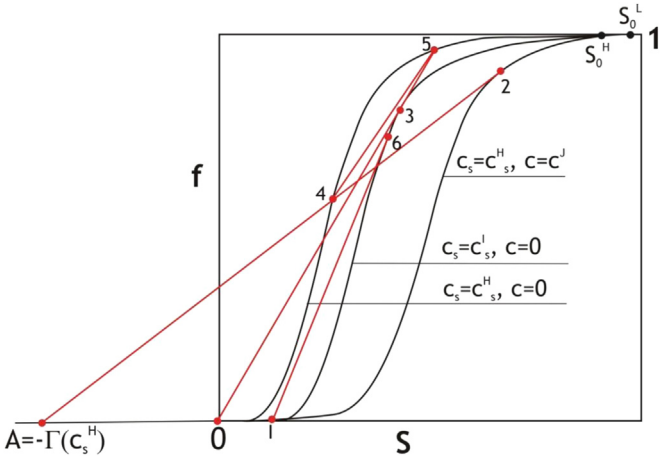

Fig.7. Graphical construction of the Riemann solution for displacement of oil by polymer with salinity higher than the formation water salinity and calculation of the basic points 2, 3…6.

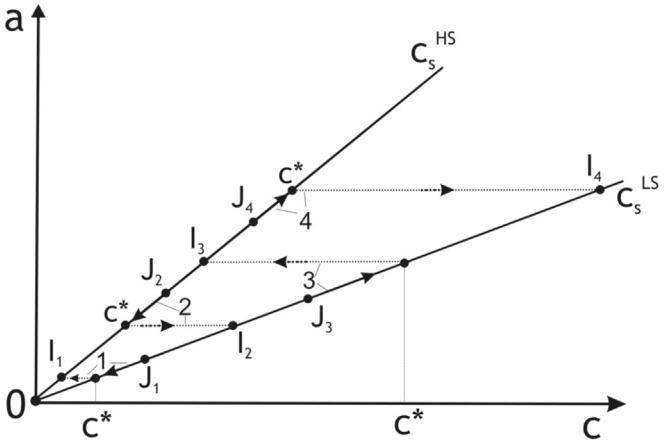

Fig.8. Riemann solutions for auxiliary system for: 1-injection of low-salinity high-concentration polymer solution into the rock with high salinity low-concentration polymer; 2-injection of high-salinity, high-concentration polymer solution into the rock with low salinity, low-concentration polymer; 3-injection of low-salinity, low-concentration polymer solution into the rock with high salinity, high-concentration polymer; 4-injection of high-salinity, low-concentration polymer solution into the rock with low salinity, high-concentration polymer.

the increase in injection velocity shifts the fractional-flow function to higher water saturations because of the decrease in polymer viscosity. Consequently, both the polymer breakthrough time and the oil recovery increase with decreasing velocity. The increase in exponent n (from 0.5 to 0.7) for a fixed velocity and polymer concentration slightly increases the breakthrough time and oil recovery.

Table 3
Parameters for Corey correlation, power law function and polymer adsorption in different salinities.

	Low salinity water	High salinity water
End point water relative permeability	0.17	0.29
End point oil relative permeability	0.57	0.57
Oil residual saturation	0.2	0.23
Connate water saturation	0.2	0.2
Corey exponent for water	4.5	3.1
Corey exponent for oil	3	4.6
Power-law exponential index	*0.5*	*0.65*
Bulk power law coefficient	*0.212*	*0.039*
Concentration of adsorbed polymer	$a=0.2c$	$a=0.4c$

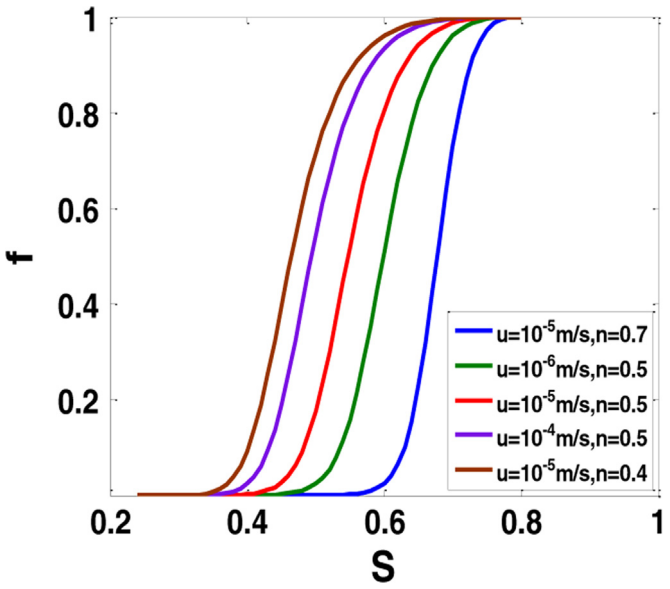

Fig.9. Fractional flow curve for two-phase flow of non-Newtonian and Newtonian liquids for three different velocities u and different power-law exponents n.

The salinity-dependent Corey relative-permeability parameters were used to study the effect of salinity variations on efficiency of polymer flooding. With the parameter listed in Table 3, the salinity reduction results in decrease of the fractional-flow function.

The example considered in this paper reveals that the salinity reduction in the polymer slug slows the waterfront and increases the water breakthrough time. Even after the water breakthrough, higher oil cuts are observed in the effluent for LSP flooding than for HSP flooding. The solution of LSP flooding contains an additional shock, which is the low-salinity water shock. The lower adsorption of polymer in the LSP case leads to later breakthrough

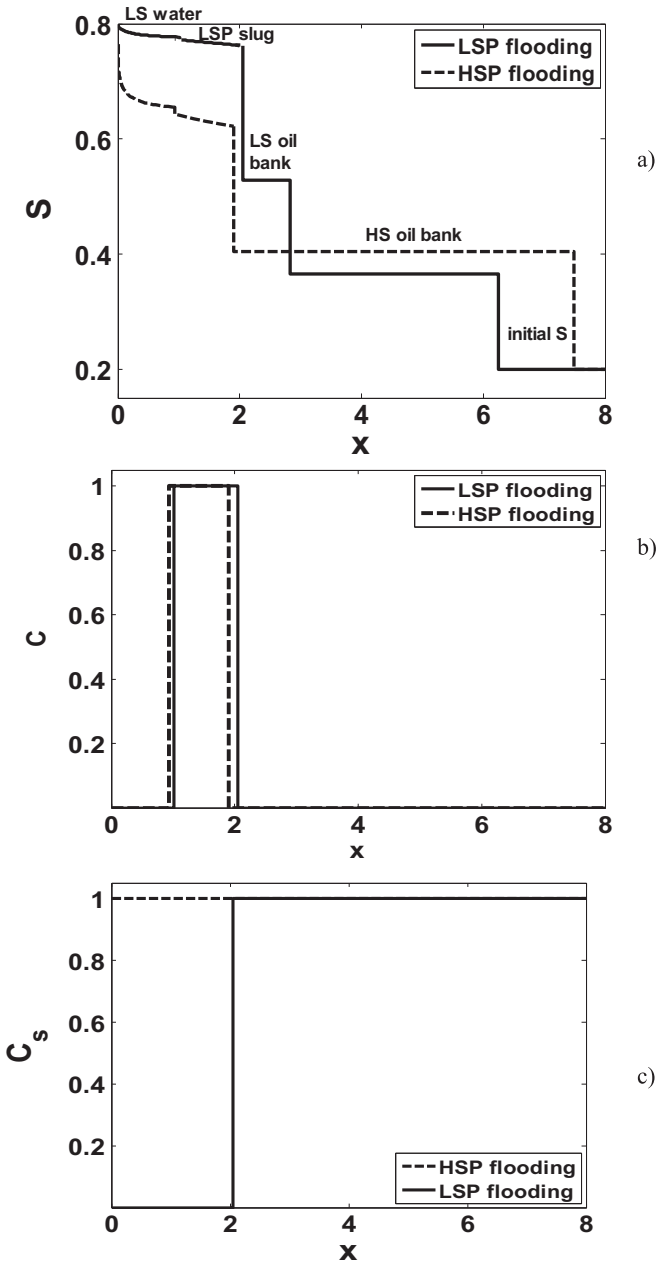

Fig.10. Comparisons of two flooding cases by low salinity polymer slug followed by low-salinity water (LSP) and by the high salinity polymer slug driven by high-salinity water (HSP) at the moment $t=2$ PVI: (a) saturation profiles; (b) polymer concentration profiles; (c) salt concentration profiles.

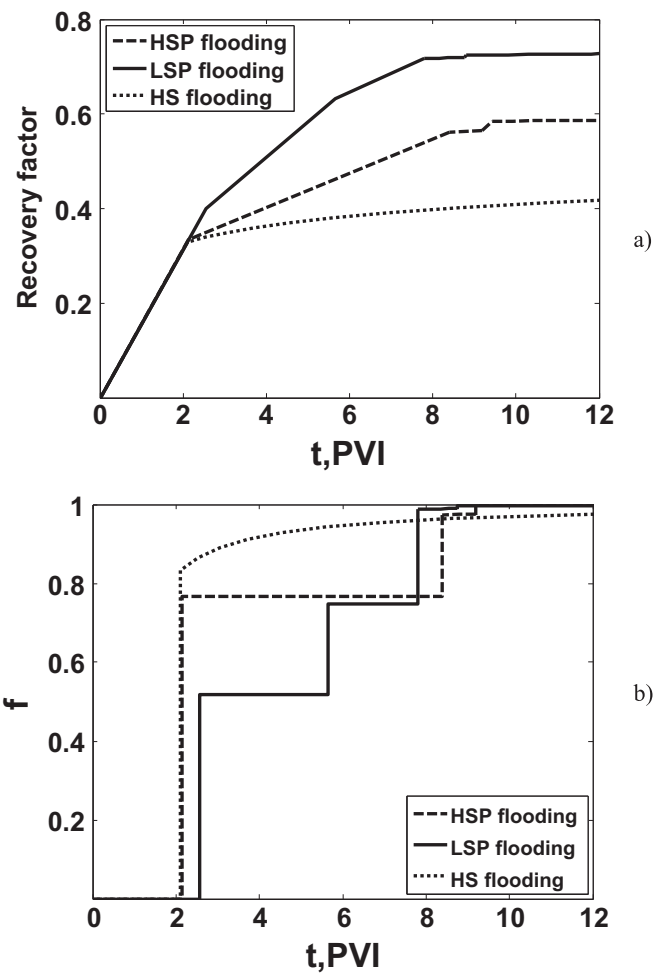

Fig.11. Comparison between cases of oil displacement by formation high salinity water (HS), low salinity polymer slug followed by low-salinity water (LSP) and by the high salinity polymer slug driven by high-salinity water (HSP) (a) recovery factor versus PVI; (b) water cut history.

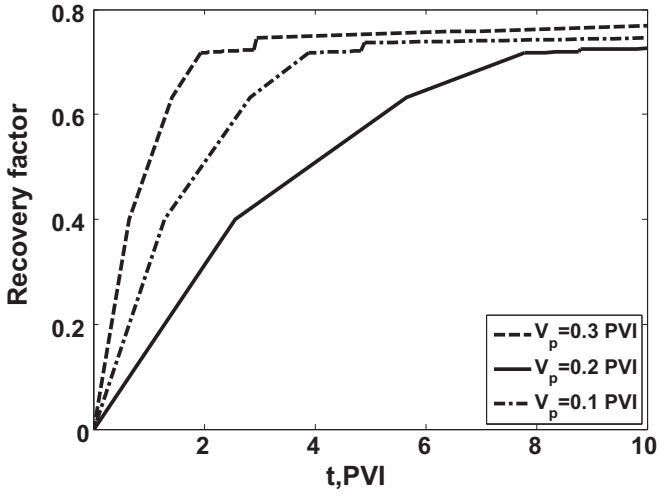

Fig.12. Effect of polymer slug size on oil recovery for low salinity polymer flooding (LSP) (low salinity polymer slug followed by low-salinity water).

of polymer and slight increase in oil cut after polymer breakthrough.

Application of the splitting method to non-self-similar, two-phase, multi-component problems of polymer slug with alternated water salinity injections in oil reservoirs, with the assumptions made in this paper, leads to the following conclusions:

- Accounting for non-Newtonian properties of the injected polymer allows for fractional-flow description of the problem using a velocity-dependent fractional-flow function.
- Application of the splitting technique to the one-dimensional problem of displacement of oil by non-Newtonian polymer slug with varying water salinity yields an exact solution. The solution contains explicit expressions for water saturation and polymer and salt concentrations, and an implicit expression for polymer- and salt-slug trajectories.
- Salinity-dependency of polymer sorption results in appearance of a shock with simultaneous jump in salinity and polymer

concentrations. The polymer concentration jump in this shock disappears at zero initial polymer concentration.

- The solution for $c^I=0$ depends on three fractional-flow curves corresponding to initial salinity, injected fluid and the injected salinity, and zero polymer concentration.
- The low-salinity front moves faster than the polymer front because of polymer adsorption, yielding the oil–water bank with the injected salinity moves ahead of the polymer. It prevents contact between the polymer and formation water.
- Similarly, the back front of the low-salinity slug moves faster than the rear front of the polymer slug, which can also result in a reduction in polymer viscosity. The analytical solution allows calculating the minimum size of the low-salinity slug, preventing the mixing between the polymer and high-salinity water drive.
- Compared to constant-salinity polymer slug flooding, using low-salinity water in the polymer slug results in an increase of water breakthrough time and decrease of water-cut after water breakthrough.

Acknowledgements

The authors thank Prof. A. Shapiro from Technical University of Denmark for long-time co-operation on analytical solutions.

Appendix A. Splitting method for system of two-phase, multicomponent polymer flooding

Following Pires et al. (2006), this appendix shows briefly the splitting procedure for the hyperbolic system (1–3). The stream function $\varphi(x, t)$ can be introduced from the conservation law in Eq. (1):

$$S = -\frac{\partial\varphi}{\partial x}, \quad f = \frac{\partial\varphi}{\partial t}, \tag{A-1}$$

i.e., substitution of Eq. (A-1) into Eq. (1) yields the equality of mixed second-order derivatives of the potential φ, and the potential function has the following form:

$$d\varphi = fdt - Sdx. \tag{A-2}$$

The differential dt can be expressed from Eq. (A-2) as

$$dt = \frac{d\varphi}{f} + \frac{Sdx}{f}. \tag{A-3}$$

Calculating the differential of dt in Eq. (A-3) yields the expressions for Eq. (1) in (x, φ)-coordinates, Eq. (14).

Applying Green's theorem, over any arbitrary domain ϖ with continuous boundary $\partial\varpi$, to Eq. (2) and accounting for Eq. (A-2), yields the transformation of Eq. (2) into Eq. (15):

$$\oint_{\partial\varpi}(cf)dt - (cS + a)dx = \oint_{\partial\varpi} c(fdt - Sdx) - adx = \oint_{\partial\varpi} cd\varphi - adx = \iint_{\varpi}\left(\frac{\partial a}{\partial\varphi} + \frac{\partial c}{\partial x}\right)dxd\varphi = 0 \tag{A-4}$$

Applying Green's theorem, over any arbitrary domain ϖ, to Eq. (3) and accounting for Eq. (A-2),

$$\oint_{\partial\varpi}(c_s f)dt - (c_s S)dx = \oint_{\partial\varpi} c_s(fdt - Sdx) = \oint_{\partial\varpi} c_s d\varphi = \iint_{\varpi}\left(\frac{\partial c_s}{\partial x}\right)dx = 0 \tag{A-5}$$

transforms Eq. (3) to Eq. (16).

Therefore, the original system (1–3) has the form of Eqs. (14–16) in (x, φ)-coordinates. Velocities of rarefaction and shock waves in planes (x, φ) and (x, t) (V and D, respectively) are related as

$$\frac{1}{V} = \frac{f}{D} - S. \tag{A-6}$$

The values of real D and auxiliary V velocities fulfil Eq. (A-6).

System (14–16) has three real distinct eigenvalues $\lambda = \frac{d\varphi}{dx}$:

$$\lambda_1 = \frac{\partial F}{\partial U};\ \lambda_2 = \Gamma(c_s);\ \lambda_3 = 0. \tag{A-7}$$

For discontinuous solutions, the mass balance (Hugoniot-Rankine) conditions on shocks associated with conservation laws (14–16) are

$$[U] = V[F], \quad [c] = V\left[\Gamma(c_s)c\right], \quad [c_s] = 0 \tag{A-8}$$

and

$$\left[\Gamma(c_s)c\right] = 0, \quad [F] = 0, \quad [c_s] = \ \forall\ , \quad V = \infty. \tag{A-9}$$

Eq (A-8) shows that salinity, c_s,, can jump only across the lines φ=const that correspond to the infinite V.

From Eq. (A-8), it follows that the velocity of c-shocks is

$$\frac{1}{V} = \Gamma(c_s) = \frac{[F]}{[U]}, \ [c_s] = 0, [c] \neq 0 \tag{A-10}$$

and that the velocity of S-shocks is

$$V = \frac{[U]}{[F]}, \quad [c_s] = 0, [c] = 0. \tag{A-11}$$

Finally, the auxiliary system (15, 16) permits two types of shocks: c_s-shocks given by Eq. (A-9) and c-shocks given by Eq. (A-10).

Continuous solutions of both general and auxiliary systems correspond to a constant salinity. Therefore, c-rarefactions for Henry's adsorption (9) degenerate into c-shocks. It yields constant concentrations of salt and polymer in the continuous S-waves:

$$\frac{dF(U, a, c, c_s)}{dU} = \eta,\ \Gamma(c_s) = \eta,\ \frac{dc_s}{d\eta} = 0, \tag{A-12}$$

where $\eta=\varphi/x$. The above elementary waves are used to solve the auxiliary and lifting problems in Sections 3.3, 3.4, and 3.5.

Appendix B. Calculation of the recovery factor

The exact solution of system (1–3) allows deriving explicit formulae for recovery factor

$$RF(t) = \frac{\bar{S}(t) - S^I}{1 - S^I}, \tag{B-1}$$

where $\bar{S}$ is the average water saturation in the reservoir and is defined by

$$\bar{S} = \int_0^{\frac{\phi L}{V_p}} S(x, t)dx. \tag{B-2}$$

The contour integration method can be used to derive the explicit formulae for the average saturation $\bar{S}$(Bedrikovetsky, 1993). For $t<1$, integration of Eq. (1) over the domain bounded by the contour ω: $(0, 0)\rightarrow(0, t)\rightarrow(\frac{\phi L}{V_p}, t)\rightarrow(0, 0)$ with further application of Green's formula yields

$$\iint_{\varpi}\frac{\partial S}{\partial t} + \frac{\partial f(S, c)}{\partial x}dxdt = \oint_{\partial\varpi} fdt - Sdx = t - \bar{S}(t)\frac{\phi L}{V_p} - f\left(\frac{\phi L}{V_p t}\right)t + S\left(\frac{\phi L}{V_p t}\right)\frac{\phi L}{V_p} = 0, \tag{B-3}$$

which results in

$$\bar{S}(t) = V_p t/\phi L\left(1 - f\left(\frac{\phi L}{V_p t}\right)\right) + S\left(\frac{\phi L}{V_p t}\right). \tag{B-4}$$

The average saturation (B-4) allows for the graphical calculation. The intersection of a straight line with slope $\frac{\phi L}{V_p t}$ originating from points S^J (zone I), S_4 (zone II), and S_3 (zone III) with $f=1$ in the (S, f) plane gives $\bar{S}$ in zones I, II, and III, respectively.

In zone IV where $1 < t < t_w$ (t_w is found from Eqs. (38, 40) at $x = \frac{\phi L}{V_p}$), the intersection of a straight line with slope $\frac{\phi L}{V_p t}$ originating from $(S_1(x/t), c^J, c_s^J)$ and with $f=1$ gives $\bar{S}$.

To find $\bar{S}$ for $t > t_w$, we integrate Eq. (B-3) over the region bounded by $(0, 0)\rightarrow(0, t_w{}^-)\rightarrow(\frac{\phi L}{V_p}, t_w{}^-)\rightarrow(x(t_w{}^+), t_w{}^+)\rightarrow(0, 0)$:

$$\bar{t_w} - \bar{S}\frac{\phi L}{V_p} = \left(f^+ - S^+ f'\left(S^+, c^J\right)\right)t_w^+ + \left(f^- - S^- f'(S^-, 0)\right)\left(\left(\bar{t_w} - t_w^+\right)\right). \tag{B-5}$$

That yields

$$\bar{S} = -V_p/\phi L\left(\left(f^+ - S^+ f'\left(S^+, c^J\right)\right)t_w^+ + \left(f^- - S^- f'(S^-, 0)\right)\left(\left(\bar{t_w} - t_w^+\right)\right) - \bar{t_w}\right). \tag{B-6}$$

Here, superscripts + and – represent the values ahead of and behind the polymer-slug rear. Grouping the terms in (B-6) and using Eqs. (36, 37), we finally obtain the formula for $\bar{S}$

$$\bar{S} = \bar{S}^- + \left(\bar{S}^- - \bar{S}^+\right)\frac{f'\left(S^+, c^J, c_s^J\right)V_p}{\Delta\left(S^+, c^J, c_s^J\right)\phi L}, \tag{B-7}$$

where $\bar{S}^-$ and $\bar{S}^+$ are

$$\bar{S}^- = S^- + \frac{1 - f\left(S^-, c = 0, c_s^J\right)}{f'\left(S^-, c = 0, c_s^J\right)},\ \bar{S}^+ = S^+ + \frac{1 - f\left(S^+, c^J, c_s^J\right)}{f'\left(S^+, c^J, c_s^J\right)}. \tag{B-8}$$

References

Bedrikovetsky, P., 1982. Displacement of oil by a chemical slug with water drive. J. Fluid Dyn. 3, 102–111.

Bedrikovetsky, P., 1993. Mathematical Theory of Oil and Gas Recovery: With Applications to Ex-USSR Oil and Gas Fields. Kluwer Academic, Dordrecht.

Borazjani, S., Bedrikovetsky, P., Farajzadeh, R., 2014. Exact solution for non-self-similar wave-interaction problem during two-phase four-component flow in porous media. Abstr. Appl. Anal. 2014, 13.

Borazjani, S., Roberts, A.J., Bedrikovetsky, P., 2016. Splitting in systems of PDEs for two-phase multicomponent flow in porous media. Appl. Math. Lett. 53, 25–32.

Braginskaya, G., Entov, V., 1980. Nonisothermal displacement of oil by a solution of an active additive. J. Fluid Dyn. 15 (6), 873–880.

Claridge, E., Bondor, P., 1974. A graphical method for calculating linear displacement with mass transfer and continuously changing mobilities. SPE J. 14 (6), 609–618.

Courant, R., Friedrichs, K.O., 1976. Supersonic Flow and Shock Waves. Interscience Publisher LTD., London.

De Nevers, N., 1964. A calculation method for carbonated water flooding. SPE J. 4 (01), 9–20.

Ewing, R.E., 1983. The Mathematics of Reservoir Simulation. SIAM, Philadelphia.

Fayers, F., 1962. Some theoretical results concerning the displacement of a viscous oil by a hot fluid in a porous medium. J. Fluid Mech. 13, 65–76.

Gel'fand, I.M., 1959. Some problems in the theory of quasi-linear equations. Usp. Mat. Nauk. 14 (2), 87–158.

Helfferich, F.G., 1981. Theory of multicomponent multiphase displacement in porous media. SPE J. 21 (01), 51–62.

Hirasaki, G., 1981. Application of the theory of multicomponent, multiphase displacement to three-component, two-phase surfactant flooding. SPE J. 21 (2), 191–204.

Holden, H., Risebro, N.H., 2002. Front Tracking for Hyperbolic Conservation Laws. Springer-Verlag, New York.

Johansen, T., Winther, R., 1988. The solution of the Riemann problem for a hyperbolic system of conservation laws modelling polymer flooding. SIAM J. Math. 19 (3), 541–566.

Johansen, T., Tveito, A., Winther, R., 1989. A Riemann solver for a two-phase multicomponent process. SIAM J. Sci. Stat. Comput. 10 (5), 846–879.

Lager, A., Webb, K., Black, C., Singleton, M., Sorbie, K., 2008. Low salinity oil recovery—an experimental investigation. Petrophysics 49 (1), 28–35.

Lake, L.W., 1989. Enhanced Oil Recovery. Prentice Hall, Englewood Cliffs, N.J.

Landau, L.D., Lifshitz, E.M., 1987. Fluid Mechanics. Elsevier, Oxford.

Mahani, H., Berg, S., Ilic, D., Bartels, W.B., Joekar-Niasar, V., 2015. Kinetics of low-salinity-flooding effect. SPE J. 20 (1), 8–20.

Mohammadi, H., Gary, J., 2012. Mechanistic modeling of the benefit of combining polymer with low-salinity water for enhanced oil recovery. SPE 153161, presented at the SPE improved oil recovery symposium in Tulsa, Oklahoma.

Pires, A.P., Bedrikovetsky, P., Shapiro, A.A., 2006. A splitting technique for analytical modelling of two-phase multicomponent flow in porous media. J. Pet. Sci. Eng. 51 (1), 54–67.

Pope, G., Lake, L., Helfferich, F., 1978. Cation exchange in chemical flooding: Part 1—Basic theory without dispersion. SPE J. 18, 418–434.

Pope, G., 1980. The Application of Fractional Flow Theory to Enhanced Oil Recovery, SPE. Texas.

Rhee, H.-K., Aris, R., Amundson, N.R., 1998. Theory and Application of Hyperbolic Systems of Quasilinear Equations Vol. 2. Prentice-Hall, Englewood Cliffs, NJ.

Sorbie, K.S., 1991. Polymers-Improved Oil Recovery. Blackie and Son Ltd., Glasgow.

Vicente, B.J., Priimenko, V., Pires, A.P., 2014. Semi-analytical solution for a hyperbolic system modeling 1D polymer slug flow in porous media. J. Pet. Sci. Eng. 115, 102–109.

Wu, Y.-S., Pruess, K., Witherspoon, P.A., 1991. Displacement of a Newtonian fluid by a non-Newtonian fluid in a porous medium. Transp. Porous Media 6, 115–142.

4.3 Exact Solutions for 1-D Polymer Flooding Accounting for Mechanical Entrapment

S. Borazjani, P. Bedrikovetsky

Water Resources Research, submitted 01/ 2016

Statement of Authorship

Title of Paper	Exact solutions for 1-D polymer flooding accounting for mechanical entrapment
Publication Status	☐ Published ☐ Accepted for Publication ☑ Submitted for Publication ☐ Unpublished and Unsubmitted work written in manuscript style
Publication Details	S. Borazjani, P. Bedrikovetsky. (2016). Exact solutions for 1-D polymer flooding accounting for mechanical entrapment

Principal Author

Name of Principal Author (Candidate)	Sara Borazjani
Contribution to the Paper	Problem formulation, Derivation of the mathematical model, Analysis of results, Writing the manuscript
Overall percentage (%)	85%
Certification:	This paper reports on original research I conducted during the period of my Higher Degree by Research candidature and is not subject to any obligations or contractual agreements with a third party that would constrain its inclusion in this thesis. I am the primary author of this paper.
Signature	Date: 1.12.2015

Co-Author Contributions

By signing the Statement of Authorship, each author certifies that:

i. the candidate's stated contribution to the publication is accurate (as detailed above);

ii. permission is granted for the candidate in include the publication in the thesis; and

iii. the sum of all co-author contributions is equal to 100% less the candidate's stated contribution.

Name of Co-Author	P. Bedrikovetsky
Contribution to the Paper	Problem formulation, Manuscript review and assessment
Signature	1.12.2015

Please cut and paste additional co-author panels here as required.

Name of Co-Author			
Contribution to the Paper			
Signature		Date	

Exact solutions for 1-D polymer flooding accounting for mechanical entrapment

S. Borazjani, P. Bedrikovetsky

The University of Adelaide, Faculty of Engineering and Mathematical Sciences, Adelaide, Australia

Abstract Two-phase transport of aqueous colloids and solutes occurs in numerous areas of chemical, environmental, geo-, and petroleum engineering. The main effects are particle capture by the rock, its adsorption and altering the flux by the changing suspended, adsorbed and retained concentrations. The mathematical model for the component capture and adsorption is considered, resulting in a 3×3 system of partial differential equations. Using the stream-function as an independent variable instead of time splits the system into a 2×2 auxiliary system, containing only concentrations, and one lifting hydrodynamic equation for unknown phase saturation. The auxiliary problem is linear and allows for exact solution. The exact formulae allow predicting the profiles and breakthrough histories for the suspended, adsorbed and retained concentrations and phase saturations. The solution shows that for small retained concentrations, the suspended concentration is steady-state behind the concentration front, where all retained concentrations are proportional to the mass of suspended particles that passed via a given reservoir cross-section. The maximum penetration depths for suspended and retained particles are the same and are equal to those for a single-phase flow.

1. Introduction

Suspension-colloidal and solute flows in porous media occur in numerous engineering areas, such as disposal of industrial wastes in aquifers with propagation of contaminants and pollutants, industrial water treatment and filtering, injection of hot or low-salinity water into aquifers for storage purposes, or water injection into geothermal reservoirs [*Dagan*, 1989; *Benson et al*., 1991; *Dagan et al*., 2008; *Bradford et al.*, 2011, 2012; *Chrysikopoulos et al.*, 2012; *Katzourakis and Chrysikopoulos*, 2014, 2015]. An aqueous suspension of solid particles invades formations during well drilling; the penetration depth highly affects the formation damage and skin factor; these effects are also important for interpretation of electrical logging based on the salinity contrast between the invaded drilling fluid and reservoir water [*Civan*, 2015]. Similar invasion by the fracturing fluid occurs during hydraulic fracturing of artesian, oil, and geothermal wells. Clay and soil suspensions and colloids flow in the vadose zone and during irrigation. Two-phase suspension-colloidal flows occur in unsaturated aquifers. All metal cations adsorb on clays that are present in the rock. Almost all subterranean flows are accompanied by the ionic exchange between the aqueous brines and the rock minerals. In the petroleum industry, low-quality water with solid or liquid particles is injected into oilfields, impairing the wells but often enhancing oil recovery [*Civan*, 2015].

Numerical models for two-phase solute and colloidal-suspension flows have been used to study propagation of viruses, bacteria, and nano-particles in under-saturated aquifers

[*Mitropoulou et al.*, 2013; *Zhang et al.*, 2013, 2014]. The one-dimensional problems for solute invasion/injection with adsorption (so-called multicomponent polymer flooding) correspond to Riemann problem and allow for self-similar solutions [*Johansen and Winther* 1988]. However, kinetic capture of the aqueous components by the rock breaks the conservation-law type of the governing system, and one-dimensional flow is not self-similar anymore. To our knowledge, analytical models for two-phase flow of solutes and colloids in porous media are unavailable in the literature.

In the current paper, non-self-similar solutions for one-dimensional problem of two-phase flow accounting for mechanical entrapment and adsorption of component by the rock is obtained. To be specific, the component is called "the polymer", since that exhibits both retention and adsorption in porous media. The effects of continuous increase of the pressure drop and reduction of the breakthrough concentration if compared with the injected concentration, which was observed in laboratory tests and was not described the model that ignores the capture, are clearly exhibited. Both cases of continuous polymer injection and of polymer slug with the water chase drive are discussed.

The structure of the text is as follows. Section 2 presents a 3×3 system of governing equations along with initial and boundary conditions for one-dimensional flow. Section 3 derives the analytical solution using the splitting method for the case of linear sorption isotherm and constant filtration coefficient. Section 4 analyses the obtained solution and describes the structure of the flow zone. Section 5 derives exact solutions for the cases of non-linear sorption isotherm and varying filtration coefficient. Sections 6 and 7 discuss the results of the analytical modelling of two-phase solute and colloidal flows in porous media, which concludes the paper.

2. Basic system of equations

This section formulates the one-dimensional two-phase flow of aqueous polymer solution through porous media, including the main assumptions (Section 2.1), derivation of governing equations (Section 2.2).and the initial and boundary conditions (Section 2.3).

2.1 Assumptions

Consider incompressible, one-dimensional flow of an aqueous polymer solution in porous media with polymer sorption and mechanical entrapment. Figure 1 shows rock porosity ϕ, water saturation s, concentrations of flowing, adsorbed and entrapped polymer c, a, and σ_s, respectively. Figure 2 shows polymer capture mechanisms include adsorption and mechanical entrapment.

The polymer concentration is small enough not to affect the volumetric balance of the aqueous solution. The deep-bed-filtration formula is assumed for the polymer entrapment rate, where, the polymer-capture rate is proportional to the dispersion-free polymer flu*x cu* [*Lotfollahi et al.*, 2015]. The linear equilibrium sorption isotherm is assumed. We assume that the relative permeability of the aqueous phase is a monotonically decreasing function of the

sum of sorbed and entrapped concentrations. Capillary pressure between phases is considered negligible compared with phase pressures.

2.2 Governing equations

System of governing equations for 1-D flow of polymer solution through porous media includes equation for mass balances of water, dissolved (*c*), adsorbed (*a*), and trapped polymer concentrations (σ_s) in dimensionless form are [*Lake* 1989, *Bedrikovetsky* 1993]:

$$\frac{\partial s}{\partial t}+\frac{\partial f(s,c,\sigma_s)}{\partial x}=0 \tag{1}$$

$$\frac{\partial}{\partial t}(sc+a+\sigma_s)+\frac{\partial cf}{\partial x}=0 \tag{2}$$

$$\frac{\partial \sigma_s}{\partial t}=\lambda cf\left(s,c,\sigma_s\right) \tag{3}$$

where, λ is the filtration coefficient and is assumed to be constant, f is fractional flow of water, x and t are dimensionless coordinates.

The dimensionless concentrations and coordinates are defined as follow:

$$x\to\frac{x}{L},\ t\to\frac{1}{\phi L}\int_0^t U(t)dt,\ \lambda\to\lambda L,\ \ c\to\frac{c}{c^J},\ \sigma_s\to\frac{\sigma_s}{\phi c^J} \tag{4}$$

For small concentration *c*, the equilibrium polymer-adsorption isotherm is described by the linear Henry's sorption

$$a=\Gamma c \tag{5}$$

2.3 Initial and boundary conditions

Initial conditions for one-dimensional flow correspond to connate water saturation with no polymer in the porous medium

$$t=0,\quad c=0,\quad \sigma_s=0,\quad s=s^I \tag{6}$$

Slug injection of polymer solution corresponds to boundary conditions with the fixed injected fractional flow, and a piecewise constant injected concentration

$$x=0,\quad f\left(s^J,1,\sigma_s\left(0,t\right)\right)=1,\begin{cases}c=1 & t<t_s\\ c=0 & t>t_s\end{cases} \tag{7}$$

For unknown concentrations of captured polymer, Goursat boundary conditions are formulated [*Tikhonov and Samarskii,* 1990]. Substituting *c*=1, *c*=0 and *f*=1 from the boundary condition (7) into rate equations (3) yields

$$x=0,\ \begin{cases} \dfrac{d\sigma_s(0,t)}{dt}=\lambda, & t<t_s \\ \dfrac{d\sigma_s(0,t)}{dt}=0, & t>t_s \end{cases} \tag{8}$$

3. Splitting method

This section reduces the 3×3 system of quasi-linear hyperbolic equations (1-3) to one scalar hyperbolic equation and 2×2 retention-kinetic equations. The governing system (1-3), subject to the initial and boundary conditions of the previous section, is solved using the splitting method [*Wagner*, 1987; *Pires et al.*, 2006; *Borazjani et al.*, 2016]. Section 3.1 introduces the stream-function and splits the system into the retention-kinetics auxiliary system and the lifting equation for unknown saturation. Section 3.2 presents the solution of the auxiliary system. Sections 3.3 and 3.4 present the solution of the lifting problem and inverse mapping, respectively.

3.1 Stream function and splitting mapping

Consider a stream function $\varphi(x,t)$ associated with the conservation law in Eq. (1)

$$s=-\frac{\partial\varphi}{\partial x}, \qquad f=\frac{\partial\varphi}{\partial t} \tag{9}$$

The corresponding differential form for two-phase flux is

$$d\varphi = f dt - s dx \tag{10}$$

which determines the stream-function

$$\varphi(x,t)=\int_{00}^{(x,t)} f dt - s dx \tag{11}$$

The transformation of system (1-3) from (x, t) into (x, φ) coordinate using Eq. (10) yields the following

$$\frac{\partial F(G,\sigma_1\ldots\sigma_m,c)}{\partial\varphi}+\frac{\partial G}{\partial x}=0, \qquad F=-\frac{s}{f(s,c,\sigma_s)},\ G=\frac{1}{f(s,c,\sigma_s)} \tag{12}$$

$$\frac{\partial c}{\partial x}+\frac{\partial(\sigma_s+\Gamma c)}{\partial\varphi}=0 \tag{13}$$

$$\frac{\partial\sigma_s}{\partial\varphi}=\lambda c \tag{14}$$

For detailed derivations see *Pires et al.*, 2006 and *Borazjani et al.*, 2016.

The inlet boundary conditions (7) in co-ordinates (x,φ) become

$$x=0: \quad \begin{cases} c=1, & \dfrac{d\sigma(0,\varphi)}{d\varphi}=\lambda, \quad \varphi<\varphi_s \\ c=0, & \dfrac{d\sigma(0,\varphi)}{d\varphi}=0, \quad \varphi>\varphi_s \end{cases} \tag{15}$$

$$x=0: \quad U=1 \tag{16}$$

and initial conditions (6) take the form

$$\varphi=-s^I x: \quad c=0, \quad \sigma_s=0 \tag{17}$$

$$\varphi=-s^I x \quad : \; F=-\infty \tag{18}$$

Thus, in the system of co-ordinates (x,φ), the auxiliary problem (13, 14) separates from the lifting problem (12). The auxiliary system contains unknown kinetics variables c and σ_s, whereas the lifting equation depends also on unknown saturation s. Here the uniform initial conditions (17, 18) are set along the straight line $\varphi=-s^I x$, which is the image of axes $t=0$ in (x,φ) coordinates. The solution of lifting equation (12) $G(x,\varphi)$ is also presented in the plane (x,φ).

3.2. Solution of the auxiliary system

The characteristic form of the first-order-partial-differential Eq. (13) substituting (14) is

$$\frac{d\varphi}{dx}=\Gamma, \frac{dc}{dx}=-\lambda c \tag{19}$$

Equation (19) with boundary condition Eq. (15) behind the front $\Gamma x<\varphi<\Gamma x+\varphi_s$ is solved by separation of variables to obtain polymer concentration in the aqueous solution:

$$c=e^{-\lambda x} \tag{20}$$

Derivation of the characteristic form of the first order partial differential Eq. (19) along the characteristics $\varphi=\Gamma(x-x_0)+\varphi_0$ ahead of the front $-s^I x<\varphi<\Gamma x$, and behind the slug front $\Gamma x+\varphi_s<\varphi$ and solving it yields to zero concentration.

Therefore, the polymer concentration is:

$$c(x,\varphi)=\begin{cases} c=0 & \Gamma x+\varphi_s<\varphi<\infty \\ c=e^{-\lambda x} & \Gamma x<\varphi<\Gamma x+\varphi_s \\ c=0 & -s^I x<\varphi<\Gamma x \end{cases} \tag{21}$$

Integrating both sides of Eq. (14) in φ and using (21) results in an expression for the concentration of the entrapped polymer

$$\sigma_s(x,\varphi)=\begin{cases}\sigma_s=\lambda e^{-\lambda x_0}\left(\Gamma x_0+\varphi_s\right) & \varphi>\Gamma x+\varphi_s\\ \sigma_s=\lambda e^{-\lambda x}\left(\varphi-\Gamma x\right) & \Gamma x<\varphi<\Gamma x+\varphi_s\\ \sigma_s=0 & -s^I x<\varphi<\Gamma x\end{cases} \quad (22)$$

The solution of auxiliary problem (13, 14) $c(x, \varphi)$, $\sigma_s(x, \varphi)$ as obtained by the method of characteristics can be presented in the (x, φ)-plane (Figure 3).

3.3. Lifting procedure

Let us solve lifting equation (12) for the already known suspended and retained concentrations (21-22). Subjecting lifting equation (12) to initial and boundary conditions (16, 18) yields a hyperbolic PDE and has the conservation law type.
The characteristic form of lifting equation (12) is

$$\frac{d\varphi}{dx}=\frac{\partial F(G,c,\sigma_s)}{\partial G},\quad \frac{dG}{dx}=-\frac{\partial F(G,c,\sigma_s)}{\partial c}\frac{\partial c}{\partial \varphi}-\frac{\partial F(G,c,\sigma_s)}{\partial \sigma}\frac{\partial \sigma_s}{\partial \varphi} \quad (23)$$

As follows from Eq. (23), for $-s^I x<\varphi<\Gamma x$ and $\varphi>\Gamma x+\varphi_s$ where $c=\sigma_s=0$, saturation is constant along the characteristics, which become straight lines. In zone $\Gamma x<\varphi<\Gamma x+\varphi_s$ the characteristic curves are obtained by solving two equation (23) simultaneously.

3.4. Inverse mapping

To obtain the solution of problem (1-3), the inverse transformation of (x, φ) to (x, t) in the solution of auxiliary and lifting problems is performed

As follows from Eq. (10),

$$t(x,\varphi)=\int_{0,0}^{x,\varphi}\left(\frac{1}{f(x,\varphi)}d\varphi+\frac{s(x,\varphi)}{f(x,\varphi)}dx\right), \quad (24)$$

expressing the inverse mapping. Substitution of Eq. (24) into the auxiliary and lifting solutions yields the solution of general problem (1-3).

4. Exact Solution for the Case of Fractional Flow Independent of Retained Concentrations

Consider the injection of a high-concentration suspension that affects the aqueous phase viscosity. We also assume that the effect of retained concentration on relative permeability of water is neglected. These assumptions are valid in the following cases: low capture rate, low values of formation damage coefficients, low injected concentration, and short times. In all those cases, the process is described by system (1-3) where the fractional flow is independent of retention concentrations. The solution of auxiliary problem (13–14) is given by Eqs. (21, 22).

$$\frac{d\varphi}{dx}=\frac{\partial F\left(G,c(x)\right)}{\partial G},\quad \frac{dG}{dx}=0 \tag{25}$$

Substituting the expression for functions F and G from the second and third terms in system (12) into (23) yields

$$\frac{d\varphi}{dx}=\frac{\Delta(s,c,\sigma)}{f_s'(s,c,\sigma)},\ \Delta(s,c,\sigma)=f(s,c,\sigma)-sf_s'(s,c,\sigma)$$
$$\frac{df(s,c)}{dx}=0 \tag{26}$$

Let us solve the lifting problem using the method of characteristics. First we discuss the characteristic lines that start at the axis x=0, which corresponds to zone V (Figure 5). In zone IV, the characteristic curves start at the axis $\varphi=\Gamma x$ and propagate inside the area $\varphi>\Gamma x$. Zone III is formed by straight characteristic lines that start at the axis $\varphi=\Gamma x$ and propagate inside the area $\varphi<\Gamma x$. Zone II is a shock s-wave 3-s^I for $c=0$. Zone VI

In zone V, consider a characteristic that starts in point (0, 0) and corresponds to any arbitrary value s_0, $s_2<s_0<s^J$. Here point 2 is determined by

$$\frac{\partial F\left(G,1\right)}{\partial G}=\Gamma \tag{27}$$

The solution $s=s_I(x,s_0)$ is determined from the condition of fractional flow conservation along the characteristic $\varphi=\varphi(x)$:

$$f\left(s_0,1\right)=f\left(s(x,\varphi(x)),c(x)\right) \tag{28}$$

Substituting eqs (28) and (21) into eq (26), we obtain the equation of the characteristic curve, presented in first line of fifth column (Table 1). The curve with $s_0=s_2$ separates zones V and IV.

Change of parameters along characteristic curves in zone V corresponds to straight horizontal lines f=const that start at the fractional flow c=1 in the saturation interval [2, s^J] and finish up at the fractional flow $c=e^{-\lambda xa}$ (Figure 5). The tangent $dF/dG>0$ increases along the characteristic curves, therefore, the characteristic curves do not intersect in zone V. No s-shocks appear in zone V.

In zone IV, all characteristic lines start at axis $\varphi=\Gamma x$. Concentration c above this line is given by eq (21); below this line, concentration c is equal zero. The concentration-saturation shock occurs along this line. It determines the saturation $s(x_0)$ above the line $\varphi=\Gamma x$ for each point x_0:

$$\frac{\partial F(G^-,\exp(-\lambda x_0))}{\partial G}=\Gamma \tag{29}$$

Saturation $s(x_0)$ above the axis φ=0 change from s_2 for x_0=0 to s_5 with x_0 tending to infinity. The points 2…5 behind the shock front correspond to maxima of curves $F(G,c)$ (Figure 5).

The fractional flow is constant along the characteristics $\varphi=\varphi(x)$:

$$f\left(s\left(x,\varphi(x)\right),\exp\left(-\lambda x\right)\right)=f\left(s^{-}\left(x_0\right),\exp\left(-\lambda x_0\right)\right) \tag{30}$$

Expressing $s(x,\ \varphi(x))$ from (30) and substituting it into first eq (26) yields the explicit expression for the characteristic line presented in second line of the fifth column in Table 1.

Now let us consider saturation distribution in zone III. Saturation s^{+} ahead of c-shock (at $\varphi<\Gamma x$) is calculated from mass balance across the shock

$$\frac{\left[-\frac{s}{f}\right]}{\left[\frac{1}{f}\right]}=\Gamma \tag{31}$$

Eq (90) shows that the points below and above axis $\varphi=\Gamma x$ in plane (s, f) are located on the straight line that crosses three points $s^{-}=s_2$, $s^{+}=s_3$, and $(0,-\Gamma)$ (Figure 5).

Below the axis $\varphi=\Gamma x$, the solution is given by the characteristics emanating from a point $(x_0,0)$. In this zone, c=0, so the characteristics are straight lines and given by the equation presented in Table 1 (third line and fifth column).

In zone II, c=0 and the solution is given by a constant value s_3.

In zone VI all characteristic lines start at axis $\varphi=\Gamma x+\varphi_s$. In this zone, c=0, so the characteristics are straight lines, saturation behind of $\varphi=\Gamma x+\varphi_s$ is calculated from the equality of the concentration shock velocity and saturation and given by the equation presented in Table 1 (third line and fifth column).

$$\frac{\left[-\frac{s}{f}\right]}{\left[\frac{1}{f}\right]}=\Gamma \tag{32}$$

The boundaries between six zones are given in Table 2.

Applying formula (24) for inverse mapping of independent co-ordinate t results in the representation of the solution in plane (x, t) (Figure 6a). The explicit formulae for saturation distribution in six zones are presented in Table 3, where the boundaries between six zones are given in Table 4. The c-s-shocks are exhibited in suspended-concentration and saturation profiles in Figures 6b and 6c; the continuous retention profiles are shown in Figure 6c.

The exact solution of eqs (16-18) exhibits the following structure of two-phase (Figure 6):

I - unperturbed zone with initial saturation and no polymer;

II - first polymer-free bank with constant water saturation;

III - second particle-free bank with increase of water saturation s_3 to s_5;

IV - first two-phase flow zone with suspended and retained particles behind the concentration front;

V - two-phase flow zone with suspended and retained particles where saturation increases up to s^J-value;

VI - particle free zone with saturation s^J to s_5.

5. Solutions for Non-linear sorption and capture.

Consider the auxiliary system with non-linear adsorption isotherm $a=a(c)$:

$$\frac{\partial c}{\partial x}+\frac{\partial\left(\sigma_s+a(c)\right)}{\partial \varphi}=0 \tag{33}$$

Substitution of the expression (14) for the retention rate into Eq (33) yields

$$\frac{\partial a(c)}{\partial \varphi}+\frac{\partial c}{\partial x}=-\lambda c \tag{34}$$

The analytical solution for Eq (34) with initial and boundary conditions (6) and (7) have been found by *Lotfollahi et al.,* 2016.

Another non-linear case allowing for analytical solution corresponds to high concentration of strained particles, where the filtration coefficient is σ_s–dependent:

$$\frac{\partial \sigma_s}{\partial \varphi}=\lambda(\sigma_s)c \tag{35}$$

The problem can be solved by introduction of the potential (see Alvares, 2005, 2006)

$$c=\int_0^{\sigma_s}\frac{du}{\lambda(u)}$$

Substituting the expression (36) into Eq (13) yields the decreasing of its order by one. The solution of the obtained first-order hyperbolic equation allows for exact integration.

6. Discussions

The system for two-phase flow of polymer solution with sorption and capture mechanisms consists of 3 equations. It was found that using the stream function φ (10) as an independent variable instead of time separates 2×2 auxiliary equations with unknowns c, σ_s from one scalar lifting equation for unknown saturation s. The 2×2 auxiliary problem with uniform initial and boundary data allows for an exact solution in the cases linear sorption and varying filtration function, and non-linear adsorption and constant filtration coefficient.

Structure of the two-phase polymer flow zone. The solution exhibits the following flow zone structure: the undisturbed zone with initial saturation and no polymer is followed by the

polymer-free two-phase bank with higher saturation; then follows the concentration front with saturation increasing as far as the core inlet. Suspension concentration jumps across the concentration front, whereas the captured concentration is continuous. For slug injection, the polymer two-phase flow bank is followed by the polymer free zone with increasing water saturation.

In the case of small adsorbed and captured concentrations that correspond to constant filtration coefficient, the solution shows that the suspension concentration is zero ahead of the concentration front. The suspension concentration instantly becomes steady-state at any given reservoir point behind the front after the front passes this point. The polymer captured concentration is proportional to the mass of particles that passes this point; the proportionality coefficient for each retained concentration is the corresponding filtration coefficient.

The above quantitative observations aid in interpreting the breakthrough data during laboratory experiments and production data from the field tests.

Conclusions

The analytical modelling of two-phase flow of polymer solution in porous media accounting for the polymer adsorption and mechanical entrapment allows drawing the following conclusions:

1. Using the Lagrangian co-ordinate (stream-function) as an independent variable instead of time, in the 3×3 system of water and polymer conservation laws along with the mechanical entrapment rate expression, recasts the system into an auxiliary 2×2 system and one scalar lifting equation. The auxiliary problem allows for exact solution in the cases of non-linear adsorption isotherm and varying filtration coefficient.
2. In the case of small dissolved retention concentrations, where the adsorption isotherms has Henry's type and the filtration coefficient is constant, the suspended concentration is zero ahead of the particle motion front and instantly becomes steady-state after the front passes a given reservoir point. The breakthrough suspended concentration in this case is constant. The retained concentration is proportional to the mass of particles that passes this point; the proportionality coefficient is the filtration coefficient.
3. In the case of negligible formation damage coefficients, the lifting equation is solved analytically.
4. Larger filtration coefficients imply a faster concentration-saturation front, lower breakthrough saturation, higher retained concentrations, and a lower breakthrough concentration.

Acknowledgements. The authors thank Prof. A. Roberts from the University of Adelaide and Dr. R. Farajzadeh from Delft University for fruitful discussions. Many thanks are due to David H. Levin (Murphy, NC, USA) who provided professional English-language editing of this article.

References

Alvarez, A. C., P. Bedrikovetsky, G. Hime, D., Marchesin, J. R., Rodríguez (2006), A fast inverse solver for the filtration function for flow of water with particles in porous media, *Journal of Inverse Problems*, 22, 69-88.

Alvarez, A. C., G. Hime, D. Marchesin, and P. G. Bedrikovetsky (2007), The inverse problem of determining the filtration function and permeability reduction in flow of water with particles in porous media, *Transp. Porous Media*, 70(1), 43–62.

Bedrikovetsky, P. (1993), *Mathematical Theory of Oil and Gas Recovery*, Kluwer Academic Publishers, Boston.

Benson, S. M., A. F. White, S. Halfman, S. Flexser, and M. Alavi (1991), Groundwater contamination at the Kesterson Reservoir, California: 1. Hydrogeologic setting and conservative solute transport, *Water Resour. Res.*, 27(6), 1071–1084.

Borazjani, S., A. Roberts, and P. Bedrikovetsky (2016), Splitting in systems of PDEs for two-phase multicomponent flow in porous media, *Appl. Math. Let.*, 53, 25–32.

Bradford, S. A., S.Torkzaban, and J. Simunek (2011), Modeling colloid transport and retention in saturated porous media under unfavorable attachment conditions, *Water Resour. Res.*, 47(10), W10503.

Bradford, S. A., S. Torkzaban, H. Kim, and J. Simunek (2012), Modeling colloid and microorganism transport and release with transients in solution ionic strength, *Water Resour. Res.*, 48(9), W09509.

Chrysikopoulos, C. V., V. I. Syngouna, I. A. Vasiliadou, and V. E. Katzourakis (2012), Transport of pseudomonas putida in a 3-D bench scale experimental aquifer, *Transp. Porous Media*, 94(3), 617–642.

Civan, F. (2015), *Reservoir Formation Damage*, Gulf Professional Publishing, N. Y.

Dagan, G. (1989), *Flow and Transport in Porous Formations*, Springer, Berlin, N. Y.

Dagan, G., A. Fiori and I. Jankovic (2008), Transport in Porous Media, article in Vol. 5 "Ecological Processes" of "*Encyclopedia of Ecology*", 3575-3582, Elsevier, Oxford.

Johansen, T., and R. Winther (1988), The solution of the Riemann problem for a hyperbolic system of conservation laws modeling polymer flooding, *SIAM J. Math. Anal.*, 19(3), 541–566.

Katzourakis, V. E., and C. V. Chrysikopoulos (2014), Mathematical modeling of colloid and virus cotransport in porous media: Application to experimental data, *Adv. Water Resour.*, 68, 62–73.

Katzourakis, V. E., and C. V. Chrysikopoulos (2015), Modeling dense-colloid and virus cotransport in three-dimensional porous media, *J. Contam. Hydrol.*

Lake, L. W. (1989), *Enhanced Oil Recovery*, Prentice Hall, Englewood Cliffs, NJ.

Lotfollahi, M., R. Farajzadeh, M. Delshad, K., Al-Abri, B. M., Wassing, R., Mjeni, K., Awan, and P., Bedrikovetsky (2015), Mechanistic Simulation of Polymer Injectivity in Field Tests. In SPE Asia Pacific Enhanced Oil Recovery Conference, *SPE*.

Mitropoulou, P. N., V. I. Syngouna, and C.V. Chrysikopoulos (2013), Transport of colloids in unsaturated packed columns: Role of ionic strength and sand grain size, *Chem. Eng. J.*, 232, 237–248.

Pires, A. P. and P. G. Bedrikovetsky (2006), A splitting technique for analytical modelling of two-phase multicomponent flow in porous media, *J. Petr. Sci. Eng*., 51(1), 54–67.

Tikhonov, A. N., and A. A. Samarskii (1990), *Equations of Mathematical Physics*, Courier Corporation, Dover, New York.

Wagner, D. H. (1987), Equivalence of the Euler and Lagrangian equations of gas dynamics for weak solutions, *J. Differ. Equat*., 68(1), 118–136

Zhang, Q., S. Hassanizadeh, N. Karadimitriou, A. Raoof, B. Liu, P. Kleingeld, and A. Imhof (2013), Retention and remobilization of colloids during steady-state and transient two-phase flow, *Water Resour. Res.*, 49(12), 8005–8016.

Zhang, Q., S. Hassanizadeh, B. Liu, J. Schijven, and N. Karadimitriou (2014), Effect of hydrophobicity on colloid transport during two-phase flow in a micromodel, *Water Resour. Res*., 50(10), 7677–7691.

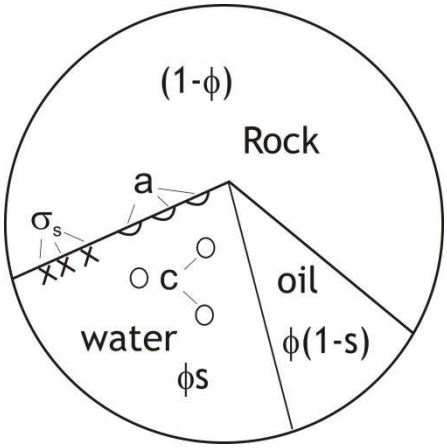

Fig.1. Schematic for phase saturations along with dissolved, adsorbed and retained polymer in porous media

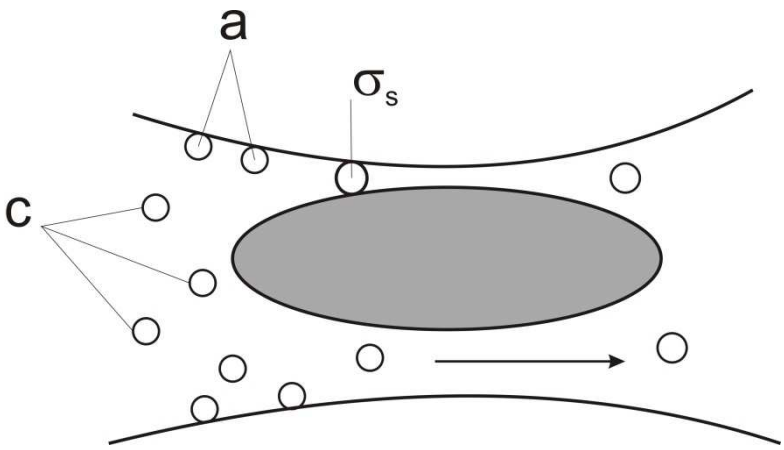

Fig.2. Dissolved, adsorbed and strained polymer molecules in porous space

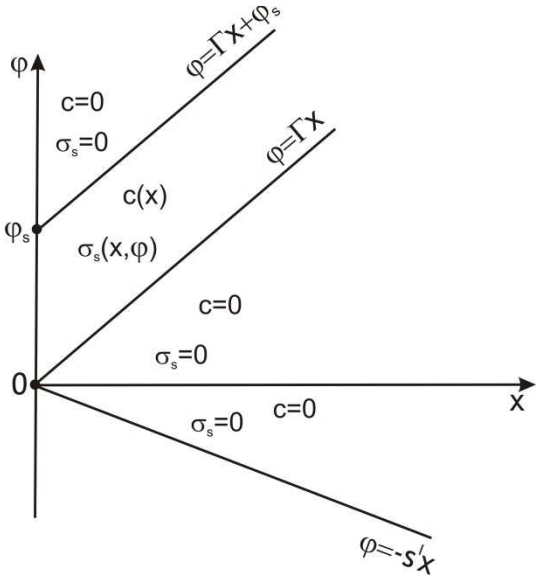

Fig.3. Auxiliary solution for a polymer slug problem.

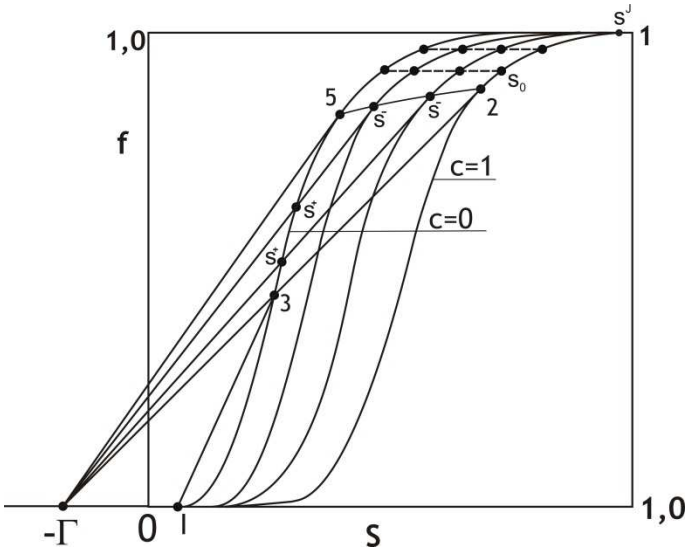

Fig.4. Lifting solution path in (*s*,*f*) plane.

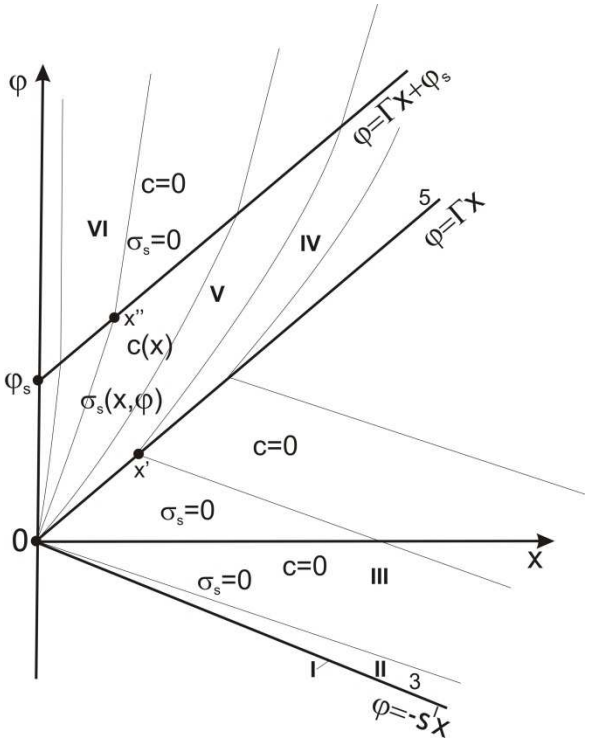

Fig.5. Solution of the lifting problem for one-dimensional polymer slug injection with typical flow zones I, II …VI.

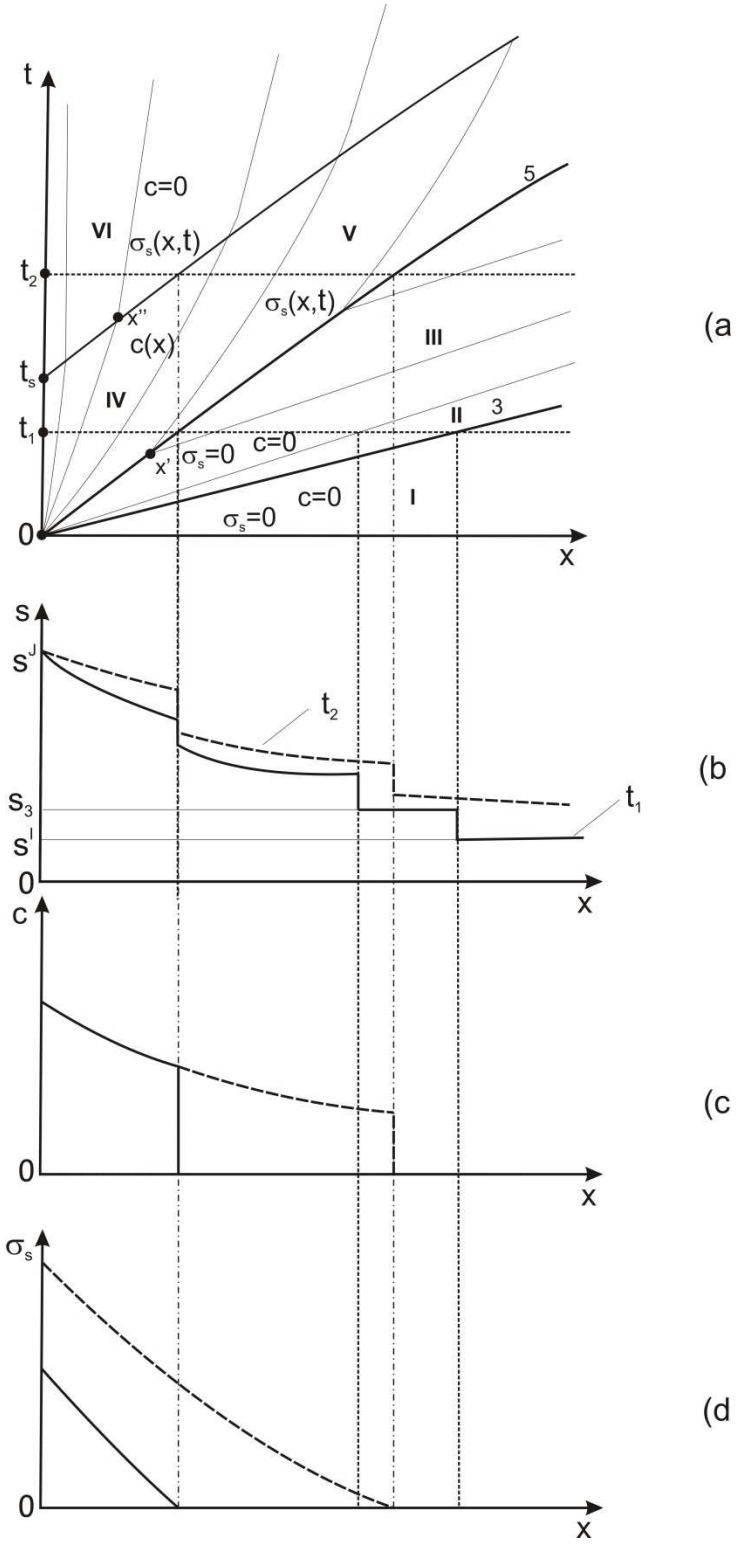

Fig.6. Analytical solution in(*x*,*t*) plane (a) Characteristic and shock wave trajectories for polymer slug flow in (*x*, *t*)-plane; profiles of (b) saturation and concentrations of dissolved (c) and retained (d) polymer before and after chase water drive injection

Table 1. Exact solution of the auxiliary and lifting problems in the (x, φ)-plane

Zone	c	σ	s	Characteristic
I	$c=0$	$\sigma=0$	s^I	$\varphi=-s^I x$
II	$c=0$	$\sigma=0$	s_3	
III	$c=0$	$\sigma=0$	$s_{III}(x,\varphi)$	$\varphi=\int_{x0}^{x}\Delta\left(s_{III}(u),c(u)\right)\left[f_s'\left(s_{III}(u),c(u)\right)\right]^{-1}du+\Gamma x$
IV	$c=0$	$\sigma=\lambda e^{-\lambda x}(\varphi-\Gamma x)$	$s_{IV}(x,\varphi)$	$\frac{\varphi-\Gamma x_0}{x-x_0}=\Delta\left(s_{IV},0\right)\left[f_s'\left(s_{IV},0\right)\right]^{-1}$
V	$c=e^{-\lambda x}$	$\sigma=\lambda e^{-\lambda x}(\varphi-\Gamma x)$	$s_I(x,\varphi)$	$\varphi=\int_{0}^{x}\Delta\left(s_I(u),c(u)\right)\left[f_s'\left(s_I(u),c(u)\right)\right]^{-1}du$
VI	$c=e^{-\lambda x}$	$\sigma=\lambda e^{-\lambda x_0}(\Gamma x_0+\varphi_s)$	$s_{VI}(x,\varphi)$	$\varphi=\int_{x0}^{x}\Delta\left(s_{VI}(u),0\right)\left[f_s'\left(s_{III}(u),0\right)\right]^{-1}du+\varphi_0$

Table 2. Five flow zones in the (x, φ)-plane for the solution of auxiliary and lifting problems

Zone	Domain
I	$\varphi=-s^I x$
II	$-s^I x<\varphi<\Delta\left(s_3,0\right)\left[f_s'\left(s_3,0\right)\right]^{-1}$
III	$\Delta\left(s_3,0\right)\left[f_s'\left(s_3,0\right)\right]^{-1}<\varphi<\Gamma x$
IV	$\Gamma x<\varphi<\int_{0}^{x}\Delta\left(s_{II}(u),c(u)\right)\left[f_s'\left(s_{II}(u),c(u)\right)\right]^{-1}du$
V	$\int_{0}^{x}\Delta\left(s_{II}(u),c(u)\right)\left[f_s'\left(s_{II}(u),c(u)\right)\right]^{-1}du<\varphi<\Gamma x+\varphi_s$

Table 3. Exact solution in the (x, t) plane after the inverse mapping

Zone	c	σ	s	Characteristic
I	$c=0$	$\sigma=0$	s^I	
II	$c=0$	$\sigma=0$	s_3	
III	$c=0$	$\sigma=0$	$s_{III}(x,\varphi)$	$t=\int_{x0}^{x}\left[f_s'(s_{III}(u),c(u))\right]^{-1}du+\Gamma x$
IV	$c=0$	$\sigma=\lambda e^{-\lambda x}(\varphi-\Gamma x)$	$s_{IV}(x,\varphi)$	$\frac{t-t_0}{x-x_0}=\left[f_s'(s_{IV},0)\right]^{-1}$
V	$c=e^{-\lambda x}$	$\sigma=\lambda e^{-\lambda x}(\varphi-\Gamma x)$	$s_I(x,\varphi)$	$t=\int_{0}^{x}\left[f_s'(s_I(u),c(u))\right]^{-1}du$
VI	$c=e^{-\lambda x}$	$\sigma=\lambda e^{-\lambda x_0}(\Gamma x_0+\varphi_s)$	$s_{VI}(x,\varphi)$	$t=\int_{x0}^{x}\left[f_s'(s_{III}(u),0)\right]^{-1}du+t_0$

Table 4. Six flow zones in the (x, t)-plane for the solution of 1-d flow problem

Zone	Domain
I	$0<t<\frac{s_3-s^I}{f_3}$
II	$\frac{s_3-s^I}{f_3}<t<\left[f_s'(s_3,0)\right]^{-1}$
III	$\left[f_s'(s_3,0)\right]^{-1}<t<\frac{\Gamma+s_{III}}{f_{III}}x$
IV	$\frac{\Gamma+s_{III}}{f_{III}}x<t<\int_{0}^{x}\left[f_s'(s_{IV}(u),c(u))\right]^{-1}du$
V	$\int_{0}^{x}\left[f_s'(s_{IV}(u),c(u))\right]^{-1}du<t<\frac{(\Gamma+s_V)}{f_V}x+\varphi_s$

5 Exact Solutions for Two-Phase Colloidal-Suspension Transport in Porous Media

S. Borazjani, P. Bedrikovetsky

Water Resources Research, submitted 11/ 2015

Statement of Authorship

Title of Paper	Exact solutions for two-phase colloidal-suspension transport in porous media
Publication Status	☐ Published ☐ Accepted for Publication ☑ Submitted for Publication ☐ Unpublished and Unsubmitted work written in manuscript style
Publication Details	S. Borazjani, P. Bedrikovetsky, Exact solutions for two-phase colloidal-suspension transport in porous media. Submitted to Water Resources Research (2015)

Principal Author

Name of Principal Author (Candidate)	Sara Borazjani
Contribution to the Paper	Problem formulation, Derivation of the mathematical model, Analysis of results, Writing the manuscript
Overall percentage (%)	85%
Certification:	This paper reports on original research I conducted during the period of my Higher Degree by Research candidature and is not subject to any obligations or contractual agreements with a third party that would constrain its inclusion in this thesis. I am the primary author of this paper.
Signature	Date: 22.11.2015

Co-Author Contributions

By signing the Statement of Authorship, each author certifies that:

i. the candidate's stated contribution to the publication is accurate (as detailed above);

ii. permission is granted for the candidate in include the publication in the thesis; and

iii. the sum of all co-author contributions is equal to 100% less the candidate's stated contribution.

Please cut and paste additional co-author panels here as required.

Name of Co-Author	P. Bedrikovetsky
Contribution to the Paper	Supervised development of the work, Manuscript review and assessment
Signature	22.11.2015

Exact solutions for two-phase colloidal-suspension transport in porous media

S. Borazjani, P. Bedrikovetsky

The University of Adelaide, Faculty of Engineering and Mathematical Sciences, Adelaide, Australia

Abstract Two-phase transport of colloids and suspensions occur in numerous areas of chemical, environmental, geo- and petroleum engineering. The main effects are particle capture by the rock and alternation of the flux by the changing suspended and retained concentrations. Multiple mechanisms of suspended particle capture are discussed. The mathematical model for m independent particle capture mechanisms is considered resulting in $(m+2)\times(m+2)$ system of partial differential equations. Using the stream-function as an independent variable instead of time splits the system into $(m+1)\times(m+1)$ auxiliary system, containing only concentrations and one lifting hydrodynamic equation for unknown phase saturation. Introduction of the concentration potential linked with retention concentrations yields an exact solution for auxiliary problem. The exact formulae allow predicting the profiles and breakthrough histories for the suspended and retained concentrations and phase saturations. The solution shows that for small retained concentrations, the suspended concentration is steady-state behind the concentration front, where all retained concentrations are proportional to the mass of suspended particles that passed via a given reservoir cross-section. The maximum penetration depths for suspended and retained particles are the same, and are equal to those for a single-phase flow.

1. Introduction

Suspension-colloidal flow in porous media occurs in numerous engineering areas, like disposal of industrial wastes in aquifers with propagation of contaminants an pollutants, industrial water treatment and filtering, injection of hot- or low-salinity water into aquifers for storage purposes, water injection into geothermal reservoirs [*Bradford et al.,* 2011, 2012, *Chrysikopoulos et al.,* 2012; *Katzourakis and Chrysikopoulos,* 2014, 2015]. An aqueous suspension of solid particles invades formations during well drilling; the penetration depth is important for evaluation of formation damage and prediction of skin factor; it is also important for interpretation of electrical logging based on the salinity contrast between the invaded drilling fluid and reservoir water [*Civan,* 2015]. Similar processes of fracturing fluid invasion occur during hydraulic fracturing of artesian, oil- and geothermal wells. Clay- and soil suspensions and colloids flow in vadose zone and during irrigation. Two-phase suspension-colloidal flows correspond to under-saturated aquifers. Two-phase gas-water flow with colloidal products of chemical reactions occurs with CO_2 geo-sequestration [*Perrin and Benson,* 2010; *Krevor et al.,* 2012; *Mijic et al.,* 2014; *Kuo and Benson,* 2015]. In petroleum industry, the low-quality water with solid or liquid particles is injected in oilfields, causing significant well impairment but some oil-recovery enhancement [*Civan,* 2015].

Planning and design of the above mentioned technologies is based on the results of mathematical modelling. Exact analytical solutions are used for interpretation of the results of laboratory coreflooding and calculation of the model coefficients. The comparison of the concentration and saturation waves provided by the analytical models with the breakthrough of colloids and water during the corefloods or field tests yields more profound understanding of the processes. The analytical models are also widely used in three-dimensional reservoir simulation using stream-line and front-tracking techniques [*Oladyshkin and Panfilov,* 2007; *Holden and Risebro,* 2013]. The above applications motivate numerous studies on exact solutions for one-dimensional two-phase multicomponent flows in porous media. Those include self-similar solutions for continuous injection of constant-composition fluids into formations, corresponding to Riemann problems for conservation law systems [*Braginskaya and Entov,* 1980; *Pope,* 1980; *Johansen and Winther,* 1988; *Barenblatt et al.,* 1989; *Lake,* 1989; *LaForce et al.,* 2008; *LaForce and Jessen,* 2010]. The non-self-similar solutions for injection of different-composition slugs are obtained by interaction of non-linear hyperbolic waves [*Fayers,* 1962; *Bedrikovetsky,* 1993]. Recently obtained semi-analytical solutions accounting for capillary pressure and diffusion are based on integral representation of the saturation field and significantly extend the class of 1-d flows permitting for analytical modelling [*Schmid et al.,* 2011].The continuous-mechanics model for a single-phase suspension-colloidal flow in porous media consists of mass balance for suspended and retained particles, equation of the retention rate and Darcy's law accounting for permeability damage by the retained particles[*Herzig et al.,* 1970]:

$$\frac{\partial}{\partial t}\left(\phi c+\sigma\right)+U\frac{\partial c}{\partial x}=0 \tag{1}$$

$$\frac{\partial \sigma}{\partial t}=\lambda\left(\sigma\right)cU \tag{2}$$

$$U=-\frac{k}{\mu(c)(1+\beta\sigma)}\frac{\partial p}{\partial x} \tag{3}$$

where ϕ is the rock porosity, c is the concentration of particles suspended in aqueous phase and σ is the retained concentration on the accessible to water rock surface, U is the Darcy's flow velocity, $\lambda(\sigma)$ is the filtration function, k is the absolute permeability, μ is the viscosity, β is the formation damage coefficient and p is the pore pressure.

Here the filtration function λ is related to the attachment rate coefficient k_d from the Colloid Filtration Theory transport in porous media [*Tufenkji and Elimelech,* 2004; *Elimelech et al.,* 2013] as

$$\lambda=\frac{k_d\phi}{U}=\frac{3}{2}\frac{1-\phi}{d_c\phi}\alpha\eta_0 \tag{4}$$

where d_c is the average grain diameter, α is the attachment efficiency (probability that the particle collided a grain remains attached to the grain surface), η_0 is the single collector contact efficiency (probability for the particle flowing towards the grain to strike this grain).

The exact solutions for one-dimensional single-phase flows with constant, linear and power-law filtration functions $\lambda(\sigma)$ are presented by [*Herzig et al.,* 1970]:. Introduction of the concentration potential from the capture rate equation allows for derivation of the exact solution for any form of the filtration function [*Polyanin and Zaitsev,* 2003; *Alvares et al.,* 2007]. In particular, *Santos and Araujo*, [2015] derive the exact solution for the case where the filtration function remains zero above some critical retention concentration.

The exact solutions, obtained by the concentration potential method permit for well-posed inverse problems of determining the model functions from the results of laboratory flow tests. *Alvares et al.,* [2007] determines the filtration function $\lambda(\sigma)$ from the breakthrough concentration and the permeability damage function $k(\sigma)$ from the pressure drop growth across the core.

The phenomenological model (1-4) is formulated for average particle and pore sizes. The population balance models account for probabilistic particle and pore size distributions [*Payatakes et al.,* 1974; *Sharma and Yortsos,* 1987]. The exact solution can be obtained for mono-sized suspension flow in the rock with the pores distributed by sizes [*Bedrikovetsky*, 2008]. The solution allows for the averaging of the flow, yielding the generalisation of the model (1-4) that accounts for the pore volume, inaccessible for finite-size particles, and the fractional flows via the accessible and inaccessible parts of the porous space. [*You et al.,* 2013].

The stochastic models for a single-phase colloidal-suspension flows include the particle-trajectory calculations [*Payatakes et al.,* 1974; *Lin et al.,* 2009], random-walk equations [*Shapiro,* 2007; *Yuan and Shapiro,* 2010; *Araujo and Santos*, 2013].

Presently, the numerical models for two-phase colloidal-suspension flows are used in studies of propagation of viruses, bacteria and nano-particles in porous media [*Mitropoulou et al.,* 2013; *Zhang et al.,* 2013; 2014]. To the best of our knowledge, the analytical models for two-phase flow of suspensions and colloids in porous media are unavailable in the literature.

The splitting method, proposed by *Wagner* [1987] allows the derivation of numerous analytical solutions for two-phase multi-component flows in porous media. Change of time to stream-function as an independent variable in the system of conservation laws (the Lagrangian approach) decreases the number of equations by one. For two-phase flows in porous media, the method has been applied to conservation law systems under thermodynamic equilibrium [*Pires et al.,* 2006] and non-equilibrium phase transitions and chemical reactions [*Borazjani et al.,* 2016].

The present work generalises the splitting method for suspended-colloidal flow with quasi-linear kinetics of the particle capture and derives the analytical solutions for two-phase flow with multiple ($m>1$) capture mechanisms. The splitting procedure separates the $(m+2)\times(m+2)$ system into $(m+1)\times(m+1)$ auxiliary system containing only one suspension and m retained concentrations, and one lifting equation for phase saturation The exact solution of the auxiliary system is found for any form of filtration functions $\lambda_k(\sigma_1, \ldots\sigma_m)$, $k=1,2\ldots m$. The lifting equation allows for exact solution for the case of negligible retained

concentrations. It was found out that in the case of constant filtration coefficients $\lambda_k=const$, the suspended concentration is steady-state behind the concentration front, and all retained concentrations are proportional to the amount of passing suspended particles. The maximum propagation depths for suspended and retained particles are the same and equal to those for a one-phase flow.

The structure of the text is as follows. Second Section presents the formulation of basic governing equations and assumptions along with the initial- and boundary-value problem for one-dimensional flows. The splitting technique with exact solution of auxiliary problem is presented in third Section. Section 4 contains the exact solution the case of constant filtration coefficients and the retention-independent fraction flow. The calculation results are given in Section 5. The extended discussion of the analytical model and wave propagation is Sections 6 and 7 conclude the paper.

2. Governing system

The Current Section formulates one-dimensional problem of two-phase colloidal-suspension flow in porous media, including the main assumptions (Section 2.1), derivation of governing equations (Section 2.2), transformation of the system with dimensionless parameters (Section 2.3) and the initial and boundary conditions (Section 2.4).

2.1. Assumptions

Consider two-phase transport of aqueous suspension with different mechanisms of particle retention in the porous medium. Figure 1(a) shows rock porosity ϕ, water saturation s, concentration c of particles suspended in aqueous phase and retained concentrations σ_1, $\sigma_2 \ldots \sigma_m$ on the accessible to water rock surface. The particle capture mechanisms include straining, attachment, diffusion, sedimentation and bridging (see Figure 1(b)). The above capture mechanisms have been extensively discussed for propagation of bacteria, viruses and nano-particles in aquifers with consequent contamination.[*Benson et al.* 1991; *Bradford et al.,* 2011; *Elimelech et al.*, 2013; *Mitropoulou et al., 2013; Syngouna and Chrisikopoulos*, 2013; *Molnar et al.,* 2015].

Two immiscible incompressible phases are assumed. Capillary pressure between phases is neglected if compared with phase pressures. We assume that the rock is water-wet, so the subscript w is used for water (wetting phase). For non-wetting phase (air, oil, gas), the subscript n is used. We discuss water-wet suspended particles transported by aqueous phase.

Concentrations of suspended and retained particles are small and do not affect the volumetric balance of the carrier water. Particle diffusion/dispersion in aqueous phase is neglected as compared with the advective flux, which is typical for large-scale systems. We discuss water-wet suspended-colloidal particles only, assuming that they are transported by the aqueous phase [*Zhang et al.,* 2014].

2.2. Governing equations

Mass balance equations for both phases are [*Barenblatt et al.*, 1989; *Bedrikovetsky*, 1993]:

$$\phi\frac{\partial \rho_w s}{\partial t}+\frac{\partial \rho_w u_w}{\partial x}=0,\ \phi\frac{\partial \rho_n (1-s)}{\partial t}+\frac{\partial \rho_n u_n}{\partial x}=0 \tag{5}$$

where ρ_w and ρ_n are water and air (oil) densities, respectively, u_w and u_n are phase velocities.

Aqueous phase viscosity is the suspension-concentration dependent. Relative permeability of the aqueous phase depends on suspended and all retained concentrations:

$$u_w=-k\frac{k_{rw}(s,c,\sigma_1...\sigma_m)}{\mu_w(c)}\frac{\partial p}{\partial x},u_n=-k\frac{k_{rn}(s,c)}{\mu_n}\frac{\partial p}{\partial x} \tag{6}$$

where k_{rw} and k_{rn} are the relative permeabilities of wetting and non-wetting phases, respectively.

Cancelling the constant phase densities in eqs (5) and (6) and adding the resulting equations yield conservation of the overall flux U for two-phase flow of incompressible phases:

$$u_w+u_n=U(t) \tag{7}$$

Introduce the fractional flow f for water as a fraction of the aqueous phase flux in the overall flux:

$$u_w=fU \tag{8}$$

The expression for fractional flow follows from eqs (6, 7)

$$f(s,\sigma_1...\sigma_m,c)=\left[1+\frac{k_{rn}(s,c)}{\mu_n}\frac{\mu_w(c)}{k_{rw}(s,c,\sigma_1...\sigma_m)}\right]^{-1} \tag{9}$$

Substituting expression for water flux (8) into mass balance (5) yields

$$\phi\frac{\partial s}{\partial t}+U\frac{\partial f(s,c,\sigma_1...\sigma_m)}{\partial x}=0 \tag{10}$$

Mass balance for suspended and retained particles accounting for eq (9) is

$$\frac{\partial}{\partial t}\left(\phi sc+\sum_{i=1}^{m}\sigma_i\right)+U\frac{\partial cf}{\partial x}=0 \tag{11}$$

For a single-phase suspension transport in porous media, it is assumed that the retention rate is proportional to the suspension flux cU, see eqs (5-7) [*Herzig et al.*, 1970]. For each particle capture mechanism by the rock from the aqueous suspension in two-phase flow, it is also assumed that the retention rate is proportional to the suspended flux of the particles:

$$\frac{\partial \sigma_i}{\partial t}=\lambda_i(\sigma_1...\sigma_m)cf(s,\sigma_1...\sigma_m)U \tag{12}$$

In the case where the overall retained concentration σ is negligibly small if compared with the number of the capture sites, the retained particle accumulation does not affect the particle capture probability, and the filtration functions λ_k are assumed to be constant. For small

retention concentrations, the form of the Langmuir blocking functions follow from the active mass low for the "interaction" between the particle and capture site populations [*Kuhnen et al.*, 2000]

$$\lambda(\sigma) = \lambda_0 \left(1 - \sigma \sigma_{\max}^{-1}\right) \tag{13}$$

More complex dependencies $\lambda_k(\sigma_k)$ take place for large retention concentrations [*Herzig et al.*, 1970].

The expression for the total flux follows from (7)

$$U = -k\left(k_{rw}(s,c,\sigma_1 \ldots \sigma_m)\mu_w(c)^{-1} + k_{rn}(s,c)\mu_n^{-1}\right)\frac{\partial p}{\partial x} \tag{14}$$

System of m+3 equations (10-14) determines the unknowns s,c, $\sigma_1,\ldots\sigma_m$ and p.

2.3. Dimensionless parameters

Introduce the following dimensionless independent variables and parameters

$$x \to \frac{x}{L}, \quad t \to \frac{1}{\phi L}\int_0^t U(t)dt, \; p \to \frac{k}{UL\mu_n} p, \; \lambda \to \lambda L, \; c \to \frac{c}{c^J}, \sigma_i \to \frac{\sigma_i}{\phi c^J}, \mu_w \to \frac{\mu_w}{\mu_n} \tag{15}$$

Substituting the dimensionless parameters (15) into eqs (10-14) yield the dimensionless form of the system for two-phase suspension flow in porous media

$$\frac{\partial s}{\partial t} + \frac{\partial f(s,c,\sigma_1 \ldots \sigma_m)}{\partial x} = 0 \tag{16}$$

$$\frac{\partial}{\partial t}\left(sc + \sum_{i=1}^{m}\sigma_i\right) + \frac{\partial cf}{\partial x} = 0 \tag{17}$$

$$\frac{\partial \sigma_i}{\partial t} = \lambda_i c f\left(s,c,\sigma_1 \ldots \sigma_m\right) \tag{18}$$

$$1 = -\left(k_{rw}(s,c,\sigma_1 \ldots \sigma_m)\mu_w(c)^{-1} + k_{rn}(s,c)\right)\frac{\partial p}{\partial x} \tag{19}$$

Eq (19) separates from the rest of the system (16-18), which consists of m+2 equations for m+2 unknowns s, c, $\sigma_1,\ldots\sigma_m$.

Consider the normalised inverse to relative permeability for wetting phase as monotonically increasing function of retained concentrations. Keeping zero and first order terms in Taylor's expansion over retained concentrations $\sigma_1,\ldots\sigma_m$ for this function yields

$$\frac{k_{rw}\left(s,c,0 \ldots 0\right)}{k_{rw}\left(s,c,\sigma_1 \ldots \sigma_m\right)} = 1 + \sum_{i=1}^{m}\beta_i\sigma_i \tag{20}$$

resulting in explicit expression for relative permeability of water vs retained concentrations. The effects of individual retained concentrations σ_k on relative permeability are expressed via the formation damage coefficients β_k.

2.4. Initial-boundary value problem for one-dimensional flows

Initial conditions for one-dimensional flow correspond to connate water saturation with no particles in the porous medium (so-called clean-bed filtration):

$$t = 0, \quad c = 0, \quad \sigma_i = 0, \quad s = s^I \tag{21}$$

Injection of suspension with constant particle concentration correspond to boundary conditions with the fixed injected fractional flow and injected concentration

$$x = 0, \quad c = 1, \; f\left(s^J, 1, \sigma_1(0,t) ..., \sigma_m(0,t)\right) = 1 \tag{22}$$

For concentrations of immobile (retained) components, the Goursat boundary conditions are formulated [*Tikhonov and Samarskii*, 1990]. Substituting c=1 and f=1 from the boundary condition (22) into rate equations (18) yields:

$$x = 0, \; \frac{d\sigma_i(0,t)}{dt} = \lambda_i\left(\sigma_1 ... \sigma_m\right) \tag{23}$$

forming a system of m ordinary equations for retained concentrations at the inlet $\sigma_k(0,t)$, i=1…m.

3. Splitting method

The solution of the governing system (16-18) subject to initial and boundary conditions, formulated in the previous Section, is solved using the splitting method [*Wagner*, 1987; *Pires et al.*, 2006; *Borazjani et al.*, 2016]. Introduction of stream-function and splitting the system into the retention-kinetics auxiliary system and the lifting equation for unknown saturation is performed in Section 3.1. Section 3.2 presents the reduction of the auxiliary system with m different retention mechanisms to that with a single “aggregated” mechanism of the particle capture. The exact solution for auxiliary problem with an overall capture mechanism is derived in Section 3.3. Sections 3.4 and 3.5 present the solution of the lifting problem and inverse mapping, respectively. Finally, (m+2)×(m+2) system of quasilinear hyperbolic equations (16-18) is reduced to one scalar hyperbolic equation.

3.1. Stream function and splitting mapping

Let us introduce a stream function associated with the conservation law (16):

$$s = -\frac{\partial \varphi}{\partial x}, \qquad f = \frac{\partial \varphi}{\partial t} \tag{24}$$

The corresponding differential form for two-phase flux is

$$d\varphi = fdt - sdx \tag{25}$$

It determines the stream-function $\varphi(x,t)$

$$\varphi(x,t) = \int_{00}^{(x,t)} fdt - sdx \tag{26}$$

Stream-lines correspond to the curves where φ=const (Figure 2). The difference $\varphi(x,t+\tau)$-$\varphi(x,t)$ is equal to the water volume flowing through the cross-section x during the period τ [*Landau and Lifshitz*, 1987].

Consider change of independent variables in system (16-18) from (x, t) to (x,φ), which corresponds to the following mapping from (x,t)-plane to (x,φ)-plane (Figure 2):

$$\mathrm{K}:(x,t)\to(x,\varphi) \tag{27}$$

Let us express differential form dt from (25)

$$dt = \frac{d\varphi}{f} + \frac{sdx}{f} \tag{28}$$

The equality of mixed partials of $t(x,\varphi)$ yields the K-transformation of eq (16), which is called the lifting equation

$$\frac{\partial F(G,\sigma_1...\sigma_m,c)}{\partial\varphi} + \frac{\partial G}{\partial x} = 0, \quad F = -\frac{s}{f(s,c,\sigma_1...\sigma_m)}, \; G = \frac{1}{f(s,c,\sigma_1...\sigma_m)} \tag{29}$$

Variables F and G are called the density and the flux in the lifting equation, respectively. Figure 3 shows curves $F=F(G,c,\sigma_1,\ldots\sigma_m)$ for (c=1, $\sigma_1,\ldots\sigma_m$=0), (c=0 $\sigma_1,\ldots\sigma_m$=0) and ($c=c^*$, $\sigma_1=\sigma_1^*\ldots\sigma_m=\sigma_m^*$) for a S-shaped fractional flow function $f(s,c,\sigma_1,\ldots\sigma_m)$. Eq (29) defines the solution $G(x,\varphi)$ or $s(x,\varphi)$ provided the concentrations $c(x,\varphi)$ and $\sigma_k(x,\varphi)$ are known.

Integrating both sides of eq (17) over any arbitrary closed simply-connected domain in plane (x, t) and applying Green's theorem [*Wagner*, 1987; *Rhee et al.*, 2001] yield

$$\iint_D \left[\frac{\partial}{\partial t}\left(sc + \sum_{i=1}^{n}\sigma_i\right) + \frac{\partial cf}{\partial x}\right]dxdt = \oint_{\partial D} cfdt - scdx - \left(\sum_{i=1}^{m}\sigma_i\right)dx = \oint_{\partial D_\varphi} cd\varphi - \left(\sum_{i=1}^{m}\sigma_i\right)dx = \iint_D \left[\frac{\partial}{\partial\varphi}\left(\sum_{i=1}^{m}\sigma_i\right) + \frac{\partial c}{\partial x}\right]dxd\varphi \tag{30}$$

resulting in an independent-variable transformation (27) in eq (17):

$$\frac{\partial}{\partial\varphi}\left(\sum_{i=1}^{m}\sigma_i\right) + \frac{\partial c}{\partial x} = 0 \tag{31}$$

The calculations analogous to (30) as performed with eq (18) results in:

$$\frac{\partial\sigma_i}{\partial\varphi} = \lambda_i(\sigma_1...\sigma_m)c, \; i = 1,2...m \tag{32}$$

System (31, 32) consists of scalar eq (31) and m equations (32); it defines the unknowns c and σ.

The initial and boundary conditions (21, 22) for auxiliary system become:

$$\varphi = -s^I x: \quad c = 0, \quad \sigma_i = 0 \tag{33}$$

$$x = 0: \quad c = 1, \quad \frac{d\sigma_i(0,\varphi)}{d\varphi} = \lambda_i(\sigma_1 ... \sigma_m) \tag{34}$$

For lifting equation (29), the initial and boundary conditions become:

$$\varphi = -s^I x: \quad s = s^I \tag{35}$$

$$x = 0: \quad f\left(s^J, 1, \sigma_1(0,\varphi) ... \sigma_m(0,\varphi)\right) = 1 \tag{36}$$

For uniform initial conditions (21), those are set in (x,φ)-plane along the straight line $\varphi=-s^Ix$ (33, 35). Figure 2 also shows the image of the initial-condition axis t=0 for non-uniform initial conditions (33) with given $s(x,0)$, $c(x,0)$ and $\sigma(x,0)$.

So, in the system of co-ordinates (x,φ), the auxiliary problem (31,32) separates from the lifting problem (29). The auxiliary system contains the kinetics variables c and σ_k, while the lifting equation depends on saturation s also; it includes the relative permeability (9) and phase viscosities. The solution of auxiliary problem (31, 32) $c(x, \varphi)$, $\sigma_1(x, \varphi),\ldots, \sigma_m(x, \varphi)$ as obtained by method of characteristics can be presented in (x, φ)-plane (Figure 4). Here the uniform initial conditions (21) are set along the straight line $\varphi=-s^Ix$, which is the image of axes t=0 with K-transformation. The solution of lifting equation (29) $G(x,\varphi)$ is also presented in the plane (x,φ). Figure 5 presents the projection of solution of the system (29, 31-32) $s(x,\varphi)$, $\sigma(x,\varphi)$, $c(x,\varphi)$ into the solution of the auxiliary system $\sigma(x,\varphi)$, $c(x,\varphi)$ (31-32), given by the splitting mapping.

3.2. Shock waves

Consider a trajectory $x(t)$ and its image $x(\varphi)$ with the mapping K (Figure 2). Substitution of the trajectories $x(t)$ and $x(\varphi)$ into differential form (25) yields

$$\frac{d\varphi}{dx} = f\frac{dt}{dx} - s \tag{37}$$

resulting in the following relationship between the Eulerian and Lagrangian speeds speeds D and V [*Landau and Lifshitz,* 1987; *Dagan et al.*, 1996]:

$$\frac{1}{V} = \frac{f}{D} - s, \quad D = \frac{dx(t)}{dt}, \quad V = \frac{dx(\varphi)}{d\varphi} \tag{38}$$

Formula (38) is interpreted geometrically in (s, f)-plane (Figure 2(c)).

The mass balance conditions on shock waves (Hugoniot-Rankine conditions) for eqs (16-18), are formulated as equality of out- and incoming fluxes for the discontinuity trajectory (see

[*Landau and Lifshitz,* 1987; *Bedrikovetsky,* 1993] for detailed derivations) for water, suspended particles and retained particles

$$[s]D = [\, f(s, c, \sigma_1 ... \sigma_m)] \tag{39}$$

$$\left[cs + \sum_{i=1}^{m} \sigma_i \right] D = [cf(s, c, \sigma_1 ... \sigma_m)] \tag{40}$$

$$[\sigma_i] D = 0 \tag{41}$$

where the jump of the parameter A across the front $[A]=A^+-A^-$ is the difference between A-values ahead and behind the front.

Eqs (41) show that the retained concentrations σ_i are continuous for $D\neq 0$. As it follows from eqs (39) and (40), the velocity of a concentration and saturation c-shock with $c^-\neq c^+$ is

$$D_c = \frac{f(s^-, c^-, \sigma_1 ... \sigma_m)}{s^-} = \frac{f(s^+, c^+, \sigma_1 ... \sigma_m)}{s^+} \tag{42}$$

Formula (42) shows that three points (0,0), "-" and "+" are located on the same straight line in plane (s,f) for c-shocks (Figure 2(c)).

The velocity of the saturation s-shock with $c^-=c^+$, as it follows from eq (39), is

$$D = \frac{f(s^-, c, \sigma_1 ... \sigma_m) - f(s^+, c, \sigma_1 ... \sigma_m)}{s^- - s^+} \tag{43}$$

Speeds of both $c^-$and s^- shocks are equal to tangents of straight lines connecting points "-" and "+" in plane (s,f) (Figure 2(c)).

The mass balance (Hugoniot-Rankine) conditions for auxiliary equations (31) and (32) are

$$[\sigma]V = [c] \tag{44}$$

$$[\sigma_i]V = 0 \tag{45}$$

respectively. As it follows from eq (45), the retained concentrations are continuous for $V\neq 0$. Therefore, eq (44) can be fulfilled for c-shocks with $V=\infty$ only, corresponding to shock trajectory $\varphi=0$. The value of c-jump $[c]$ can be any arbitrary number. The speeds for c-shocks V and D_c (42) fulfil eq (38). Finally, c-shocks can occur along the axis x only.

Consider shock conditions for lifting equation (29):

$$\left[-\frac{s}{f}\right]V = \left[\frac{1}{f}\right] \tag{46}$$

Formula (46) defines speeds for *s*-shocks with $c^-=c^+$. For *c*-shocks propagating with infinite speed, eq (46) degenerates into the continuity condition for function *s*/*f*. Figure 5 shows the projection of shocks of the general system (39-41) into those in auxiliary system (44, 45).

3.3. Aggregation in the auxiliary system

Now let us derive an exact solution for the auxiliary problem (31-32).

Summing eqs (32) and introducing the overall retained concentration σ and filtration coefficient λ yield

$$\frac{\partial \sigma}{\partial \varphi} = \lambda(\sigma_1,...\sigma_m)c, \quad \sigma = \sum_{i=1}^{m}\sigma_i, \quad \lambda(\sigma_1,...\sigma_m) = \sum_{i=1}^{m}\lambda_i(\sigma_1,...\sigma_m) \tag{47}$$

Let us show that the total filtration coefficient λ is a function of a single variable, which is the overall retained concentration σ. Looking for solution of eqs (32, 47) in the form $\sigma_i=\sigma_i(\sigma)$ results in system of *m* ordinary differential equations

$$\frac{d\sigma_i(\sigma)}{d\sigma} = \frac{\lambda_i(\sigma_i(\sigma))}{\lambda(\sigma)} \tag{48}$$

subject to initial conditions

$$\sigma = 0 : \sigma_i = 0, i = 1, 2...m \tag{49}$$

Substituting the solution of the problem (48, 49) into the expressions (47) yield the σ-dependency for the overall filtration coefficient:

$$\lambda(\sigma) = \sum_{i=1}^{m}\lambda_i(\sigma_1(\sigma),...\sigma_m(\sigma)) \tag{50}$$

Assume that the functions in right hand side of system (48) have bounded first derivatives. Substituting the solution of system (48) into eqs (31, 47) yields the 2×2 system

$$\frac{\partial \sigma}{\partial \varphi} = \lambda(\sigma)c, \quad \frac{\partial \sigma}{\partial \varphi} + \frac{\partial c}{\partial x} = 0 \tag{51}$$

subject to initial and boundary conditions

$$\varphi = -s^I x : \quad c = 0, \quad \sigma = 0 \tag{52}$$

$$x = 0 : \quad c = 1, \quad \int_0^{\sigma(0,\varphi)} \frac{du}{\lambda(u)} = \varphi \tag{53}$$

Here the Goursat boundary condition (53) is obtained from first eq (51) by separation of variables.

So, the procedure (47) aggregates the (m+1)×(m+1) auxiliary system into 2×2 system (51) (see analogous derivations by *Polyanin and Zaitsev* [2003]; *Polyanin and Manzhirov* [2006]). Finally, the system (51) allows for exact solution, which is derived in the next Section.
Below are some examples of aggregation.

Example 1. Consider the case of small particle retention, where all filtration coefficient λ_i are constant (see the discussion of the cases where the filtration coefficient can considered to be constant in *Bedrikovetsky* [2008]; *Herzig et al.* [1970]). The result of the aggregation procedure (47) is:

$$\sigma = \sum_{i=1}^{m} \sigma_i, \quad \lambda = \sum_{i=1}^{m} \lambda_i = const \tag{54}$$

Example 2. Consider the case where each filtration coefficient depends on the corresponding retention concentration only, i.e. $\lambda=\lambda_i(\sigma_i)$, i=1,2…m. Keeping zero and first order terms in Taylor expansions near to points $\sigma_i=\sigma_{imax}$ for functions $\lambda_i(\sigma_i)$ results in so-called blocking (Langmuir) filtration function with the form of blocking filtration function (13).

The system (48) becomes

$$\frac{d\sigma_i}{d\sigma} = \lambda_{0i}\left(1-\sigma_i{\sigma_{1\max}}^{-1}\right)\left[\sum_{i=1}^{m}\lambda_{0i}\left(1-\sigma_i{\sigma_{1\max}}^{-1}\right)\right]^{-1} \tag{55}$$

Let us change the independent variable in (55) from σ to σ_1:

$$\frac{d\sigma_i}{d\sigma_1} = \lambda_{0i}\left(1-\sigma_i{\sigma_{1\max}}^{-1}\right)\left[\lambda_{01}\left(1-\sigma_i{\sigma_{1\max}}^{-1}\right)\right]^{-1}, \; i = 2,3...m \tag{56}$$

Separation of variables in (56) yields the solution in the implicit form

$$\sigma_1 = \sigma_{1\max}\left(1-e^{\frac{\sigma_{2\max}}{\sigma_{1\max}}}\left(1-\sigma_2{\sigma_{2\max}}^{-1}\right)\right) = ... = \sigma_{m\max}\left(1-e^{\frac{\sigma_{m\max}}{\sigma_{1\max}}}\left(1-\sigma_m{\sigma_{m\max}}^{-1}\right)\right) \tag{57}$$

allowing for the implicit expression of all retained concentrations σ_i via their total σ by solving the following transcendental equation in σ_1:

$$\sigma = \sigma_1 + \sigma_2(\sigma_1) + ... + \sigma_m(\sigma_1) \tag{58}$$

Substituting the solution of (58) into third eq (47) yields the expression for the overall filtration coefficient:

$$\lambda(\sigma) = \sum_{i=1}^{n}\lambda_{0i}\left(1-\sigma_i\left(\sigma_1(\sigma)\right){\sigma_{i\max}}^{-1}\right) \tag{59}$$

Example 3. Let us discuss the case for two commingled particle capture mechanisms. The filtration coefficient corresponding to the first mechanism is given by a blocking (Langmuir)

function (13) of the first retained concentration. The retention concentration for the particles captured by the second mechanism is small, so the corresponding filtration coefficient is assumed to be constant:

$$\lambda_1 = \lambda_0\left(1-\sigma_1\sigma_{\max}^{-1}\right),\quad \lambda_2 = const \tag{60}$$

The system (48) becomes:

$$\frac{d\sigma_1}{d\sigma} = \frac{\lambda_0\left(1-\sigma_1\sigma_{\max}^{-1}\right)}{\lambda_0\left(1-\sigma_1\sigma_{\max}^{-1}\right)+\lambda_2},\quad \frac{d\sigma_2}{d\sigma} = \frac{\lambda_2}{\lambda_0\left(1-\sigma_1\sigma_{\max}^{-1}\right)+\lambda_2} \tag{61}$$

Changing the independent variable in (61) from σ to σ_1 and separating the variable in the obtained ordinary differential equation results in

$$\sigma_2 = -\lambda_0^{-1}\lambda_2\sigma_{\max}\ln\left(1-\sigma_1\sigma_{\max}^{-1}\right) \tag{62}$$

The aggregation result for σ and $\lambda(\sigma)$ is given in the following implicit forms for:

$$\sigma = -\lambda_0^{-1}\lambda_2\sigma_{\max}\ln\left(1-\sigma_1\sigma_{\max}^{-1}\right)+\sigma_1 \tag{63}$$

$$\lambda(\sigma) = \lambda_0\left(1-\sigma_1(\sigma)\sigma_{\max}^{-1}\right)+\lambda_2 \tag{64}$$

3.4. Exact solution for an aggregated auxiliary system

Introduction of the concentration potential $\Phi(\sigma)$

$$\Phi(\sigma) = \int_0^{\sigma}\frac{dz}{\lambda(z)} \tag{65}$$

transforms first eq (51) into

$$\frac{\partial\Phi(\sigma)}{\partial\varphi} = c \tag{66}$$

Substituting the expression for suspended concentration (66) into second eq (51) and integrating in φ yields

$$\sigma + \frac{\partial\Phi(\sigma)}{\partial x} = a(x) \tag{67}$$

where the right hand side can be determined from initial conditions (33). The retained concentration is equal to zero along the line φ=-$s^I x$. Since c=0 along this line, x-derivative of σ is zero also. Therefore, $a(x)$=0.

Boundary condition (34) accounting for definition of the potential function (65) becomes

$$x=0,\quad c=1,\quad \Phi\left[\sigma(0,\varphi)\right]=\varphi \tag{68}$$

Separation of variables in ordinary differential equation (67) with *a(x)*=0 and accounting for boundary condition (34) yields

$$\int_{\sigma(0,\varphi)}^{\sigma(x,\varphi)} \lambda(\sigma)^{-1}\frac{d\sigma}{\sigma}=-x,\ \ \varphi>0 \tag{69}$$

Since boundary value $\sigma(0,\varphi)$ is already determined by eq (53), the unknown $\sigma(x,\varphi)$ can be uniquely determined from the above transcendental equation. Afterwards, suspension concentration *c(x,φ)* is determined by eq (66) for $\varphi>0$. For $\varphi<0$, we obtain $c=\sigma=0$.

Example 4. For the case of low retained concentrations where λ constant, integration (53) results in the following retained concentration at the inlet:

$$x=0:\quad \sigma(0,\varphi)=\lambda\varphi \tag{70}$$

Integration in (69) for this case yields the following auxiliary solution:

$$\sigma(x,\varphi)=\begin{cases}\sigma=\lambda\varphi e^{-\lambda x} & \varphi>0\\ \sigma=0 & -s^I x<\varphi<0\end{cases} \tag{71}$$

Suspended concentration is determined by substituting solution (71) into second eq (51):

$$c(x,\varphi)=\begin{cases}c=e^{-\lambda x} & \varphi>0\\ c=0 & -s^I x<\varphi<0\end{cases} \tag{72}$$

Example 5. For the case of the Langmuir filtration coefficient $\lambda=\lambda_0\left(1-\sigma\sigma_{\max}{}^{-1}\right)$, the concentration potential is

$$\Phi(\sigma)=-\frac{\sigma_{\max}}{\lambda_0}\ln\left(1-\sigma\sigma_{\max}{}^{-1}\right) \tag{73}$$

It allows for explicit expression for the boundary retained concentration (53):

$$x=0,\quad \sigma=\sigma_{\max}\left(1-e^{\frac{\lambda_0\varphi}{-\sigma_{\max}}}\right) \tag{74}$$

Performing integration (69) for two cases of negative and positiveφ, the solution for retained concentration is

$$\sigma = \begin{cases} \sigma_{\max}\left(1-e^{\frac{\lambda_0\varphi}{-\sigma_{\max}}}\right)\left[1-e^{\frac{\lambda_0\varphi}{-\sigma_{\max}}}\left(1-e^{\lambda_0 x}\right)\right]^{-1} & \varphi > 0 \\ 0 & -s^I x < \varphi < 0 \end{cases} \tag{75}$$

Suspended concentration is calculated from second eq (51) after substitution of the solution (75)

$$c = \begin{cases} \left(1-e^{\frac{\lambda_0\varphi}{-\sigma_{\max}}}\left(1-e^{\lambda_0 x}\right)\right)^{-1} & \varphi > 0 \\ 0 & -s^I x < \varphi < 0 \end{cases} \tag{76}$$

At φ=0, function σ is continuous while c is discontinuous.

3.5. Lifting equation

Let us discuss lifting equation (29) assuming that suspended and retained concentrations are already known from the solution of the auxiliary problem (51-53, 66, 69). The lifting equation (29) subject to initial and boundary conditions (35-36) is a hyperbolic PDE and has the conservation law type.

The characteristic form of the lifting equation (29) is

$$\frac{d\varphi}{dx} = \frac{\partial F(G,c,\sigma)}{\partial G}, \quad \frac{dG}{dx} = -\frac{\partial F(G,c,\sigma)}{\partial c}\frac{\partial c}{\partial \varphi} - \frac{\partial F(G,c,\sigma)}{\partial \sigma}\frac{\partial \sigma}{\partial \varphi} \tag{77}$$

Substituting the expression for functions F and G from second and third terms in (29) into (77) yields

$$\begin{gathered} \frac{d\varphi}{dx} = \frac{\Delta(s,c,\sigma)}{f_s'(s,c,\sigma)}, \ \Delta(s,c,\sigma) = f(s,c,\sigma) - sf_s'(s,c,\sigma) \\ \frac{ds}{dx} = \frac{\frac{\partial f(s,c,\sigma)}{\partial \sigma}\left(\frac{\partial \sigma}{\partial \varphi}s - \frac{\partial \sigma}{\partial x}\right) + \frac{\partial f(s,c,\sigma)}{\partial c}\left(-\frac{\partial c}{\partial x}\right)}{f_s'(s,c,\sigma)} \end{gathered} \tag{78}$$

The geometric interpretation of the characteristic speed for lifting equation is presented in Figures 2c and 3. The point with abscissa Δ/f_s' that is equal to the characteristic speed (78) is shown in Figure 2c. It allows determining the characteristic speed during the solution of the lifting problem graphically, which is used with derivation of the exact solution in Section 4.

As it follows from eq (78), for $\varphi<0$ where c=σ=0, saturation is constant along the characteristics, which become straight lines.

Consider the solution of the lifting problem for small x and φ, i.e. in the neighbourhood of point (0,0) in (x,φ)-plane. The retention concentration in small vicinity is equal zero. So, the solution of auxiliary system (51) in small neighbourhood of point (0,0) degenerates into

$$c(x,\varphi)=\begin{cases}1, & \varphi>0\\ 0, & \varphi<0\end{cases} \tag{79}$$

Solution of the lifting equation in this neighbourhood is self-similar (see *Polyanin and Manzhirov*, [2006]; *Polyanin and Zaitsev*, [2003] for method of characteristics and the solution of the Riemann problem of one hyperbolic conservation-law equation). It corresponds to the sequence of rarefaction wave *J*-2, *c*-shock 2→3 and *s*-shock 3→*I*:

$$s(x,\varphi)=\begin{cases}s^J & \dfrac{\varphi}{x}>\dfrac{\partial F(s^J,1,0)}{\partial G}\\ s_1(x,\varphi) & 0<\dfrac{\varphi}{x}<\dfrac{\partial F(s^J,1,0)}{\partial G}\\ s_3 & -s^I x<\varphi<0\end{cases} \tag{80}$$

Here $s_1(x, \varphi)$ is expressed implicitly from rarefaction wave

$$\frac{\varphi}{x}=\frac{\partial F(G,1,0)}{\partial G} \tag{81}$$

Points 2 and 3 corresponds to the tangent and intersection points shown in Figure 3; the points are determined by the following relationships

$$\frac{\partial F(G_2,1,0)}{\partial G}=0 \qquad F(G_2,1,0)=F(G_3,0,0) \tag{82}$$

The graphical solution (81-82) is presented in Figure 3 by the path $-s^J$-2→3→*I*.

At small times, particle capture and retention can be neglected. So, solution (80-82) described the displacement of initial fluid I without particles (c=0) by more viscous suspension *J* with c=1 without particle capture, i.e. λ=0.

3.6. Inverse mapping

In order to obtain the solution of the problem (16-18), let us consider the inverse transformation of independent variable in the solution of auxiliary and lifting problems

$$K^{-1}:(x,\varphi)\to(x,t) \tag{83}$$

As it follows from (28)

$$t(x,\varphi)=\int_{0,0}^{x,\varphi}\left(\frac{1}{f(x,\varphi)}d\varphi+\frac{s(x,\varphi)}{f(x,\varphi)}dx\right) \tag{84}$$

expressing the inverse mapping. Substitution of (84) into auxiliary and lifting solutions yields the solution of the general problem (16-19).

4. Exact solution for the case of fractional flow independent of retained concentrations

Consider the injection of high-concentration suspension that affects the aqueous phase viscosity. The particular case under consideration in this Section corresponds to small capture rate, low values of formation damage coefficients β_i, low injected concentration or small times, where the effect of retained concentration on relative permeability of water in eq (20) can be neglected. So, the process is described by system (16-19) where the formation damage coefficients are equal zero, fractional flow is independent of retention concentrations and filtration coefficients are constant, λ_i =const. Therefore, the aggregation in system (12) corresponds to overall retained concentration with the constant total filtration coefficient, see eq (54) of Example 1. The solution of auxiliary problem (51-53) is given by eqs (71, 72).

The characteristic form of lifting eq (77, 78) for $\varphi>0$ becomes

$$\frac{d\varphi}{dx}=\frac{\partial F\left(G,c\left(x\right)\right)}{\partial G},\quad \frac{dG}{dx}=0 \tag{85}$$

i.e. $G(s,c)$ is a Riemann invariant. As it follows from expression (29) for density $G(s,c)$, the fractional flow function $f(s,c)$ conserves along the characteristics. Recalculation of the characteristic speed (81) in terms of s and $f(s,c)$ yields

$$\frac{d\varphi}{dx}=\frac{\Delta\left(s,c\left(x\right)\right)}{f'_s\left(s,c\left(x\right)\right)},\quad \frac{df\left(s,c\right)}{dx}=0 \tag{86}$$

The characteristic speed (86) as shown in Figure 2c allows to determine it graphically along with the solution of the lifting problem (29, 35, 36) in (s,f) plane (Figure 6a).

Let us first consider the case of convex fractional flow curve (Figure 6a). It corresponds to the convex relative phase permeability that appears at the length scale above the core-scale as a result of upscaling ; it can be also encountered at the core scale [*Honarpour et al.*, 1986].

The phase portrait of characteristics is presented in Figure 6a for fractional flow curves and in Figure 6b for density and flux in lifting equation (29).The curve 2-s^--5 corresponds to tangents to the fractional flow curves drawn from the origin of co-ordinates. The area above this curve corresponds to $dF/dG>0$, in the area below the curve $dF/dG<0$ (see *Bedrikovetsky* [1993], Chapter 5 for detailed derivations). The shock wave trajectories and the characteristic lines and shown in Figure 6c.

Now, let us solve the lifting problem using the method of characteristics. First we discuss the characteristic lines that start at the axis $x=0$, which corresponds to zone I (Figure 6c). The solution has self-similar asymptotical limit (80-82) in the vicinity of point (0, 0). The corresponding self-similar path is $-s^J$–2→3–I. Zone II is covered by the characteristic lines that are continuation of centred wave $s_1(x,\varphi)$, eq (81). In zone III, the characteristic curves start at the axis $\varphi=0$ and propagate inside the area $\varphi>0$. Zone IV is formed by straight characteristic lines that start at the axis $\varphi=0$ and propagate inside the area $\varphi<0$. Zone V is a rarefaction s-wave 3-s^I for $c=0$.

Saturation is constant in zone I, $s(x,\varphi)=s^J$. The characteristic curves $\varphi(x)$ are obtained by substitution of solution (72) into first eq (85) and integration in x; the explicit formula is presented in first line and fifth column of Table 1. This formula with $\varphi_0=0$ gives a separation curve between zones I and II.

In zone II, consider a characteristic that starts in point (0, 0) and corresponds to any arbitrary value s_0, $s_2<s_0<s^J$. Here point 2 is determined by eq (82). The characteristic line leaves the singular point (0,0) with velocity determined by the equation of rarefaction wave (81) with the fractional flow independent of σ. The solution $s=s_{II}(x,s_0)$ is determined from the condition of fractional flow conservation along the characteristic $\varphi=\varphi(x)$:

$$f\left(s_0,1\right)=f\left(s(x,\varphi(x)),c(x)\right) \tag{87}$$

Substituting eqs (87) and (72) into eq (86), we obtain the equation of the characteristic curve, presented in second line of fifth column (Table 1). The curve with $s_0=s_2$ separates zones II and III.

Change of parameters along characteristic curves in zone II corresponds to straight horizontal lines f=const that start at the fractional flow c=1 in the saturation interval [2, s^J] and finish up at the fractional flow c=0 in the saturation interval [4, s^J] (Figure 6a). The wave values are located above the tangent-point curve 2-5, so the tangent $dF/dG>0$ increases along the characteristic curves. Therefore, the characteristic curves do not intersect in zone II. No s-shocks appear in zone II.

In zone III, all characteristic lines start at axis φ=0. Concentration c above this line is given by eq (72); below this line, concentration c is equal zero. The concentration-saturation shock occurs along this line; the speed V of the shock is infinity. It determines the saturation $s(x_0)$ above the line φ=0 for each point x_0:

$$\frac{\partial F(G^-,\exp(-\lambda x_0))}{\partial G}=0 \tag{88}$$

Saturation $s(x_0)$ above the axis φ=0 change from s_2 for x_0=0 to s_5 with x_0 tending to infinity. The points 2…5 behind the shock front correspond to maxima of curves $F(G,c)$ (Figure 6b).

The fractional flow is constant along the characteristics $\varphi=\varphi(x)$:

$$f\left(s\left(x,\varphi(x)\right),\exp(-\lambda x)\right)=f\left(s^-(x_0),\exp(-\lambda x_0)\right) \tag{89}$$

Expressing $s(x,\ \varphi(x))$ from (89) and substituting it into first eq (86) yields the explicit expression for the characteristic line presented in third line of the fifth column in Table 1.

Now let us consider saturation distribution in zone IV. Saturation s^+ ahead of c-shock (at $\varphi<0$) is calculated from mass balance eq (46) for the shock with infinite speed, i.e. by continuity of the density F. In Figure 6b, the points above and below the shock are located on the same horizontal straight line. Points 2 and 3 in Figure 3 are found from eqs (82) for c=1.

At the point (x_0, 0), x_0>0, saturation s^- is determined by eq (88). As it follows from the conditions on *c*-shock,

$$-s^- f\left(s^-, c\left(x_0\right)\right)^{-1} = -s^+ f\left(s^+, 0\right)^{-1} \tag{90}$$

So, the points above and below the shock trajectory in plane (*G*, *F*) are located on the same horizontal lines (Figure 6b). Eq (90) shows that the points below and above axes $\varphi=0$ in plane (*s*, *f*) are located on the straight line that crosses three points $s^-=s_2$, $s^+=s_3$, and (0,0) (Figure 6a).

Below the axes φ=0, the solution is given by the characteristics emanating from a point (x_0,0). In this zone, *c*=0, so the characteristics are straight lines and given by the equation presented in Table 1 (fourth line and fifth column).

In zone V, *c*=0 and the solution is given by a centred wave presented in Table 1 (fifth line and fifth column). The boundaries between five zones are given in Table 2.

Eqs (86-90) and those in Table 1 allows expressing the images of $s(x,\varphi)$ with given $c(x,\varphi)$ on (*s*,*f*) plane. Figure 6a shows convex fractional flow curves for *c*=0 and *c*=1 along with intermediate curves. Lines *f*=const correspond to movement along the characteristics. Applying formula (84) for inverse mapping of independent co-ordinate *t* results in the representation of the solution in plane (*x*, *t*) (Figure 6d). The explicit formulae for saturation distribution in six zones are presented in Table 3, where the boundaries between six zones are given in Table 4. The *c*-*s*-shocks are exhibited in suspended-concentration and saturation profiles in Figures 7a and 7b; the continuous retention profiles are shown in Figure 7c.

The exact solution of eqs (16-18) exhibits the following structure of two-phase flow with the clean-bed injection of colloid or suspension (Figure 6d):

VI - unperturbed zone with initial saturation and no particles;

V - first particle-free bank where water saturation increases from s^I to s_3;

IV - second particle-free bank with further increase of water saturation;

III - first two-phase flow zone with suspended and retained particles behind the concentration front;

II - two-phase flow zone with suspended and retained particles where saturation increases up to S^J-value;

I- suspension-flow zone expanding from the core inlet, where saturation is equal to its maximum value s^J.

The exact solution presented in Table 1 allows deriving the explicit formulae for propagation depths of suspended and retained particles, presented in Figure 8.

In the case of more common *S*-shaped fractional flow function, the slope f'_s increases from point I to point 3 in Figure 9a, while it decreases in Figure 6a for a convex fractional flow curve. Therefore, the centred waves 3-I in zone V of Figure 6c and d is replaced by a s-shock in Figure 9c and d. The slope of S-shaped fractional flow function in the point s^J is assumed to be zero, so zone I disappears in Figure 6c,d disappears. The fractional flows curves, the lifting density-flux curves along with characteristic lines and different flow zones are presented in Figures. 9a, b, c and d, respectively. Formulae for zones II, III and IVare the same as those in Tables 1-4. In zone V, $s=s_3$ instead of rarefaction wave s_V.

5. Results

Let us first analyse the case where the fractional flow curves are independent of retained concentration, using the exact solution obtained in Section 4. We start by discussing convex fractional flow curves.

Figure 7 shows the profiles of saturation, suspended and retained concentrations for three different filtration coefficients, and also for the cases with the particle-free water injection (c=0) and with the capture-free flow (λ=0) the profile correspond to the moment t=0.2. Here dimensionless wetting phase viscosity is (1+4c)/10; s_{wi} =0.2 and s_{nr} =0.3. The relative phase permeability for wetting and non-wetting phases correspond to segregated flow of immiscible fluids in homogeneous reservoir [*Barenblatt et al.,* 1989] $0.75(s-s_{wi})/(1-s_{nr}-s_{wi})$, $0.75(1-s_{nr}-s)/(1-s_{nr}-s_{wi})$. The corresponding fractional flow curves and flux function for lifting equation and shown in Figures. 6a and 6b, respectively.

For one-phase flow, the *c*-jump trajectory coincides with the water-particle trajectory, i.e. it is independent of filtration coefficient. So, *c*-jump speed is equal to one, and it propagates in the overall porous space. For convex fractional flow functions, velocity of water *f/s* is higher than water velocity for a single-phase flow, which is equal to one. Other *c*- and *s*-fronts in Figures 7a and 7b are significantly ahead of the position x=0.2 of *c*-front for a single-phase flow, since those fronts propagate in water-filled fraction of the porous space.

In Figures 7, two-phase suspension-colloidal flow is compared with the case of particle-free water injection (c=0, black curve for s-profile), and also with the case where particles are not captured (λ=0, brown curves for *s*- and *c*-profiles). For the particle-free water injection, the problem degenerates into solution of one equation (16) subject to initial and boundary conditions (21, 22) with $c=\sigma=0$. The Riemann solution for this problem is self-similar and given by the rarefaction wave s^J-s^I along the curve c=0 [*Barenblatt et al.,* 1989; *Bedrikovetsky,* 1993]. If the suspended concentration does not affect the fractional flow, the saturation $s(x, t)$ for suspension injection is the same as that with the particle-free water injection. In this case, the solution also contains *c*-shock 5→5 with the concentration jump from one to zero (this case is denoted as $c=0^+$ in the legends to Figures 7). The profile of this *c*-shock is shown in black in in Figures 7b; its breakthrough is shown in Figures 7e also in black. The capture-free solution corresponds to σ_i=0 in system (16-18).The Riemann solution is also self-similar and is given by the rarefaction wave s^J-2 at c=1, jump 2→3 and rarefaction 3-s^I at c=0 (see Figures 6a and 6b). The corresponding profiles and breakthrough

curves are presented in Figure 7 in brown. Blue, red and green curves correspond to the increasing filtration coefficient.

The penetration depths of retained and suspended particles for single- and two-phase flows for different filtration coefficients are presented in Figure 8. The retention depth for two-phase flow is given by the following formula

$$x_\sigma(t) = \int_0^\infty x\sigma(x,t)\,s(x,t)\,dx \left[\int_0^\infty \sigma(x,t)\,s(x,t)\,dx\right]^{-1} \qquad (91)$$

Changing the retained concentration $\sigma(x,t)$ to suspended concentration $c(x,t)$ in eq (91) results in the definition of the suspension penetration depth $x_c(t)$. Exact solution for a single-phase deep bed filtration (s=1) shows that at $t\to\infty$ both depths x_c and x_σ tend to $1/\lambda$ [*Herzig et al.*, 1970]. For two-phase flow, saturation tends to s^J, so the limits for x_c and x_σ also tend to $1/\lambda$. In Figure 8, red and blue continuous and dotted curve tend to the same limit.

Now let us discuss more common S-shaped fractional flow curves, corresponding to concave relative permeability, which is typical for core-scale [*Barenblatt et al.*, 1989]. Figures 6a and 9a show that in this case the shock $3\to s^I$ substitutes the rarefaction wave $3\text{-}s^I$ for the capture-free particle transport. The decay configuration for the particle-free water injection becomes $s^J\text{-}2\to 3\to s^I$ (Figure 9a). Here relative phase permeability for wetting and non-wetting phases are $0.75((s\text{-}s_{wi})/(1\text{-}s_{nr}\text{-}s_{wi}))^2$ and $0.75((1\text{-}s_{nr}\text{-}s)/(1\text{-}s_{nr}\text{-}s_{wi}))^2$, other coefficients are the same as in the previous example [*Barenblatt et al.*, 1989]. Figures 10 a, b and c present the calculated saturation and concentration profiles; the breakthrough histories of water flux and concentration are presented in Figures 10d and e.

Now consider the effect of formation damage coefficient on two-phase suspended-colloidal flow. In this case, the fractional flow depends on saturation and both concentrations c and σ. Intermediate values of retained concentration are considered, so the Langmuir filtration function (13) is assumed. The auxiliary solution is taken from Example 5. The following data are used for calculations: initial filtration coefficient λ_0=7, maximum retention concentration σ_{max}=1. Relative permeability for non-wetting phase is the same as in the previous example. For wetting phase, the relative permeability from the previous example is divided by $1+4\sigma$.

The exact solution for auxiliary problem is given by formulae (75) and (76). The lifting problem (78) is solved numerically using the computer code presented by *Shampine,* [2005] and available from http://faculty.smu.edu/shampine/current.html, which implements the second order Richtmyer's two-step variant of the Lax-Wendroff method. The software was compared with the MATLAB-based numerical method of characteristics. The ordinary differential equations (78), which are the characteristic form of the lifting equation (29) have been solved by the fifth order Runge-Kutta method with a variable time step (MATLAB, Version 7.10.0499). The coincidence of the results calculated by two different codes has been observed.

Figure 11 presents the saturation and concentration profiles for the above-described case of *c*- and σ-dependencies of the fractional flow curve. As in the previous example, the fractional flow curve is S-shaped. The phase portraits of characteristic lines and the flow zones in (x,φ)- and (x,t)-planes are the same as that shown in Figure 9a,b. The two-phase bank without particles (c=0) follow the water-breakthrough front. The solution contains one s-shock and one *c*-shock. The higher is the formation damage coefficient the lower is the water velocity and the lower is the fractional flow. So, the increase in formation damage coefficient delays both *s*- and *c*-fronts and reduces water-flux after the particle breakthrough, as it is shown in Figures 11 a, b. The formation damage coefficient increase causes also increase in saturation at the late stage with more complete displacement by less mobile phase with reduced relative permeability. The saturation profile behind the *c*-jump change the form from concave at β=20 to convex at β=2000. Figure 11 shows the early stage profile at t=0.1. After reaching the maximum retention value σ=100, the retention profile stabilises, and the breakthrough concentration is equal one.

During waterflooding of oilfields, the recovery factor is the ratio between the produced and initial oil in the reservoir

$$RF\left(t\right)=\left[\int_0^1 s\left(x,t\right)dx-s_{wi}\right]\left(1-s_{wi}\right)^{-1} \qquad (92)$$

Solid particles and oleic droplets are always present in the injected water. For the previous example, Figure 12 shows that the formation damage coefficient enhances the recovery factor. The higher is the formation damage coefficient, the lower is the aqueous phase velocity and, consequently, the higher is the oil flux 1-*f*.

6. Summary and Discussions

The mathematical model for two-phase suspended-colloidal flow with the multiple particle-capture mechanisms and water deceleration by the retained particles exhibits several competitive effects. The particle capture decreases the suspended concentration and aqueous phase viscosity, yielding the enhanced water mobility, while the particle retention decreases relative permeability for water causing its mobility reduction. The suspended concentration reduction due to particle capture and water acceleration due to its viscosity reduction are also competitive factors. The analytical modelling allows for detailed investigation of this complex behavior.

The system of two-phase suspension transport with m particle retention mechanisms consists of m+2 equations. It was found out that introduction of the stream function (25) and using it as an independent variable instead of time separates (m+1)×(m+1) auxiliary equations with unknowns c, $\sigma_1 \ldots \sigma_m$ from one scalar lifting equation for unknown saturation s. The auxiliary system has *m-1* first integrals and can be reduced to system 2×2 for unknown overall retained concentration and suspended concentration; this 2×2 auxiliary problem with uniform initial and boundary data allows for exact solution.

The solution exhibits the following flow zone structure: the undisturbed zone with initial saturation and no particles is followed by the particle-free two-phase bank with enhanced saturation; then follows the concentration front with saturation increasing up to the core inlet. Suspension concentration jumps across the concentration front while all retained concentrations corresponding to all different retention mechanisms are continuous. In the case of convex fractional flow, the particle-free two-phase bank enters the undisturbed zone by the continuous simple wave and zone with maximum saturation expands from the core inlet. For S-shaped fractional flow, the saturation front separates the particle-free two-phase bank and undisturbed zone; the maximum-saturation zone adjacent to the core inlet may disappear. So, the solution always contains *c*-jump; it also contains the fast *s*-shock in the wide-spread case of an S-shape fractional flow.

Consider the case of small retained concentrations, which corresponds either to constant filtration coefficients or small flow times. However, the effect of retained concentration on relative permeability for aqueous phase is accounted for. The solution shows that the suspension concentration is zero ahead of the concentration front; it instantly becomes steady-state in any reservoir point behind the front after the front pass this point. All retained concentrations are proportional to the amount of particles that pass this point; the proportionality coefficient for each retained concentration is the corresponding filtration coefficient.

The above quantitative observations are important for interpreting the breakthrough data during laboratory experiments and production data from the field tests.

The formation damage coefficients β_k exhibit a significant variation depending on the particle capture mechanism. In the case of size exclusion, even small amounts of retained fines yield a significant permeability reduction, so the formation damage coefficient is high [*Civan*, 2010; *Bedrikovetsky et al.*, 2011]. If the particle attachment results in the grain coating, the permeability variation is negligible [*Civan*, 2015]. Yet, in the case of dendritic growth of the attached particles, the formation damage coefficient is high. Gravity segregation of fine particles yields low permeability decline. For diffusion of particles into the stagnant flow zones, the formation damage coefficient can be assumed to be zero.
In the case of negligible formation damage coefficients, where the effect of retained concentration on relative permeability for aqueous phase is not accounted for, the lifting equation allows for exact solution. The formulae are presented in the Tables 1-4. Otherwise, the lifting problem is solved numerically.

Let us analyse the effects of particle capture on the suspension-colloidal flow. The higher is the filtration coefficient, the lower is the suspended concentration, the smaller is the aqueous phase viscosity the higher is the fractional flow and the higher is its velocity. The increase of filtration coefficient increases the fractional flow. It results in the increase of *c*-shock speed 2→3, in the decrease of saturation behind the front and increase of saturation ahead of the front (Figures 6a, b). In Figure 7b, the *c*-shocks in order of decreasing their speed are green, red, blue and brown; it corresponds to the decrease in filtration coefficient. The *c*-profile

curves correspond to the same sequence of suspended concentration increase. The higher is the filtration coefficient the lower is the breakthrough moment due to water viscosity increase (Figure 7e). The water viscosity is lowest for the case c=0, so the black c-profiles in Figure 7 b are ahead of all other profiles. The effects of water flux delay with decreasing of filtration coefficient are shown in Figure 7a for saturation profile and in Figure 7d for water flux breakthrough. The higher is the filtration coefficient, the faster is the concentration front and the higher is the retention profile (Figure 7c). Since the suspension concentration is steady-state behind the concentration front, the breakthrough concentration is constant (Figure 7e).

The propagation depths x_c and x_σ increase with time. For the constant filtration coefficient in two and one phase flow as time tends to infinity x_c and x_σ tend to the same limit $1/\lambda$ (Figure 8). Both lengths x_c and x_σ propagate faster for two-phase flow, since the particles are transported by water that occupies only a fraction of porous space in the case of two-phase flow, while the particles occupy the overall space during the one-phase transport.

The propagation depths $x_c(t)$ and $x_\sigma(t)$ decrease as filtration coefficient increases, due to suspension concentration reduction. However, the filtration coefficient increase causes increase of aqueous phase velocity and deeper particle penetration. The propagation depths curves for larger λ in Figure 8 are located below those for lower λ. So, the effect of suspension concentration reduction dominates over the water acceleration effect.

In the case of more common S-shaped fractional flow, the fractional flows curves, the lifting density-flux curves along with characteristic lines and different flow zones in planes (x,φ) and (x,t) are presented in Figures 9a, b, c and d, respectively. Both fractional flow function and the flux function for the lifting equation have an inflection point; both curves are concave in the interval between the inflection point and point I. Therefore, the centred wave in zone V in the convex case is replaced by a s-shock; saturation profiles in Figure 10a exhibit two jumps while the profiles in Figure 7a continuously tend to s^I ahead of the c-s-shock. The breakthrough water flux histories in Figure 10d have two shocks while those in Figure 7d exhibit only one jump.

The S-shaped fractional flow curve is assumed to have zero derivative at the point s^J, so zone I disappears (Figures 6 and 9, c and d). The formulae for zones I-IV are the same as those in Tables 1-4. In zone V, s=s_3 instead of rarefaction wave $s_V(x,t)$.

The qualitative observations about the forms and dynamics of saturation and concentration profiles and histories are useful for interpretation of the laboratory coreflood data and for the analysis of field data. The saturation and concentration profiles are important for selection of the drilling fluid causing minimum formation damage in artesian, geothermal and oil wells. The retention profiles allow selecting the perforation depths with re-perforation of the damaged wells; they also permit the definition of the acid volume for the damage removal. The penetration depths facilitate interpretation of simultaneous shallow and deep electrical logging.

The paper discusses initial connate water saturation in the reservoir. For higher initial saturation, solution for particle-free injection corresponds to rarefaction wave s^J-$s(x,0)$. If $s(x,0)>s_3$, the solution for the capture-free injection contains shock $3 \rightarrow s(x,0)$ instead of rarefaction wave 3-s^I. The speculations about the competition between filtration and formation damage coefficients with regards to their effects on fractional flow with consequent alternation of two-phase flux remain the same for any initial saturation.

So far, the suspended-colloidal injection into clean bed, corresponding to initial and boundary conditions (21, 22) has been discussed in the paper. Fine particle detachment with further fines migration and capture corresponds to the same system (16-19) [*Civan,* 2010; *Bedrikovetsky et al.,* 2011] subject to another initial and boundary conditions:

$$t = 0 : c = 1, \sigma_1 = ... = \sigma_n = 0; \;\; x = 0 : c = 0 \tag{93}$$

The developed splitting procedure allows for exact solution derivations for the process of natural reservoir fines migration and retention too. It permits the analysis of the effects of suspended and retained particles on two-phase flow in porous media.

The developed splitting procedure is also applied to two-phase colloidal-suspension transport in axi-symmetric geometry, allowing analyzing particle propagation and permeability damage during the injection into vertical well.

The work considers the particles wetted by either of phases, assuming that the wetted phase transports the particles [*Civan,* 2010]. The mixed-wet particles are transported by the water-air menisci, where the model must involve the flux and density of the phase interface [*Hassanizadeh and Gray,* 1993; *Zhang et al.,* 2013, 2014; *Shapiro,* 2015].

One-dimensional (x, t)-flow is discussed. It corresponds to laboratory coreflood and injection into fractured well. It also describes the situation of injection with the "line" like irrigation or seawater invasion into aquifers. Besides, the one-dimensional exact solutions obtained can be applied for three-dimensional reservoir simulation using the stream-line or front-tracking technique [*Oladyshkin, Panfilov,* 2007; *Holden, Risebro,* 2013].

7. Conclusions

The analytical modelling of two-phase suspension-colloidal flow in porous media allows drawing the following conclusions:

1. Using the stream-function as an independent variable instead of time in the $(m+2)\times(m+2)$-system of two-phase suspension-colloidal flow with m different retention mechanisms, splits the system into auxiliary $(m+1)\times(m+1)$-system and one scalar lifting equation. The auxiliary problem allows for exact solution.
2. In the case of small retention concentrations, the suspended concentration is zero ahead of the particle motion front and instantly become steady-state after the front passes a given reservoir point; the breakthrough suspended concentration is constant. The retained

concentration is proportional to the amount of particles that pass this point; the proportionality coefficient is the filtration coefficient.

3. In the case of negligible formation damage coefficients, the lifting equation is solved analytically.

4. The larger are the filtration coefficients the faster move the concentration-saturation front, the lower is the breakthrough saturation the higher are retained concentrations and the lower is the breakthrough concentration.

5. At finite times, the particle penetration depth is higher for two-phase flows than for a single-phase transport. The maximum penetration depths for suspended and retained particles are the same and equal to inverse to filtration coefficient; i.e. they are the same for two-phase and one-phase transport.

6. For S-shaped fractional flow function, the particle-free two-phase flux with intermediate saturation follows the un-disturbed zone with initial saturation and the saturation front, while the saturation decreases continuously ahead of c-front until s^I for a convex fractional flow.

7. Increase in formation damage coefficient delays s- and c-shocks and decrease water flux behind the c-front. It increases saturation at the late stage of suspension-colloidal injection. In the case of waterflooding in oilfield, the Increase in formation damage coefficient results in delay of water breakthrough, and increase of oil production during arrival of particle-free oil-water bank and sometime after particle breakthrough. It also yields more complete displacement at the late stage of the suspension-colloidal injection.

Acknowledgements. The authors thank Prof. A. Roberts for multiple fruitful discussions.

References

Alvarez, A. C., G. Hime, D. Marchesin, and P. G. Bedrikovetsky (2007), The inverse problem of determining the filtration function and permeability reduction in flow of water with particles in porous media, Transport in Porous Media, 70(1), 43-62.

Araújo, J. A., and A. Santos (2013), Analytic model for DBF under multiple particle retention mechanisms, Transport in porous media, 97(2), 135-145.

Barenblatt, G. I., V. M. Entov, and V. M. Ryzhik (1989), Theory of fluid flows through natural rocks, Kluwer Academic Publishers, London.

Bedrikovetsky, P. (1993), Mathematical theory of oil and gas recovery: with applications to ex-USSR oil and gas fields, Kluwer Academic, Boston.

Bedrikovetsky, P. (2008), Upscaling of stochastic micro model for suspension transport in porous media, Transport in Porous Media, 75(3), 335-369.

Bedrikovetsky, P., F. D. Siqueira, C. A. Furtado, and A. L. S. Souza (2011), Modified particle detachment model for colloidal transport in porous media, Transport in porous media, 86(2), 353-383.

Benson, S. M., A. F. White, S. Halfman, S. Flexser, and M. Alavi (1991), Groundwater contamination at the Kesterson Reservoir, California: 1. Hydrogeologic setting and conservative solute transport, Water resources research, 27(6), 1071-1084.

Borazjani, S., A. Roberts, and P. Bedrikovetsky (2016), Splitting in systems of PDEs for two-phase multicomponent flow in porous media, Applied Mathematics Letters, 53, 25-32.

Bradford, S. A., S. Torkzaban, and J. Simunek (2011), Modeling colloid transport and retention in saturated porous media under unfavorable attachment conditions, Water Resources Research, 47(10).

Bradford, S. A., S. Torkzaban, H. Kim, and J. Simunek (2012), Modeling colloid and microorganism transport and release with transients in solution ionic strength, Water Resources Research, 48(9).

Bradford, S. A., S. Torkzaban, and A. Shapiro (2013), A theoretical analysis of colloid attachment and straining in chemically heterogeneous porous media, Langmuir, 29(23), 6944-6952.

Braginskaya, G., and V. Entov (1980), Nonisothermal displacement of oil by a solution of an active additive, Fluid Dynamics, 15(6), 873-880.

Chrysikopoulos, C. V., V. I. Syngouna, I. A. Vasiliadou, and V. E. Katzourakis (2012), Transport of pseudomonas putida in a 3-D bench scale experimental aquifer, Transport in porous media, 94(3), 617-642.

Civan, F. (2010), Non-isothermal permeability impairment by fines migration and deposition in porous media including dispersive transport, Transport in porous media, 85(1), 233-258.

Civan, F. (2015), Reservoir formation damage, Gulf Professional Publishing.

Dagan, G., A. Bellin, and Y. Rubin (1996), Lagrangian analysis of transport in heterogeneous formations under transient flow conditions, Water Resources Research, 32(4), 891-899.

Elimelech, M., J. Gregory, and X. Jia (2013), Particle deposition and aggregation: measurement, modelling and simulation, Butterworth-Heinemann.

Entov, V., and A. Zazovskii (1989), Hydrodynamics of Enhanced Oil Recovery Processes, Nedra, Moscow.

Fayers, F. (1962), Some theoretical results concerning the displacement of a viscous oil by a hot fluid in a porous medium, Journal of Fluid Mechanics, 13, 65-76.

Hassanizadeh, S. M., and W. G. Gray (1993), Thermodynamic basis of capillary pressure in porous media, Water Resources Research, 29(10), 3389-3405.

Herzig, J., D. Leclerk, and P. Legoff (1970), Flow of suspensions through porous media, Industrial and Engineering Chemistry, 62(5), 8-35.

Holden, H., and N. H. Risebro (2013), Front tracking for hyperbolic conservation laws, Springer.

Honarpour, M., F. Koederitz, and A. Herbert (1986), Relative permeability of petroleum reservoirs.

Johansen, T., and R. Winther (1988), The solution of the Riemann problem for a hyperbolic system of conservation laws modeling polymer flooding, SIAM journal on mathematical analysis, 19(3), 541-566.

Katzourakis, V. E., and C. V. Chrysikopoulos (2014), Mathematical modeling of colloid and virus cotransport in porous media: Application to experimental data, Advances in Water Resources, 68, 62-73.

Katzourakis, V. E., and C. V. Chrysikopoulos (2015), Modeling dense-colloid and virus cotransport in three-dimensional porous media, Journal of Contaminant Hydrology.

Krevor, S., R. Pini, L. Zuo, and S. M. Benson (2012), Relative permeability and trapping of CO2 and water in sandstone rocks at reservoir conditions, Water Resources Research, 48(2).

Kuhnen, F., K. Barmettler, S. Bhattacharjee, M. Elimelech, and R. Kretzschmar (2000), Transport of iron oxide colloids in packed quartz sand media: monolayer and multilayer deposition, Journal of Colloid and Interface Science, 231(1), 32-41.

Kuo, C.-W., and S. M. Benson (2015), Numerical and analytical study of effects of small scale heterogeneity on CO 2/brine multiphase flow system in horizontal corefloods, Advances in Water Resources, 79, 1-17.

LaForce, T., and K. Jessen (2010), Analytical and numerical investigation of multicomponent multiphase WAG displacements, Computational Geosciences, 14(4), 745-754.

LaForce, T., K. Jessen, and F. M. Orr Jr (2008), Four-component gas/water/oil displacements in one dimension: Part I. structure of the conservation law, Transport in Porous Media, 71(2), 199-216.

Lake, L. W. (1989), Enhanced oil recovery, Prentice Hall: Englewood Cliffs, NJ.

Landau, L. D., and E. M. Lifshitz (1987), Fluid mechanics, Elsevier, Oxford.

Lin, H.-K., L. P. Pryadko, S. Walker, and R. Zandi (2009), Attachment and detachment rate distributions in deep-bed filtration, Physical Review E, 79(4), 046321.

MATLAB version 7.10.0. Natick, Massachusetts: The MathWorks Inc., 2010.

Mijic, A., T. C. LaForce, and A. H. Muggeridge (2014), CO2 injectivity in saline aquifers: The impact of non-Darcy flow, phase miscibility, and gas compressibility, Water Resources Research, 50(5), 4163-4185.

Mitropoulou, P. N., V. I. Syngouna, and C. V. Chrysikopoulos (2013), Transport of colloids in unsaturated packed columns: Role of ionic strength and sand grain size, Chemical Engineering Journal, 232, 237-248.

Molnar, I. L., W. P. Johnson, J. I. Gerhard, C. S. Willson, and D. M. O'Carroll (2015), Predicting colloid transport through saturated porous media: A critical review, Water Resources Research, 51(9), 6804-6845.

Oladyshkin, S., and M. Panfilov (2007), Streamline splitting between thermodynamics and hydrodynamics in a compositional gas–liquid flow through porous media, Comptes Rendus Mécanique, 335(1), 7-12.

Payatakes, A., R. Rajagopalan, and C. Tien (1974), Application of porous media models to the study of deep bed filtration, The canadian journal of chemical engineering, 52(6), 722-731.

Perrin, J.-C., and S. Benson (2010), An experimental study on the influence of sub-core scale heterogeneities on CO2 distribution in reservoir rocks, Transport in porous media, 82(1), 93-109.

Pires, A. P., P. G. Bedrikovetsky, and A. A. Shapiro (2006), A splitting technique for analytical modelling of two-phase multicomponent flow in porous media, Journal of Petroleum Science and Engineering, 51(1), 54-67.

Polyanin, A. D., and V. F. Zaitsev (2003), Handbook of nonlinear partial differential equations, CRC press, Boca Raton.

Polyanin, A. D., and A. V. Manzhirov (2006), Handbook of mathematics for engineers and scientists, CRC Press, Boca Raton, London.

Pope, G. A. (1980), The application of fractional flow theory to enhanced oil recovery, Society of Petroleum Engineers Journal, 20(03), 191-205.

Rhee, H., R. Aris, and N. R. Amundson (2001), First-order Partial Differential Equations: Theory and application of hyperbolic systems of quasilinear equations, Dover publications, INC., New York.

Santos, A., and J. Araújo (2015), Modeling Deep Bed Filtration Considering Limited Particle Retention, Transport in Porous Media, 1-16.

Schmid, K., S. Geiger, and K. Sorbie (2011), Semianalytical solutions for cocurrent and countercurrent imbibition and dispersion of solutes in immiscible two-phase flow, Water Resources Research, 47(2).

Shampine, L. (2005), Solving hyperbolic PDEs in MATLAB, Applied Numerical Analysis and Computational Mathematics, 2(3), 346.

Shapiro, A. A. (2007), Elliptic equation for random walks. Application to transport in microporous media, Physica A: Statistical Mechanics and its Applications, 375(1), 81-96.

Shapiro, A. A. (2015), Two-Phase Immiscible Flows in Porous Media: The Mesocopic Maxwell–Stefan Approach, Transport in Porous Media, 107(2), 335-363.

Sharma, M., and Y. Yortsos (1987), Transport of particulate suspensions in porous media: model formulation, AIChE Journal, 33(10), 1636-1643.

Syngouna, V. I., and C. V. Chrysikopoulos (2013), Cotransport of clay colloids and viruses in water saturated porous media, Colloids and Surfaces A: Physicochemical and Engineering Aspects, 416, 56-65.

Tikhonov, A. N., and A. A. Samarskii (1990), Equations of mathematical physics, Courier Corporation, Dover, New York.

Tufenkji, N., and M. Elimelech (2004), Correlation equation for predicting single-collector efficiency in physicochemical filtration in saturated porous media, Environmental science & technology, 38(2), 529-536.

Wagner, D. H. (1987), Equivalence of the Euler and Lagrangian equations of gas dynamics for weak solutions, Journal of differential equations, 68(1), 118-136.

You, Z., P. Bedrikovetsky, and L. Kuzmina (2013), Exact solution for long-term size exclusion suspension-colloidal transport in porous media, paper presented at Abstract and Applied Analysis, Hindawi Publishing Corporation.

Yuan, H., and A. A. Shapiro (2010), Modeling non-Fickian transport and hyperexponential deposition for deep bed filtration, Chemical Engineering Journal, 162(3), 974-988.

Yuan, H., A. Shapiro, Z. You, and A. Badalyan (2012), Estimating filtration coefficients for straining from percolation and random walk theories, Chemical Engineering Journal, 210, 63-73.

Zhang, Q., S. Hassanizadeh, N. Karadimitriou, A. Raoof, B. Liu, P. Kleingeld, and A. Imhof (2013), Retention and remobilization of colloids during steady-state and transient two-phase flow, Water Resources Research, 49(12), 8005-8016.

Zhang, Q., S. Hassanizadeh, B. Liu, J. Schijven, and N. Karadimitriou (2014), Effect of hydrophobicity on colloid transport during two-phase flow in a micromodel, Water Resources Research, 50(10), 7677-7691.

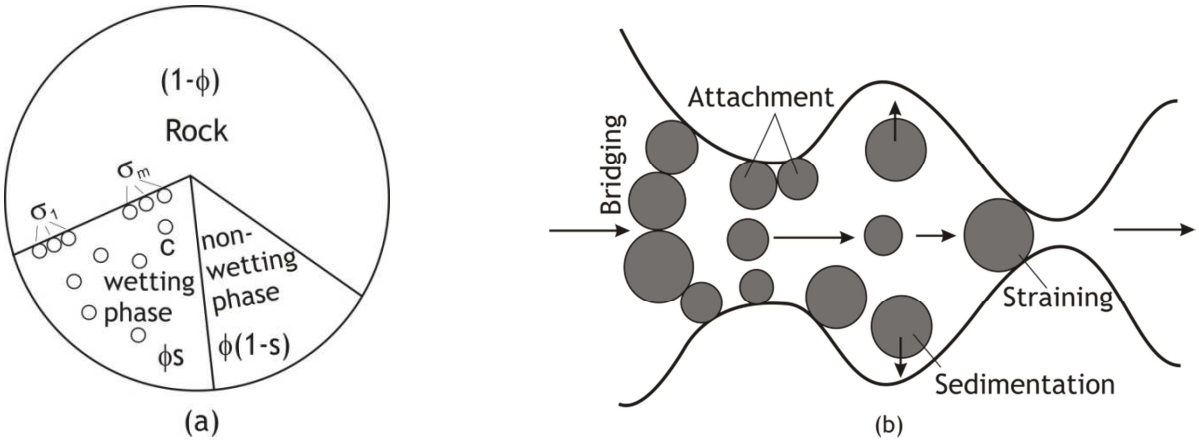

Figure 1. Schema of particle capture and placing in the porous space during suspension transport: (a) different mechanisms of particle capture pores, (b) suspension and retained particles in porous media

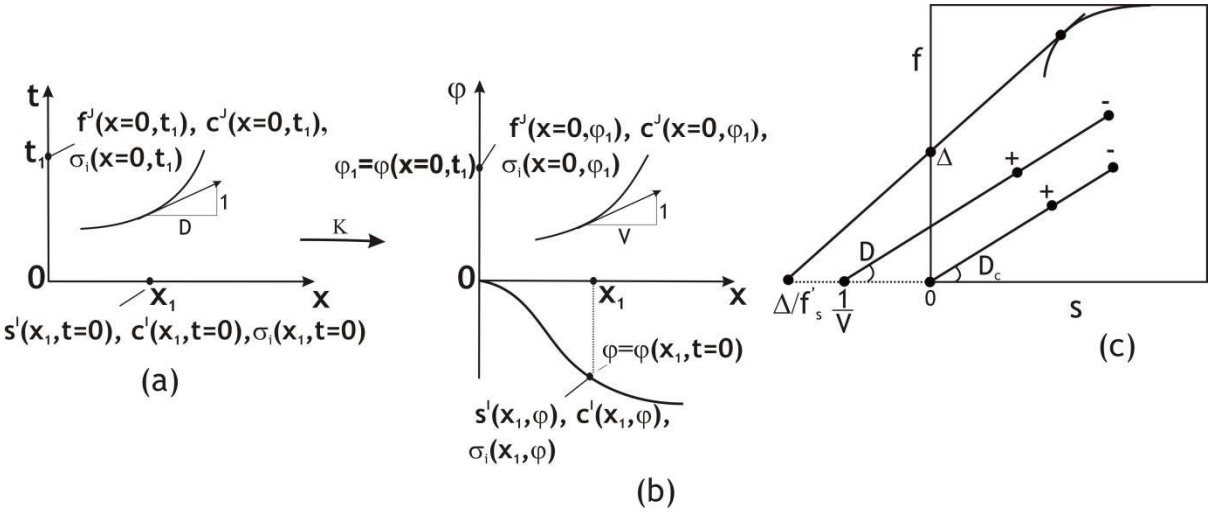

Figure 2. Mapping *K: (x,t)→(x,φ)* using a stream function *φ(x,t)*: (a) initial and boundary conditions in the plane (*x, t*); (b) mapped initial and boundary conditions in the plane (*x, φ*); (c) geometric relationships between the speeds *D* in general system and *V* in the auxiliary system

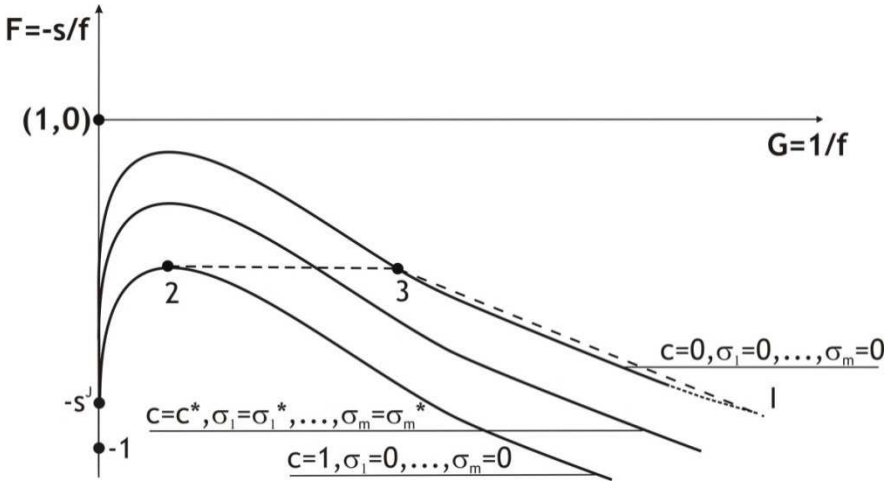

Figure 3. Density G and flux F in the lifting equation for different suspended and retained concentrations; path $-s^J$-2→3→I corresponds to self-similar solution for two-phase capture-free flow

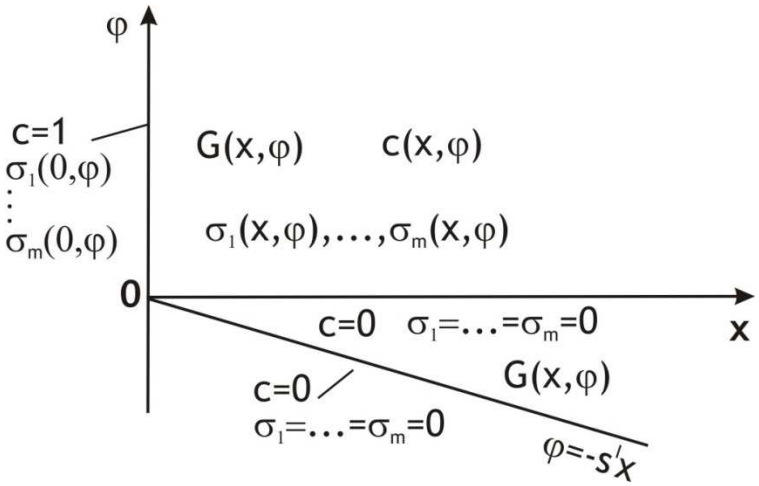

Figure 4. The solutions of the auxillary and lifting systems

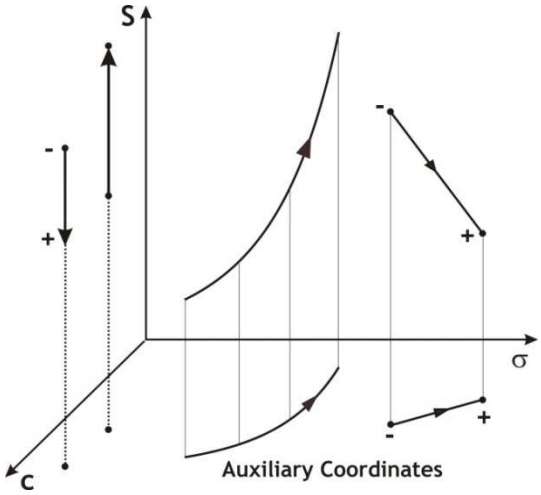

Figure 5. Elementary waves, projection and lifting for auxiliary and general systems

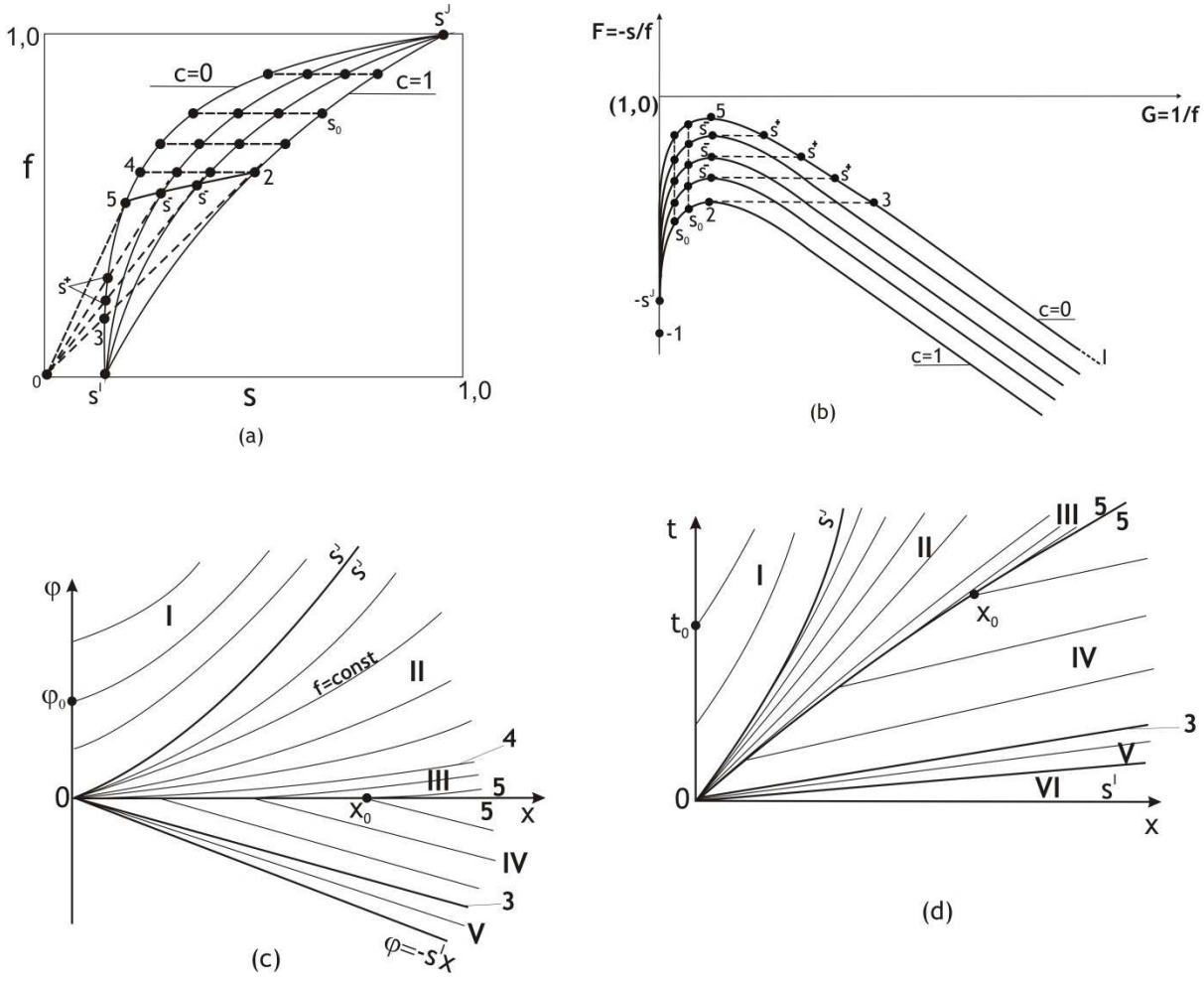

Figure 6. Exact solution for the case of concave fractional flow function, which is independent of retained concentrations: (a) graphical solution in the plane of fractional flow curves; (b) the solution representation in the plane (G,F) of the density and flux for the lifting equation; (c) five-zone solution in (x,φ) plane, (d) shocks and characteristics in (x,t) plane

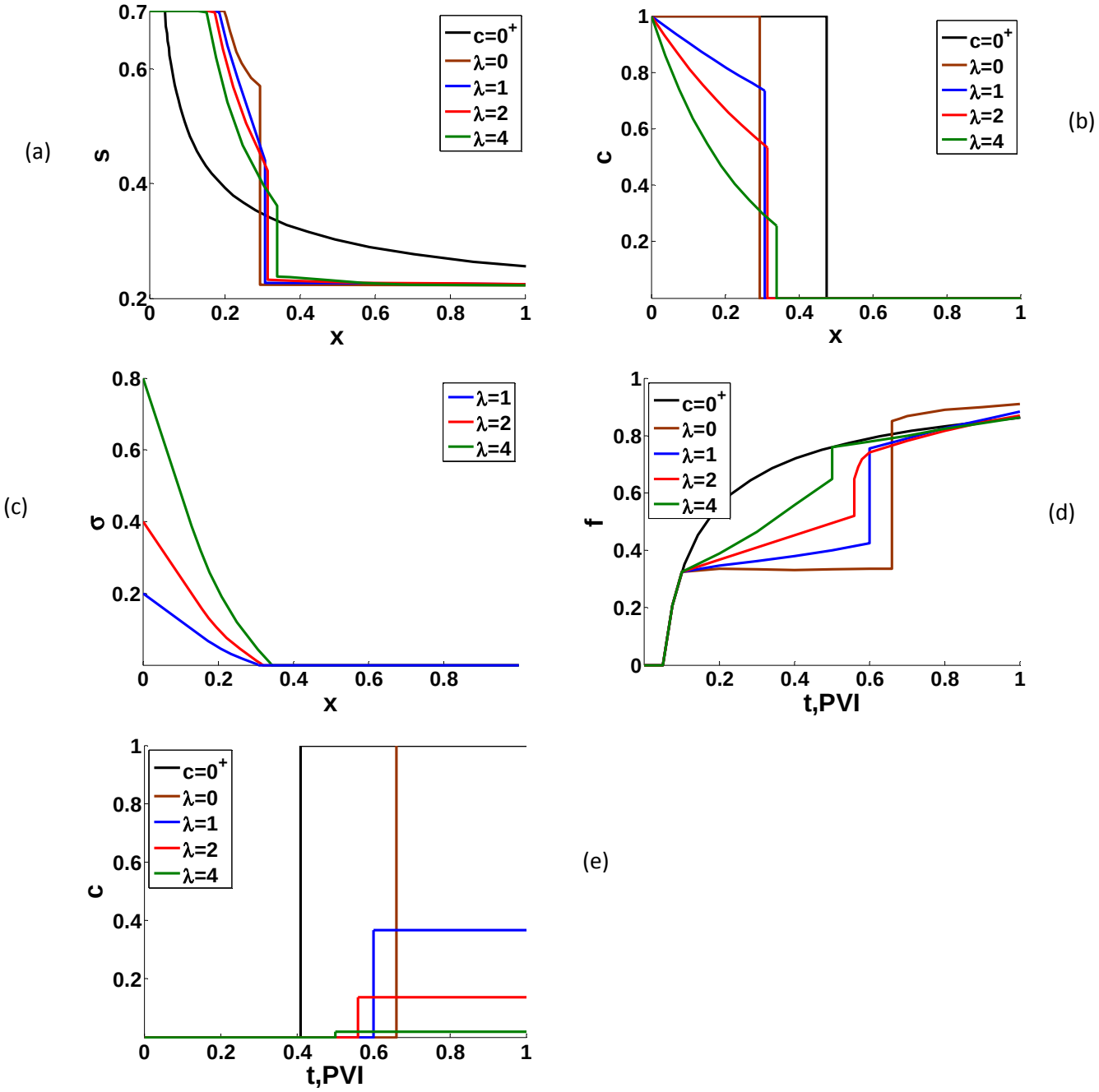

Figure 7. Saturation and concentration profiles and histories as obtained from the exact solution for different filtration coefficients λ in the case of negligible formation damage coefficients and concave fractional flow: (a) water saturation profiles at the moment t=0.2, (b) suspended particle concentration profiles, (c) retained particle concentration profiles, (d) water flux breakthrough at x=1, (e) breakthrough concentration.

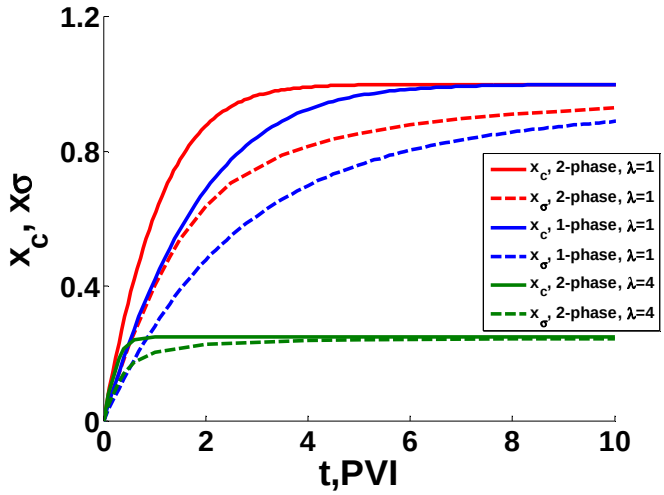

Figure 8. The penetration depths for suspension and retained particles (x_c and x_σ) with a single- and two-phase flows and different filtration coefficients

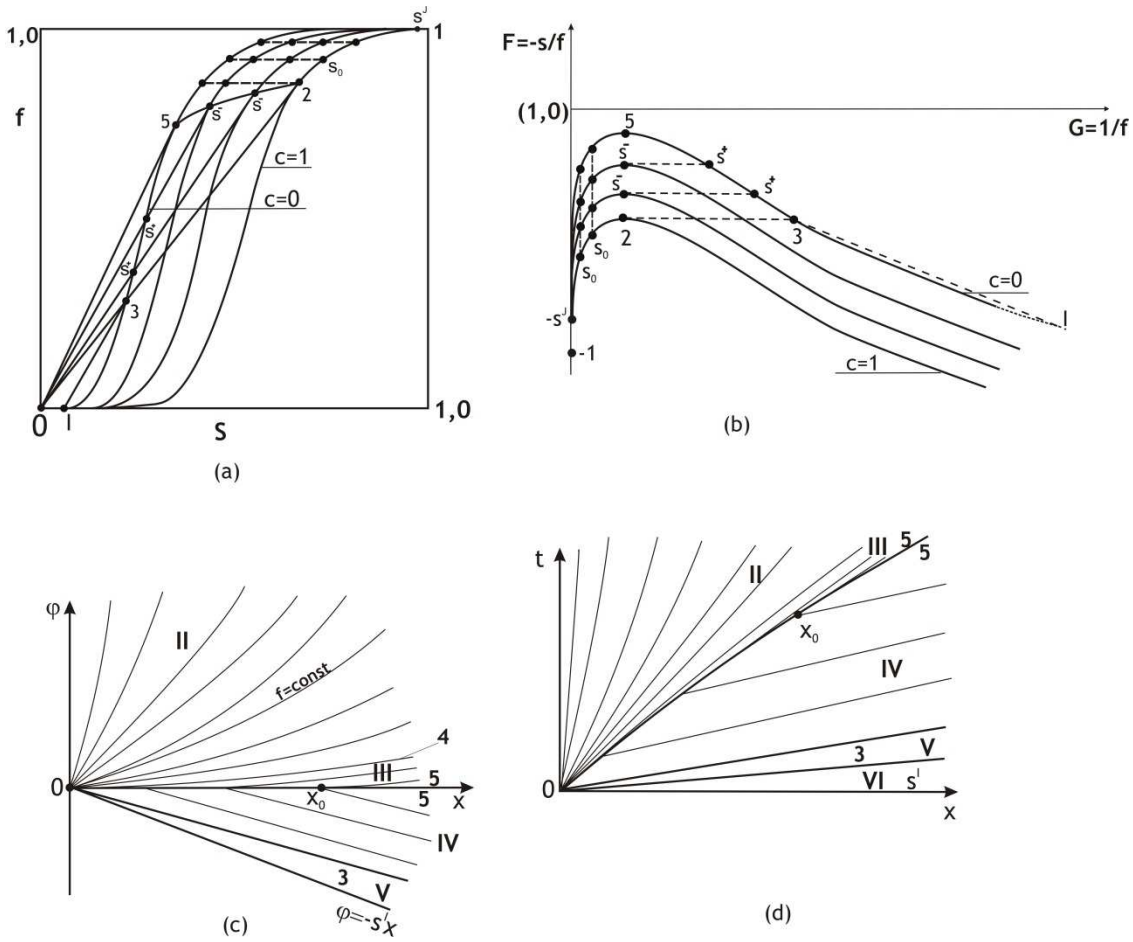

Figure 9. Exact solution for the case of *S*-shaped fractional flow function that is independent of retained concentration: (a) presentation of solution in the plane of fractional flow curves; (b) solution in the plane of density and flux for the lifting equation; (c) five-zone solution in (x,φ) plane, (d) six-zone solution in (x,t) plane

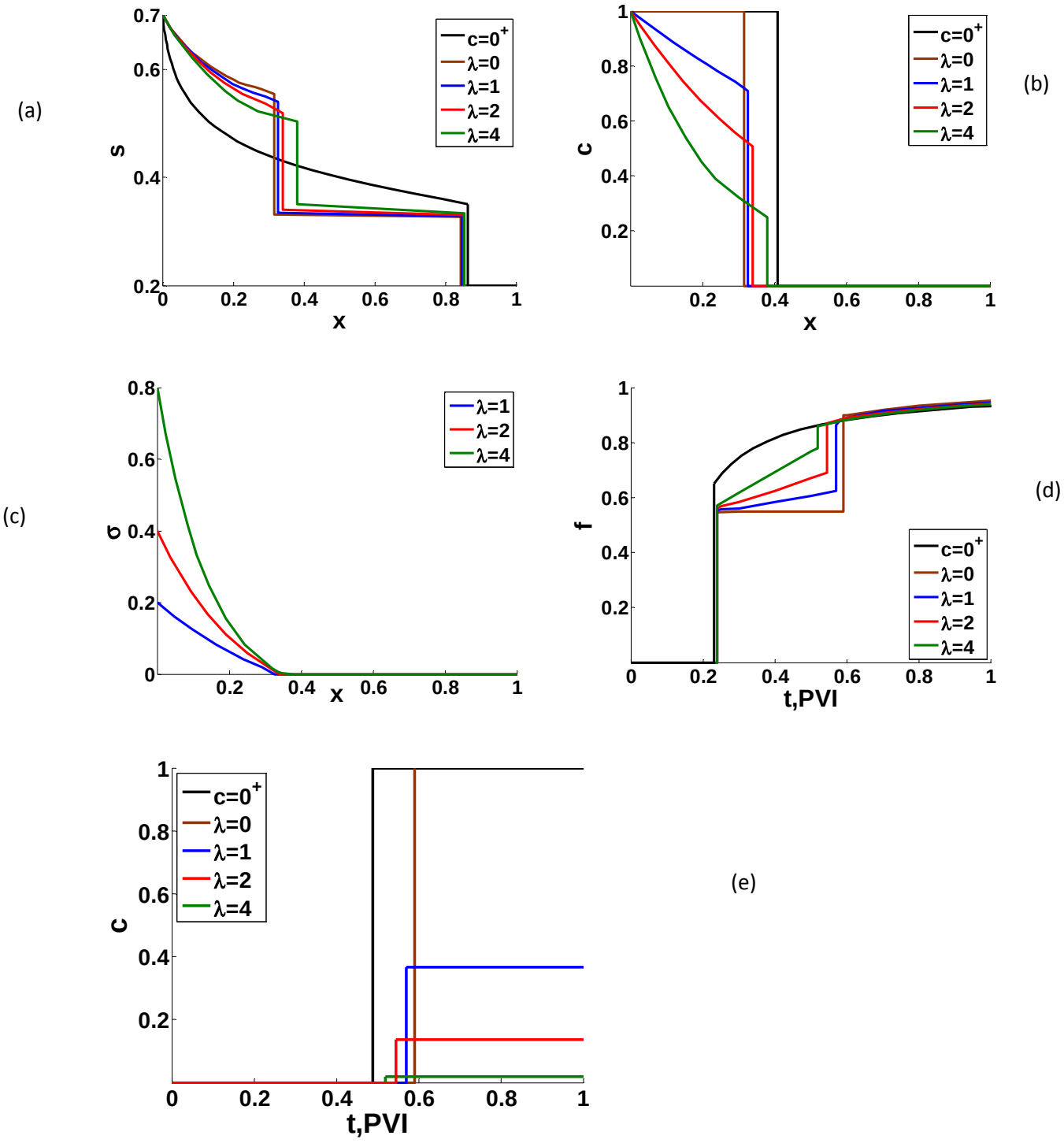

Figure 10. Saturation and concentration profiles and histories as obtained from the exact solution for different filtration coefficients λ for S-shape fractional flow, which is independent of particle retention concentration (a) water saturation profiles at the moment t=0.2, (b) retained particle concentration and (c) suspended particle concentration profiles for three different λ at t=0.2 (d) water flux breakthrough at x=1 (e) concentration breakthrough

(a)

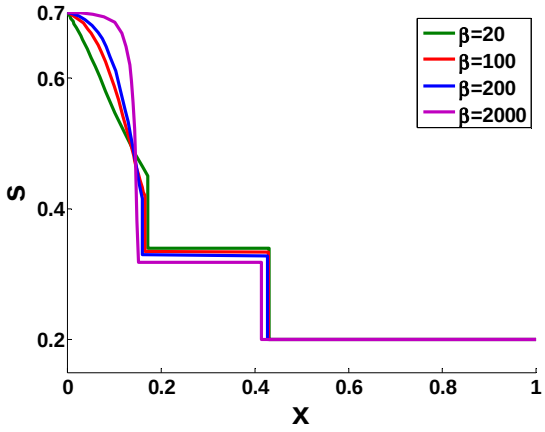

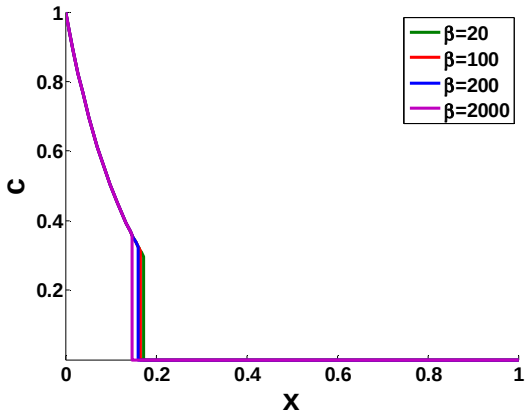

(b)

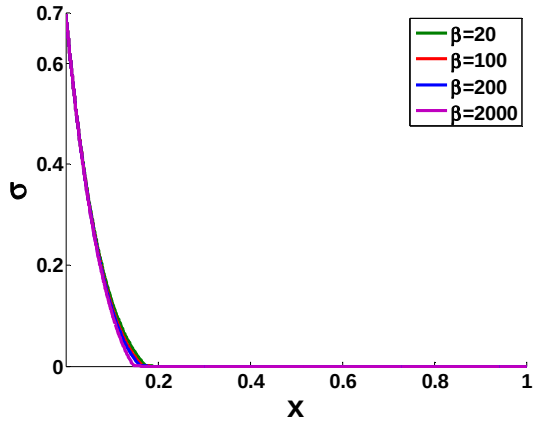

(c)

Figure 11. Effects of formation damage coefficient β on two-phase suspension-colloidal flow with the Langmuir blocking function for the particle capture (a) saturation profiles for different β for t=0.1, (b) suspended particle concentration, (c) retained concentration profiles

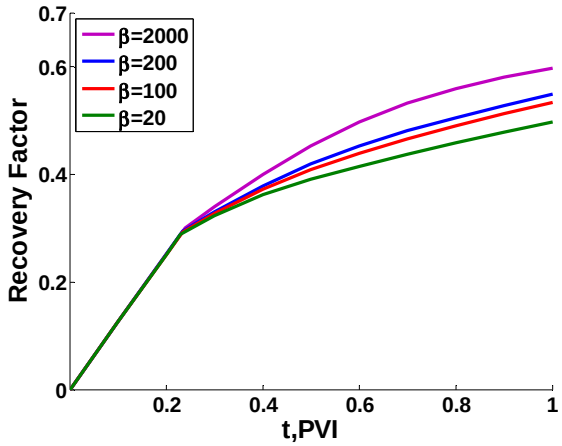

Figure 12. Effect of formation damage coefficient β on recovery factor, for the case of the blocking filtration function

Table 1. Exact solution of the auxiliary and lifting problems in (x, φ)-plane

Zones	c	σ	s	characteristic
I	$c = e^{-\lambda x}$	$\sigma = \lambda\varphi e^{-\lambda x}$	s^J	$\varphi = \varphi_0 + \int_0^x \Delta\left(s^J, e^{-\lambda u}\right)\left[f_s'\left(s^J, e^{-\lambda u}\right)\right]^{-1} du$
II	$c = e^{-\lambda x}$	$\sigma = \lambda\varphi e^{-\lambda x}$	$s_{II}(x,\varphi)$	$\varphi = \int_0^x \Delta\left(s_{II}(u), c(u)\right)\left[f_s'\left(s_{II}(u), c(u)\right)\right]^{-1} du$
III	$c = e^{-\lambda x}$	$\sigma = \lambda\varphi e^{-\lambda x}$	$s_{III}(x,\varphi)$	$\varphi = \int_{x0}^x \Delta\left(s_{III}(u), c(u)\right)\left[f_s'\left(s_{III}(u), c(u)\right)\right]^{-1} du$
IV	$c = 0$	$\sigma = 0$	$s_{IV}(x,\varphi)$	$\frac{\varphi}{x - x_0} = \Delta\left(s^+, 0\right)\left[f_s'\left(s^+, 0\right)\right]^{-1}, s_{IV}(x,\varphi) = s^+(x_0, 0)$
V	$c = 0$	$\sigma = 0$	$s_V(x,\varphi)$	$\frac{\varphi}{x} = \Delta\left(s_V, 0\right)\left[f_s'\left(s_V, 0\right)\right]^{-1}$

Table 2. Five flow zones in (x, φ)-plane for the solution of auxiliary and lifting problems

Zones	domain
I	$\varphi > \int_0^x \Delta\left(s^J, e^{-\lambda u}\right)\left[f_s'\left(s^J, e^{-\lambda u}\right)\right]^{-1} du$
II	$\int_0^x \Delta\left(s_{II}(u), c(u)\right)\left[f_s'\left(s_{II}(u), c(u)\right)\right]^{-1} du < \varphi < \int_0^x \Delta\left(s^J, e^{-\lambda u}\right)\left[f_s'\left(s^J, e^{-\lambda u}\right)\right]^{-1} du$
III	$0 < \varphi < \int_0^x \Delta\left(s_{II}(u), c(u)\right)\left[f_s'\left(s_{II}(u), c(u)\right)\right]^{-1} du$
IV	$\Delta\left(s_3, 0\right)\left[f_s'\left(s_3, 0\right)\right]^{-1} x < \varphi < 0$
V	$-s^I x < \varphi < \Delta\left(s_3, 0\right)\left[f_s'\left(s_3, 0\right)\right]^{-1} x$

Table 3. Exact solution in (x, t) plane after the inverse mapping

Zones	c	σ	s	characteristic
I	$c = e^{-\lambda x}$	$\sigma = \lambda\varphi e^{-\lambda x}$	s^J	$t = t_0 + \int_0^x \left[f_s'\left(s^J, c(u)\right)\right]^{-1} du$
II	$c = e^{-\lambda x}$	$\sigma = \lambda\varphi e^{-\lambda x}$	$s_{II}(x,t)$	$t = \int_0^x \left[f_s'\left(s_{II}(u), c(u)\right)\right]^{-1} du$
III	$c = e^{-\lambda x}$	$\sigma = \lambda\varphi e^{-\lambda x}$	$s_{III}(x,t)$	$t = \int_{x0}^x \left[f_s'\left(s_{III}(u), c(u)\right)\right]^{-1} du$
IV	$c = 0$	$\sigma = 0$	$s_{IV}(x,t)$	$\frac{t}{x - x_0} = \left[f_s'\left(s^+, 0\right)\right]^{-1}, s_{IV}(x,\varphi) = s^+(x,0)$
V	$c = 0$	$\sigma = 0$	$s_V(x,\varphi)$	$\frac{t}{x} = \left[f_s^{/}(s_V, 0)\right]^{-1}$
VI	$c = 0$	$\sigma = 0$	s^I	

Table 4. Six flow zones in (x, t)-plane for the solution of 1-d flow problem

Zones	domain
I	$t > \int_0^x \left[f_s'\left(s^J, c(u)\right)\right]^{-1} du$
II	$\int_0^x \left[f_s'\left(s_{II}(u), c(u)\right)\right]^{-1} du < t < \int_0^x \left[f_s'\left(s^J, c(u)\right)\right]^{-1} du$
III	$\int_0^x s^- \left[f\left(s^-(u), c(u)\right)\right]^{-1} du < t < \int_0^x \left[f_s'\left(s_{II}(u), c(u)\right)\right]^{-1} du$
IV	$\left[f_s'(s_3, 0)\right]^{-1} x < t < \int_0^x s^- \left[f\left(s^-(u), c(u)\right)\right]^{-1} du$
V	$\left[f_s'\left(s^I, 0\right)\right]^{-1} x < t < \left[f_s'\left(s_3, 0\right)\right]^{-1} x$
VI	$0 < t < \left[f_s'\left(s^I, 0\right)\right]^{-1} x$

Nomenclature

c	Concentration of particles suspended in aqueous phase
D	Front velocity in (x, t) coordinates
d_c	Average grain diameter
f	Fractional flow for wetting phase
F	Density in lifting equation
G	Flux in lifting equation
k	Absolute permeability, L^2
k_r	Relative permeability
L	Reservoir size, L
u	Flow velocity, LT^{-1}
U	Overall flow velocity, LT^{-1}
p	Pressure
s	Saturation
t	Time
V	Front velocity in (x, φ) coordinates
x	Coordinate
RF	Recovery factor

Greek letters

α	Attachment efficiency
β	Formation damage coefficient
λ	Filtration coefficient, L^{-1}
η_0	Single collector contact efficiency
μ	Viscosity, $ML^{-1}T^{-1}$
σ	Concentration of retained particles
ρ	Density, ML^{-3}
ϕ	Porosity
φ	Stream function
Φ	Retention concentration potential

Subscripts

n	Non wetting phase
w	Wetting phase

Superscript

I	Initial value
J	Injected value

6 Splitting Method for Flow System with Dissipation and Non-Equilibrium Effects

S. Borazjani, A.J. Roberts, P. Bedrikovetsky

Applied Mathematics Letters, 53 (2016) 25-32

Statement of Authorship

Title of Paper	Splitting in systems of PDEs for two-phase multicomponent flow in porous media
Publication Status	
Publication Details	S. Borazjani, A.J. Roberts, P. Bedrikovetsky (2016). Splitting in systems of PDEs for two-phase multicomponent flow in porous media. Applied Mathematics Letters.

Principal Author

Name of Principal Author (Candidate)	Sara Borazjani
Contribution to the Paper	Problem formulation, Derivation of the mathematical model, Writing the manuscript
Overall percentage (%)	80%
Certification:	This paper reports on original research I conducted during the period of my Higher Degree by Research candidature and is not subject to any obligations or contractual agreements with a third party that would constrain its inclusion in this thesis. I am the primary author of this paper.
Signature	Date: 22.11.2015

Co-Author Contributions

By signing the Statement of Authorship, each author certifies that:

i. the candidate's stated contribution to the publication is accurate (as detailed above);

ii. permission is granted for the candidate in include the publication in the thesis; and

iii. the sum of all co-author contributions is equal to 100% less the candidate's stated contribution.

Name of Co-Author	Anthony John Roberts
Contribution to the Paper	Supervised development of the work, Manuscript review and assessment
Signature	Date: 20/11/2015

Name of Co-Author	Pavel Bedrikovetsky
Contribution to the Paper	Supervised development of the work, Manuscript review and assessment
Signature	22.11.2015

Please cut and paste additional co-author panels here as required.

Applied Mathematics Letters 53 (2016) 25–32

Contents lists available at ScienceDirect

Applied Mathematics Letters

www.elsevier.com/locate/aml

Splitting in systems of PDEs for two-phase multicomponent flow in porous media

S. Borazjani*, A.J. Roberts, P. Bedrikovetsky

The University of Adelaide, Adelaide SA 5005, Australia

ARTICLE INFO

Article history:
Received 3 August 2015
Received in revised form 23 September 2015
Accepted 23 September 2015
Available online 3 October 2015

Keywords:
Non-linear PDEs
Exact solutions
Conservation laws
Splitting
Dissipative systems
Advective reaction–diffusion equations

ABSTRACT

The paper investigates the system of PDEs for two-phase n-component flow in porous media consisting of hyperbolic terms for advective transport, parabolic terms of dissipative effects and relaxation non-equilibrium equations. We found that for several dissipative and non-equilibrium systems, using the stream-function as a free variable instead of time separates the general $(n+1)\times(n+1)$ system into an $n\times n$ auxiliary system and one scalar lifting equation. In numerous cases, where the auxiliary system allows for exact solution, the general flow problem is reduced to numerical or semi-analytical solution of one lifting equation.

1. Introduction

Consider one-dimensional two-phase multicomponent flow of water and oil in porous media. The independent dimensionless variables are linear co-ordinate $0 < x < 1$ and time $t > 0$. We seek for water saturation $s(x,t)$, concentration of ith component in water $c_i(x,t)$ and non-equilibrium adsorbed concentrations, $\bar{a}_i(x,t)$. The system consists of mass conservation laws for water and each component, and of sorption kinetics for each component:

$$\frac{\partial s}{\partial t}+\frac{\partial q}{\partial x}=0,\quad q=f\left(s,c,\bar{a}\right)\left[1+\varepsilon_c k_{ro}\left(s,c,\bar{a}\right)\frac{\partial J\left(s,c,\bar{a}\right)}{\partial x}\right] \tag{1}$$

$$\frac{\partial\left(cs+\bar{a}\right)}{\partial t}+\frac{\partial cq}{\partial x}=0,\quad c=\left(c_1,\ldots,c_i,\ldots,c_n\right),\ \bar{a}=\left(\bar{a}_1,\ldots\bar{a}_i,\ldots,\bar{a}_n\right),\ i=1,2\ldots,n \tag{2}$$

$$\varepsilon_t\frac{\partial\bar{a}}{\partial t}=\left[a\left(c\right)-\bar{a}\right]f\left(s,c,\bar{a}\right),\quad a=\left(a_1,\ldots,a_i,\ldots,a_n\right),\ a_i=a_i\left(c\right),\ i=1,2,\ldots,n \tag{3}$$

* Corresponding author.
E-mail address: sara.borazjani@adelaide.edu.au (S. Borazjani).

http://dx.doi.org/10.1016/j.aml.2015.09.014
0893-9659/

where q is the water flux, f is the fractional flow of water, k_{ro} is the relative permeability for oil, J is the capillary pressure, ε_c and ε_t are the dimensionless groups for capillary pressure and delay, respectively [1,2]. The functions $f(s, c, \bar{a})$, $k_{ro}(s, c, \bar{a})$, $J(s, c, \bar{a})$ and $a(c)$ are known. Diffusion of components is neglected in Eq. (2).

System (1)–(3) arises in numerous areas of chemical, petroleum and environmental engineering, in geology and petroleum exploration. For large n, even a one-dimensional numerical solution is very cumbersome. Therefore, analytical solutions for (1)–(3) are very useful in reservoir simulation, particularly in three-dimensional stream-line and front-tracking models [1,3]. Matched asymptotic expansion solutions and also recently developed semi-analytical methods for the system (1)–(3) with dissipation and non-equilibrium ($\varepsilon_c, \varepsilon_t \neq 0$) allow for significant acceleration of numerical computations [4,5].

At $\varepsilon_c = \varepsilon_t = 0$ (large scale approximation) the system (1)–(3) becomes hyperbolic; self-similar solutions of the Riemann problems have been presented in numerous works [6–8]. Exact solutions for non-self-similar initial–boundary problems with piecewise-constant values have been obtained by solving the interactions of the Riemann configurations in [2,6]. Direct projection of the system (1)–(3) onto a one-phase system causes splitting of the Riemann problems for (1)–(3) at $\varepsilon_c = \varepsilon_t = 0$ into those for an auxiliary $n \times n$ system and a scalar lifting equation [8]. Pires et al. [9] showed that using the stream-function $\varphi(x, t)$ as an independent variable instead of time t

$$s = -\frac{\partial \varphi}{\partial x},\ f = \frac{\partial \varphi}{\partial t}, \quad \varphi\,(x, t) = \int_{(0,0)}^{(x,t)} (f dt - s dx) \tag{4}$$

results in the splitting for any initial–boundary value problems for $\varepsilon_c = \varepsilon_t = 0$. It significantly multiplies the number of exact solutions and encompasses those obtained previously [9].

In this work, we develop a new splitting method for system (1)–(3) accounting for the dissipative and non-equilibrium phenomena (ε_c, $\varepsilon_t \neq 0$) along with derivation of new associated exact and semi-analytical solutions (Sections 2 and 3). For the cases of exact auxiliary solutions, the splitting reduces the general flow problem to the solution of one non-linear lifting equation. Exact solution of the inverse problem for the system (1), (2) under thermodynamic equilibrium (Section 2.5) is obtained. Section 4 discusses two-phase flows with inter-phase mass transfer.

2. Splitting for two-phase multi-component flow with equilibrium sorption

This section applies the splitting procedure to system (1)–(3) with $\varepsilon_t = 0$ and finite ε_c, which corresponds to low velocities flows. In this case, all adsorbed concentrations are at equilibrium, $\bar{a} = a(c)$.

2.1. Initial–boundary value problem

The initial saturation s_R and concentrations c_R at $t = 0$ are bounded functions of x. Inlet boundary water flux q_L and concentrations c_L at $x = 0$ are bounded functions of t. Outlet boundary condition at $x = 1$ corresponds to saturation, for which the capillary pressure equals zero [4].

System (1)–(3) is parabolic with respect to unknown saturation $s(x, t)$ and hyperbolic in the unknown concentrations $c_i(x, t)$, $i = 1, 2, \ldots, n$.

2.2. Splitting procedure

Introduce the stream-function φ with respect to the conservation law (1)

$$s = -\frac{\partial \varphi}{\partial x},\ q = \frac{\partial \varphi}{\partial t}, \quad d\varphi = q dt - s dx. \tag{5}$$

Let us map system (1), (2) from independent variables (x, t) to (x, φ). Expressing dt from (5) and calculating its differential yield the following expressions for Eq. (1) in (x, φ)-coordinates with the water flux q given by the second equation (1)

$$\frac{\partial F}{\partial \varphi} + \frac{\partial G}{\partial x} = 0, \quad G = \frac{1}{q}, \; F = -\frac{s}{q}. \tag{6}$$

Integrating Eq. (2) over any simply-connected domain in plane (x, t), applying Green's theorem and using (5) transform Eq. (2) to (x, φ)-coordinates:

$$\frac{\partial a\,(c)}{\partial \varphi} + \frac{\partial c}{\partial x} = 0. \tag{7}$$

For constant initial data s_R and c_R, the initial conditions for Eqs. (6), (7) now apply along the straight line $\varphi = -s_R x, \; x > 0$.

The system for $(n + 1)$ unknowns (s, c) is separated into the $n \times n$ auxiliary system (7) for unknown $c(x, \varphi)$ and one scalar parabolic lifting equation (6) with unknown $s(x, \varphi)$. The auxiliary system (7) contains functions $a(c)$ only, whereas the lifting equation contains the hydrodynamic functions $f(s, c, a), \; J(s, c, a)$ and $k_{ro}(s, c)$.

2.3. Solution of the auxiliary problem

The auxiliary system (7) is a hyperbolic system of conservation laws [10]. Initial and boundary conditions with constant values correspond to a Riemann problem that allows for self-similar solutions: $c(x, \varphi) = C(\varphi/x)$. Solution of the initial–boundary problem with piecewise-constant values is obtained by interactions of Riemann configurations, occurring in the points of discontinuity of initial and boundary values [2,11,12].

Consider the projection of a solution $s(x, t), \; c(x, t)$ of system (1)–(3) onto the auxiliary solution $c(x, \varphi)$. As it follows from the mapping (5), the shock trajectory $x_0(t)$ with velocity D projects into the trajectory $x_0(\varphi)$ with velocity V

$$\frac{1}{V} = \frac{q}{D} - s, \quad D = \frac{dx_0\,(t)}{dt}, \; V = \frac{dx_0\,(\varphi)}{d\varphi}. \tag{8}$$

Lemma 1. *Mass balance (Hugoniot–Rankine) conditions on a discontinuity for system (1)–(3) project onto those for the auxiliary system (7).*

Lemma 2. *Lax's stability conditions for discontinuities of system (1)–(3) project onto those for the auxiliary system (7)* [13].

Now let us introduce diffusion with corresponding Peclet number $1/\varepsilon_d$ into system (1)–(3) (see [2,5] for detailed derivations). The system (1)–(3) becomes hyperbolic for $\varepsilon_c = \varepsilon_t = \varepsilon_d = 0$. A discontinuity in the hyperbolic system is admissible if it is a limit of continuous solutions of the system (1)–(3) with ε_c, ε_t and ε_d tending to zero. The admissibility of shocks in the auxiliary system corresponds to vanishing diffusion and non-equilibrium effects.

Lemma 3. *Admissibility conditions for a discontinuity of system (1)–(3) project on those for the auxiliary system (7)* [2,12].

Now let us discuss some cases where the auxiliary problem allows for exact solution.

Example 1. Polymer slug injection with water drive corresponds to inlet boundary conditions for water flux $q(0,t)=1$ and for concentration $c(0,t)=1,\ t<t_0$ and $c(0,t)=0$ for $t>t_0$. The solution of the auxiliary problem for any arbitrary adsorption isotherm is presented in [2,11].

Example 2. Rhee et al. [11] derive complete integration of the auxiliary system (7) for Langmuir adsorption isotherms

$$a_i=\frac{N_iK_ic_i}{1+\sum\limits_{j=1}^{n}K_jc_j},\quad i=1,2,\ldots,n \tag{9}$$

where N_i are the saturation concentrations and K_i are the equilibrium constants. The system (7) becomes strictly hyperbolic. Rarefaction waves for the auxiliary system (7), corresponding to eigenvalues $p_k\omega_k^2$ are

$$\left(\frac{d\varphi}{dx}\right)_{\omega_k}=p_k\omega_k^2,\quad p_k=\frac{1}{N_kK_k}\prod_{i=1,k}^{n}\frac{\omega_i}{N_iK_i},\qquad \sum_{i=1}^{n}\frac{K_ia_i}{N_iK_i-\omega_i}=1 \tag{10}$$

where p_k and ω_k are determined by second and third Eq. (10), respectively.

Consider the shock and rarefaction waves of the ith family, $\omega_i=\text{const}$. Consider a hyper-rectangle in R^n with opposite vertices corresponding to Riemann problem values R and L. The solution of the Riemann problem corresponds to shocks and/or rarefactions along the rectangular sides. The problem of the interactions of rarefaction waves allows for exact solution by the hodograph method. Therefore, any initial–boundary problem with piecewise-constant data also allows for an exact solution.

Example 3. For the case of small concentrations c_i, formula (9) gives $a_i\approx N_iK_ic_i$; the rarefaction waves degenerate into shocks, and the global solution degenerates into a sequence of n shocks with velocities $\varphi/x=N_iK_i$ [14,15].

For the above examples, the general $(n+1)\times(n+1)$ system (1), (2) is reduced to one parabolic lifting equation (6), where the solutions of the auxiliary system (7), $c_i(x,\varphi)$, are already known.

2.4. Lifting solution and inverse mapping

In a general case, the lifting equation (6) can be solved either numerically or by matched asymptotic expansions [4,16]. The inverse mapping $(x,\varphi)\to(x,t)$ is determined by

$$t=\int_{(0,0)}^{(x,\varphi)}\frac{d\varphi}{q}+\frac{sdx}{q} \tag{11}$$

where $s(x,\varphi)$ is the solution of the lifting equation (6).

2.5. Solution of the inverse problem

Consider a laboratory experiment on injection of water with constant composition c_L into a porous medium with initial saturation s_R and concentrations c_R. The measurements of water flux $q(1,t)$ and breakthrough concentrations $c(1,t)$ are carried out during the experiment. The inverse problem is the determination of the adsorption isotherms $a(c)$. The solution of the Riemann problem for the auxiliary system for initial and boundary conditions c_R and c_L is self-similar, i.e. it is constant along each line $\varphi/x=\text{const}$.

Integration of Eq. (7) over the triangle, bounded by the contour $\Gamma : (0,0) \to (1,-s_R) \to (1,\varphi) \to (0,0)$ and applying Green's theorem yields

$$0 = \oint\!\!\!\!\!\!\square_{\Gamma} c d\varphi - a(c)\, dx = -c_R s_R - a(c_R) + \int_{-s_R}^{\varphi} c(1,u) du - c(1,\varphi)\,\varphi + a(c(1,\varphi)). \tag{12}$$

It allows for explicit calculation of the sorption isotherm

$$a(c(1,\varphi)) = c_R s_R + a(c_R) - \int_0^t c(1,u) q(u)\, du + c(1,\varphi)\,\varphi, \qquad \varphi(1,t) = \int_0^t q(1,u)\, du + s_R. \tag{13}$$

However, the solution of the inverse problem (13) involves only c-values, which are exhibited in the forward solution of the Riemann problem. The solution of the inverse problem for $a(c)$ does not use the direct Riemann solution and is based on its self-similarity only.

3. Two-phase flow with non-equilibrium sorption and chemical reactions

This section considers two-phase flow at high velocities, where capillary pressure effects are negligible ($\varepsilon_c = 0$), but thermodynamic equilibrium conditions are not valid anymore ($\varepsilon_t > 0$ is a finite value).

3.1. Two-phase multicomponent flow with non-equilibrium sorption

Eqs. (3) can be obtained from the system with finite delay [17,18] as first order approximation with regard to small parameter ε_t; the zero order approximation corresponds to equilibrium sorption $a(c)$. The relaxation time is inversely proportional to hydrodynamic dispersion of the components, which in turn is proportional to the velocity [2,4]. The dimensionless group ε_t is the ratio between the relaxation and flight times.

The stream-function and mapping are defined by Eqs. (4). The lifting equation has the form (6), where the density and the flux are

$$G = f^{-1}(s,c,\bar{a}), \qquad F = -s f^{-1}(s,c,\bar{a}). \tag{14}$$

The auxiliary $2n \times 2n$ system is hyperbolic with n zero-speed characteristics

$$\frac{\partial \bar{a}}{\partial \varphi} + \frac{\partial c}{\partial x} = 0, \qquad \varepsilon_t \frac{\partial \bar{a}}{\partial \varphi} = a(c) - \bar{a}. \tag{15}$$

The Goursat values $\bar{a}$ at $x = 0$ are obtained from inlet boundary conditions for $c(0,\varphi)$ and kinetics equations (15) [19].

Lemma 4. *Goursat conditions for the general system (1)–(3) with $\varepsilon_c = 0$ project into those for auxiliary system (15).*

Example 4. The auxiliary system is linear for small concentrations, that is, $a_i = \Gamma_{ij} c_j$ for some matrix Γ_{ij}, and is solved using Green's functions [15]. The lifting equation is hyperbolic. Despite the lifting solution being discontinuous, the mapping (4) is continuous.

3.2. Two-phase multicomponent flow with chemical reactions between salt components and rock

Consider r non-equilibrium reversible chemical reactions between the ith component in aqueous solution (c_i) and that adsorbed on the clay ($\bar{a}_i$) with the following stoichiometry

$$\sum_{i=1}^{n} v_{i\alpha}^{c} c_i + \sum_{i=1}^{n} v_{i\alpha}^{a} \bar{a}_i = 0, \quad \alpha = 1,2,\ldots,r \tag{16}$$

where $\nu^c_{i\alpha}$ and $\nu^a_{i\alpha}$ are the stoichiometric coefficients of suspended and adsorbed component i in reaction α, respectively [2,11]. The reaction kinetics of component i involved in n_k reactions, is given by the active mass law

$$\varepsilon_t \frac{\partial \bar{a}_i}{\partial t} = \sum_{\alpha=1}^{n_k} \left(K^f_\alpha \prod_{i=1}^{n} (c_i)^{\nu^c_{i\alpha}} (\bar{a}_i)^{\nu^a_{i\alpha}} - K^b_\alpha \prod_{i=1}^{n} (c_i)^{\nu^c_{i\alpha}} (\bar{a}_i)^{\nu^a_{i\alpha}} \right) f, \quad i = 1, 2, \ldots, n. \tag{17}$$

Here, the reaction kinetics coefficients are assumed to be proportional to the flow velocity; therefore, K^f_α and K^b_α are the forward and backward reaction rate constants for reaction α, divided by the flow velocity.

The equations for conservation of water and component masses (1) and (2) for $\varepsilon_c = 0$ hold. Introduction of the stream-function (4) yields the lifting equation (6) with density and flux (14); the auxiliary system consists of conservation laws first equation (15) and the kinetics equation

$$\varepsilon_t \frac{\partial \bar{a}_i}{\partial \varphi} = \sum_{\alpha=1}^{n_k} \left(K^f_\alpha \prod_{i=1}^{n} (c_i)^{\nu^c_{i\alpha}} (\bar{a}_i)^{\nu^a_{i\alpha}} - K^b_\alpha \prod_{i=1}^{n} (c_i)^{\nu^c_{i\alpha}} (\bar{a}_i)^{\nu^a_{i\alpha}} \right), \quad i = 1, \ldots, n. \tag{18}$$

At low flow velocities, ε_t tends to zero. The system becomes equivalent to Eqs. (1), (2) with sorption isotherms $a = a(c)$ expressed from (17) for $\varepsilon_t = 0$. The splitting mapping in this case is given by Eq. (5).

4. Two-phase flow with inter-phase mass transfer

Mass balance equations for two-phase flow, where n components are distributed between the aqueous and oil phases are

$$\frac{\partial C_i}{\partial t} + \frac{\partial F_i}{\partial x} = 0, \quad C_i = c_i s + y_i (1 - s), \; F_i = c_i q + y_i (1 - q), \; i = 1, 2, \ldots, n-1 \tag{19}$$

where concentrations $c_1, c_2 \ldots c_{n-1}$ and y_1 are thermodynamic functions of concentrations $y_2, \; y_3 \ldots y_{n-1}$ and q is given by second equation (1). The $(n-1) \times (n-1)$ system (19) defines unknowns $y_2, \; y_3 \ldots y_{n-1}$ and s [2,20].

Introduction of the thermodynamic variables α_i and β_i

$$\alpha_i (c_2 \ldots c_{n-1}) = \frac{c_i - y_i}{c_1 - y_1}, \qquad \beta_i (c_2 \ldots c_{n-1}) = y_i - \alpha_i y_1, \quad i = 2, 3, \ldots, n-1 \tag{20}$$

transforms system (19) into

$$\frac{\partial C_1}{\partial t} + \frac{\partial F_1 (C, \beta)}{\partial x} = 0, \qquad \frac{\partial (\alpha_i (\beta) C_1 + \beta_i)}{\partial t} + \frac{\partial (\alpha_i (\beta) F_1 + \beta_i)}{\partial x} = 0, \quad \beta = (\beta_2, \beta_3 \ldots \beta_{n-1}). \tag{21}$$

Using the potential ϕ and variable ψ instead of independent variables (x, t)

$$C = -\frac{\partial \phi}{\partial x}, \qquad F = \frac{\partial \phi}{\partial t}, \qquad \psi = x - t \tag{22}$$

separates the following auxiliary $(n-2) \times (n-2)$ system from the first equation (19)

$$\frac{\partial}{\partial \phi} \left(\frac{C_1}{F_1 - C_1} \right) - \frac{\partial}{\partial \psi} \left(\frac{1}{F_1 - C_1} \right) = 0, \qquad \frac{\partial \beta_i}{\partial \phi} + \frac{\partial \alpha_i (\beta)}{\partial \psi} = 0. \tag{23}$$

The auxiliary system second (23) allows for exact solutions analogous to those described above for the system with sorption (7). Besides, the inverse problem for determining the thermodynamic relationship $\alpha = \alpha(\beta)$ from laboratory data allows for exact solutions like (13).

5. General applications

The splitting transformations (4) and (5) can be generalized to non-isothermal systems, where the energy conservation law adds to system (1)–(3). Also, denoting s as oil saturation allows using system (1)–(3) for secondary migration of hydrocarbons during the geological formation of petroleum accumulations; it allows description of water-alternate gas injection into oilfields too [2].

The system for two-phase immiscible colloidal-suspension transport in porous media, that appears in numerous areas of environmental and chemical engineering consists of mass balance for one of the phases (Eq. (1) with $\varepsilon c = 0$), mass balance of suspended and captured particles and n capture-rate equations corresponding to different capture mechanisms [21]. It also allows for splitting using the mapping (4). For the Riemann problem, the auxiliary $(n+1) \times (n+1)$ system allows for exact solution [14].

The governing system for compressible multi-component non-isothermal single-phase flow in porous media consists of the overall mass balance equation and the mass balance equations for each component, accounting for non-equilibrium sorption and chemical reactions [2]. The mapping (5) splits the overall balance equation for unknown pressure from equations for unknown concentrations and temperature. For those cases, the auxiliary system is hyperbolic and the lifting equation is parabolic.

Consider the general system (1)–(3) with either vanishing relaxation ($\varepsilon = \varepsilon_t$) or dispersion/diffusion ($\varepsilon = \varepsilon_d$). The difference between the solutions is an infinitesimal quantity of the second order ε^2 [22]. Therefore, the transformation (5) splits the systems with diffusion too.

The splitting method (5) can be extended to three-dimensional flows in the case where the total mobility of two phases is constant. Introduction of a linear co-ordinate along the stream-lines splits the three-dimensional system into one-dimensional system (1)–(3) and a Laplace equation for a real pressure distribution (see the corresponding derivations in [2,23]). Then mapping (5) is applied to the one-dimensional system (1)–(3) yielding the splitting.

6. Conclusions

For advective conservation systems with capillary-pressure dissipation (1), (2) or non-equilibrium kinetics (3), (17), the introduction of the stream-function instead of time splits the system into an auxiliary system and one lifting equation. In numerous cases, where the auxiliary problem allows for exact solution, the general system is reduced to one scalar equation. Auxiliary systems in the models (1)–(3), (16), (17) or (19), (20) depend on thermodynamic functions only, whereas the lifting equation (6) contains all hydrodynamic parameters.

Acknowledgments

The authors are grateful to Profs. A. Polyanin (Russian Academy of Sciences) and A. Shapiro (Technical University of Denmark) for fruitful co-operation.

References

[1] R.E. Ewing, The Mathematics of Reservoir Simulation, SIAM, Philadelphia, 1983.
[2] P. Bedrikovetsky, Mathematical Theory of Oil and Gas Recovery, Kluwer, London, 1993.
[3] H. Holden, N.H. Risebro, Front Tracking for Hyperbolic Conservation Laws, Springer-Verlag, New York, 2002.
[4] G.I. Barenblatt, V.M. Entov, V.M. Ryzhik, Theory of Fluid Flows through Natural Rocks, Kluwer, Dordrecht, 1990.
[5] S. Geiger, K.S. Schmid, Y. Zaretskiy, Curr. Opin. Colloid Interface Sci. 17 (3) (2012) 147–155.
[6] F. Fayers, J. Fluid Mech. 13 (1962) 65–76.
[7] V. Entov, A. Zazovskii, Hydrodynamics of Enhanced Oil Recovery Processes, Nauka, Moscow, 1989 (in Russian).
[8] T. Johansen, R. Winther, SIAM J. Math. Anal. 19 (3) (1988) 541–566.

[9] A.P. Pires, P.G. Bedrikovetsky, A.A. Shapiro, J. Pet. Sci. Eng. 51 (1) (2006) 54–67.
[10] R. Courant, D. Hilbert, Methods of Mathematical Physics: Partial Differential Equations, Interscience, New York, 1962.
[11] H.K. Rhee, R. Aris, N.R. Amundson, Theory and Application of Hyperbolic Systems of Quasilinear Equations, Prentice-Hall, Englewood Cliffs, 1998.
[12] B.L. Rozdestvenskii, N.N. Janenko, Systems of Quasilinear Equations and their Applications to Gas Dynamics, American Mathematical Society, Providence, 1983.
[13] P.D. Lax, Hyperbolic Systems of Conservation Laws and the Mathematical Theory of Shock Waves, SIAM, Philadelphia, 1972.
[14] A.D. Polyanin, V.E. Zaitsev, Handbook of Nonlinear Partial Differential Equations, Chapman & Hall/CRC, Boca Raton, 2004.
[15] A.D. Polyanin, Handbook of Linear Partial Differential Equations for Engineers and Scientists, Chapman and Hall/CRC, Boca Raton, 2002.
[16] L. Shampine, Appl. Numer. Anal. Comput. Math. 2 (3) (2005) 346–358.
[17] A.D. Polyanin, A.I. Zhurov, Appl. Math. Lett. 37 (2014) 43–48.
[18] A.D. Polyanin, V.G. Sorokin, Appl. Math. Lett. 46 (2015) 38–43.
[19] A.N. Tikhonov, A.A. Samarskii, Equations of Mathematical Physics, Dover, New York, 1990.
[20] T. Johansen, Y. Wang, F.M. Orr, B. Dindoruk, Transp. Porous Media 61 (1) (2005) 59–76.
[21] M.S. Espedal, A. Fasano, A. Mikelic, Filtration in Porous Media and Industrial Application, in: Lecture Notes in Mathematics, Springer, Berlin, 1981.
[22] A.J. Roberts, Model Emergent Dynamics in Complex Systems, SIAM, Philadelphia, 2014.
[23] S. Oladyshkin, M. Panfilov, C. R. Mec. 335 (2007) 7–12.

7 Conclusions

The derivation of new governing equations for low-salinity water-flooding and analytical modelling of two-phase multi-component flows in natural reservoirs allows drawing the following conclusions:

1. The effective splitting method for PDEs of conservation laws, allowing for derivation of numerous exact analytical solutions for two-phase multicomponent flows in porous media, permits the generalization for the cases of dissipative and non-equilibrium systems.

2. For advective conservation law systems for two-phase multicomponent flow in porous media with capillary-pressure dissipation, chemical reactions or non-equilibrium phase transitions, the introduction of the stream-function instead of time, splits the system into an auxiliary system and one lifting equation. In numerous cases, where the auxiliary problem allows for exact solution, the general system is reduced to one scalar equation. Auxiliary systems in the models with chemical reactions or non-equilibrium phase transitions depend on thermodynamics functions only, whereas the lifting equation contains all hydrodynamic parameters.

3. In the general case, the lifting equation is solved numerically, using the method of characteristics. However, for the cases of steady-state distribution of concentrations in different flow zones, the lifting equation allows for exact solution.

4. In particular, the exact solution for displacement of oil by high salinity slug followed by the slug with low salinity and, finally, by high salinity water chase drive is presented in the form of explicit formulae for saturation, salinity, suspended and

retained concentrations of fines during the displacement. Also, the explicit formulae for oil recovery follow from the exact solution.

5. 1D problem for displacement of oil during low-salinity polymer flooding also allows for exact solution. The saturation, polymer concentration and salinity profiles and their dynamics during the displacement are described by the explicit formulae. The solution along with oil-recovery expressions permits for illustrative visualization in the plane of the fractional flow curves.

6. The problems of 1D oil displacement by suspensions and colloids also allows for analytical modelling. Using the stream-function as an independent variable instead of time in the $(m+2)\times(m+2)$-system of two-phase suspension-colloidal flow with m different retention mechanisms, splits the system into auxiliary $(m+1)\times(m+1)$-system and one scalar lifting equation. The auxiliary problem allows for exact solution. In the case of negligible formation damage coefficients, the lifting equation is solved analytically.

7. For the case of small retained concentrations, which corresponds to either constant filtration coefficients or small flow times, the analytical model exhibits a new feature of two-phase colloidal-suspended flux. However, the effect of suspension concentration on viscosity of aqueous phase is accounted for. The solution shows that the suspension concentration is zero ahead of the concentration front; it instantly becomes steady-state in any reservoir point behind the front after the front pass this point. All retained concentrations are proportional to the amount of particles that pass this point; the proportionality coefficient for each retained concentration is the corresponding filtration coefficient.

8. The exact solutions of 1D flow problems can be used for 3D reservoir simulation using stream-line or front-tracking options.